# Molecular Pathogenesis of *Helicobacter hepaticus* Induced Liver Disease

by

Samuel R. Boutin

DVM, University of Minnesota, 1998
MBA, University of Chicago, 1985
MSEE, Illinois Institute of Technology, 1980
BSEE, University of Michigan, 1974

SUBMITTED TO THE DIVISION OF BIOLOGICAL ENGINEERING IN PARTIAL FULFILLMENT OF THE REQUIRMENTS FOR THE DEGREE OF

DOCTOR OF PHILOSOPHY DEGREE IN MOLECULAR AND SYSTEMS BACTERIAL PATHOGENESIS

at the

MASSACHUSETTS INSTITUTE OF TECHNOLOGY
February, 2005



Signature of Author_____
Division of Biological Engineering
Division of Comparative Medicine
January 28, 2005

Certified by_____
James G. Fox
Professor, Division of Biological Engineering
Director, Division of Comparative Medicine
Thesis Supervisor

Accepted by_____
Ram Sasisekharan
Professor, Division of Biological Engineering
Chairman, Departmental Committee on Graduate Students

This doctoral thesis has been examined by thesis committee as follows:

_____

Professor David B. Schauer
Chairman

_____

Professor James L. Sherley

_____

Professor Timothy C. Wang

# Molecular Pathogenesis of *Helicobacter hepaticus* Induced Liver Disease

**by**

**Samuel R. Boutin**

SUBMITTED TO THE DIVISION OF BIOLOGICAL ENGINEERING ON JANUARY 28, 2005 IN PARTIAL FULFILLMENT OF THE REQUIRMENTS FOR THE DOCTOR OF PHILOSOPHY DEGREE IN MOLECULAR AND SYSTEMS BACTERIAL PATHOGENESIS

## Abstract

*Helicobacter hepaticus* infection of A/JCr mice is a model of liver cancer resulting from chronic active inflammation. We monitored hepatic global gene expression profiles and correlated them to histological liver lesions in *H. hepaticus* infected and control male A/JCr mice at 3 months, 6 months, and 1 year of age. We used an Affymetrix-based oligonucleotide microarray platform on the premise that a specific genetic expression signature at isolated time points would be indicative of disease status. Model based expression index comparisons generated by dChip yielded consistent profiles of differential gene expression for *H. hepaticus* infected male mice with progressive liver disease versus uninfected control mice within each age group. Linear discriminant analysis and principal component analysis allowed segregation of mice based on combined age and lesion status, or age alone. Up-regulated genes present throughout the 12 month study involved inflammation, tissue repair, and host immune function. Up-regulation of putative tumor and proliferation markers correlated with advancing hepatocellular dysplasia. Transcriptionally down-regulated genes in mice with liver lesions included those related to peroxisome proliferator, cholesterol, and steroid metabolism pathways. Transcriptional profiling of hepatic genes documented gene expression signatures in the livers of *H. hepaticus* infected male A/JCr mice with chronic progressive hepatitis and preneoplastic liver lesions, complemented the histopathological diagnosis, and suggested molecular targets for the monitoring and intervention of disease progression prior to the onset of hepatocellular neoplasia.

Our laboratory, in collaboration with Professors Suerbaum and Schauer, recently identified a 70kb genomic island in *Helicobacter hepaticus* strain ATCC 51488 as a putative pathogenicity island (HhPAI) (Suerbaum et al, PNAS, 2003). This region within *H. hepaticus* contains genes HH0233-HH0302, a differential GC content, several long tandem repeats but no flanking repeats, and three components of a type IV secretion system (T4SS). A/JCr mice were experimentally infected with three naturally occurring strains of *H. hepaticus* including the type strain *H. hepaticus* ATCC 51488 strain (Hh 3B1) isolated from A/JCr mice, MIT 96-1809 (Hh NET) isolated from mice shipped from the Netherlands, and MIT-96-284 (HhG) isolated from mice acquired from Germany.

HhNET (missing most of the HhPAI) infected male A/JCR mice exhibited a significantly lower prevalence ($p<.05$) of hepatic lesions at 6 months post infection than Hh 3B1 with an intact HhPAI. Hh G also has a large segment of the genomic island deleted, but not as many genes are deleted as compared to Hh NET. Hh G also demonstrated a lower prevalence of hepatic lesions. This variable pathological effect was evident in male mice only. The severity of chronic active inflammation in the liver of the *H. hepaticus* infected A/JCr mice depended on *H. hepaticus* liver colonization levels. The *in vivo* results support the presence of the HhPAI as a legitimate virulence determinant and predictor of severity of liver lesions in *H. hepaticus* infected A/JCr male mice.

To further determine the differences in virulence of the *H. hepaticus* strains Hh 3B1, Hh NET, Hh G and an isogenic mutant *H. hepaticus* mutant lacking genes HH0250-HH0268 (containing two of the *vir* homologues of a T4SS) of the HhPAI, *in vitro* experiments were performed. Since the macrophage participates in the immune response to *H. hepaticus* infection in the liver as demonstrated by histopathology and microarray studies, a murine macrophage cell line, RAW264.7, was chosen for the *in vitro* experiments. RAW264.7 murine macrophage cell cultures were infected with three wild type strains (Hh3B1, HhG, HhNET) and a mutant strain (HhBac26) of *H. hepaticus* at a multiplicity of infection (MOI) of 0.1 for 24 hours. Cytokine Cxcl4, Cxcl10, Cxcl1, Cxcl2, Ccl2, Ccl3, and Tnf expression levels were monitored by real time PCR. These *in vitro* experiments demonstrated statistical significance ($p<.05$) of *H. hepaticus* strain differences (i.e. higher levels in Hh3B1 versus HhNET and HhBac26) compared to controls in the Cxcl2, Ccl2, Ccl3, and Tnf cytokine responses of a murine macrophage cell line, RAW 264.7. These *in vitro* results generated additional evidence of virulence differences in *H. hepaticus* strains based on the pathogenicity island, HhPAI. In conclusion, these studies provided further insight into the host-pathogen interaction of infectious liver cancer by identifying genes in both the murine host and the pathogenicity island in *H. hepaticus,* as well as the importance of macrophages in eliciting and profiling the hosts tissue responses that participate in chronic active inflammation-associated preneoplasia which ultimately progresses to hepatocellular carcinoma.

Thesis Supervisor: James G. Fox
Title: Professor, Division of Biological Engineering
Director, Division of Comparative Medicine

**Acknowledgements**

My wife Sue has been my pillar of support. I could not have completed this degree without her love, help, understanding, and encouragement. I regret my parents did not live long enough to see me receive this degree. In fact, my mother passed away while I was a graduate student. Sue was completely devoted to her, and unselfishly cared for her at our home until the end. There were many personal challenges for Sue while I was at MIT. She was instrumental in obtaining the finest medical care for her father and sister at Massachusetts General Hospital. Sue tirelessly cared for them too. Although her father could not be saved, her sister survived two neurosurgeries. It seemed there were more personally trying events concentrated during our six years in Massachusetts than any other time in our 23 years of marriage. Sue persevered through all of it. I am very fortunate to have such a wonderful wife. I dedicate this MIT PhD to her.

I am also very fortunate to have had such wonderful parents. My parents always encouraged me to seek formal education and provided the means to do so. My father was a mechanical engineer. Since I was an electrical engineer, it created a friendly competition and rivalry, with constant teasing as to which field of engineering was superior. He worked very hard to support his family, and his work demanded long periods of time away from home. I am very proud of the work he did in installing and maintaining turbines and generators at power plants all over the country.

My mother had the chore of raising the likes of me. She was a wonderful mother. She provided the best in care for me, and spoiled me with her wonderful cooking. She would drive me all over town, at all hours of the day, for swimming practice, Boy Scouts, and other activities. She loved to laugh and I have many pleasant memories of us laughing together. She was also a "big tease" like my father, and they had plenty of material to work with having a son like me.

My advisor, Dr. James G. Fox, made everything possible for me at MIT. I am very grateful for all the time and effort he has devoted to me. We have spent many a Saturday together at MIT. He is a Professor and a Director at the Massachusetts Institute of Technology, which says it all. He has had, and continues to have, an exemplary career in research and veterinary medicine. I am proud to have been mentored by a member of the Institute of Medicine of the National Academies of Science. His grants have provided an exceptional research and training environment, providing equipment and resources to perform experiments that could not have been accomplished in very many places. The other aspect of an excellent research environment is the people. Dr. Fox has assembled an exceptional team of veterinarians, research scientists, technicians, administrators, and postdoctoral fellows. Finally, I want to thank Dr. Fox for introducing me to the fascinating world of *Helicobacter* spp. I feel very fortunate to have studied two fields of tremendous interest to me, infectious disease and cancer. It has been very interesting to focus on a bacterial genus that causes cancer in people and animals. I have enjoyed the research immensely.

My committee chairman, Dr. David B. Schauer, has been outstanding. He has shared a tremendous amount of his time and expertise with me, and I am most grateful. I have been the benefactor of Dr. Schauer's marvelous intellect, knowledge, and teaching. I have often been struck with his ability to recognize the strengths and weaknesses of experiments and experimental results. His scrutiny is unsurpassed. Dr. Schauer is an expert in bacteriology and molecular biology. He has generously shared his knowledge of *Helicobacter* spp., *E. coli*, and *Citrobacter* spp. His research and research lab have been excellent and have helped me enormously.

Dr. James L. Sherley is an adult stem cell, cell kinetics, and cancer expert. He introduced me to the fascinating "immortal strand hypothesis" and his seminal work in this area has contributed enormously to the understanding of adult stem cells. His intellectual courage to challenge the biological tenet of semi-conservative replication in adult stem cells has been inspiring. He has generously provided his time and tremendous insight into cancer mechanisms in helping me with my research. Dr. Sherley has also shared his statistics expertise in our respective microarray studies, and we have had many fruitful and stimulating conservations in this discovery field. I am very grateful to him and am proud to have had him on my committee.

Dr. Timothy C. Wang is presently Dorothy L. and Daniel H. Silberberg Professor of Medicine and Chief, Division of Digestive and Liver Diseases at Columbia University, College of Physicians & Surgeons in New York City, New York. Dr. Wang was offered this position while I was a graduate student. While he was in Massachusetts, he attended my committee meetings and contributed to our research direction. At meetings and at a distance, he has been very supportive of my pursuits and has been a wonderful collaborator of the Fox lab.

Dr. Arlin Rogers (aka "Brisket") is a great researcher, an excellent pathologist, and a dear friend. Simply put, I am forever in his debt.

I need to acknowledge my favorite lab mates. Zeli Shen has been a joy to work with, and I learned so much molecular biology and microbiology from her. I am very indebted to her for teaching me and helping me. Research was both interesting and fun with Zeli around. I think we made a great research team, and I will miss her day to day camaraderie. Nancy Taylor also helped me in the lab and is a great teacher. Her experience and knowledge of microbiology was a wonderful resource for me, and she was always generous with her time. Two other people that were instrumental in my training in the lab include Zhonming Ge and Yan Feng. Their cheerful attitudes day-in and day-out are inspirational.

Other people, past and present, in DCM including Bob Marini, Prashant Nambiar, Sandy Xu, Charlie Corcoran, Ellen Buckley, Vivian Ng, Keith Astrofsky, Katie Madden, Kirk Maurer, Betsy Theve, Alex Garcia, Rao Varada, Scooter Holcombe, Mark Whary, Susan Erdman, Sue Chow, Lucy Wilhelm, Elaine Robbins, Pam Slot, Cheryl Buccieri, Leslie Hopper, Glenda Inciong, Steve Downey, Jeff Bajko, Erinn Stefanich, Bobi Young, Ernie Smith, Kathy Cormier, Chuck Dangler, Mark Schrenzel, Kris Hewes, Kevin Milne, Tony

Chavarria, Dina Chojnacky, Jane Sohn, Ming Chen, and Kim Knox, have all helped me and I want to thank them, and anybody I inadvertently neglected to mention, for all their efforts.

**Table of Contents**

**List of Figures**

4-7 Hepatitis index (combined lobular and portal hepatitis scores) of all male groups of A/JCr mice infected with the type strain *H. hepaticus* 3B1 and two other wild type strains of *H. hepaticus* at 6 months post-inoculation.

4-8 Dual fluorescence immunohistochemistry

5-1 Macrophage cell line RAW264.7 infection assay.

**List of Tables**

# Chapter 1

## Introduction to the molecular pathogenesis of *Helicobacter* spp.

## ***Helicobacter*** **species**

### History of *Helicobacter* species

In 1982, gastroscopic antral biopsies revealed curved, gram negative, flagellate bacilli in patients with chronic gastritis, gastric ulceration, and duodenal ulceration (Marshall and Warren 1984). Marshall and Warren identified the bacterium as a *Campylobacter* sp., a member of a genus noted for strains that cause enterocolitis and diarrhea in humans and animals. The bacterium was initially named *Campylobacter pyloridis* but the nomenclature was later revised to *Campylobacter pylori* (Marshall and Goodwin 1987). *Campylobacter pylori* experimental infections satisfied Koch's postulates when two human volunteers, with histologically normal gastric mucosa, were orally inoculated with the new bacterial species and exhibited gastritis within days (Marshall *et al.* 1985; Morris and Nicholson 1987). Due to ultrastructural differences including sheathed flagella and 16S rRNA sequence differences between this new species and existing *Campylobacter* spp. (Romaniuk *et al.* 1987), a new genus was formally created and *Campylobacter pylori* was renamed *Helicobacter pylori* in 1989 (Goodwin *et al.* 1989).

The *Helicobacter* genus is expanding as different anatomical niches within numerous vertebrate hosts yield novel species. There are 26 *Helicobacter* species at the date of this writing, with more proceeding through formal taxonomic classification (Fox and Lee 1997; Whary and Fox 2004a). *Helicobacter* spp. colonize the stomach, liver, cecum,

colon, and gall bladder in various animals species, and can be grouped as either gastric or enterohepatic.

Gastric *Helicobacter* species

Spiral-shaped bacteria occupying the gastrointestinal tract have been observed for over a century. Gastric spiral-shaped bacteria were reported in animals by Rappin (1881), Bizzozero (1893), and Salomon (1898) and their association with gastric carcinoma by Krienitz (1906) and Celler and Thalheimer (1916) (Fox 1995; Fox and Lee 1989; Versalovic and Fox 2003). In 1939, JL Doenges observed gastric spiral bacteria in 43% of 243 human samples and 100% of 43 rhesus macaque samples (Fox and Lee 1989). Ultrastructural studies in the 1970's of duodenal ulceration and gastric metaplasia revealed spiral bacteria (Steer 1975, 1984). The successful isolation of the gastric spiral bacteria from human patients with gastritis initiated intensive research into an infectious cause of gastric and duodenal disease (Marshall and Warren 1984). Electron microscopy revealed various morphologies of the gastric spiral bacteria in humans and animals including the distribution of periplasmic fibrils, and the location, number, and sheathing of flagella (Fox and Lee 1989; Lockard and Boler 1970). As mentioned earlier, the ultrastructure and 16S rRNA sequence differentiated the gastric spiral bacteria from *Campylobacter*, thus justifying the establishment of the *Helicobacter* genus (Goodwin et al, 1989).

*H. pylori* usually colonizes people for life within the mucus layer of the gastric mucosa. The infection is often acquired in childhood and may be transient in childhood.

However, once the infection is re-established, the organism usually persists for life. *H. pylori* demonstrates gastric tissue tropism and a narrow host range. Natural *H. pylori* infection and gastritis also occurs in rhesus monkeys (Handt *et al.* 1997; Newell *et al.* 1987; Suerbaum *et al.* 2002) and the domestic cat (Fox *et al.* 1995a). The first successful experimental infections of *H. pylori* were established in neonatal gnotobiotic piglets (Krakowka *et al.* 1987) but the inflammatory infiltrate was distinctly different between humans and piglets (Bertram *et al.* 1991). Subsequently, *H. pylori* also successfully colonized and produced gastritis in macaques (Fujioka *et al.* 1994; Shuto *et al.* 1993). Unfortunately, *H. pylori* would not colonize mice and other laboratory animals in early experimental infections despite numerous attempts. Experimental infections of BALB/c nude and BALB/c euthymic mice with freshly isolated *H. pylori* strains from human patients colonized the gastric mucosa of the mice for 20 weeks and 2 weeks, respectively. However, the established *H. pylori* strain did not colonize these BALB/c nude and BALB/c euthymic mice (Karita *et al.* 1991). The same group colonized athymic germ-free mice with *H. pylori* (Karita *et al.* 1994). A standardized mouse model of *H. pylori* infection, the Sydney strain SS1, was not attained until the late 1990's (Lee *et al.* 1997; Marchetti *et al.* 1995). A second *H. pylori* strain, B128, induces pangastritis, ulcerations, and gastric atrophy in the Mongolian gerbil and gastric adenocarcinoma in the INS-GAS mouse model (Fox *et al.* 2003b; Wang *et al.* 2000). Recently, a third mouse-adapted strain of *H. pylori* was isolated and characterized, allowing comparative studies of both *H. pylori* strains and their effect on various rodent host strains (Thompson *et al.* 2004). In addition to *H. pylori*, another gastric *Helicobacter* sp. identified from humans in a small percentage of gastritis cases is "*H. heilmannii*". *H. heilmannii*, although not yet

formally classified because it has been cultured only once, is more prevalent in animals. A homogenized human gastric biopsy infected with *H.heilmannii* was used as a inoculum and the organism colonized mice (Dick *et al.* 1989). *H. heilmannii* has also been associated with human duodenal ulceration, gastric carcinoma, and gastric B-cell mucosa-associated lymphoid tissue (MALT) lymphoma (Heilmann and Borchard 1991; O'Rourke *et al.* 2004).

*H. mustelae* in the ferret was the second gastric *Helicobacter* species to be isolated and characterized (Fox *et al.* 1988). The ferret became the first natural infection animal model of *Helicobacter*-induced gastritis (Fox *et al.* 1990). *H. felis*, isolated from the gastric mucosa of a cat, is another natural gastric *Helicobacter* species (Paster *et al.* 1991). *H. felis* exhibits a wider host range, with experimental infection colonizing many other animals, including the gnotobiotic rat (Fox *et al.* 1991), the mouse (Chen *et al.* 1992; Lee *et al.* 1990), and the beagle dog (Lee *et al.* 1992a).

Enterohepatic *Helicobacter* species

Cecal and colonic colonization

Historically, culturing the spiral shaped bacteria in the gastrointestinal tracts of animals was problematic. Morphologically distinct spiral bacteria colonizing the mucus layer of the colon of a rat were first cultured in 1978 (Lee and Phillips 1978). Later, these gram negative spiral bacteria were isolated from the ileum, cecum, and colon of mice and rats

and were cultured on *Campylobacter* medium in a microaerobic environment (Phillips and Lee 1983). The bacterial morphology did not correspond to any known genus at the time, and this spiral bacterium with "9 to 11 helically coiled periplasmic fibers and bipolar tufts of flagellum-like appendages" would eventually be designated as belonging to a *Helicobacter* sp. and was subsequently named *H. muridarum* (Lee *et al.* 1992b; Phillips and Lee 1983).

The first human enterohepatic *Helicobacter*s, *H. cinaedi* and *H. fennelliae*, formerly classified as a *Campylobacter* spp., were first isolated from homosexual men with proctitis, protocolitis, and/or enteritis (Totten *et al.* 1985) and later from patients with Human Immunodeficiency Virus (HIV) exhibiting multifocal cellulitis and arthritis (Burman *et al.* 1995; Kiehlbauch *et al.* 1994). *H. cineadi* has also been isolated from the feces and blood of clinically normal female adults and children (Vandamme *et al.* 1990) and the cerebrospinal fluid and blood of a neonate with meningitis and septicemia (Orlicek *et al.* 1993). Molecular evidence of gastric colonization of *H. cinaedi* has been reported once (Pena *et al.* 2002). Experimental infection of infant pig-tailed macaques (*Macaca nemestrina*) with *H. cinaedi* and *H. fennelliae* produced acute diarrhea and bacteremia, and gastrointestinal infection (Flores *et al.* 1990). *H. cinaedi* has been isolated from other animal reservoirs (Kiehlbauch *et al.* 1994; Vandamme *et al.* 2000) including hamsters, presumed to be enzootically infected (Gebhart *et al.* 1989), and captive rhesus macaques with chronic hepatitis and colitis (Fox *et al.* 2001a; Fox *et al.* 2001b).

Other enteroheptic *Helicobacter* spp. include *H. canis*, *H. pullorum*, *H. marmotae*, and *H. canadensis*. *H. canis* was isolated from healthy and diarrheic dogs and from humans with a history of gastroenteritis (Stanley *et al.* 1993). *H. canis* has also been associated with hepatitis in a dog (Fox *et al.* 1996a) and colitis in Bengal cats (Foley *et al.* 1999). The avian enterohepatic species, *H. pullorum*, has been cultured from chickens with and without gastrointestinal lesions, including hepatitis, and has been associated with human gastroenteritis (Burnens *et al.* 1994; Stanley *et al.* 1994). *H. canadensis* was isolated from diarrheic humans (Fox *et al.* 2000b) and subsequently was isolated from geese in Europe (Waldenstrom *et al.* 2003).

Hepatic colonization

In 1992, the first enterohepatic *Helicobacter* sp. colonizing liver was discovered in the liver and cecal scrapings of of untreated control A/JCr mice s in a long term toxicology study at the National Cancer Institute (Fox *et al.* 1994; Ward *et al.* 1994). The A/JCr mice with chronic, active hepatatis exhibited a high incidence of hepatic tumors. This new species, *Helicobacter hepaticus*, was spiral-shaped and exhibited bipolar single sheathed flagella. *Helicobacter hepaticus* is now associated with chronic hepatitis and hepatocellular carcinoma (HCC) in A/JCr and other susceptible mouse strains, including BALB/CAnNCr, SJL/NCr, C3H/HeNCr, SCID/NCr, AxB recombinant inbred mice, B6C3F1 mice, and B6AF1 mice (Fox *et al.* 1996b; Fox *et al.* 1996d; Garcia *et al.* 2004; Hailey *et al.* 1998; Ihrig *et al.* 1999). *H. hepaticus* has since been isolated from mice housed in many other academic and commercial mouse colonies, and continues to be a

risk factor for compromising experimental enteric studies (Shames *et al.* 1995; Taylor *et al.* 2004).

Eventually, more murine enterohepatic species were isolated, including *'Flexispira rappini'* (now recognized as a *Helicobacter* sp. but not formally named) (Dewhirst *et al.* 2000; Schauer *et al.* 1993), *Helicobacter bilis* in 1995 (Fox *et al.* 1995b), *Helicobacter rodentium* in 1997 (Shen *et al.* 1997), *H. ganmani* (Robertson *et al.* 2001), *H. typhlonius* (Franklin *et al.* 2001) as well as rat enterohepatic species, *H. trogontum* (Mendes *et al.* 1996). *H. rodentium*, however, appears to be part of the normal murine microbiota and is sometimes found in *Helicobacter* spp. co-infections of mouse colonies (Shen *et al.* 1997; Shomer *et al.* 1998). *H. bilis* was found to colonize the liver, bile, and intestines of aged mice and is pathogenic in some murine strains (Fox *et al.* 2004b; Fox *et al.* 1995b; Shomer *et al.* 1998; Whary and Fox 2004a). *H. bilis* colonizes several other laboratory animals, including a mouse, dog, rat, and gerbil, (Ge *et al.* 2001) and has been associated with biliary disease and biliary tract cancer in humans (Fox *et al.* 1998; Matsukura *et al.* 2002; Murata *et al.* 2004). Other *Helicobacter* spp. isolated from the liver of animals include *H. marmotae* from the woodchuck (Fox *et al.* 2002), *H. cinaedi* from rhesus macaques, and *H. canis* from dogs (Fox *et al.* 1996a; Fox *et al.* 2001a; Fox *et al.* 2001b).

**Infection, inflammation and cancer**

The link between inflammation and cancer has been recognized for some time, as has the relationship between infectious agents and cancer (Balkwill and Coussens 2004; Balkwill

and Mantovani 2001; Clevers 2004; Coussens and Werb 2002; Shacter and Weitzman 2002; van Kempen *et al.* 2003). Persistent infection initiates an estimated 15%-20% of cancer cases worldwide, amounting to 1.2 million cases per year (Kuper *et al.* 2000; Pisani *et al.* 1999). *H. pylori*, Hepatitis B virus, Hepatitis C virus, Epstein-Barr virus, the liver fluke (*Opisthorchis viverrini*), human immunodeficiency virus, human herpes virus type 8, human papilloma virus, and *Schistosoma* spp.are some of the infectious agents associated with cancer (Coussens and Werb 2002; Giordano *et al.* 2004; Stewart *et al.* 2003).

Chronic inflammation results in persistent tissue injury and possible DNA damage due to reactive oxygen and nitrogen species from inflammatory cells (Dedon and Tannenbaum 2004). Continual cell proliferation in this inflammtory microenvironment increases the risk of neoplasia due to the possibility of DNA damage and tumor initiation. The inflammatory mileu consists of cytokines, chemokines, and growth factors that are an integral part of tissue regeneration. Thus, infectious agents not eliminated by the host produces a continual innate and acquired immune responses and chronic, active inflammation, thus establishing a putative causal link to cancer due to the promotion and progression of initiated cells (Coussens and Werb 2002).

*Helicobacter* sp. infection causes chronic, active inflammation of varying severity in susceptible hosts. *Helicobacter* spp. may cause chronic active gastritis, colitis, hepatitis, and cholecystitis. The location of the infection and severity of the disease depends on the genetics of the host and the bacteria. The inflammatory response is cell mediated and is

predominantly a Th1 phenotype. Proinflammatory cytokines interferon gamma (IFN-γ), interleukin 2 (IL-2) and tumor necrosis factor beta (TNFβ) are secreted, and activation of macrophages and other phagocytes observed. (Hauer *et al.* 1997; Mohammadi *et al.* 1996; Mohammadi *et al.* 1997; Whary *et al.* 1998). Anti-inflammatory Th2 responses presumably areinhibited unless there is co-colonization with a pathogen that induces a Th2 response (Fox *et al.* 2000a; Whary and Fox 2004b)

Persistent infection causes a large percentage of cancer cases, nearly 1 in 5. *H. pylori* is the infectious agent responsible for the highest cancer mortality. Estimates of the percentage of all cancer cases caused by *H. pylori* are just under 6% (Kuper *et al.* 2000; Parsonnet 1999; Pisani *et al.* 1999). Therefore, a large number of gastric cancer cases can be avoided by the prevention of this infectious disease. Recent studies report the association of *Helicobacter* spp. with cancer of other segments of the gastrointestinal tract, including the liver and the gall bladder. We propose the paradigm of *H. pylori* and gastric cancer may extend to persisent enterohepatic *Helicobacter* spp. infection in other gastrointestinal organs.

***Helicobacter pylori***

Overview

It is estimated that *H. pylori* infects around 50% of the world's population. *H. pylori* persistently colonizes the gastric mucosa, a unique niche for bacterial colonization. The

gastric niche, as opposed to the enterohepatic niche, contains few bacterial species due to the pH of the environment. A series of prospective case-control studies using stored serum from well-characterized populations yielded epidemiological evidence established a link between *H. pylori* infection and gastric cancer (Aromaa *et al.* 1996; Forman *et al.* 1991; Ley and Parsonnet 2000; Lin *et al.* 1995; Nomura *et al.* 1991; Parsonnet *et al.* 1991; Siman *et al.* 1997; Watanabe *et al.* 1997; Webb *et al.* 1996).

Gastric cancer is the second leading cause of cancer-related mortality (Mathers *et al.* 2002; Shibuya *et al.* 2002). *H. pylori* is listed as a group I (definite) carcinogen by the World Health Organization due to its association with gastric adenocarcinoma. The National Cancer Institute Surveillance, Epidemiology, and End Results (SEER, http://seer.cancer.gov/) report of Estimated New Cancer Cases and Deaths for 2004 approximates the number of deaths in the United States for the year 2004 from cancers of the digestive system to reach approximately 135,000 people, and the number of new digestive system cancers to approach 256,000 people. In the year 2000, 7 million deaths was the estimated total mortality worldwide, and 13% of these deaths were cancer related. Ten million new cancer cases were diagnosed (Mathers *et al.* 2002; Shibuya *et al.* 2002). In the year 2002, it is estimated 445,000 male and 254,000 female deaths per year worldwide due to gastric cancer (GLOBOCAN, 2002, Tables by cancer, http://www-depdb.iarc.fr/globocan/GLOBOframe.htm). Gastric cancer is ranked second only to lung cancer (lung cancer deaths per year: 848,000 males, 330,000 females) as the leading cause of cancer mortality in the world. Liver cancer accounts for 417,000 male

and 181,000 female deaths per year worldwide, and is the third leading cause of cancer mortality.

The clinical outcome for the majority of *H. pylori* infected people is a mild gastritis. However, *H. pylori* is a risk factor for duodenal ulcers and gastric cancer, yet only a small percentage of those infected develop disease. The reason for these disparate outcomes is unknown. Antral-predominant gastritis increases the risk of hyperchloridia and duodenal ulcers. Corpus predominant gastritis increases the risk of gastric atrophy, hypochloridia, and gastric cancer. Experimental evidence suggests both host genetics, and bacterial genetics contribute to the development of lesions. Human interleukin-1 (IL-1), interleukin 1 receptor 1 (IL1-R1), interleukin 1 receptor antagonist (IL1-RN*2), and interleukin 8 (IL-8) polymorphisms correlate with the differences in host response (El-Omar *et al.* 2000; Gyulai *et al.* 2004; Hartland *et al.* 2004; Hsu *et al.* 2004). *H. pylori* strains possessing putative virulence factors are also associated with increased gastric cancer risk (Azuma *et al.* 2004; Blaser *et al.* 1995a; Blaser *et al.* 1995b; Covacci *et al.* 1999; Parsonnet *et al.* 1997).

*H. pylori* genome

The extensive genetic diversity of *H. pylori* has been known for some time (Langenberg *et al.* 1986). The genome of *H. pylori* is 1.6 Mb (Alm *et al.* 1999; Tomb *et al.* 1997). Genomic analysis suggests that specific DNA mismatch repair systems are not present in this species, suggesting that mutation may be responsible for the highly variable genome

of *H. pylori* (Alm *et al.* 1999; Alm and Trust 1999; Tomb *et al.* 1997). Further, strain-specific restriction and modification systems (R-M) comprise a significant percentage of *H. pylori* strain specific genes, contributing to the variability (Alm *et al.* 1999; Alm and Trust 1999; Tomb *et al.* 1997). Suerbaum and Achtman state "the nucleotide sequence diversity of *H. pylori* exceeds that of many bacterial species" and that "almost every nucleotide sequence from unrelated isolates is unique, an unprecedented situation" (Achtman and Suerbaum 2000). Thus, many studies propose a non-clonal population structure of *H. pylori* with frequent recombination (Achtman and Suerbaum 2000; Falush *et al.* 2001; Falush *et al.* 2003; Salaun *et al.* 1998; Suerbaum and Achtman 1999; Suerbaum *et al.* 1998). Consequently, *H. pylori* virulence factors containing specific nucleotide sequences could explain the small percentage of the infected population developing disease from a bacterial genetics standpoint.

## Virulence factors

### Pathogenicity islands

Evolution has given bacterial pathogens various mechanisms to survive against the host's immune system and commensal competition. For example, strains of *E. coli* (Holden and Gally 2004; Kaper *et al.* 2004; Karmali 2004; Landraud *et al.* 2004), *Legionella* spp.(Bitar *et al.* 2004; Heuner and Steinert 2003), *Brucella* spp. (Delrue *et al.* 2004) invade host epithelial cells, *Salmonella* spp (Waterman and Holden 2003)and *Yersinia* spp.(Carniel 2001) target the antigen presenting M cells in the gastrointestinal tract, while

*H. pylori* remains extracellular, residing in the mucous layer coating the gastric epithelium and possessing a secretion system enabling protein injection into epithelial cells. One aspect of pathogenicity common across many bacterial species is a pathogenicity island (PAI). The term "pathogenicity island" was coined to denote a genomic island or a cluster of genes in close physical proximity on the bacterial chromosome correlated to virulence (Blum *et al.* 1995; Hacker *et al.* 1990). It often includes a group of genes transferred from other species contributing to a different GC content than the rest of the genome. The GC content of the PAI suggests the age of the island, implying increased similarity in GC content over time. Other common attributes of a PAI are the lack of stability, the site of integration being near tRNA genes, and direct repeats at the flanking sequences.

Type III and Type IV secretion systems

Several species of bacteria export virulence factors into host cells using Type III (T3SS) or Type IV secretion systems (T4SS). Bacteria possessing the T3SS include *Salmonella* spp., *E. coli*, *Yersinia* spp., and *Shigella* spp. T3SS probably evolved from flagellar secretion systems. Bacteria utilizing T4SS include *Agrobacterium tumefasciens, Brucella* spp*., Wolbachia* spp., *Campylobacter jejeuni, Bordetella pertussis,* and *Helicobacter pylori* with probable common ancestral functions of conjugation systems for transferring nucleoprotein complexes (Batchelor *et al.* 2004; Boschiroli *et al.* 2002; Celli and Gorvel 2004; Cheung *et al.* 2004; Christie 2001; den Hartigh *et al.* 2004; Hoppner *et al.* 2004; Larsen *et al.* 2004; Masui *et al.* 2000; McGraw and O'Neill 2004;

Poly *et al.* 2004; Rambow-Larsen and Weiss 2004). Both types of secretion systems stabilize effector molecules via chaperones and utilize ATP-hydrolysis as a transport energy source. *H. pylori* possesses two functional independent T4SS, *cag* and *comB*. The *cag* system involves protein translocation while the *comB* promotes uptake of DNA by natural transformation.

*Cag* pathogenicity island of *H. pylori*

The *H. pylori* PAI was named "cag" as an abbreviation for the cytotoxin associated gene (Sharma *et al.* 1995). The PAI is 40kb, has 31 open reading frames, and is flanked by repeats. Insertion element(s) are variably located on the ends or within the island. (Alm *et al.* 1999; Alm and Trust 1999; Blomstergren *et al.* 2004; Tomb *et al.* 1997). An important component of the PAI is the CagA protein, also variable in size due to the number of repeats. Most *H. pylori* strains can be classified into two major types. Type I strains possess the gene for CagA and express both the CagA protein and the vacuolating cytotoxin (see below). Type II *H. pylori* strains do not possess *cagA* and do not express either the CagA protein or the vacuolating cytotoxin. The *H. pylori* T4SS inserts CagA into AGS gastric epithelial cells producing a morphological transformation termed the "hummingbird" phenotype. A model of *H. pylori* pathogenesis is depicted in Figure 1 (Suerbaum and Michetti 2002). CagA is tyrosine phosphorylated within the epithelium and deregulates the SHP2 oncoprotein (Higashi *et al.* 2002a; Higashi *et al.* 2002b; Higuchi *et al.* 2004). CagA exhibits high sequence variability within *H. pylori*,

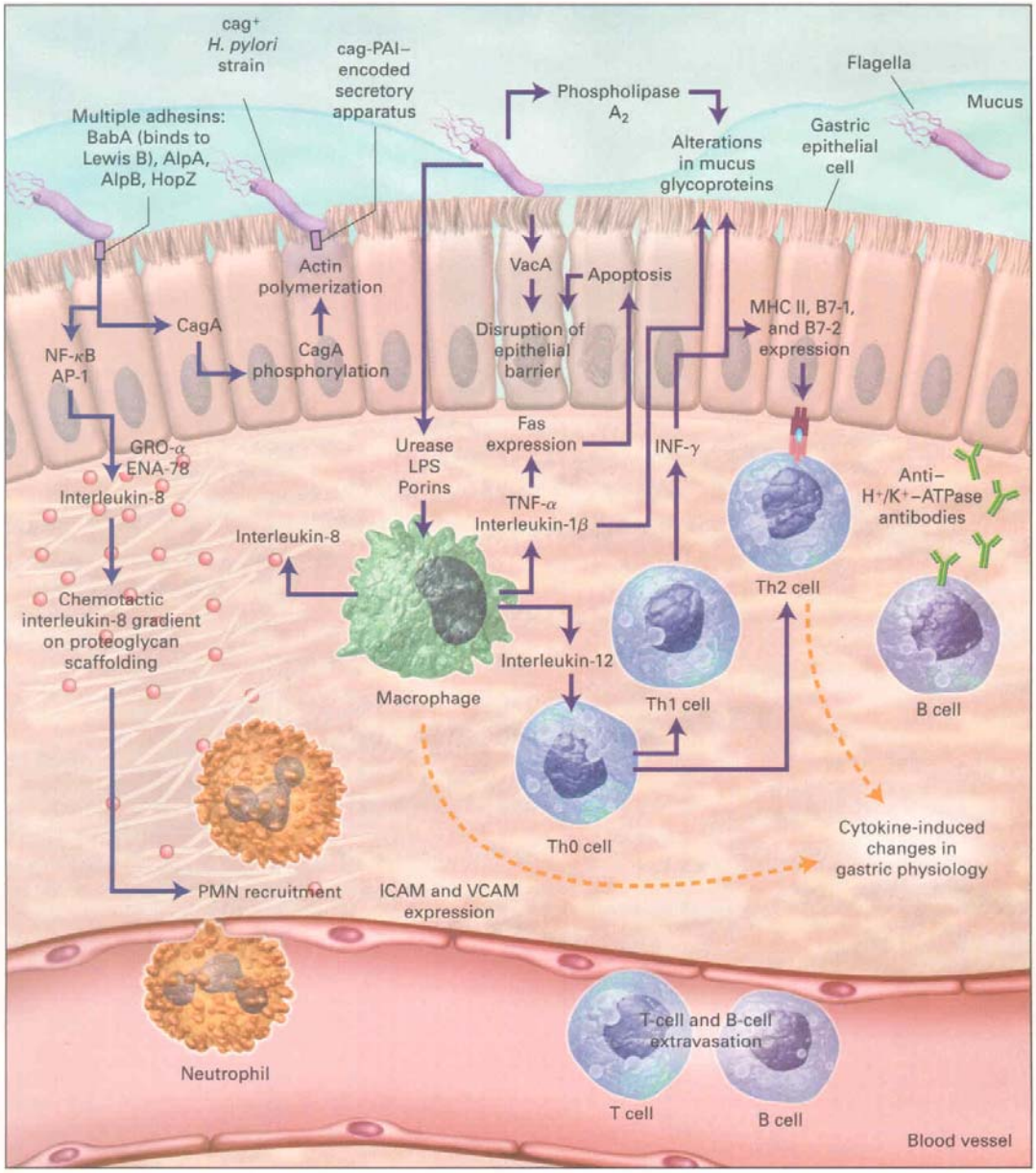


**Figure 1 (Suerbaum and Michetti, 2002; with permission)**

**Figure 1** Pathogen-Host Interactions in the Pathogenesis of *Helicobacter pylori* Infection.

The host response to *H. pylori* participates in the induction of damage to the gastric epithelium and therefore has an integral role in *H. pylori* pathogenesis. During the early phase of the infection, binding of *H. pylori* to gastric epithelial cells, in particular through BabA and by strains harboring the *cag* pathogenicity island, results in the production of interleukin 8 and other chemokines, such as epithelial-cell-derived neutrophil-activating peptide 78 (ENA-78) and growth-related oncogene a (GRO-α), by epithelial cells. Nuclear factor-κB (NF-κB) and the erly-response transcription-factor activator protein 1 (AP-1) are the intracellular messengers involved in this process. The chemokines secreted by epithelial cells bind to the proteoglycan scaffolding, generating a gradient along which polymorphonuclear cells (PMN) are recruited. The chronic phase of *H. pylori* gastritis associates an adaptive lymphocyte response with the initial innate response. Lymphocyte recruitment is facilitated by chemokine mediated expression of vascular addressins such as vascular-cell adhesion molecule 1 (VCAM-1) and intercellular adhesion molecule (ICAM-1) that are required for lymphocyte extravasation. Macrophages that participate in interleukin-8 production produce proinflammatory cytokines involved in the activation of the recruited cells, in particular T helper cells (Th0, Th1, Th2) that respond with a biased TH1 response to *H. pylori*. In turn, Th1-type cytokines such as interferon-γ (INF-γ) induce the expression of class II major histocompatibility complexes (MHC) and accessory molecules B7-1 and B7-2 by epithelial cells, making them competent for antigen presentation. The cytotoxin VacA and Fas-mediated apoptosis induced by tumor necrosis factor α leads to disruption of the epithelial barrier, facilitating translocation of bacterial antigens and leading to futher activation of macrophages. Cytokines produced by macrophages can also alter the secretion of mucus, contributing to *H. pylori*-mediated disruption of the mucous layer. Cytokines produced in the gastric mucosa induce changes in gastric acid secretion and homeostasis (dashed lines). TNF-α, interleukin 1β, and interferon γ increase gastrin release, stimulating parietal and enterochromaffin cells and thus acid secretion. TNF-α also induces a decrease in the number of antral D cells, leading to decreased somatostatin production and indirectly enhancing acid production. LPS denotes lipopolysaccharide.

particularly at the SHP2-binding site. This again suggests nucleotide differences affect the carcinogenic potential of different strains of *H. pylori* (Azuma 2004; Hatakeyama 2004; Higashi *et al.* 2004; Higuchi *et al.* 2004).

Vacuolating cytotoxin

The vacuolating cytotoxin of *H. pylori* induces vacuolation of eukaryotic cells *in vitro* and produces a serum immune response in patients, suggesting *in vivo* synthesis (Cover and Blaser 1992; Cover *et al.* 1992a; Cover *et al.* 1992b). Recent work demonstrates variable toxicity, depending on sequence of the vacuolating cytotoxin, affecting apoptosis in epithelial cells. Other vacuolating cytotoxin capabilities include modulating the immune response via affecting the cytokine response of T cells, activation and proliferation of T cells, and antigen presentation of B cells (Aviles-Jimenez *et al.* 2004; Fischer *et al.* 2004; Gebert *et al.* 2004; Sundrud *et al.* 2004; Yahiro *et al.* 2004).

*H. pylori* colonization factors

*H. pylori*, with one of the smallest genomes of an extracellular, free-living bacteria, possesses the remarkable ability to colonize some hosts indefinitely. The colonization factors allow gastic adherence and nutrient acquisition (Eppinger *et al.* 2004). *H. pylori* colonization factor genes include *alpA*, *alpB*(de Jonge *et al.* 2004a), *babA* (Aspholm-Hurtig *et al.* 2004; Hennig *et al.* 2004), *sabA* (de Jonge *et al.* 2004b; Lehours *et al.* 2004), *hopZ* (Lehours *et al.* 2004; Yamaoka *et al.* 2004), *hpaA*, *omp18* (Voland *et al.* 2003a),

*Nap* (Nishioka *et al.* 2003), *Hsp60*, *Hsp70*, and genes encoding LPS, LPS core, LPS O antigen (Testerman et al, 2001).

Urease, a gene expressed in *H. pylori*, consists of two subunits, UreA and UreB. Urease protects *H. pylori* from gastic acid by the catalysis of urea to ammonium and carbon dioxide (Benoit and Maier 2003; Eaton *et al.* 1991; Hartmann and von Graevenitz 1987; Mobley *et al.* 1991; Sidebotham and Baron 1990; Voland *et al.* 2003b). Urease isogenic mutants of *H. pylori* do not colonize mice nor gnotobiotic piglets (Eaton *et al.* 1991; Karita *et al.* 1995; Tsuda *et al.* 1994a; Tsuda *et al.* 1994b).

Another colonization factor related to motility within the mucous layer of the gastric mucosa is the 2 to 6 unipolar sheathed flagella of *H. pylori.* The flagellar system is complex, consist of over 40 genes that are expressed in a defined sequence for flagella construction (Niehus *et al.* 2004). *H. pylori* isogenic mutants of flagellin genes *flaA* and/or *flaB* have reduced motility, or are non-motile, and exhibit reduced colonization or no colonization in gnotobiotic piglets and gerbils (Eaton *et al.* 1996; McGee *et al.* 2002; Niehus *et al.* 2004; Schmitz *et al.* 1997)

Rodent models of gastric cancer

Two rodent models of *H. pylori*-induced gastric cancer include *H. pylori* infection of the Mongolian gerbil and the INS-GAS FVB mouse. *H. felis* infection of the C57BL/6

**Table 1.** ***Summary of key rodent models of infectious gastrointestinal and liver cancer***

| Rodent | Infectious Agent/Transgene | Tumor | Comment |
|---|---|---|---|
| C57BL mice | *H. felis* | Gastric adenocarcinoma | Natural gastric pathogen, but lacks *cag* and *vacA* |
| INS-GAS FVB mice* | *H. felis* and *H. pylori* | Gastric adenocarcinoma | Constitutive hypergastrinemia promotes tumorigenesis |
| Mongolian gerbil | *H. pylori* | Gastric adenocarcinoma | Closely mimics human disease, but long time course and few reagents |
| BALB/c mice | Several *Helicobacter* spp. | Gastric MALT lymphoma | Usually requires 18—24 mo |
| Genetically engineered mice: IL-10-, IL-2-, $G_{i2}$-, Muc2-, etc.-deficient; especially on 129Sv background | "Endogenous microbiota" or *H. hepaticus* | Lower bowel carcinoma | Bacteria in endogenous microbiota models not well defined; *H. hepaticus* reliably induces disease |
| Lymphocyte-deficient mice: SCID or $Rag^{-/-}$; especially on 129Sv background | "Endogenous microbiota" or *H. hepaticus* | Lower bowel carcinoma | Often used for adoptive transfer studies; *H. hepaticus* induces tumors in untreated $Rag2^{-/-}$ mice |
| Transgenic mice* | HBV or HCV transgene(s) | Hepatocellular carcinoma | Prove tumorigenic potential of viral gene products; adoptive transfer or inducible gene strategies required for hepatitis |
| A/JCr and other mice* | *H. hepaticus* | Hepatocellular carcinoma | Natural murine pathogen induces chronic active hepatitis and HCC |

**Rogers and Fox, 2004, with permission**

**MALT, mucosal-associated lymphoid tissue; PAI, pathogenicity-associated islands; HBV, hepatitis B virus; HCV, hepatitis C virus; HCC, hepatocellular carcinoma.**
***Male predominant.**

mouse and the INS-GAS mouse also induces gastric cancer but *H. felis* lacks the *cag* PAI and *vacA*. (Fox 1998; Rogers and Fox 2004; Wang *et al.* 2000) (Table 1). The Mongolian gerbil model mimics *H. pylori* pathogenesis in the human, but gastric adenocarcinoma develops only after a long period of time, i.e. greater than 15 months. The Mongolian gerbil model produces gastric ulcers prior to gastric atrophy and intestinal metaplasia (Bergin *et al.* 2003; Court *et al.* 2002; Wang and Fox 1998; Watanabe *et al.* 1998; Yang *et al.* 2003). The ING-GAS mouse exhibits constitutive hypergastrinemia, and combined with *H. pylori* or *H. felis* infection, promotes gastric cancer in less than 8 months (Fox *et al.* 2003a; Wang *et al.* 2000). As previously mentioned, the anatomical location of *H. pylori* induced gastritis is associated with two distinct clinical outcomes. The antral predominant gastritis promotes decreased somatostatin release from the D cells and increased gastrin release from the G cells, resulting in hypergastrinemia and increasing enterochromaffin-like cell histamine release (Blaser and Atherton 2004). Gastrin is a growth factor for *H. pylori* (Chowers *et al.* 2002). The gastrin and histamine co-stimulate parietal cell acid production and increased parietal cell proliferation, thus decreasing gastric pH. The increased acidity promotes duodenal ulceration, gastric metaplasia, and gastro-esophageal reflux disease. Pangastritis also promotes hypergastrinemia, but inflammation inhibits enterochromaffin-like and parietal cell output. The inhibition increases pH and hypochlorhydria persists, a risk factor for gastric ulcer, and gastric adenocarcinoma. *H. pylori* associated gastric atrophy, intestinal metaplasia, and increased colonization of diverse enteric bacterial species due to increased gastric pH are also risk factors of gastric cancer (Blaser and Atherton 2004).

The signaling pathways contributing to gastric cancer likely include gastrin and incompletely processed gastrin, due to the growth factor's trophic capabilities and involvement in other forms of cancer (Koh *et al.* 2004). Gastrin is a downstream target of the Wnt/wingless pathway and a promoter of gastrointestinal cancer. In the mouse, TGFβ/Smads and β-catenin/T-cell factors regulate the gastrin promoter (Lei *et al.* 2004). Other pathways affected include MAPK signaling and NF-κB signaling (Higashi *et al.* 2004; Maeda *et al.* 2002; Sebkova *et al.* 2004; Yanai *et al.* 2003).

Human gastric B-cell mucosa associated lymphoid tissue (MALT) lymphoma has been associated with *H. pylori* infection (Stolte 1992). As previously mentioned, *H. heilmannii* has only been reported in a small number of human cases, but is associated with gastritis, peptic ulcers, gastric adenomcarcinoma, and MALT lymphoma. *H. heilmannii* has a broader host range than *H. pylori*. Experimental *H. heilmannii* and *H. felis* infections of BALB/c mice are animal models of MALT lymphoma (Enno *et al.* 1995; Mueller *et al.* 2003; O'Rourke *et al.* 2004). Temporal laser dissection of the lymphoid nodules and microarray profiling of the tissue has yielded insight into the stages of the molecular pathogenesis of MALT. The microarry analysis revealed increased expression of genes previously associated with malignancy like laminin receptor 1 and multi-drug resistance channel 1 (Mueller *et al.* 2003).

***Helicobacter hepaticus***

Overview

*H. hepaticus* was initially discovered and isolated from control A/JCr mice in a long term toxicology study. The control mice exhibited chronic hepatitis and there was a high inidence of hepatocellular carcinoma (HCC). Mouse strains A/JCr, BALB/CAnNCr, SJL/NCr, C3H/HeNCr, SCID/NCr, AxB recombinant inbred mice, B6C3F1 mice, and B6AF1 mice exhibit susceptibility to *H. hepaticus* induced hepatitis (Fox *et al.* 1996b; Fox *et al.* 1996d; Hailey *et al.* 1998; Ihrig *et al.* 1999). Many rodent models of gastrointestinal disease utilize *H. hepaticus* (Table 1, Rogers and Fox, 2004). *H. hepaticus* causes chronic hepatitis and HCC in A/JCr mice (Fox *et al.* 1994; Fox *et al.* 1996b; Ward *et al.* 1994). A/JCr mice develop necrogranulomatous lobular and/or lymphocytic portal hepatitis. Male A/JCr mice are more susceptible to hepatitis and tumors than females. For reasons that are not clear, only a subset of *H. hepaticus* infected male mice are exhibit hepatitis (Boutin *et al.* 2004; Fox *et al.* 1996b; Rogers *et al.* 2004). Many rodent studies, including long term carcinogenesis bioassays, have been confounded due to this murine pathogen (Fox *et al.* 1994; Hailey *et al.* 1998; Ward *et al.* 1994; Whary and Fox 2004a).

*H. hepaticus* also induces typhlocolitis in immunodeficient strains including athymic NCr-nu/nu, BALB/c, AnNCr-nu/nu, C57BL/6NCr-nu/nu, and C.B17/Icr-scid/NCr

(Ward *et al.* 1996) and other mutant strains (Chin *et al.* 2000; Foltz *et al.* 1998; Kullberg *et al.* 2002; Kullberg *et al.* 2001; Kullberg *et al.* 1998; Li *et al.* 1998; Myles *et al.* 2003). Early experimental infections of *Helicobacter* free interleukin 10 deficient (IL-$10^{-/-}$) mice with *H. hepaticus* produced typhlocolitis through an IL-12 and interferon gamma (IFNγ) dependent mechanism (Kullberg *et al.* 1998). A novel urease negative *Helicobacter* species was also found to induce typhlocolitis in an IL-$10^{-/-}$ (Fox *et al.* 1999) and was subsequently named *H. typhlonius* (Franklin *et al.* 2001). Another novel urease negative *Helicobacter* species induced typhlocolitis and cholangiohepatitis in A/JCr and Tac:Icr:Ha(ICR)-scidfRF mice and is associated with the formation of chronic, active lymphoid aggregates in the liver (Shomer *et al.* 2001; Shomer *et al.* 2003). Further studies demonstrated *H. hepaticus* infected mice deficient in both IL-10 and IL-12p40 did not exhibit typhlocolitis, contributing additional evidence of a role for IL-12 (Kullberg *et al.* 2001). CD4(+) T cells from IL-$10^{-/-}$ animals transferred to infected recombination activating gene (RAG) deficient mice initiated intestinal inflammation while the cotransfer of CD4(+) T cells from *H. hepaticus*-infected wild type mice (WT), but not uninfected WT mice prevented the colitis (Kullberg *et al.* 2002). Regulatory T cells (TR) express the activation marker CD25 and represent 5%-10% of the total normal human CD4+ T cell population, and prevent immune mediated diseases (Powrie and Maloy 2003). Aberrant effector or regulator T cell responses to gut microbiota antigens may be the reason for the colonic and cecal inflammation (Kullberg *et al.* 2003; Thompson and Powrie 2004).

Recently, *H. hepaticus* infection in 129/SvEvRAG$^{-/-}$ mice has been demonstrated to induce chronic typhlocolitis progressing to colonic carcinogenesis. (Erdman *et al.* 2003a; Erdman *et al.* 2003b). These experiments demonstrated that the unregulated innate immune response, in this mouse strain, was sufficient to induce cancer due to persistent *H. hepaticus* infection. Further, adoptive transfer with CD4+ CD45RB$^{lo}$ CD25+ regulatory T cells from uninfected 129/SvEv donors significantly inhibited *H. hepaticus*-induced inflammation and development of cancer. Past experiments had demonstrated accelerated colitis in RAG$^{-/-}$ can be induced by adoptive transfer of CD4+ CD45RB$^{hi}$ T cells (Malmstrom *et al.* 2001; Singh *et al.* 2001a) The experiments also indicated the timing of the adoptive transfer relative to the *H. hepaticus* incoculation was an important consideration, and that regulatory T-cell IL-10 was a necessary component for inhibition of chronic typhlocolitis and colonic carcinoma (Erdman *et al.* 2003b).

*Helicobacter hepaticus* genome

The complete genome sequence of *H. hepaticus,* the first enterohepatic *Helicobacter* spp. to be sequenced, revealed a larger genome and different virulence factors than *H. pylori* (Suerbaum *et al.* 2003). The genome contains 1,799,146 base pairs, 1875 predicted proteins predicted, and a GC content of 35.9%. *H. hepaticus* contains one large region and several smaller regions that differ from the rest of the genome in their GC content, suggesting horizontal transfer of genes. There are 499 proteins without similarity to any other known proteins. The *H. hepaticus* genome exhibits features of *H. pylori, C. jejuni,* and other enteric species (Eppinger *et al.* 2004).

Virulence factors

*H. hepaticus* putative pathogenicity island

Although *H. hepaticus* lacks orthologs of most known *H. pylori* virulence factors, it does possesse a putative pathogenicity island (HHGI1) of 71.0 kb (Figure 2). HHGI1 contains 70 ORFs and encompasses genes HH0233-HH0302. It encodes at least 3 components of a T4SS including HH0252, HH0224, and HH260 which are orthologs of icmF/virB1, virD4, and virB4, respectively. However, the percentage identities and similarities are low (Suerbaum *et al.* 2003). The proteins VirB1, VirD4, and VirB4 are all components of the T4SS in *A. tumefasciens*, the most intensively studied T4SS, which translocates T-DNA (Hoppner *et al.* 2004). Five out of six male mice naturally infected with HHGI1-carrying strains had liver disease (4 SCIDS, 1 A/J had lesions; 1 Swiss Webster did not). None of four mice (DBA/2 female 4 weeks, C57BL/6 female 4 weeks, Nude with Swiss Webster background female 1year, and unknown) naturally infected with HHGI1-negative strains had evidence of liver disease (Suerbaum *et al.* 2003). Further evidence of HHGI1 correlation with virulence is discussed in Chapter 4.

Genes *icmF/virB1*, with similarity to HH0252, resides on the *dot/icm* 22kb genomic island in *L pneumophila.* The genomic island contains 24 genes in *L. pneumophila*.

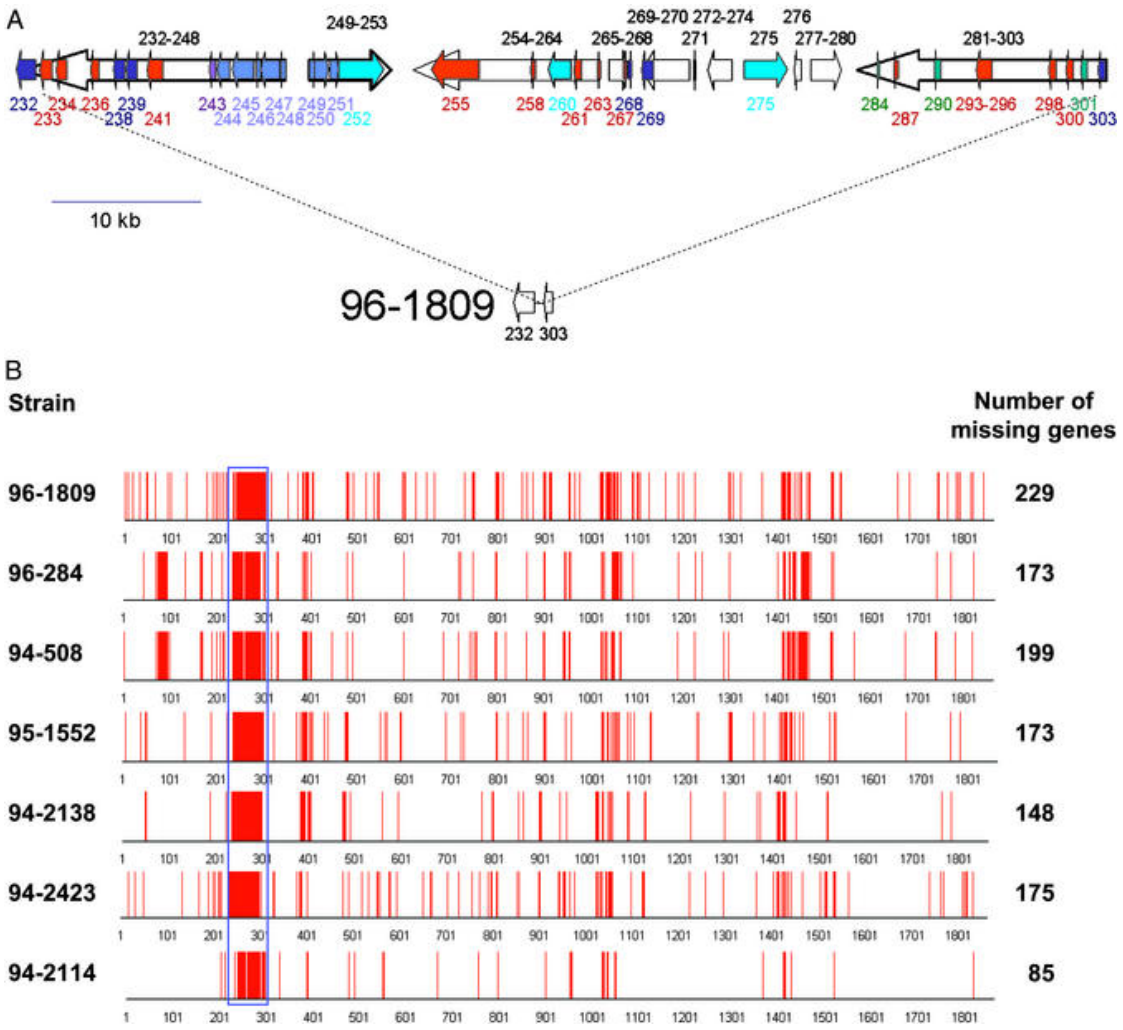


**Figure 2 (Suerbaum et al, 2003; with permission)** (*A*) The large genomic island of *H. hepaticus* (HHGI1). Red arrows represent genes encoding putative membrane-associated proteins, green arrows represent genes encoding proteins with a leader peptide, and blue arrows indicate genes coding for apparent homologs of other bacterial proteins (light blue, *V. cholerae* VCA0107–VCA0115; violet, *V. cholerae* Hcp; dark blue, proteins from other bacteria). Turquoise arrows indicate the three genes that encode proteins (HH0252, HH0259, and HH0275) with homology to VirB10, VirD4, and VirB4. Some smaller ORFs transcribed in the same orientation are not depicted individually but shown as open arrows representing a block of genes. The lower part of the figure shows the same genomic region in one strain, 96-1809, where the complete island is lacking and where only the flanking sequences, HH0232 and HH0303, are present. (*B*) Genomic variation in *H. hepaticus*. Twelve *H. hepaticus* strains were tested for hybridization with a whole-genome DNA microarray. Five strains (ATCC51448, ATCC51450, 95-225, 95-557, and 94-739) contained all genes detected by the array. The other seven strains did not hybridize with 85-229 probes, and the positions of these missing genes in the genome of the sequenced strain ATCC51449 are indicated by red lines. The location of the genomic island HHGI1 that is totally or partially deleted in all seven strains is indicated by the blue rectangle. The array experiments identified six more clusters of at least five genes that were not detected in at least one of the strains.

The *icm* gene (intracellular multiplication locus gene), also know as *dot* (defect of organelle trafficking), encodes a protein which enables survival and multiplication within a macrophage, ultimately killing the macrophage. The *dot/icm* locus possesses 4 operons: *icmTS*, *icmPO*, *icmMLKE*, and *icmJB*; and 6 individual genes: *icmR*, *icmQ*, *icmG*, *icmC*, *icmD*, and *icmF*. Genes *icmP icmO*, *icmL*, and *icmE* show sequence similarity to plasmid genes involved in conjugation and macrophage killing. In particular, *icmT* and *icmR* mutants showed a severe reduction in conjugation frequency and macrophage killing (Segal *et al.* 1999; Segal and Shuman 1999a, b). The *dot/icm* genes also correlate to growth and survival within certain protozoa and nonlytic release of the bacteria (Chen *et al.* 2004).

The *icmF* gene exhibits homology among numerous gram negative bacteria in addition to *H. hepaticus*. However, many of these gram negative bacteria do not possess a T4SS (Sexton *et al.* 2004a; Sexton *et al.* 2004b). The gene is unique in that other constituents of the *dot/icm* locus do not possess this widespread homology. Insertional mutants of *icmF* in *L. pneumophila* possess partially defective macrophage killing and were incapable of intracellular growth within *Acanthameoba castellanii* (Segal and Shuman 1999b). Double mutants of *dotU* and *icmF* exhibit decreased plasmid transfer capability (Sexton *et al.* 2004a).

Chapter 4 and Chapter 5 provides experimental evidence that *H.hepaticus* strains with a partial deletion of the genomic island HHGI1, including HH0252 with IcmF homology, are less virulent in A/JCr mice (Chapter 4) and produce a reduced cytokine response in RAW264.7 murine macrophages (Chapter 5).

*H. hepaticus* cytolethal distending toxin

Another virulence factor in enterohepatic *Helicobacter* spp. is cytolethal distending toxin (CDT). CDT in *H. hepaticus* induces cell cycle arrest in the $G_2$/M phase and progressive cell distension and eventual cytotoxicity *in vitro* (Chien *et al.* 2000; Taylor *et al.* 1995; Taylor *et al.* 2003; Young *et al.* 2004; Young *et al.* 2000). CDT was first discovered in *E. coli* and *Camplybacter* spp. (Anderson *et al.* 1987; Johnson and Lior 1988a, b). *Haemophilus ducreyi* which produces the ulcerative lesions of chancroid also produces CDT (Cope *et al.* 1997). The oral pathogen *Actinobacillus actinomycetemcomitans* produces CDT from a polymorphic region of its chromosome (Mayer *et al.* 1999). *Salmonella typhi* exhibits virulence when internalized and secretes only a protein subunit of CDT, CdtB. This negates the need for the CdtA and CdtC subunits, putatively related to transport of CdtB into the cell (Haghjoo and Galan 2004).

$IL10^{-/-}$ mice, on a C57BL/6 background, experimentally infected with an isogenic CDT mutant of *H. hepaticus* develop less severe disease than $IL10^{-/-}$ mice infected with wild type *H. hepaticus* (Young *et al.* 2004). The authors also demonstrated that CDT in *H. hepaticus* appears to be the granulating cytotoxin previously reported by Taylor et al (Taylor *et al.* 1995; Young *et al.* 2004). NF-kappa B-deficient mice infected with *C. jejuni* lacking CDT did not exhibit gastroenteritis whereas NF-kappaB-deficient mice infected with wild-type *C. jejuni* did develop severe gastroenteritis (Fox *et al.* 2004a). Previous studies of isogenic CDT mutants in *H. ducreyi* (Lewis *et al.* 2001; Stevens *et al.*

1999; Young *et al.* 2001) and *C. jejuni* (Purdy *et al.* 2000) did not yield conclusive evidence of a pathogenic role for CDT.

*H. hepaticus* urease

Urease contributes to pathogenesis in *H. pylori* and is a very stable and highly conserved gene in *H. hepaticus* (Fox *et al.* 1994; Mobley *et al.* 1991). *H. hepaticus* urease isogenic mutants, constructed by allelic exchange, failed to colonize Swiss Webster and C57BL/6 infected mice. Since the isogenic urease mutant may not survive transit through the low pH in the stomach, experimental infection via the intragastric and intraperitoneal routes was performed and *H. hepaticus* colonization monitored. These results suggest urease is an essential colonization factor for *H. hepaticus* (Chin et al, in press).

Hepatocellular carcinoma in humans

The major cause of hepatocellular carcinoma (HCC) in people is Hepatitis B virus (HBV) followed by the Hepatitis C virus (HCV). The number of HCC cases worldwide caused by these two viruses is approximately 4% of all cancer cases. A minority of HCC cases are associated with non-viral causes (Block *et al.* 2003; O'Brien *et al.* 2004; Omata and Yoshida 2004). Human HCC presumably progresses from pre-neoplastic lesions, often in conjunction with cirrhosis. While genetic alterations to the *p53*, *Rb*, and *Wnt* pathways do occur in HCC, the molecular pathogenesis of HBV-related HCC and HCV-related HCC differ (Suriawinata and Xu 2004). HBV and HCV induce increased hepatocyte

turnover due to the immune system's attack on infected hepatocytes, a commonality in the pathogenesis of viral-related HCC.

Enteritis, hepatitis, and cholecystitis in humans, and even more severe disease in immunocompromised individuals, have recently been associated with enterohepatic *Helicobacter* sp. infection (Blaser and Atherton 2004; Chen *et al.* 2003; Fox 2002; Fox *et al.* 1998; Matsukura *et al.* 2002; Murakami *et al.* 2003; Murata *et al.* 2004; Nilsson *et al.* 2003; Solnick and Schauer 2001; Sykora *et al.* 2004). There is also definitive evidence of enteritis, hepatitis, and cholecystitis caused by enterohepatic *Helicobacter* sp. in animals (Rogers and Fox 2004; Solnick and Schauer 2001; Whary and Fox 2004a). However, non-viral related HCC, and HCC without the background of cirrhosis, receives little attention in the literature due to the low percentage of cases. *Helicobacter* spp. association with HCC has been reported (Verhoef *et al.* 2003). There is considerable debate regarding *Helicobacter* spp. involvement in HCC (Coppola *et al.* 2003). *Helicobacter* sp. infection in pediatric liver disease has received recent attention (Tolia *et al.* 2004), as has *Helicobacter* spp.autoimmune hepatic disease (Nilsson *et al.* 2003).

Hepatocellular carcinoma in mice

*H. hepaticus* infection of A/JCr mice induces HCC and is a mouse models of infectious liver cancer (Fox *et al.* 1996c). Cumulative evidence suggests *H. hepaticus* is non-genotoxic and possesses characteristics of a tumor promoter(Canella *et al.* 1996; Diwan *et al.* 1997). One factor supporting its role in tumor promotion is mouse strain

susceptibility to *H. hepaticus* induced disease. Tumor promoting agents have historically exhibited strain susceptibility differences. Other evidence includes a persistent inflammatory state with increased exposure time to reactive oxygen species (ROS) and reactive nitrogen species (RNS) (Whary *et al.* 1998). Increased hepatocyte proliferation, the lack of *p53* and *ras* mutations, a negative Ames assay, and the promotion of HCC by *H. hepaticus* after tumor initiation by hepatocarcinogenic chemicals are other examples (Canella *et al.* 1996; Diwan *et al.* 1997; Sipowicz *et al.* 1997).

However, evidence demonstrating genotoxic activity of *H. hepaticus* has also been reported. DNA adduct formation by *H. hepaticus* infection suggests a role of a tumor inititator (Josyula *et al.* 2000; Singh *et al.* 2001b; Sipowicz *et al.* 1997). Both ROS and RNS species increase the risk of DNA mutation and adducts, particularly 8-oxo-2"-deoxyguanosine (8-oxodG). *In vitro* evidence suggests this adduct may be prone to peroxynitrite attack. Peroxynitrite, a product of nitric oxide and superoxide from macrophages, may form other DNA adducts instead (Dedon and Tannenbaum 2004).Methylation of CpG islands has been associated with HCC (Yu *et al.* 2003). Whether *H. hepaticus* has any epigenetic effects is an area of future investigation.

The cumulative evidence to date suggests *H. hepaticus* may be a complete carcinogen, since it possesses characteristics of tumor initiation, promotion, and progression. Further studies on the biochemical pathways affected by *H. hepaticus* are necessary, and comparison to pathways affected by chemical carcinogens or well established tumor promoters (e.g. phenobarbital) appear to be a fruitful areas of investigation. Rodent

chemical carcinogenesis studies focus on gene expression and biochemical pathways afftected by the chemicals (van Delft *et al.* 2004). Phenobarbital is non-genotoxic and has been the prototypical tumor promoter for decades. It activates the constitutive active/androstane receptor (CAR) and promotes HCC in rodents after diethylnitrosamine (DEN) initiation. CAR deficient mice do not get HCC after DEN initiation and phenobarbital promotion. Recent evidence suggests commonality in biochemical pathways of phenobarbital promotion and *H. hepaticus* infection (Yamamoto *et al.* 2004).

The biochemical pathways and genes associated with preneoplastic lesions exhibited during promotion are important in understanding tumor promotion and progression, and potential therapeutic intervention. Microarray analysis of preneoplastic lesions in the liver due to *H. hepaticus* infection are the subject of Chapter 3. An overview of microarray analysis is the subject of Chapter 2.

**References**


Achtman, M., and Suerbaum, S. (2000). Sequence variation in *Helicobacter pylori*. *Trends Microbiol* **8**, 57-8.

Alm, R. A., Ling, L. S., Moir, D. T., King, B. L., Brown, E. D., Doig, P. C., Smith, D. R., Noonan, B., Guild, B. C., deJonge, B. L., Carmel, G., Tummino, P. J., Caruso, A., Uria-Nickelsen, M., Mills, D. M., Ives, C., Gibson, R., Merberg, D., Mills, S. D., Jiang, Q., Taylor, D. E., Vovis, G. F., and Trust, T. J. (1999). Genomic-sequence comparison of two unrelated isolates of the human gastric pathogen *Helicobacter pylori*. *Nature* **397**, 176-80.

Alm, R. A., and Trust, T. J. (1999). Analysis of the genetic diversity of *Helicobacter pylori*: the tale of two genomes. *J Mol Med* **77**, 834-46.

Anderson, J. D., MacNab, A. J., Gransden, W. R., Damm, S. M., Johnson, W. M., and Lior, H. (1987). Gastroenteritis and encephalopathy associated with a strain of *Escherichia coli* 055:K59:H4 that produced a cytolethal distending toxin. *Pediatr Infect Dis J* **6**, 1135-6.

Aromaa, A., Kosunen, T. U., Knekt, P., Maatela, J., Teppo, L., Heinonen, O. P., Harkonen, M., and Hakama, M. K. (1996). Circulating anti-*Helicobacter pylori* immunoglobulin A antibodies and low serum pepsinogen I level are associated with increased risk of gastric cancer. *Am J Epidemiol* **144**, 142-9.

Aspholm-Hurtig, M., Dailide, G., Lahmann, M., Kalia, A., Ilver, D., Roche, N., Vikstrom, S., Sjostrom, R., Linden, S., Backstrom, A., Lundberg, C., Arnqvist, A., Mahdavi, J., Nilsson, U. J., Velapatino, B., Gilman, R. H., Gerhard, M., Alarcon, T., Lopez-Brea, M., Nakazawa, T., Fox, J. G., Correa, P., Dominguez-Bello, M. G., Perez-Perez, G. I., Blaser, M. J., Normark, S., Carlstedt, I., Oscarson, S., Teneberg, S., Berg, D. E., and Boren, T. (2004). Functional adaptation of BabA, the *H. pylori* ABO blood group antigen binding adhesin. *Science* **305**, 519-22.

Aviles-Jimenez, F., Letley, D. P., Gonzalez-Valencia, G., Salama, N., Torres, J., and Atherton, J. C. (2004). Evolution of the *Helicobacter pylori* vacuolating cytotoxin in a human stomach. *J Bacteriol* **186**, 5182-5.

Azuma, T. (2004). *Helicobacter pylori* CagA protein variation associated with gastric cancer in Asia. *J Gastroenterol* **39**, 97-103.

Azuma, T., Ohtani, M., Yamazaki, Y., Higashi, H., and Hatakeyama, M. (2004). Meta-analysis of the relationship between CagA seropositivity and gastric cancer. *Gastroenterology* **126**, 1926-7; author reply 1927-8.

Balkwill, F., and Coussens, L. M. (2004). Cancer: an inflammatory link. *Nature* **431**, 405-6.

Balkwill, F., and Mantovani, A. (2001). Inflammation and cancer: back to Virchow? *Lancet* **357**, 539-45.

Batchelor, R. A., Pearson, B. M., Friis, L. M., Guerry, P., and Wells, J. M. (2004). Nucleotide sequences and comparison of two large conjugative plasmids from different *Campylobacter* species. *Microbiology* **150**, 3507-17.

Benoit, S., and Maier, R. J. (2003). Dependence of *Helicobacter pylori* urease activity on the nickel-sequestering ability of the UreE accessory protein. *J Bacteriol* **185**, 4787-95.

Bergin, I. L., Sheppard, B. J., and Fox, J. G. (2003). *Helicobacter pylori* infection and high dietary salt independently induce atrophic gastritis and intestinal metaplasia in commercially available outbred Mongolian gerbils. *Dig Dis Sci* **48**, 475-85.

Bertram, T. A., Krakowka, S., and Morgan, D. R. (1991). Gastritis associated with infection by *Helicobacter pylori*: comparative pathology in humans and swine. *Rev Infect Dis* **13 Suppl 8**, S714-22.

Bitar, D. M., Molmeret, M., and Abu Kwaik, Y. (2004). Molecular and cell biology of Legionella pneumophila. *Int J Med Microbiol* **293**, 519-27.

Blaser, M. J., and Atherton, J. C. (2004). *Helicobacter pylori* persistence: biology and disease. *J Clin Invest* **113**, 321-33.

Blaser, M. J., Chyou, P. H., and Nomura, A. (1995a). Age at establishment of *Helicobacter pylori* infection and gastric carcinoma, gastric ulcer, and duodenal ulcer risk. *Cancer Res* **55**, 562-5.

Blaser, M. J., Perez-Perez, G. I., Kleanthous, H., Cover, T. L., Peek, R. M., Chyou, P. H., Stemmermann, G. N., and Nomura, A. (1995b). Infection with *Helicobacter pylori* strains possessing cagA is associated with an increased risk of developing adenocarcinoma of the stomach. *Cancer Res* **55**, 2111-5.

Block, T. M., Mehta, A. S., Fimmel, C. J., and Jordan, R. (2003). Molecular viral oncology of hepatocellular carcinoma. *Oncogene* **22**, 5093-107.

Blomstergren, A., Lundin, A., Nilsson, C., Engstrand, L., and Lundeberg, J. (2004). Comparative analysis of the complete cag pathogenicity island sequence in four *Helicobacter pylori* isolates. *Gene* **328**, 85-93.

Blum, G., Falbo, V., Caprioli, A., and Hacker, J. (1995). Gene clusters encoding the cytotoxic necrotizing factor type 1, Prs-fimbriae and alpha-hemolysin form the pathogenicity island II of the uropathogenic *Escherichia coli* strain J96. *FEMS Microbiol Lett* **126**, 189-95.

Boschiroli, M. L., Ouahrani-Bettache, S., Foulongne, V., Michaux-Charachon, S., Bourg, G., Allardet-Servent, A., Cazevieille, C., Lavigne, J. P., Liautard, J. P., Ramuz, M., and O'Callaghan, D. (2002). Type IV secretion and *Brucella* virulence. *Vet Microbiol* **90**, 341-8.

Boutin, S., Rogers, A., Shen, Z., Fry, R., Love, J., Nambiar, P., Suerbaum, S., and Fox, J. (2004). Hepatic Temporal Gene Expression Profiling in *Helicobacter hepaticus*-Infected A/JCr Mice. *Toxicol Pathol* **32**, 678-93.

Burman, W. J., Cohn, D. L., Reves, R. R., and Wilson, M. L. (1995). Multifocal cellulitis and monoarticular arthritis as manifestations of *Helicobacter cinaedi* bacteremia. *Clin Infect Dis* **20**, 564-70.

Burnens, A. P., Stanley, J., Morgenstern, R., and Nicolet, J. (1994). Gastroenteritis associated with *Helicobacter pullorum*. *Lancet* **344**, 1569-70.

Canella, K. A., Diwan, B. A., Gorelick, P. L., Donovan, P. J., Sipowicz, M. A., Kasprzak, K. S., Weghorst, C. M., Snyderwine, E. G., Davis, C. D., Keefer, L. K., Kyrtopoulos, S. A., Hecht, S. S., Wang, M., Anderson, L. M., and Rice, J. M. (1996). Liver tumorigenesis by *Helicobacter hepaticus*: considerations of mechanism. *In Vivo* **10**, 285-92.

Carniel, E. (2001). The *Yersinia* high-pathogenicity island: an iron-uptake island. *Microbes Infect* **3**, 561-9.

Celli, J., and Gorvel, J. P. (2004). Organelle robbery: *Brucella* interactions with the endoplasmic reticulum. *Curr Opin Microbiol* **7**, 93-7.

Chen, J., de Felipe, K. S., Clarke, M., Lu, H., Anderson, O. R., Segal, G., and Shuman, H. A. (2004). *Legionella* effectors that promote nonlytic release from protozoa. *Science* **303**, 1358-61.

Chen, M., Lee, A., and Hazell, S. (1992). Immunisation against gastric *Helicobacter* infection in a mouse/*Helicobacter felis* model. *Lancet* **339**, 1120-1.

Chen, X., Hoda, S. A., and Petrovic, L. (2003). Images in pathology: *Helicobacter heilmannii* gastritis. *Int J Surg Pathol* **11**, 315.

Cheung, A. M., Farizo, K. M., and Burns, D. L. (2004). Analysis of relative levels of production of pertussis toxin subunits and Ptl proteins in *Bordetella pertussis*. *Infect Immun* **72**, 2057-66.

Chien, C. C., Taylor, N. S., Ge, Z., Schauer, D. B., Young, V. B., and Fox, J. G. (2000). Identification of cdtB homologues and cytolethal distending toxin activity in enterohepatic *Helicobacter* spp. *J Med Microbiol* **49**, 525-34.

Chin, E. Y., Dangler, C. A., Fox, J. G., and Schauer, D. B. (2000). *Helicobacter hepaticus* infection triggers inflammatory bowel disease in T cell receptor alphabeta mutant mice. *Comp Med* **50**, 586-94.

Chowers, M. Y., Keller, N., Bar-Meir, S., and Chowers, Y. (2002). A defined human gastrin sequence stimulates the growth of *Helicobacter pylori*. *FEMS Microbiol Lett* **217**, 231-6.

Christie, P. J. (2001). Type IV secretion: intercellular transfer of macromolecules by systems ancestrally related to conjugation machines. *Mol Microbiol* **40**, 294-305.

Clevers, H. (2004). At the crossroads of inflammation and cancer. *Cell* **118**, 671-4.

Cope, L. D., Lumbley, S., Latimer, J. L., Klesney-Tait, J., Stevens, M. K., Johnson, L. S., Purven, M., Munson, R. S., Jr., Lagergard, T., Radolf, J. D., and Hansen, E. J. (1997). A diffusible cytotoxin of *Haemophilus ducreyi*. *Proc Natl Acad Sci U S A* **94**, 4056-61.

Coppola, N., De Stefano, G., Marrocco, C., Scarano, F., Scolastico, C., Tarantino, L., Rossi, G., Battaglia, M., Onofrio, M., D'Aniello, F., Pisapia, R., Sagnelli, C., Sagnelli, E., Piccinino, F., Giorgio, A., and Filippini, P. (2003). *Helicobacter* spp. and liver diseases. *Infez Med* **11**, 201-7.

Court, M., Robinson, P. A., Dixon, M. F., and Crabtree, J. E. (2002). Gastric *Helicobacter* species infection in murine and gerbil models: comparative analysis of effects of *H. pylori* and *H. felis* on gastric epithelial cell proliferation. *J Infect Dis* **186**, 1348-52.

Coussens, L. M., and Werb, Z. (2002). Inflammation and cancer. *Nature* **420**, 860-7.

Covacci, A., Telford, J. L., Del Giudice, G., Parsonnet, J., and Rappuoli, R. (1999). *Helicobacter pylori* virulence and genetic geography. *Science* **284**, 1328-33.

Cover, T. L., and Blaser, M. J. (1992). Purification and characterization of the vacuolating toxin from *Helicobacter pylori*. *J Biol Chem* **267**, 10570-5.

Cover, T. L., Cao, P., Murthy, U. K., Sipple, M. S., and Blaser, M. J. (1992a). Serum neutralizing antibody response to the vacuolating cytotoxin of *Helicobacter pylori*. *J Clin Invest* **90**, 913-8.

Cover, T. L., Vaughn, S. G., Cao, P., and Blaser, M. J. (1992b). Potentiation of *Helicobacter pylori* vacuolating toxin activity by nicotine and other weak bases. *J Infect Dis* **166**, 1073-8.

de Jonge, R., Durrani, Z., Rijpkema, S. G., Kuipers, E. J., van Vliet, A. H., and Kusters, J. G. (2004a). Role of the *Helicobacter pylori* outer-membrane proteins AlpA and AlpB in colonization of the guinea pig stomach. *J Med Microbiol* **53**, 375-9.

de Jonge, R., Pot, R. G., Loffeld, R. J., van Vliet, A. H., Kuipers, E. J., and Kusters, J. G. (2004b). The functional status of the *Helicobacter pylori* sabB adhesin gene as a putative marker for disease outcome. *Helicobacter* **9**, 158-64.

Dedon, P. C., and Tannenbaum, S. R. (2004). Reactive nitrogen species in the chemical biology of inflammation. *Arch Biochem Biophys* **423**, 12-22.

Delrue, R. M., Lestrate, P., Tibor, A., Letesson, J. J., and De Bolle, X. (2004). Brucella pathogenesis, genes identified from random large-scale screens. *FEMS Microbiol Lett* **231**, 1-12.

den Hartigh, A. B., Sun, Y. H., Sondervan, D., Heuvelmans, N., Reinders, M. O., Ficht, T. A., and Tsolis, R. M. (2004). Differential requirements for VirB1 and VirB2 during *Brucella abortus* infection. *Infect Immun* **72**, 5143-9.

Dewhirst, F. E., Fox, J. G., Mendes, E. N., Paster, B. J., Gates, C. E., Kirkbride, C. A., and Eaton, K. A. (2000). *'Flexispira rappini'* strains represent at least 10 *Helicobacter* taxa. *Int J Syst Evol Microbiol* **50 Pt 5**, 1781-7.

Dick, E., Lee, A., Watson, G., and O'Rourke, J. (1989). Use of the mouse for the isolation and investigation of stomach-associated, spiral-helical shaped bacteria from man and other animals. *J Med Microbiol* **29**, 55-62.

Diwan, B. A., Ward, J. M., Ramljak, D., and Anderson, L. M. (1997). Promotion by *Helicobacter hepaticus*-induced hepatitis of hepatic tumors initiated by N-nitrosodimethylamine in male A/JCr mice. *Toxicol Pathol* **25**, 597-605.

Eaton, K. A., Brooks, C. L., Morgan, D. R., and Krakowka, S. (1991). Essential role of urease in pathogenesis of gastritis induced by *Helicobacter pylori* in gnotobiotic piglets. *Infect Immun* **59**, 2470-5.

Eaton, K. A., Suerbaum, S., Josenhans, C., and Krakowka, S. (1996). Colonization of gnotobiotic piglets by *Helicobacter pylori* deficient in two flagellin genes. *Infect Immun* **64**, 2445-8.

El-Omar, E. M., Carrington, M., Chow, W. H., McColl, K. E., Bream, J. H., Young, H. A., Herrera, J., Lissowska, J., Yuan, C. C., Rothman, N., Lanyon, G., Martin, M., Fraumeni, J. F., Jr., and Rabkin, C. S. (2000). Interleukin-1 polymorphisms associated with increased risk of gastric cancer. *Nature* **404**, 398-402.

Enno, A., O'Rourke, J. L., Howlett, C. R., Jack, A., Dixon, M. F., and Lee, A. (1995). MALToma-like lesions in the murine gastric mucosa after long-term infection with *Helicobacter felis*. A mouse model of *Helicobacter pylori*-induced gastric lymphoma. *Am J Pathol* **147**, 217-22.

Eppinger, M., Baar, C., Raddatz, G., Huson, D. H., and Schuster, S. C. (2004). Comparative analysis of four *Campylobacterales. Nat Rev Microbiol* **2**, 872-85.

Erdman, S. E., Poutahidis, T., Tomczak, M., Rogers, A. B., Cormier, K., Plank, B., Horwitz, B. H., and Fox, J. G. (2003a). CD4+ CD25+ regulatory T lymphocytes inhibit microbially induced colon cancer in Rag2-deficient mice. *Am J Pathol* **162**, 691-702.

Erdman, S. E., Rao, V. P., Poutahidis, T., Ihrig, M. M., Ge, Z., Feng, Y., Tomczak, M., Rogers, A. B., Horwitz, B. H., and Fox, J. G. (2003b). CD4(+)CD25(+) regulatory lymphocytes require interleukin 10 to interrupt colon carcinogenesis in mice. *Cancer Res* **63**, 6042-50.

Falush, D., Kraft, C., Taylor, N. S., Correa, P., Fox, J. G., Achtman, M., and Suerbaum, S. (2001). Recombination and mutation during long-term gastric colonization by *Helicobacter pylori*: estimates of clock rates, recombination size, and minimal age. *Proc Natl Acad Sci U S A* **98**, 15056-61.

Falush, D., Wirth, T., Linz, B., Pritchard, J. K., Stephens, M., Kidd, M., Blaser, M. J., Graham, D. Y., Vacher, S., Perez-Perez, G. I., Yamaoka, Y., Megraud, F., Otto, K., Reichard, U., Katzowitsch, E., Wang, X., Achtman, M., and Suerbaum, S. (2003). Traces of human migrations in *Helicobacter pylori* populations. *Science* **299**, 1582-5.

Fischer, W., Gebert, B., and Haas, R. (2004). Novel activities of the *Helicobacter pylori* vacuolating cytotoxin: from epithelial cells towards the immune system. *Int J Med Microbiol* **293**, 539-47.

Flores, B. M., Fennell, C. L., Kuller, L., Bronsdon, M. A., Morton, W. R., and Stamm, W. E. (1990). Experimental infection of pig-tailed macaques (Macaca nemestrina) with *Campylobacter cinaedi* and *Campylobacter fennelliae*. *Infect Immun* **58**, 3947-53.

Foley, J. E., Marks, S. L., Munson, L., Melli, A., Dewhirst, F. E., Yu, S., Shen, Z., and Fox, J. G. (1999). Isolation of *Helicobacter canis* from a colony of bengal cats with endemic diarrhea. *J Clin Microbiol* **37**, 3271-5.

Foltz, C. J., Fox, J. G., Cahill, R., Murphy, J. C., Yan, L., Shames, B., and Schauer, D. B. (1998). Spontaneous inflammatory bowel disease in multiple mutant mouse lines: association with colonization by *Helicobacter hepaticus*. *Helicobacter* **3**, 69-78.

Forman, D., Newell, D. G., Fullerton, F., Yarnell, J. W., Stacey, A. R., Wald, N., and Sitas, F. (1991). Association between infection with *Helicobacter pylori* and risk of gastric cancer: evidence from a prospective investigation. *Bmj* **302**, 1302-5.

Fox, J. G. (1995). Non-human reservoirs of *Helicobacter pylori*. *Aliment Pharmacol Ther* **9 Suppl 2**, 93-103.

Fox, J. G. (1998). Review article: *Helicobacter* species and in vivo models of gastrointestinal cancer. *Aliment Pharmacol Ther* **12 Suppl 1**, 37-60.

Fox, J. G. (2002). Other *Helicobacter*s involved in human diseases. *Acta Gastroenterol Belg* **65**, 24-32.

Fox, J. G., Batchelder, M., Marini, R., Yan, L., Handt, L., Li, X., Shames, B., Hayward, A., Campbell, J., and Murphy, J. C. (1995a). *Helicobacter pylori*-induced gastritis in the domestic cat. *Infect Immun* **63**, 2674-81.

Fox, J. G., Beck, P., Dangler, C. A., Whary, M. T., Wang, T. C., Shi, H. N., and Nagler-Anderson, C. (2000a). Concurrent enteric helminth infection modulates inflammation and gastric immune responses and reduces *Helicobacter*-induced gastric atrophy. *Nat Med* **6**, 536-42.

Fox, J. G., Cabot, E. B., Taylor, N. S., and Laraway, R. (1988). Gastric colonization by *Campylobacter pylori* subsp. mustelae in ferrets. *Infect Immun* **56**, 2994-6.

Fox, J. G., Chien, C. C., Dewhirst, F. E., Paster, B. J., Shen, Z., Melito, P. L., Woodward, D. L., and Rodgers, F. G. (2000b). *Helicobacter canadensis* sp. nov. isolated from humans with diarrhea as an example of an emerging pathogen. *J Clin Microbiol* **38**, 2546-9.

Fox, J. G., Correa, P., Taylor, N. S., Lee, A., Otto, G., Murphy, J. C., and Rose, R. (1990). *Helicobacter mustelae*-associated gastritis in ferrets. An animal model of *Helicobacter pylori* gastritis in humans. *Gastroenterology* **99**, 352-61.

Fox, J. G., Dewhirst, F. E., Shen, Z., Feng, Y., Taylor, N. S., Paster, B. J., Ericson, R. L., Lau, C. N., Correa, P., Araya, J. C., and Roa, I. (1998). Hepatic *Helicobacter* species identified in bile and gallbladder tissue from Chileans with chronic cholecystitis. *Gastroenterology* **114**, 755-63.

Fox, J. G., Dewhirst, F. E., Tully, J. G., Paster, B. J., Yan, L., Taylor, N. S., Collins, M. J., Jr., Gorelick, P. L., and Ward, J. M. (1994). *Helicobacter hepaticus* sp. nov., a microaerophilic bacterium isolated from livers and intestinal mucosal scrapings from mice. *J Clin Microbiol* **32**, 1238-45.

Fox, J. G., Drolet, R., Higgins, R., Messier, S., Yan, L., Coleman, B. E., Paster, B. J., and Dewhirst, F. E. (1996a). *Helicobacter canis* isolated from a dog liver with multifocal necrotizing hepatitis. *J Clin Microbiol* **34**, 2479-82.

Fox, J. G., Gorelick, P. L., Kullberg, M. C., Ge, Z., Dewhirst, F. E., and Ward, J. M. (1999). A novel urease-negative *Helicobacter* species associated with colitis and typhlitis in IL-10-deficient mice. *Infect Immun* **67**, 1757-62.

Fox, J. G., Handt, L., Sheppard, B. J., Xu, S., Dewhirst, F. E., Motzel, S., and Klein, H. (2001a). Isolation of *Helicobacter cinaedi* from the colon, liver, and mesenteric lymph node of a rhesus monkey with chronic colitis and hepatitis. *J Clin Microbiol* **39**, 1580-5.

Fox, J. G., Handt, L., Xu, S., Shen, Z., Dewhirst, F. E., Paster, B. J., Dangler, C. A., Lodge, K., Motzel, S., and Klein, H. (2001b). Novel *Helicobacter* species isolated from rhesus monkeys with chronic idiopathic colitis. *J Med Microbiol* **50**, 421-9.

Fox, J. G., and Lee, A. (1989). Gastric *Campylobacter*-like organisms: their role in gastric disease of laboratory animals. *Lab Anim Sci* **39**, 543-53.

Fox, J. G., and Lee, A. (1997). The role of *Helicobacter* species in newly recognized gastrointestinal tract diseases of animals. *Lab Anim Sci* **47**, 222-55.

Fox, J. G., Lee, A., Otto, G., Taylor, N. S., and Murphy, J. C. (1991). *Helicobacter felis* gastritis in gnotobiotic rats: an animal model of *Helicobacter pylori* gastritis. *Infect Immun* **59**, 785-91.

Fox, J. G., Li, X., Yan, L., Cahill, R. J., Hurley, R., Lewis, R., and Murphy, J. C. (1996b). Chronic proliferative hepatitis in A/JCr mice associated with persistent *Helicobacter hepaticus* infection: a model of *Helicobacter*- induced carcinogenesis. *Infect Immun* **64**, 1548-58.

Fox, J. G., Li, X., Yan, L., Cahill, R. J., Hurley, R., Lewis, R., and Murphy, J. C. (1996c). Chronic proliferative hepatitis in A/JCr mice associated with persistent *Helicobacter hepaticus* infection: a model of *Helicobacter*-induced carcinogenesis. *Infect Immun* **64**, 1548-58.

Fox, J. G., Rogers, A. B., Ihrig, M., Taylor, N. S., Whary, M. T., Dockray, G., Varro, A., and Wang, T. C. (2003a). *Helicobacter pylori*-associated gastric cancer in INS-GAS mice is gender specific. *Cancer Res* **63**, 942-50.

Fox, J. G., Rogers, A. B., Whary, M. T., Ge, Z., Taylor, N. S., Xu, S., Horwitz, B. H., and Erdman, S. E. (2004a). Gastroenteritis in NF-kappaB-deficient mice is produced with wild-type *Camplyobacter jejuni* but not with *C. jejuni* lacking cytolethal distending toxin despite persistent colonization with both strains. *Infect Immun* **72**, 1116-25.

Fox, J. G., Rogers, A. B., Whary, M. T., Taylor, N. S., Xu, S., Feng, Y., and Keys, S. (2004b). *Helicobacter bilis*-associated hepatitis in outbred mice. *Comp Med* **54**, 571-7.

Fox, J. G., Shen, Z., Xu, S., Feng, Y., Dangler, C. A., Dewhirst, F. E., Paster, B. J., and Cullen, J. M. (2002). *Helicobacter marmotae* sp. nov. isolated from livers of woodchucks and intestines of cats. *J Clin Microbiol* **40**, 2513-9.

Fox, J. G., Wang, T. C., Rogers, A. B., Poutahidis, T., Ge, Z., Taylor, N., Dangler, C. A., Israel, D. A., Krishna, U., Gaus, K., and Peek, R. M., Jr. (2003b). Host and microbial

constituents influence *Helicobacter pylori*-induced cancer in a murine model of hypergastrinemia. *Gastroenterology* **124**, 1879-90.

Fox, J. G., Yan, L., Shames, B., Campbell, J., Murphy, J. C., and Li, X. (1996d). Persistent hepatitis and enterocolitis in germfree mice infected with *Helicobacter hepaticus*. *Infect Immun* **64**, 3673-81.

Fox, J. G., Yan, L. L., Dewhirst, F. E., Paster, B. J., Shames, B., Murphy, J. C., Hayward, A., Belcher, J. C., and Mendes, E. N. (1995b). *Helicobacter bilis* sp. nov., a novel *Helicobacter* species isolated from bile, livers, and intestines of aged, inbred mice. *J Clin Microbiol* **33**, 445-54.

Franklin, C. L., Gorelick, P. L., Riley, L. K., Dewhirst, F. E., Livingston, R. S., Ward, J. M., Beckwith, C. S., and Fox, J. G. (2001). *Helicobacter typhlonius* sp. nov., a Novel Murine Urease-Negative *Helicobacter* Species. *J Clin Microbiol* **39**, 3920-6.

Fujioka, T., Kubota, T., Shuto, R., Kodama, R., Murakami, K., Perparim, K., and Nasu, M. (1994). Establishment of an animal model for chronic gastritis with *Helicobacter pylori*: potential model for long-term observations. *Eur J Gastroenterol Hepatol* **6 Suppl 1**, S73-8.

Garcia, A., Ihrig, M. M., Whary, M. T., Feng, Y., Xu, S., Roger, A. B., and Fox, J. G. (2004). A Mouse Model of Hepatocellular Carcinoma: Dominant Responsiveness in *Helicobacter-hepaticus*-Induced Liver Cancer in F1 Hybrid Male Mice. In Digestive Disease Week (Gastroenterology, ed., Vol. 126, pp. A-40. American Gastroenterological Association, New Orleans, LA.

Ge, Z., Doig, P., and Fox, J. G. (2001). Characterization of proteins in the outer membrane preparation of a murine pathogen, *Helicobacter bilis*. *Infect Immun* **69**, 3502-6.

Gebert, B., Fischer, W., and Haas, R. (2004). The *Helicobacter pylori* vacuolating cytotoxin: from cellular vacuolation to immunosuppressive activities. *Rev Physiol Biochem Pharmacol*.

Gebhart, C. J., Fennell, C. L., Murtaugh, M. P., and Stamm, W. E. (1989). *Campylobacter* cinaedi is normal intestinal flora in hamsters. *J Clin Microbiol* **27**, 1692-4.

Giordano, T. P., Kramer, J. R., Souchek, J., Richardson, P., and El-Serag, H. B. (2004). Cirrhosis and hepatocellular carcinoma in HIV-infected veterans with and without the hepatitis C virus: a cohort study, 1992-2001. *Arch Intern Med* **164**, 2349-54.

Goodwin, C. S., Armstrong, J. A., Chilvers, T., Peters, M., Collins, M. D., Sly, L. I., McConnell, W., and Harper, W. E. S. (1989). Transfer of *Campylorbacter pylori* and

*Campylobacter mustelae* to *Helicobacter* gen. nov. as *Helicobacter pylori* comb. nov. and *Helicobacter mustelae* comb. now., respectively. *Int. J. Syst. Bacteriol.* **39**, 397-405.

Gyulai, Z., Klausz, G., Tiszai, A., Lenart, Z., Kasa, I. T., Lonovics, J., and Mandi, Y. (2004). Genetic polymorphism of interleukin-8 (IL-8) is associated with *Helicobacter pylori*-induced duodenal ulcer. *Eur Cytokine Netw* **15**, 353-8.

Hacker, J., Bender, L., Ott, M., Wingender, J., Lund, B., Marre, R., and Goebel, W. (1990). Deletions of chromosomal regions coding for fimbriae and hemolysins occur in vitro and in vivo in various extraintestinal *Escherichia coli* isolates. *Microb Pathog* **8**, 213-25.

Haghjoo, E., and Galan, J. E. (2004). *Salmonella typhi* encodes a functional cytolethal distending toxin that is delivered into host cells by a bacterial-internalization pathway. *Proc Natl Acad Sci U S A* **101**, 4614-9.

Hailey, J. R., Haseman, J. K., Bucher, J. R., Radovsky, A. E., Malarkey, D. E., Miller, R. T., Nyska, A., and Maronpot, R. R. (1998). Impact of *Helicobacter hepaticus* infection in B6C3F1 mice from twelve National Toxicology Program two-year carcinogenesis studies. *Toxicol Pathol* **26**, 602-11.

Handt, L. K., Fox, J. G., Yan, L. L., Shen, Z., Pouch, W. J., Ngai, D., Motzel, S. L., Nolan, T. E., and Klein, H. J. (1997). Diagnosis of *Helicobacter pylori* infection in a colony of rhesus monkeys (*Macaca mulatta*). *J Clin Microbiol* **35**, 165-8.

Hartland, S., Newton, J. L., Griffin, S. M., and Donaldson, P. T. (2004). A functional polymorphism in the interleukin-1 receptor-1 gene is associated with increased risk of *Helicobacter pylori* infection but not with gastric cancer. *Dig Dis Sci* **49**, 1545-50.

Hartmann, D., and von Graevenitz, A. (1987). A note on name, viability and urease tests of *Campylobacter pylori*. *Eur J Clin Microbiol* **6**, 82-3.

Hatakeyama, M. (2004). Oncogenic mechanisms of the *Helicobacter pylori* CagA protein. *Nat Rev Cancer* **4**, 688-94.

Hauer, A. C., Finn, T. M., MacDonald, T. T., Spencer, J., and Isaacson, P. G. (1997). Analysis of TH1 and TH2 cytokine production in low grade B cell gastric MALT-type lymphomas stimulated in vitro with *Helicobacter pylori*. *J Clin Pathol* **50**, 957-9.

Heilmann, K. L., and Borchard, F. (1991). Gastritis due to spiral shaped bacteria other than *Helicobacter pylori*: clinical, histological, and ultrastructural findings. *Gut* **32**, 137-40.

Hennig, E. E., Mernaugh, R., Edl, J., Cao, P., and Cover, T. L. (2004). Heterogeneity among *Helicobacter pylori* strains in expression of the outer membrane protein BabA. *Infect Immun* **72**, 3429-35.

Heuner, K., and Steinert, M. (2003). The flagellum of *Legionella pneumophila* and its link to the expression of the virulent phenotype. *Int J Med Microbiol* **293**, 133-43.

Higashi, H., Nakaya, A., Tsutsumi, R., Yokoyama, K., Fujii, Y., Ishikawa, S., Higuchi, M., Takahashi, A., Kurashima, Y., Teishikata, Y., Tanaka, S., Azuma, T., and Hatakeyama, M. (2004). *Helicobacter pylori* CagA induces Ras-independent morphogenetic response through SHP-2 recruitment and activation. *J Biol Chem* **279**, 17205-16.

Higashi, H., Tsutsumi, R., Fujita, A., Yamazaki, S., Asaka, M., Azuma, T., and Hatakeyama, M. (2002a). Biological activity of the *Helicobacter pylori* virulence factor CagA is determined by variation in the tyrosine phosphorylation sites. *Proc Natl Acad Sci U S A* **99**, 14428-33.

Higashi, H., Tsutsumi, R., Muto, S., Sugiyama, T., Azuma, T., Asaka, M., and Hatakeyama, M. (2002b). SHP-2 tyrosine phosphatase as an intracellular target of *Helicobacter pylori* CagA protein. *Science* **295**, 683-6.

Higuchi, M., Tsutsumi, R., Higashi, H., and Hatakeyama, M. (2004). Conditional gene silencing utilizing the lac repressor reveals a role of SHP-2 in cagA-positive *Helicobacter pylori* pathogenicity. *Cancer Sci* **95**, 442-7.

Holden, N. J., and Gally, D. L. (2004). Switches, cross-talk and memory in *Escherichia coli* adherence. *J Med Microbiol* **53**, 585-93.

Hoppner, C., Liu, Z., Domke, N., Binns, A. N., and Baron, C. (2004). VirB1 orthologs from *Brucella suis* and pKM101 complement defects of the lytic transglycosylase required for efficient type IV secretion from *Agrobacterium tumefaciens*. *J Bacteriol* **186**, 1415-22.

Hsu, P. I., Li, C. N., Tseng, H. H., Lai, K. H., Hsu, P. N., Lo, G. H., Lo, C. C., Yeh, J. J., Ger, L. P., Hsiao, M., Yamaoka, Y., Hwang, I. R., and Chen, A. (2004). The Interleukin-1 RN Polymorphism and *Helicobacter pylori* Infection in the Development of Duodenal Ulcer. *Helicobacter* **9**, 605-13.

Ihrig, M., Schrenzel, M. D., and Fox, J. G. (1999). Differential susceptibility to hepatic inflammation and proliferation in AXB recombinant inbred mice chronically infected with *Helicobacter hepaticus*. *Am J Pathol* **155**, 571-82.

Johnson, W. M., and Lior, H. (1988a). A new heat-labile cytolethal distending toxin (CLDT) produced by *Campylobacter* spp. *Microb Pathog* **4**, 115-26.

Johnson, W. M., and Lior, H. (1988b). A new heat-labile cytolethal distending toxin (CLDT) produced by *Escherichia coli* isolates from clinical material. *Microb Pathog* **4**, 103-13.

Josyula, S., Schut, H. A., Diwan, B. A., Anver, M. R., and Anderson, L. M. (2000). Age-related alterations in 32P-postlabeled DNA adducts in livers of mice infected with the tumorigenic bacterial pathogen, *Helicobacter hepaticus*. *Int J Oncol* **17**, 811-8.

Kaper, J. B., Nataro, J. P., and Mobley, H. L. (2004). Pathogenic *Escherichia coli*. *Nat Rev Microbiol* **2**, 123-40.

Karita, M., Kouchiyama, T., Okita, K., and Nakazawa, T. (1991). New small animal model for human gastric *Helicobacter pylori* infection: success in both nude and euthymic mice. *Am J Gastroenterol* **86**, 1596-603.

Karita, M., Li, Q., Cantero, D., and Okita, K. (1994). Establishment of a small animal model for human *Helicobacter pylori* infection using germ-free mouse. *Am J Gastroenterol* **89**, 208-13.

Karita, M., Tsuda, M., and Nakazawa, T. (1995). Essential role of urease in vitro and in vivo *Helicobacter pylori* colonization study using a wild-type and isogenic urease mutant strain. *J Clin Gastroenterol* **21 Suppl 1**, S160-3.

Karmali, M. A. (2004). Infection by Shiga toxin-producing *Escherichia coli*: an overview. *Mol Biotechnol* **26**, 117-22.

Kiehlbauch, J. A., Tauxe, R. V., Baker, C. N., and Wachsmuth, I. K. (1994). *Helicobacter cinaedi*-associated bacteremia and cellulitis in immunocompromised patients. *Ann Intern Med* **121**, 90-3.

Koh, T. J., Field, J. K., Varro, A., Liloglou, T., Fielding, P., Cui, G., Houghton, J., Dockray, G. J., and Wang, T. C. (2004). Glycine-extended gastrin promotes the growth of lung cancer. *Cancer Res* **64**, 196-201.

Krakowka, S., Morgan, D. R., Kraft, W. G., and Leunk, R. D. (1987). Establishment of gastric *Campylobacter pylori* infection in the neonatal gnotobiotic piglet. *Infect Immun* **55**, 2789-96.

Kullberg, M. C., Andersen, J. F., Gorelick, P. L., Caspar, P., Suerbaum, S., Fox, J. G., Cheever, A. W., Jankovic, D., and Sher, A. (2003). Induction of colitis by a CD4+ T cell clone specific for a bacterial epitope. *Proc Natl Acad Sci U S A* **100**, 15830-5.

Kullberg, M. C., Jankovic, D., Gorelick, P. L., Caspar, P., Letterio, J. J., Cheever, A. W., and Sher, A. (2002). Bacteria-triggered CD4(+) T regulatory cells suppress *Helicobacter hepaticus*-induced colitis. *J Exp Med* **196**, 505-15.

Kullberg, M. C., Rothfuchs, A. G., Jankovic, D., Caspar, P., Wynn, T. A., Gorelick, P. L., Cheever, A. W., and Sher, A. (2001). *Helicobacter hepaticus*-induced colitis in

interleukin-10-deficient mice: cytokine requirements for the induction and maintenance of intestinal inflammation. *Infect Immun* **69**, 4232-41.

Kullberg, M. C., Ward, J. M., Gorelick, P. L., Caspar, P., Hieny, S., Cheever, A., Jankovic, D., and Sher, A. (1998). *Helicobacter hepaticus* triggers colitis in specific-pathogen-free interleukin-10 (IL-10)-deficient mice through an IL-12- and gamma interferon-dependent mechanism. *Infect Immun* **66**, 5157-66.

Kuper, H., Adami, H. O., and Trichopoulos, D. (2000). Infections as a major preventable cause of human cancer. *J Intern Med* **248**, 171-83.

Landraud, L., Pulcini, C., Gounon, P., Flatau, G., Boquet, P., and Lemichez, E. (2004). E. coli CNF1 toxin: a two-in-one system for host-cell invasion. *Int J Med Microbiol* **293**, 513-8.

Langenberg, W., Rauws, E. A., Widjojokusumo, A., Tytgat, G. N., and Zanen, H. C. (1986). Identification of *Campylobacter pyloridis* isolates by restriction endonuclease DNA analysis. *J Clin Microbiol* **24**, 414-7.

Larsen, J. C., Szymanski, C., and Guerry, P. (2004). N-linked protein glycosylation is required for full competence in *Campylobacter jejuni* 81-176. *J Bacteriol* **186**, 6508-14.

Lee, A., Fox, J. G., Otto, G., and Murphy, J. (1990). A small animal model of human *Helicobacter pylori* active chronic gastritis. *Gastroenterology* **99**, 1315-23.

Lee, A., Krakowka, S., Fox, J. G., Otto, G., Eaton, K. A., and Murphy, J. C. (1992a). Role of *Helicobacter felis* in chronic canine gastritis. *Vet Pathol* **29**, 487-94.

Lee, A., O'Rourke, J., De Ungria, M. C., Robertson, B., Daskalopoulos, G., and Dixon, M. F. (1997). A standardized mouse model of *Helicobacter pylori* infection: introducing the Sydney strain. *Gastroenterology* **112**, 1386-97.

Lee, A., and Phillips, M. (1978). Isolation and cultivation of spirochetes and other spiral-shaped bacteria associated with the cecal mucosa of rats and mice. *Appl Environ Microbiol* **35**, 610-3.

Lee, A., Phillips, M. W., O'Rourke, J. L., Paster, B. J., Dewhirst, F. E., Fraser, G. J., Fox, J. G., Sly, L. I., Romaniuk, P. J., and Trust, T. J. (1992b). *Helicobacter muridarum* sp. nov., a microaerophilic helical bacterium with a novel ultrastructure isolated from the intestinal mucosa of rodents. *Int J Syst Bacteriol* **42**, 27-36.

Lehours, P., Menard, A., Dupouy, S., Bergey, B., Richy, F., Zerbib, F., Ruskone-Fourmestraux, A., Delchier, J. C., and Megraud, F. (2004). Evaluation of the association of nine *Helicobacter pylori* virulence factors with strains involved in low-grade gastric mucosa-associated lymphoid tissue lymphoma. *Infect Immun* **72**, 880-8.

Lei, S., Dubeykovskiy, A., Chakladar, A., Wojtukiewicz, L., and Wang, T. C. (2004). The murine gastrin promoter is synergistically activated by transforming growth factor-beta/Smad and Wnt signaling pathways. *J Biol Chem* **279**, 42492-502.

Lewis, D. A., Stevens, M. K., Latimer, J. L., Ward, C. K., Deng, K., Blick, R., Lumbley, S. R., Ison, C. A., and Hansen, E. J. (2001). Characterization of *Haemophilus ducreyi* cdtA, cdtB, and cdtC mutants in in vitro and in vivo systems. *Infect Immun* **69**, 5626-34.

Ley, C., and Parsonnet, J. (2000). Gastric Adenocarcinoma. In Infectious Causes of Cancer, Targets for Intervention (J. J. Goedert, ed., pp. 389-410. Humana Press, Totowa, N.J.

Li, X., Fox, J. G., Whary, M. T., Yan, L., Shames, B., and Zhao, Z. (1998). SCID/NCr mice naturally infected with *Helicobacter hepaticus* develop progressive hepatitis, proliferative typhlitis, and colitis. *Infect Immun* **66**, 5477-84.

Lin, J. T., Wang, L. Y., Wang, J. T., Wang, T. H., Yang, C. S., and Chen, C. J. (1995). A nested case-control study on the association between *Helicobacter pylori* infection and gastric cancer risk in a cohort of 9775 men in Taiwan. *Anticancer Res* **15**, 603-6.

Lockard, V. G., and Boler, R. K. (1970). Ultrastructure of a spiraled microorganism in the gastric mucosa of dogs. *Am J Vet Res* **31**, 1453-62.

Maeda, S., Yoshida, H., Mitsuno, Y., Hirata, Y., Ogura, K., Shiratori, Y., and Omata, M. (2002). Analysis of apoptotic and antiapoptotic signalling pathways induced by *Helicobacter pylori*. *Gut* **50**, 771-8.

Malmstrom, V., Shipton, D., Singh, B., Al-Shamkhani, A., Puklavec, M. J., Barclay, A. N., and Powrie, F. (2001). CD134L expression on dendritic cells in the mesenteric lymph nodes drives colitis in T cell-restored SCID mice. *J Immunol* **166**, 6972-81.

Marchetti, M., Arico, B., Burroni, D., Figura, N., Rappuoli, R., and Ghiara, P. (1995). Development of a mouse model of *Helicobacter pylori* infection that mimics human disease. *Science* **267**, 1655-8.

Marshall, B. J., Armstrong, J. A., McGechie, D. B., and Glancy, R. J. (1985). Attempt to fulfil Koch's postulates for pyloric *Campylobacter*. *Med J Aust* **142**, 436-9.

Marshall, B. J., and Goodwin, C. S. (1987). Revised nomenclature of *Campylobacter pyloridis*. *Int J Syst Bacteriol* **37**.

Marshall, B. J., and Warren, J. R. (1984). Unidentified curved bacilli in the stomach of patients with gastritis and peptic ulceration. *Lancet* **1**, 1311-5.

Masui, S., Sasaki, T., and Ishikawa, H. (2000). Genes for the type IV secretion system in an intracellular symbiont, *Wolbachia*, a causative agent of various sexual alterations in arthropods. *J Bacteriol* **182**, 6529-31.

Mathers, C. D., Shibuya, K., Boschi-Pinto, C., Lopez, A. D., and Murray, C. J. (2002). Global and regional estimates of cancer mortality and incidence by site: I. Application of regional cancer survival model to estimate cancer mortality distribution by site. *BMC Cancer* **2**, 36.

Matsukura, N., Yokomuro, S., Yamada, S., Tajiri, T., Sundo, T., Hadama, T., Kamiya, S., Naito, Z., and Fox, J. G. (2002). Association between *Helicobacter bilis* in bile and biliary tract malignancies: H. bilis in bile from Japanese and Thai patients with benign and malignant diseases in the biliary tract. *Jpn J Cancer Res* **93**, 842-7.

Mayer, M. P., Bueno, L. C., Hansen, E. J., and DiRienzo, J. M. (1999). Identification of a cytolethal distending toxin gene locus and features of a virulence-associated region in *Actinobacillus actinomycetemcomitans*. *Infect Immun* **67**, 1227-37.

McGee, D. J., Coker, C., Testerman, T. L., Harro, J. M., Gibson, S. V., and Mobley, H. L. (2002). The *Helicobacter pylori* flbA flagellar biosynthesis and regulatory gene is required for motility and virulence and modulates urease of *H. pylori* and Proteus mirabilis. *J Med Microbiol* **51**, 958-70.

McGraw, E. A., and O'Neill, S. L. (2004). Wolbachia pipientis: intracellular infection and pathogenesis in Drosophila. *Curr Opin Microbiol* **7**, 67-70.

Mendes, E. N., Queiroz, D. M., Dewhirst, F. E., Paster, B. J., Moura, S. B., and Fox, J. G. (1996). *Helicobacter trogontum* sp. nov., isolated from the rat intestine. *Int J Syst Bacteriol* **46**, 916-21.

Mobley, H. L., Hu, L. T., and Foxal, P. A. (1991). *Helicobacter pylori* urease: properties and role in pathogenesis. *Scand J Gastroenterol Suppl* **187**, 39-46.

Mohammadi, M., Czinn, S., Redline, R., and Nedrud, J. (1996). *Helicobacter*-specific cell-mediated immune responses display a predominant Th1 phenotype and promote a delayed-type hypersensitivity response in the stomachs of mice. *J Immunol* **156**, 4729-38.

Mohammadi, M., Nedrud, J., Redline, R., Lycke, N., and Czinn, S. J. (1997). Murine CD4 T-cell response to *Helicobacter* infection: TH1 cells enhance gastritis and TH2 cells reduce bacterial load. *Gastroenterology* **113**, 1848-57.

Morris, A., and Nicholson, G. (1987). Ingestion of *Campylobacter pyloridis* causes gastritis and raised fasting gastric pH. *Am J Gastroenterol* **82**, 192-9.

Mueller, A., O'Rourke, J., Grimm, J., Guillemin, K., Dixon, M. F., Lee, A., and Falkow, S. (2003). Distinct gene expression profiles characterize the histopathological stages of

disease in *Helicobacter*-induced mucosa-associated lymphoid tissue lymphoma. *Proc Natl Acad Sci U S A* **100**, 1292-7.

Murakami, H., Goto, M., Ono, E., Sawabe, E., Iwata, M., Okuzumi, K., Yamaguchi, K., and Takahashi, T. (2003). Isolation of *Helicobacter cinaedi* from blood of an immunocompromised patient in Japan. *J Infect Chemother* **9**, 344-7.

Murata, H., Tsuji, S., Tsujii, M., Fu, H. Y., Tanimura, H., Tsujimoto, M., Matsuura, N., Kawano, S., and Hori, M. (2004). *Helicobacter bilis* infection in biliary tract cancer. *Aliment Pharmacol Ther* **20 Suppl 1**, 90-4.

Myles, M. H., Livingston, R. S., Livingston, B. A., Criley, J. M., and Franklin, C. L. (2003). Analysis of gene expression in ceca of *Helicobacter hepaticus*-infected A/JCr mice before and after development of typhlitis. *Infect Immun* **71**, 3885-93.

Newell, D. G., Hudson, M. J., and Baskerville, A. (1987). Naturally occurring gastritis associated with *Campylobacter pylori* infection in the rhesus monkey. *Lancet* **2**, 1338.

Niehus, E., Gressmann, H., Ye, F., Schlapbach, R., Dehio, M., Dehio, C., Stack, A., Meyer, T. F., Suerbaum, S., and Josenhans, C. (2004). Genome-wide analysis of transcriptional hierarchy and feedback regulation in the flagellar system of *Helicobacter pylori*. *Mol Microbiol* **52**, 947-61.

Nilsson, I., Kornilovs'ka, I., Lindgren, S., Ljungh, A., and Wadstrom, T. (2003). Increased prevalence of seropositivity for non-gastric *Helicobacter* species in patients with autoimmune liver disease. *J Med Microbiol* **52**, 949-53.

Nishioka, H., Baesso, I., Semenzato, G., Trentin, L., Rappuoli, R., Del Giudice, G., and Montecucco, C. (2003). The neutrophil-activating protein of *Helicobacter pylori* (HP-NAP) activates the MAPK pathway in human neutrophils. *Eur J Immunol* **33**, 840-9.

Nomura, A., Stemmermann, G. N., Chyou, P. H., Kato, I., Perez-Perez, G. I., and Blaser, M. J. (1991). *Helicobacter pylori* infection and gastric carcinoma among Japanese Americans in Hawaii. *N Engl J Med* **325**, 1132-6.

O'Brien, T. R., Kirk, G., and Zhang, M. (2004). Hepatocellular carcinoma: paradigm of preventive oncology. *Cancer J* **10**, 67-73.

Omata, M., and Yoshida, H. (2004). Prevention and treatment of hepatocellular carcinoma. *Liver Transpl* **10**, S111-4.

Orlicek, S. L., Welch, D. F., and Kuhls, T. L. (1993). Septicemia and meningitis caused by *Helicobacter cinaedi* in a neonate. *J Clin Microbiol* **31**, 569-71.

O'Rourke, J. L., Dixon, M. F., Jack, A., Enno, A., and Lee, A. (2004). Gastric B-cell mucosa-associated lymphoid tissue (MALT) lymphoma in an animal model of *'Helicobacter heilmannii'* infection. *J Pathol* **203**, 896-903.

Parsonnet, J. (1999). *Microbes and malignancy : infection as a cause of human cancers*. Oxford University Press, New York.

Parsonnet, J., Friedman, G. D., Vandersteen, D. P., Chang, Y., Vogelman, J. H., Orentreich, N., and Sibley, R. K. (1991). *Helicobacter pylori* infection and the risk of gastric carcinoma. *N Engl J Med* **325**, 1127-31.

Parsonnet, J., Replogle, M., Yang, S., and Hiatt, R. (1997). Seroprevalence of CagA-positive strains among *Helicobacter pylori*-infected, healthy young adults. *J Infect Dis* **175**, 1240-2.

Paster, B. J., Lee, A., Fox, J. G., Dewhirst, F. E., Tordoff, L. A., Fraser, G. J., O'Rourke, J. L., Taylor, N. S., and Ferrero, R. (1991). Phylogeny of *Helicobacter felis* sp. nov., *Helicobacter mustelae*, and related bacteria. *Int J Syst Bacteriol* **41**, 31-8.

Pena, J. A., McNeil, K., Fox, J. G., and Versalovic, J. (2002). Molecular evidence of *Helicobacter cinaedi* organisms in human gastric biopsy specimens. *J Clin Microbiol* **40**, 1511-3.

Phillips, M. W., and Lee, A. (1983). Isolation and characterization of a spiral bacterium from the crypts of rodent gastrointestinal tracts. *Appl Environ Microbiol* **45**, 675-83.

Pisani, P., Parkin, D. M., Bray, F., and Ferlay, J. (1999). Estimates of the worldwide mortality from 25 cancers in 1990. *Int J Cancer* **83**, 18-29.

Poly, F., Threadgill, D., and Stintzi, A. (2004). Identification of *Campylobacter jejuni* ATCC 43431-specific genes by whole microbial genome comparisons. *J Bacteriol* **186**, 4781-95.

Powrie, F., and Maloy, K. J. (2003). Immunology. Regulating the regulators. *Science* **299**, 1030-1.

Purdy, D., Buswell, C. M., Hodgson, A. E., McAlpine, K., Henderson, I., and Leach, S. A. (2000). Characterisation of cytolethal distending toxin (CDT) mutants of *Campylobacter jejuni*. *J Med Microbiol* **49**, 473-9.

Rambow-Larsen, A. A., and Weiss, A. A. (2004). Temporal expression of pertussis toxin and Ptl secretion proteins by *Bordetella pertussis*. *J Bacteriol* **186**, 43-50.

Robertson, B. R., O'Rourke, J. L., Vandamme, P., On, S. L., and Lee, A. (2001). *Helicobacter ganmani* sp. nov., a urease-negative anaerobe isolated from the intestines of laboratory mice. *Int J Syst Evol Microbiol* **51**, 1881-9.

Rogers, A., Boutin, S., Whary, M., Sundina, N., Ge, Z., Cormier, K., and Fox, J. (2004). Progression of Chronic Hepatitis and Preneoplasia in *Helicobacter hepaticus*-Infected A/JCr Mice. *Toxicol Pathol* **32**, 668-77.

Rogers, A. B., and Fox, J. G. (2004). Inflammation and Cancer. I. Rodent models of infectious gastrointestinal and liver cancer. *Am J Physiol Gastrointest Liver Physiol* **286**, G361-6.

Romaniuk, P. J., Zoltowska, B., Trust, T. J., Lane, D. J., Olsen, G. J., Pace, N. R., and Stahl, D. A. (1987). *Campylobacter pylori*, the spiral bacterium associated with human gastritis, is not a true *Campylobacter* sp. *J Bacteriol* **169**, 2137-41.

Salaun, L., Audibert, C., Le Lay, G., Burucoa, C., Fauchere, J. L., and Picard, B. (1998). Panmictic structure of *Helicobacter pylori* demonstrated by the comparative study of six genetic markers. *FEMS Microbiol Lett* **161**, 231-9.

Schauer, D. B., Ghori, N., and Falkow, S. (1993). Isolation and characterization of "Flexispira rappini" from laboratory mice. *J Clin Microbiol* **31**, 2709-14.

Schmitz, A., Josenhans, C., and Suerbaum, S. (1997). Cloning and characterization of the *Helicobacter pylori* flbA gene, which codes for a membrane protein involved in coordinated expression of flagellar genes. *J Bacteriol* **179**, 987-97.

Sebkova, L., Pellicano, A., Monteleone, G., Grazioli, B., Guarnieri, G., Imeneo, M., Pallone, F., and Luzza, F. (2004). Extracellular signal-regulated protein kinase mediates interleukin 17 (IL-17)-induced IL-8 secretion in *Helicobacter pylori*-infected human gastric epithelial cells. *Infect Immun* **72**, 5019-26.

Segal, G., Russo, J. J., and Shuman, H. A. (1999). Relationships between a new type IV secretion system and the icm/dot virulence system of Legionella pneumophila. *Mol Microbiol* **34**, 799-809.

Segal, G., and Shuman, H. A. (1999a). Legionella pneumophila utilizes the same genes to multiply within *Acanthamoeba castellanii* and human macrophages. *Infect Immun* **67**, 2117-24.

Segal, G., and Shuman, H. A. (1999b). Possible origin of the Legionella pneumophila virulence genes and their relation to *Coxiella burnetii*. *Mol Microbiol* **33**, 669-70.

Sexton, J. A., Miller, J. L., Yoneda, A., Kehl-Fie, T. E., and Vogel, J. P. (2004a). *Legionella pneumophila* DotU and IcmF are required for stability of the Dot/Icm complex. *Infect Immun* **72**, 5983-92.

Sexton, J. A., Pinkner, J. S., Roth, R., Heuser, J. E., Hultgren, S. J., and Vogel, J. P. (2004b). The *Legionella pneumophila* PilT homologue DotB exhibits ATPase activity that is critical for intracellular growth. *J Bacteriol* **186**, 1658-66.

Shacter, E., and Weitzman, S. A. (2002). Chronic inflammation and cancer. *Oncology (Huntingt)* **16**, 217-26, 229; discussion 230-2.

Shames, B., Fox, J. G., Dewhirst, F., Yan, L., Shen, Z., and Taylor, N. S. (1995). Identification of widespread *Helicobacter hepaticus* infection in feces in commercial mouse colonies by culture and PCR assay. *J Clin Microbiol* **33**, 2968-72.

Sharma, S. A., Tummuru, M. K., Miller, G. G., and Blaser, M. J. (1995). Interleukin-8 response of gastric epithelial cell lines to *Helicobacter pylori* stimulation in vitro. *Infect Immun* **63**, 1681-87.

Shen, Z., Fox, J. G., Dewhirst, F. E., Paster, B. J., Foltz, C. J., Yan, L., Shames, B., and Perry, L. (1997). *Helicobacter rodentium* sp. nov., a urease-negative *Helicobacter* species isolated from laboratory mice. *Int J Syst Bacteriol* **47**, 627-34.

Shibuya, K., Mathers, C. D., Boschi-Pinto, C., Lopez, A. D., and Murray, C. J. (2002). Global and regional estimates of cancer mortality and incidence by site: II. Results for the global burden of disease 2000. *BMC Cancer* **2**, 37.

Shomer, N. H., Dangler, C. A., Marini, R. P., and Fox, J. G. (1998). *Helicobacter* bilis/*Helicobacter rodentium* co-infection associated with diarrhea in a colony of scid mice. *Lab Anim Sci* **48**, 455-9.

Shomer, N. H., Dangler, C. A., Schrenzel, M. D., Whary, M. T., Xu, S., Feng, Y., Paster, B. J., Dewhirst, F. E., and Fox, J. G. (2001). Cholangiohepatitis and inflammatory bowel disease induced by a novel urease-negative *Helicobacter* species in A/J and Tac:ICR:HascidfRF mice. *Exp Biol Med (Maywood)* **226**, 420-8.

Shomer, N. H., Fox, J. G., Juedes, A. E., and Ruddle, N. H. (2003). *Helicobacter*-induced chronic active lymphoid aggregates have characteristics of tertiary lymphoid tissue. *Infect Immun* **71**, 3572-7.

Shuto, R., Fujioka, T., Kubota, T., and Nasu, M. (1993). Experimental gastritis induced by *Helicobacter pylori* in Japanese monkeys. *Infect Immun* **61**, 933-9.

Sidebotham, R. L., and Baron, J. H. (1990). Hypothesis: *Helicobacter pylori*, urease, mucus, and gastric ulcer. *Lancet* **335**, 193-5.

Siman, J. H., Forsgren, A., Berglund, G., and Floren, C. H. (1997). Association between *Helicobacter pylori* and gastric carcinoma in the city of Malmo, Sweden. A prospective study. *Scand J Gastroenterol* **32**, 1215-21.

Singh, B., Read, S., Asseman, C., Malmstrom, V., Mottet, C., Stephens, L. A., Stepankova, R., Tlaskalova, H., and Powrie, F. (2001a). Control of intestinal inflammation by regulatory T cells. *Immunol Rev* **182**, 190-200.

Singh, R., Leuratti, C., Josyula, S., Sipowicz, M. A., Diwan, B. A., Kasprzak, K. S., Schut, H. A., Marnett, L. J., Anderson, L. M., and Shuker, D. E. (2001b). Lobe-specific increases in malondialdehyde DNA adduct formation in the livers of mice following infection with *Helicobacter hepaticus*. *Carcinogenesis* **22**, 1281-7.

Sipowicz, M. A., Weghorst, C. M., Shiao, Y. H., Buzard, G. S., Calvert, R. J., Anver, M. R., Anderson, L. M., and Rice, J. M. (1997). Lack of p53 and ras mutations in *Helicobacter hepaticus*-induced liver tumors in A/JCr mice. *Carcinogenesis* **18**, 233-6.

Solnick, J. V., and Schauer, D. B. (2001). Emergence of diverse *Helicobacter* species in the pathogenesis of gastric and enterohepatic diseases. *Clin Microbiol Rev* **14**, 59-97.

Stanley, J., Linton, D., Burnens, A. P., Dewhirst, F. E., On, S. L., Porter, A., Owen, R. J., and Costas, M. (1994). *Helicobacter pullorum* sp. nov.-genotype and phenotype of a new species isolated from poultry and from human patients with gastroenteritis. *Microbiology* **140 ( Pt 12)**, 3441-9.

Stanley, J., Linton, D., Burnens, A. P., Dewhirst, F. E., Owen, R. J., Porter, A., On, S. L., and Costas, M. (1993). *Helicobacter canis* sp. nov., a new species from dogs: an integrated study of phenotype and genotype. *J Gen Microbiol* **139 ( Pt 10)**, 2495-504.

Steer, H. W. (1975). Ultrastructure of cell migration throught the gastric epithelium and its relationship to bacteria. *J Clin Pathol* **28**, 639-46.

Steer, H. W. (1984). Surface morphology of the gastroduodenal mucosa in duodenal ulceration. *Gut* **25**, 1203-10.

Stevens, M. K., Latimer, J. L., Lumbley, S. R., Ward, C. K., Cope, L. D., Lagergard, T., and Hansen, E. J. (1999). Characterization of a *Haemophilus ducreyi* mutant deficient in expression of cytolethal distending toxin. *Infect Immun* **67**, 3900-8.

Stewart, B. W., Kleihues, P., and International Agency for Research on Cancer. (2003). *World cancer report*. IARC Press, Lyon.

Stolte, M. (1992). *Helicobacter pylori* gastritis and gastric MALT-lymphoma. *Lancet* **339**, 745-6.

Suerbaum, S., and Achtman, M. (1999). Evolution of *Helicobacter pylori*: the role of recombination. *Trends Microbiol* **7**, 182-4.

Suerbaum, S., Josenhans, C., Sterzenbach, T., Drescher, B., Brandt, P., Bell, M., Droge, M., Fartmann, B., Fischer, H. P., Ge, Z., Horster, A., Holland, R., Klein, K., Konig, J.,

Macko, L., Mendz, G. L., Nyakatura, G., Schauer, D. B., Shen, Z., Weber, J., Frosch, M., and Fox, J. G. (2003). The complete genome sequence of the carcinogenic bacterium *Helicobacter hepaticus*. *Proc Natl Acad Sci U S A* **100**, 7901-6.

Suerbaum, S., Kraft, C., Dewhirst, F. E., and Fox, J. G. (2002). *Helicobacter* nemestrinae ATCC 49396T is a strain of *Helicobacter pylori* (Marshall et al. 1985) Goodwin et al. 1989, and *Helicobacter* nemestrinae Bronsdon et al. 1991 is therefore a junior heterotypic synonym of *Helicobacter pylori*. *Int J Syst Evol Microbiol* **52**, 437-9.

Suerbaum, S., and Michetti, P. (2002). *Helicobacter pylori* infection. *N Engl J Med* **347**, 1175-86.

Suerbaum, S., Smith, J. M., Bapumia, K., Morelli, G., Smith, N. H., Kunstmann, E., Dyrek, I., and Achtman, M. (1998). Free recombination within *Helicobacter pylori*. *Proc Natl Acad Sci U S A* **95**, 12619-24.

Sundrud, M. S., Torres, V. J., Unutmaz, D., and Cover, T. L. (2004). Inhibition of primary human T cell proliferation by *Helicobacter pylori* vacuolating toxin (VacA) is independent of VacA effects on IL-2 secretion. *Proc Natl Acad Sci U S A* **101**, 7727-32.

Suriawinata, A., and Xu, R. (2004). An update on the molecular genetics of hepatocellular carcinoma. *Semin Liver Dis* **24**, 77-88.

Sykora, J., Hejda, V., Varvarovska, J., Stozicky, F., Siala, K., and Schwarz, J. (2004). *Helicobacter heilmannii* gastroduodenal disease and clinical aspects in children with dyspeptic symptoms. *Acta Paediatr* **93**, 707-9.

Taylor, N. S., Fox, J. G., and Yan, L. (1995). In-vitro hepatotoxic factor in *Helicobacter hepaticus*, *H. pylori* and other *Helicobacter* species. *J Med Microbiol* **42**, 48-52.

Taylor, N. S., Ge, Z., Shen, Z., Dewhirst, F. E., and Fox, J. G. (2003). Cytolethal distending toxin: a potential virulence factor for *Helicobacter cinaedi*. *J Infect Dis* **188**, 1892-7.

Taylor, N. S., Xu, S., Ng, V., Dewhirst, F. E., and Fox, J. G. (2004). High Prevalence of *Helicobacter* spp. in Mouse Research Colonies in the United States , Europe, and Asia. In American Associaton of Laboratory Animal Science, Tampa, Florida.

Thompson, C., and Powrie, F. (2004). Regulatory T cells. *Curr Opin Pharmacol* **4**, 408-14.

Thompson, L. J., Danon, S. J., Wilson, J. E., O'Rourke, J. L., Salama, N. R., Falkow, S., Mitchell, H., and Lee, A. (2004). Chronic *Helicobacter pylori* infection with Sydney strain 1 and a newly identified mouse-adapted strain (Sydney strain 2000) in C57BL/6 and BALB/c mice. *Infect Immun* **72**, 4668-79.

Tolia, V., Nilsson, H. O., Boyer, K., Wuerth, A., Al-Soud, W. A., Rabah, R., and Wadstrom, T. (2004). Detection of *Helicobacter ganmani*-like 16S rDNA in pediatric liver tissue. *Helicobacter* **9**, 460-8.

Tomb, J. F., White, O., Kerlavage, A. R., Clayton, R. A., Sutton, G. G., Fleischmann, R. D., Ketchum, K. A., Klenk, H. P., Gill, S., Dougherty, B. A., Nelson, K., Quackenbush, J., Zhou, L., Kirkness, E. F., Peterson, S., Loftus, B., Richardson, D., Dodson, R., Khalak, H. G., Glodek, A., McKenney, K., Fitzegerald, L. M., Lee, N., Adams, M. D., Venter, J. C., and et al. (1997). The complete genome sequence of the gastric pathogen *Helicobacter pylori*. *Nature* **388**, 539-47.

Totten, P. A., Fennell, C. L., Tenover, F. C., Wezenberg, J. M., Perine, P. L., Stamm, W. E., and Holmes, K. K. (1985). *Campylobacter cinaedi* (sp. nov.) and *Campylobacter fennelliae* (sp. nov.): two new *Campylobacter* species associated with enteric disease in homosexual men. *J Infect Dis* **151**, 131-9.

Tsuda, M., Karita, M., Mizote, T., Morshed, M. G., Okita, K., and Nakazawa, T. (1994a). Essential role of *Helicobacter pylori* urease in gastric colonization: definite proof using a urease-negative mutant constructed by gene replacement. *Eur J Gastroenterol Hepatol* **6 Suppl 1**, S49-52.

Tsuda, M., Karita, M., Morshed, M. G., Okita, K., and Nakazawa, T. (1994b). A urease-negative mutant of *Helicobacter pylori* constructed by allelic exchange mutagenesis lacks the ability to colonize the nude mouse stomach. *Infect Immun* **62**, 3586-9.

van Delft, J. H., van Agen, E., van Breda, S. G., Herwijnen, M. H., Staal, Y. C., and Kleinjans, J. C. (2004). Discrimination of genotoxic from non-genotoxic carcinogens by gene expression profiling. *Carcinogenesis* **25**, 1265-76.

van Kempen, L. C., Ruiter, D. J., van Muijen, G. N., and Coussens, L. M. (2003). The tumor microenvironment: a critical determinant of neoplastic evolution. *Eur J Cell Biol* **82**, 539-48.

Vandamme, P., Falsen, E., Pot, B., Kersters, K., and De Ley, J. (1990). Identification of *Campylobacter cinaedi* isolated from blood and feces of children and adult females. *J Clin Microbiol* **28**, 1016-20.

Vandamme, P., Harrington, C. S., Jalava, K., and On, S. L. (2000). Misidentifying *Helicobacter*s: the *Helicobacter cinaedi* example. *J Clin Microbiol* **38**, 2261-6.

Verhoef, C., Pot, R. G., de Man, R. A., Zondervan, P. E., Kuipers, E. J., JN, I. J., and Kusters, J. G. (2003). Detection of identical *Helicobacter* DNA in the stomach and in the non-cirrhotic liver of patients with hepatocellular carcinoma. *Eur J Gastroenterol Hepatol* **15**, 1171-4.

Versalovic, J., and Fox, J. G. (2003). *Helicobacter*. In Manual of Clinical Microbiology (P. R. Murray, E. J. Baron and A. S. f. Microbiology., eds.). ASM Press, Washington, D.C.

Voland, P., Hafsi, N., Zeitner, M., Laforsch, S., Wagner, H., and Prinz, C. (2003a). Antigenic properties of HpaA and Omp18, two outer membrane proteins of *Helicobacter pylori*. *Infect Immun* **71**, 3837-43.

Voland, P., Weeks, D. L., Marcus, E. A., Prinz, C., Sachs, G., and Scott, D. (2003b). Interactions among the seven *Helicobacter pylori* proteins encoded by the urease gene cluster. *Am J Physiol Gastrointest Liver Physiol* **284**, G96-G106.

Waldenstrom, J., On, S. L., Ottvall, R., Hasselquist, D., Harrington, C. S., and Olsen, B. (2003). Avian reservoirs and zoonotic potential of the emerging human pathogen *Helicobacter canadensis*. *Appl Environ Microbiol* **69**, 7523-6.

Wang, T. C., Dangler, C. A., Chen, D., Goldenring, J. R., Koh, T., Raychowdhury, R., Coffey, R. J., Ito, S., Varro, A., Dockray, G. J., and Fox, J. G. (2000). Synergistic interaction between hypergastrinemia and *Helicobacter* infection in a mouse model of gastric cancer. *Gastroenterology* **118**, 36-47.

Wang, T. C., and Fox, J. G. (1998). *Helicobacter pylori* and gastric cancer: Koch's postulates fulfilled? *Gastroenterology* **115**, 780-3.

Ward, J. M., Anver, M. R., Haines, D. C., Melhorn, J. M., Gorelick, P., Yan, L., and Fox, J. G. (1996). Inflammatory large bowel disease in immunodeficient mice naturally infected with *Helicobacter hepaticus*. *Lab Anim Sci* **46**, 15-20.

Ward, J. M., Fox, J. G., Anver, M. R., Haines, D. C., George, C. V., Collins, M. J., Jr., Gorelick, P. L., Nagashima, K., Gonda, M. A., Gilden, R. V., and et al. (1994). Chronic active hepatitis and associated liver tumors in mice caused by a persistent bacterial infection with a novel *Helicobacter* species. *J Natl Cancer Inst* **86**, 1222-7.

Watanabe, T., Tada, M., Nagai, H., Sasaki, S., and Nakao, M. (1998). *Helicobacter pylori* infection induces gastric cancer in mongolian gerbils. *Gastroenterology* **115**, 642-8.

Watanabe, Y., Kurata, J. H., Mizuno, S., Mukai, M., Inokuchi, H., Miki, K., Ozasa, K., and Kawai, K. (1997). *Helicobacter pylori* infection and gastric cancer. A nested case-control study in a rural area of Japan. *Dig Dis Sci* **42**, 1383-7.

Waterman, S. R., and Holden, D. W. (2003). Functions and effectors of the *Salmonella* pathogenicity island 2 type III secretion system. *Cell Microbiol* **5**, 501-11.

Webb, P. M., Yu, M. C., Forman, D., Henderson, B. E., Newell, D. G., Yuan, J. M., Gao, Y. T., and Ross, R. K. (1996). An apparent lack of association between *Helicobacter pylori* infection and risk of gastric cancer in China. *Int J Cancer* **67**, 603-7.

Whary, M. T., and Fox, J. G. (2004a). Natural and experimental *Helicobacter* infections. *Comp Med* **54**, 128-58.

Whary, M. T., and Fox, J. G. (2004b). Th1-mediated pathology in mouse models of human disease is ameliorated by concurrent Th2 responses to parasite antigens. *Curr Top Med Chem* **4**, 531-8.

Whary, M. T., Morgan, T. J., Dangler, C. A., Gaudes, K. J., Taylor, N. S., and Fox, J. G. (1998). Chronic active hepatitis induced by *Helicobacter hepaticus* in the A/JCr mouse is associated with a Th1 cell-mediated immune response. *Infect Immun* **66**, 3142-8.

Yahiro, K., Wada, A., Yamasaki, E., Nakayama, M., Nishi, Y., Hisatsune, J., Morinaga, N., Sap, J., Noda, M., Moss, J., and Hirayama, T. (2004). Essential domain of receptor tyrosine phosphatase b, RPTPb, for interaction with *Helicobacter pylori* vacuolating cytotoxin. *J Biol Chem*.

Yamamoto, Y., Moore, R., Goldsworthy, T. L., Negishi, M., and Maronpot, R. R. (2004). The orphan nuclear receptor constitutive active/androstane receptor is essential for liver tumor promotion by phenobarbital in mice. *Cancer Res* **64**, 7197-200.

Yamaoka, Y., Kudo, T., Lu, H., Casola, A., Brasier, A. R., and Graham, D. Y. (2004). Role of interferon-stimulated responsive element-like element in interleukin-8 promoter in *Helicobacter pylori* infection. *Gastroenterology* **126**, 1030-43.

Yanai, A., Hirata, Y., Mitsuno, Y., Maeda, S., Shibata, W., Akanuma, M., Yoshida, H., Kawabe, T., and Omata, M. (2003). *Helicobacter pylori* induces antiapoptosis through buclear factor-kappaB activation. *J Infect Dis* **188**, 1741-51.

Yang, Y. L., Xu, B., Song, Y. G., and Zhang, W. D. (2003). Overexpression of c-fos in *Helicobacter pylori*-induced gastric precancerosis of Mongolian gerbil. *World J Gastroenterol* **9**, 521-4.

Young, R. S., Fortney, K. R., Gelfanova, V., Phillips, C. L., Katz, B. P., Hood, A. F., Latimer, J. L., Munson, R. S., Jr., Hansen, E. J., and Spinola, S. M. (2001). Expression of cytolethal distending toxin and hemolysin is not required for pustule formation by *Haemophilus ducreyi* in human volunteers. *Infect Immun* **69**, 1938-42.

Young, V. B., Knox, K. A., Pratt, J. S., Cortez, J. S., Mansfield, L. S., Rogers, A. B., Fox, J. G., and Schauer, D. B. (2004). In vitro and in vivo characterization of *Helicobacter hepaticus* cytolethal distending toxin mutants. *Infect Immun* **72**, 2521-7.

Young, V. B., Knox, K. A., and Schauer, D. B. (2000). Cytolethal distending toxin sequence and activity in the enterohepatic pathogen *Helicobacter hepaticus*. *Infect Immun* **68**, 184-91.

Yu, J., Zhang, H. Y., Ma, Z. Z., Lu, W., Wang, Y. F., and Zhu, J. D. (2003). Methylation profiling of twenty four genes and the concordant methylation behaviours of nineteen genes that may contribute to hepatocellular carcinogenesis. *Cell Res* **13**, 319-33.

## Chapter 2

## Microarray analysis of *Helicobacter* spp. infection and *Helicobacter* spp. strains

## Overview of microarrays

### History

Microarray technology has generated considerable interest in the scientific field since 1995 (Schena *et al.* 1995). Microarrays provide the entire transcriptome at a single point in time. It yields a global, instantaneous perspective of the dynamic, complex interactions among thousands of genes. This includes genes in a heterogeneous population of cells in a tissue sample or a more homogenous cell population such as yeast or bacteria. Initial applications focused primarily on cancer (DeRisi *et al.* 1996; Golub *et al.* 1999; Tamayo *et al.* 1999; Welford *et al.* 1998) and yeast cell cycle analysis (Spellman *et al.* 1998). The number and diversity of experiments has increased tremendously as more genomes are sequenced. Microarray expression databases from all types of microarray experiments, and across microarray platforms, have emerged (Ball *et al.* 2005; Su *et al.* 2002).

This chapter focuses on microarray applications as they pertain to disease and the host-pathogen interaction. A gene expression signature is a unique transcription profile that characterizes a specific physiologic or pathologic state of an organ or tissue. This has allowed the establishment of new subtypes of previously recognized diseases. These disease subtypes present prognostic implications for existing therapeutic interventions (Armstrong *et al.* 2003; Campbell and Ghazal 2004; Ebert and Golub 2004; Mirnics and Pevsner 2004; Ramaswamy and Golub 2002; Russo *et al.* 2003). Thus, microarray

technology provides a powerful approach to diagnostics and contributes to prognoses. A gene signature of lesions provides important etiological and diagnostic clues. However, lesions consist of a heterogeneous population of cells and may be highly variable in size. This necessitates increased sensitivity and technological capabilities as the cell population in tissue samples become smaller. The transcriptional profile of an individual cell is not an unrealistic goal due to linear amplification strategies of minute amounts of total RNA (Van Gelder *et al.* 1990) and the introduction of laser capture microdissection (Kunz and Chan 2004; Player *et al.* 2004). Laser capture microdissection is an advancement for analyzying small, targeted tissue samples and is discussed in appendix 2.

Microarray types and technology

The three most commonly used microarray-based platforms are spotted oligonucleotide arrays, *in situ* oligonucleotide arrays (e.g, Affymetrix, Nimblegen), and spotted cDNA arrays. Oligonucleotide arrays have shorter gene target sequences (typically between 25-70 base pairs). The arraying technique differentiates the two oligonucleotide platforms (Bjorkbacka 2004). Spotted oligonucleotides are manufactured by robotic placement of oligonucleotide probes on a chemically treated microscope slide ( www.agilent.com ). Microscope slide surface coatings reduce background fluorescence and non-specific binding (Bjorkbacka 2004). *In-situ* oligonucleotide probes are synthesized by photolithographic techniques utilizing masks for *in-situ* oligonucleotide arrays (Fodor *et al.* 1993) (www.affymetrix.com) or by maskless photodeposition chemistry using digital

light processing ( www.nimblegen.com ). Oligomer and cDNA robotic spotting technologies include spotting pens (contact spotting) and ink-jet printing (non-contact spotting). Oligomer synthesis by ink-jet spotting of free nucleotides is another popular technology (Agilent). Probes consist of one single long oligomer (50-70 bases) per gene or multiple (16-20) shorter oligomers (25 bases) per gene. Increasing the probe density of oligomer arrays allows more genes per array. Oligonucleotide arrays offer higher probe density and greater specificity than cDNA arrays. However, cDNA arrays are the only option for species where the genome has not been sequenced. Microarrays are available containing the complete genome of the species of interest on one microarray. Arrays are also available containing multiple genomes, and the number of genomes is dependent on genome size and probe density technological limitations.

Hybridization differences for microarray platforms

Spotted oligonucleotide and spotted cDNA arrays utilize two fluorescent dyes while *in situ* oligonucleotide microarrays use one. Both spotted array types are hybridized with labeled test and reference samples simultaneously. The fluorescent dyes are of a specific wavelength that allows their signals to be clearly distinguished. The *in situ* oligonucleotide microarrays use one sample per microarray. The total RNA isolated from samples are subjected to a number of processing steps that yield cDNA molecules that are labeled with fluorescent dyes. The one dye method for in-situ olignucleotide microarrays allows for array to array comparisons, with one array serving as a reference array. The two dye method for spotted arrays allows within array comparisons. The

most popular fluorescent dyes used for spotted arrays to label test and reference samples are Cyanine-3 (green) and Cyanine-5 (red). After hybridization, the microarray slides are scanned using a confocal scanner that illuminates every spot and measures fluorescence intensity for each dye.

**Microrray analysis**

Scanning and image analysis

The image acquisition, analysis, normalization, modeling, and identification of differentially expressed genes in microarray experiments are non-trivial processes. Sophisticated hardware and software tools provide robust data visualization and analysis. Image analysis software facilitates acquisition of raw signal data from each probe. A final signal value is dependent upon several important parameters such as oligomer probe(s) fabrication, location, orientation, size, shape, and uniformity. The scanner parameters, the resolution of the scanner, and the alignment of the chip represent additional important variables. Computer algorithms intrinsically account for the spatial distribution, cumulative signal, number of oligomers, and number of pixels that collectively represent the final signal value recorded for each gene.

Normalization

Normalization is an integral step of data analysis. The purpose is to minimize variation across multiple arrays from factors that are not biological. For example, the total RNA concentration initially processed and the sample concentration applied to the array(s) will exhibit sample variability. For two dye microarray experiments, dye bias occurs, thus normalization approaches differ for one dye and two dye platforms. Non-linear relationships can exist between arrays, negating the use of a simple scaling factor.

Rank invariant normalization in the dChip software package was utilized for all microarray studies in Chapter 3 (Li and Wong 2001a; Li and Wong 2001b). The model based expression index (discussed next) derived in dChip requires normalization prior to comparing expression levels between arrays. All arrays are normalized to a baseline array exhibiting the median signal intensity. The normalization is based on the assumption that non-differentially expressed genes in two arrays should have similar intensity rankings. The dChip rank invariant normalization algorithm determines a proportion rank difference (PRD) defined as the absolute rank difference in two arrays divided by the number of probes. The algorithm is an iterative procedure that utilizes an empirically determined threshold for the PRD in determining if a probe should be kept or eliminated, thus establishing a new set of probes. The algorithm is applied to each new set, during each iteration, until the number of the probes does not change.

Modeling

The statistical model utilized in dChip for probe level data generates model-based estimates for gene expression indexes (Li and Wong 2001a; Li and Wong 2001b). The Affymetrix arrays consist of 16-20 probes per gene, with a probe oligonucleotide length of 25 mer, and each probe having a corresponding mismatch probe. The mismatch probe contains a different nucleotide in the middle of the probe. The expression level for different probes of a probe set for the same gene can be highly variable. A single 50-70 mer probe per gene versus 16-20 Perfect Match (PM) and Mismatch (MM) 25 mer probe pairs per gene would imply two substantially different statistical models. The latter case provides more information due to 32-40 sample points per gene. Initial gene expression studies with Affymetrix microarrays did not employ a statistical model for expression levels, and simply used the average of the PM-MM probe values as an expression index for each gene. In earlier studies, this value was used in gene expression analysis algorithms such as hierarchical clustering and self-organizing maps (Alon *et al.* 1999; Li and Wong 2001b; Tamayo *et al.* 1999). The dChip model generates a gene expression index at the probe level, a statistical model based expression index (MBEI), and allows for probe-specific biases due to their high reproducibility and predictability. Probe-specific effects are extremely important in the model (Li and Wong 2001b). The MBEI is a weighted average of the PM and MM differences, with larger weights given to probes with larger probe sensitivities. The probe sensitivity standard error is zero for an individual probe, if there are no cross-hybridizing probes for that individual probe. Thus, the probe sensitivity standard error is large for cross-hybridizing probes. The MBEI

standard error is large for image contamination. The software thus identifies cross-hybridizing probes and contamination. Therefore, the dChip model states the PM and mismatch MM difference for one probe set is the product of the MBEI and the probe sensitivity index, plus random error.

Algorithms

Algorithms for microarray data analysis are usually classified in two categories: "unsupervised or clustering" (implying no *a priori* classification of data) and "supervised or classification" (using data from known *a priori* classifications and applying predictors from this data to new data). A hybrid approach can also be utilized. These algorithms may recognize a pattern in the data that correlates with a disease or a previously unrecognized sub-type of a disease as alluded to earlier, thus complementing histopathologic classifications. Algorithms used for microarray analysis in this thesis include comparison analysis (ratio and difference thresholds), hierarchical clustering with two dimensional dendrograms and heat-maps (Eisen *et al.* 1998), linear discriminant analysis (Dudoit and Fridlyand 2002; Hakak *et al.* 2001), and principal component analysis (Raychaudhuri *et al.* 2000)

Two dimensional dendrograms and heat maps cluster genes based on the similarity of expression. There are a number of mathematical measures of similarity, and dChip utilizes the standardized correlation coefficient (r) and defines the distance between two genes as 1-r. The algorithm merges the first two genes encountered in the search for the

closest distance into a "supergene". The genes are connected by branches to form the evolving tree (dendrogram) with length representing their distance. These individual genes are deleted for the next iteration of merging and are replaced by the "supergene." The supergene is the average of standardized expression levels of the two genes across samples. In the next iteration, the next pair of genes (including supergenes) with the smallest distance is chosen to merge and another branch of the dendrogram is formed. The number of iterations is necessary to merge all the genes (and form the final dendrogram) is n-1, where n is the number of genes. This algorithm can be applied twice to obtain two dendrograms, one across genes and the other across samples (Li and Wong 2003).

Linear discriminant analysis classifies unknown samples based on training by known classes. Each individual gene is examined as to how well it separates all samples into two groups, and how well it correlates with the samples within one of these groups. The algorithm then selects a linear combination of genes in an attempt to maximize the ratio of the " between-group variance" and the "within-group variance"(Hakak *et al.* 2001). The dChip algorithm calculates two linear discriminants that map the multidimensional samples to a plane. The number of dimensions is equal to the number of genes used. The number of genes used in linear discriminant analysis is often a list of most differentially expressed genes, which was the approach used in Chapter 3. However, other lists of genes can be used and empirically tested to find the set of genes that exhibits the best predictive value.

Principal component analysis is a technique to find patterns in multidimensional data and has been utilized in facial recognition, image compression, and microarray gene expression analysis. Formally, the principal component of a data set is the eigenvector with the highest eigenvalue. It allows the dimension of the data to be reduced. This can be accomplished when there is a high correlation between two data points. There is redundancy in this case and the two variables can be reduced to one. For example, using a mathematical transformation to convert 3 dimensional data into 2 dimensional data, can possibly maintain most of the variability of the original data. Principal component analysis can transform gene expression data into a vector of any dimension, but for visualization purposes of microarray data, it is either a 3 or 2 dimensional vector that is plotted. Hopefully, the analysis yields regions on the plot that differentiates the groups of interest, e.g. control and treated (Raychaudhuri *et al.* 2000; Smith 2002).

Gene ontology, standardized vocabulary and gene annotation

Gene annotation requires a standardized vocabulary to prevent redundant nomenclature for gene function. Standardized vocabulary for biological processes, cellular components, and molecular function has been proposed by the Gene Ontology consortium (www.geneontology.org) (Ashburner *et al.* 2000; Harris *et al.* 2004). Genes characterized as "hypothetical", an open reading frame (ORF) determined by gene prediction algorithms with no protein match in Basic Local Alignment Search Tool (BLAST)-Extend-Repraze (BER) or The Institute for Genomic Research protein families (TIGRFAM), represent a very large percentage of all the genomes sequenced at present.

The same situation exists for "conserved hypothetical proteins", a pair-wise match with a hypothetical protein from another species but no TIGRFAM match (Fraser *et al.* 2004). Transitive errors arise when an aberrant annotation on one gene is transferred to another gene(s) due to database matches and subsequent annotation based on that match. Phylogenetic classification of proteins contributes to the annotation task and the cluster of orthologous gene (COG) database (http://www.ncbi.nlm.nih.gov/COG/) established phylogenetic lineages (Karlin *et al.* 2003; Tatusov *et al.* 2001). Biochemical classification of protein function presents an arduous task and *in silico* solutions are being actively pursued. The sequencing of more genomes within a species contributes to gene annotation (Kellis *et al.* 2003).

Identification of pathways and therapeutic targets

Microarray analysis generates tremendous amounts of data, producing lists of genes exhibiting differential expression under various experimental conditions. The list reveals genes that are potential targets for therapeutic intervention. However, hundreds or thousand of genes are often affected and identifying true therapeutic targets becomes problematic. Presently, a relatively large percentage of the genes in any genome may not have a functional annotation. Therefore, the molecular pathway(s) a gene product participates in is also unknown. How genes behave as a group under various experimental perturbations can suggest potential interactions with known pathways, but not the topology of the signaling network. Microarray analysis may yield potential clues. The hierarchical clustering mentioned earlier may group genes with known function and

pathways with genes with no functional annotation. This may suggest the unknown gene is directly or indirectly influenced by the known gene and pathway, and may warrant further investigation. Common sequence motifs within differentially expressed genes may imply a common transcriptional regulatory factor, or a common co-factor, depending on the whether other genes with the same motif are also differentially expressed. Transcriptional regulation experiments highlighting protein-DNA interaction provide further insight into network topology (Harbison *et al.* 2004).

Another approach to identifying genes in a pathway is chemical genomics. Chemical genomics approaches have added alternatives to traditional high-throughput screening (HTS). This approach focuses on the microarray target list, the differentially expressed genes in an experiment, for effects on biochemical pathways (Stegmaier *et al.* 2004). Extensive chemical library screens are utilized to search for potential target interaction as well as *in-vitro* effect.

Pathways also include protein-protein interactions in multi-protein complexes which are temporally and spatially regulated, and modulated by protein kinases (Yaffe and Smerdon 2004). Identifying all the targets of the different protein kinases and all the phosphorylation states of these targets may also contribute to deciphering cellular pathways. The smallest number of pathways is presumed to be in organisms with the smallest genomes. Hence, the recent interest in minimal organisms and synthetic biology. The complete genome and proteome for "minimal organisms" may be a start to elucidating the minimal set of pathways necessary for life (Jaffe *et al.* 2004).

Verification of microarray gene expression by quantitative real-time PCR

Microarray results have been criticized for a number of reasons. The reasons most often cited include cross platform discrepancies such as cDNA versus oligo, long oligo versus multiple short oligo, spotting versus photolithography, and others. The maturation of the technology contributed to the discrepancies. Some of the advantages and disadvantages of the different technologies have already been discussed. Early microarrays were often custom printed with a multitude of manufacturing variables to be considered. The hybridization, scanning, algorithms, and other factors inherent in these assays contributed to variability. One of the most controversial topics was defining when there was differential gene expression. The problem of recognizing and pursuing false positives obviously wastes resources. Missing true positives, when low level transcript changes are biologically significant, is also a problem. (Brown *et al.* 2001; Dobbin and Simon 2005; Etienne *et al.* 2004; Kothapalli *et al.* 2002; Woo *et al.* 2004; Yauk *et al.* 2004). One approach to verifying microarray results was employing quantitative real-time PCR for randomly selected genes. We used this approach in Chapter 3 and found the technology we chose to be in complete agreement with the microarray results at higher levels of signal. In fact, the microarray fold changes appeared systematically lower for higher differential expression. This indicated a narrower dynamic range for microarray technology as compared to quantitative real-time PCR. At lower fold changes, we found general agreement, but found some discrepancies as would be expected when signal levels are close to the noise floor.

## Microarray Applications

### Gene expression

Gene expression analysis of a tissue sample represents the most common use of microarrays. In an individual human cell, transcription of a subset of roughly twenty to twenty five thousand genes produces various forms of coding and non-coding RNA. Non-coding RNA molecules may be post transcriptionally modified and perform a regulatory, enzymatic, or transport role. Coding RNAs may also undergo further processing and are subsequently translated into protein products. The population distribution of transcripts depends on the number, type, and state of the cells in the sample. The microarray signal level for each gene represents the quantity of each individual transcript within a population of transcripts in a tissue sample at a single point in time.

### DNA-DNA hybridization for strain differences

Another common application utilizes microbial species microarrays to highlight strain differences at the gene level. The utility of this approach has been demonstrated with *H. pylori*, the first bacteria to have two strains sequenced. *H. pylori* strains compared at the sequence level demonstrated 6% to 7% of the genes specific to each strain, with roughly half of those genes in a single hypervariable region (Alm *et al.* 1999; Alm and Trust 1999). Subsequent microarray analysis of *H. pylori* strain differences yielded genes

correlated to virulence. (Bjorkholm and Salama 2003; Israel *et al.* 2001a; Israel *et al.* 2001b; Suerbaum *et al.* 2003; Thompson *et al.* 2004). The same approach applied to *H. hepaticus* revealed numerous genetic differences in strains including a putative pathogenicity island (Suerbaum *et al.* 2003). Microarrays with multiple strains of microbial species are commercially available. The applicability of this technique depends on the sequence diversity of the organism and the probe capacity of the microarray.

Microarrays as a complement to histology

Histopathology provides the present-day definitive diagnosis and classification of lesions based on subjective assessment of the microarchitecture of a tissue, including assessments of cell appearance and morphology in relation to their function. Histopathology, along with other medical tests and patient history, provide the framework for diagnostic, prognostic, and therapeutic decisions. Any reduction of the subjectivity of histopathological measurements to more quantitative assessment of lesions would be an improvement. In the instance where multiple diseases look very similar histologically, a gene expression signature may be a differentiating factor. For example, a transcription profile may predict whether a neoplasia is benign or malignant, and if malignant, the risk of metastases. Molecular characterization of lesion classification may contribute previously unknown sub-classifications, potentially affording improvement in therapeutic development, the prediction of disease behavior, and the response of existing therapeutic regimens. The molecular characterization of lesions could consist of, but not

be limited to, gene expression, proteins (including modifications), metabolites, protein interactions, and protein-DNA interactions. Molecular characterization of the temporal nature of lesions may prove invaluable via capturing sequential states of molecular pathogenesis. This may provide further insight into the progression of lesions, and identify potential therapeutic targets at each stage of disease progression.

Microarray investigation of the host-pathogen interaction

The host-pathogen interaction exemplifies a temporal pathogenic process where differential gene expression due to the pathogen can be investigated by microarray analysis. It allows the transcription profile of infected and control tissues in experimental animals to be monitored at any time interval desired. The preneoplastic events leading to a tumor cannot easily be investigated in people. Microarray analysis of human tumors, although very valuable, is complicated by the noise contributed by the heterogeneity of the humanpopulation and the genomic instability of the tumor. The use of tissue outside the tumor margins as controls is problematic if that tissue is also abnormal at the molecular level. The inability to match for age, gender, nutrition, environment, and other factors may also add noise to the analysis. A mouse model of an infectious cause of HCC presents an excellent opportunity to monitor the preneoplastic molecular pathogenesis. The experimental parameters controlled in the experiment in Chapter 3 include host strain, gender, nutrition, environment, and age at infection, thus avoiding the previously mentioned effects in human molecular pathogenesis studies. Chapter 3 and appendix 1 examine the AJ/Cr mouse-*H. hepaticus* interaction in the liver at 3, 6, and 12 months post

infection. These joint papers demonstrate the utility of combining conventional histopathology and microarray analysis.

Microarray analysis of neoplasia

Some of the first microarray experiments focused on tumor biology and have yielded valuable characterizations and new diagnoses, with prognostic and therapeutic implications (DeRisi *et al.* 1996; Golub *et al.* 1999). Tumor biology focuses on neoplastic cells and their microenvironment including stromal cells, inflammatory infiltrates, and blood vessels. Transcriptional profiling of tumors from the same tissue, or different tissues, provides considerable insight into the commonality and differences of tumors. Tumors with the same histopathological classification and grade can be compared, and potentially be further differentiated by gene signature. The classification of a tumor may be even further refined as additional proteomic and metabolomic data become available. This information may correlate with prognoses or therapeutic outcomes. It may prevent a patient from being subjected to a rigorous therapeutic regimen with little chance of success. It may promote new therapeutic focus on newly defined tumor subtypes. To what degree further refinement of tumor classification represents valuable information as opposed to ancillary information remains to be seen, since genomic instability of a tumor may imply a stochastic aspect of tumor gene expression.

*Helicobacter* spp. microarray experiments

Microarray experiments associated with *Helicobacter* spp. include human peripheral blood mononuclear cell response to *H. pylori* infection (Yamasaki *et al.* 2004), tissue response in experimental *Helicobacter* spp. infection in animal models, cell response to *in-vitro* infection, mutant and wild-type *Helicobacter* spp. gene expression under various experimental conditions, and mutant and wild-type *Helicobacter* spp. strain comparison via DNA hybridization. There are numerous reports dealing with microarray analysis of primary gastric carcinoma cells and gastric cells lines which will not be discussed here. The *Helicobacter pylori* genome reportedly varies over the course of years of infection within the same host, presumably due to phase variability and/or lack of mismatch repair enzymes, deletion of nucleotides, and acquisition of DNA (Falush *et al.* 2001; Kuipers and Grool 2001; Salaun *et al.* 2004; Suerbaum *et al.* 1998). Recently, acute experimental infection of rhesus macaques demonstrated *H. pylori* genomic changes including antigen variation and phase variation within a few months post-infection (Solnick *et al.* 2004). A mouse model of mucosal associated lymphoid tissue (MALT) lymphoma due to *H. pylori* or *H. felis* infection demonstrated distinct histopathological stages correlating with a gene expression profile (Mueller *et al.* 2003). *H. pylori* infection in the gerbil model indicated gastric ulcer strain B128 induced more severe gastritis, proliferation, and apoptosis in gerbil mucosa than did duodenal ulcer strain G1.1. Microarray analysis identified several strain-specific differences in gene composition including a large deletion of the cag pathogenicity island in strain G1.1 (Israel *et al.* 2001a). Regulatory studies revealed a transcriptional hierarchy and feedback regulation in the flagellar system via mutational

analysis of *H. pylori* (Niehus *et al.* 2004). Finally, in addition to the microarray analysis of *H. hepaticus* associated gene expression in the liver discussed in Chapter 3, there has been only one other enterohepatic *Helicobacter* sp. microarray study. This was a *H. hepaticus* experimental infection in A/JCr mice demonstrating differentially expressed genes in the cecum at 3 months post-infection (Myles *et al.* 2003).

Histological and microarray analysis of *H. hepaticus* infection in the A/JCr mouse

Histopathological characterization and classification of the preneoplastic stages and types of hepatic tumors due to chemical and infectious agents have existed for decades (Bannasch *et al.* 2001). Clinical classification of liver cancer relies upon morphological characteristics of tumors, lymph node status, and histology, as well as expression of specific markers associated with clinical course. Microarray analysis of preneoplastic stages complements the existing knowledge. Chronic, active hepatitis contributes to hepatic proliferation, a key component of the development of HCC in humans as well as livers of mice infected with *H. hepaticus* (Fox *et al.* 1996; Hailey *et al.* 1998). A previous study of *H. hepaticus* infection in six 18 month old mice reported similar findings (Ramljak *et al.* 1998). The histopathology of *H. hepaticus* induced liver disease up to 12 months post inoculation of *H. hepaticus* is presented in the appendix 1. The microarray analysis of *H. hepaticus* induced liver disease is presented in Chapter 3. The combination of microarray analysis and histopathology contribute valuable insight into the preneoplastic pathophysiology of *H. hepaticus* induced liver tumorigenesis in the A/JCr mouse.

**References**


Alm, R. A., Ling, L. S., Moir, D. T., King, B. L., Brown, E. D., Doig, P. C., Smith, D. R., Noonan, B., Guild, B. C., deJonge, B. L., Carmel, G., Tummino, P. J., Caruso, A., Uria-Nickelsen, M., Mills, D. M., Ives, C., Gibson, R., Merberg, D., Mills, S. D., Jiang, Q., Taylor, D. E., Vovis, G. F., and Trust, T. J. (1999). Genomic-sequence comparison of two unrelated isolates of the human gastric pathogen *Helicobacter pylori*. *Nature* **397**, 176-80.

Alm, R. A., and Trust, T. J. (1999). Analysis of the genetic diversity of *Helicobacter pylori*: the tale of two genomes. *J Mol Med* **77**, 834-46.

Alon, U., Barkai, N., Notterman, D. A., Gish, K., Ybarra, S., Mack, D., and Levine, A. J. (1999). Broad patterns of gene expression revealed by clustering analysis of tumor and normal colon tissues probed by oligonucleotide arrays. *Proc Natl Acad Sci U S A* **96**, 6745-50.

Armstrong, S. A., Golub, T. R., and Korsmeyer, S. J. (2003). MLL-rearranged leukemias: insights from gene expression profiling. *Semin Hematol* **40**, 268-73.

Ashburner, M., Ball, C. A., Blake, J. A., Botstein, D., Butler, H., Cherry, J. M., Davis, A. P., Dolinski, K., Dwight, S. S., Eppig, J. T., Harris, M. A., Hill, D. P., Issel-Tarver, L., Kasarskis, A., Lewis, S., Matese, J. C., Richardson, J. E., Ringwald, M., Rubin, G. M., and Sherlock, G. (2000). Gene ontology: tool for the unification of biology. The Gene Ontology Consortium. *Nat Genet* **25**, 25-9.

Ball, C. A., Awad, I. A., Demeter, J., Gollub, J., Hebert, J. M., Hernandez-Boussard, T., Jin, H., Matese, J. C., Nitzberg, M., Wymore, F., Zachariah, Z. K., Brown, P. O., and Sherlock, G. (2005). The Stanford Microarray Database accommodates additional microarray platforms and data formats. *Nucleic Acids Res* **33 Database Issue**, D580-2.

Bannasch, P., Nehrbass, D., and Kopp-Schneider, A. (2001). Significance of hepatic preneoplasia for cancer chemoprevention. *IARC Sci Publ* **154**, 223-40.

Bjorkbacka, H. (2004). Microarray Technology. In Analysis of Microarray Gene Expression Data (M.-L. T. Lee, ed., pp. 19-43. Kluwer Academic Publishers Group, Norwell, Massachusetts.

Bjorkholm, B., and Salama, N. R. (2003). Genomics of helicobacter 2003. *Helicobacter* **8 Suppl 1**, 1-7.

Brown, C. S., Goodwin, P. C., and Sorger, P. K. (2001). Image metrics in the statistical analysis of DNA microarray data. *Proc Natl Acad Sci U S A* **98**, 8944-9.

Campbell, C. J., and Ghazal, P. (2004). Molecular signatures for diagnosis of infection: application of microarray technology. *J Appl Microbiol* **96**, 18-23.

DeRisi, J., Penland, L., Brown, P. O., Bittner, M. L., Meltzer, P. S., Ray, M., Chen, Y., Su, Y. A., and Trent, J. M. (1996). Use of a cDNA microarray to analyse gene expression patterns in human cancer. *Nat Genet* **14**, 457-60.

Dobbin, K., and Simon, R. (2005). Sample size determination in microarray experiments for class comparison and prognostic classification. *Biostatistics* **6**, 27-38.

Dudoit, S., and Fridlyand, J. (2002). A prediction-based resampling method for estimating the number of clusters in a dataset. *Genome Biol* **3**, RESEARCH0036.

Ebert, B. L., and Golub, T. R. (2004). Genomic approaches to hematologic malignancies. *Blood* **104**, 923-32.

Eisen, M. B., Spellman, P. T., Brown, P. O., and Botstein, D. (1998). Cluster analysis and display of genome-wide expression patterns. *Proc Natl Acad Sci U S A* **95**, 14863-8.

Etienne, W., Meyer, M. H., Peppers, J., and Meyer, R. A., Jr. (2004). Comparison of mRNA gene expression by RT-PCR and DNA microarray. *Biotechniques* **36**, 618-20, 622, 624-6.

Falush, D., Kraft, C., Taylor, N. S., Correa, P., Fox, J. G., Achtman, M., and Suerbaum, S. (2001). Recombination and mutation during long-term gastric colonization by *Helicobacter pylori*: estimates of clock rates, recombination size, and minimal age. *Proc Natl Acad Sci U S A* **98**, 15056-61.

Fodor, S. P., Rava, R. P., Huang, X. C., Pease, A. C., Holmes, C. P., and Adams, C. L. (1993). Multiplexed biochemical assays with biological chips. *Nature* **364**, 555-6.

Fox, J. G., Li, X., Yan, L., Cahill, R. J., Hurley, R., Lewis, R., and Murphy, J. C. (1996). Chronic proliferative hepatitis in A/JCr mice associated with persistent *Helicobacter hepaticus* infection: a model of helicobacter-induced carcinogenesis. *Infect Immun* **64**, 1548-58.

Fraser, C. M., Read, T. D., and Nelson, K. E. (2004). *Microbial genomes*. Humana Press, Totowa, N.J.

Golub, T. R., Slonim, D. K., Tamayo, P., Huard, C., Gaasenbeek, M., Mesirov, J. P., Coller, H., Loh, M. L., Downing, J. R., Caligiuri, M. A., Bloomfield, C. D., and Lander, E. S. (1999). Molecular classification of cancer: class discovery and class prediction by gene expression monitoring. *Science* **286**, 531-7.

Hailey, J. R., Haseman, J. K., Bucher, J. R., Radovsky, A. E., Malarkey, D. E., Miller, R. T., Nyska, A., and Maronpot, R. R. (1998). Impact of *Helicobacter hepaticus* infection in

B6C3F1 mice from twelve National Toxicology Program two-year carcinogenesis studies. *Toxicol Pathol* **26**, 602-11.

Hakak, Y., Walker, J. R., Li, C., Wong, W. H., Davis, K. L., Buxbaum, J. D., Haroutunian, V., and Fienberg, A. A. (2001). Genome-wide expression analysis reveals dysregulation of myelination-related genes in chronic schizophrenia. *Proc Natl Acad Sci U S A* **98**, 4746-51.

Harbison, C. T., Gordon, D. B., Lee, T. I., Rinaldi, N. J., Macisaac, K. D., Danford, T. W., Hannett, N. M., Tagne, J. B., Reynolds, D. B., Yoo, J., Jennings, E. G., Zeitlinger, J., Pokholok, D. K., Kellis, M., Rolfe, P. A., Takusagawa, K. T., Lander, E. S., Gifford, D. K., Fraenkel, E., and Young, R. A. (2004). Transcriptional regulatory code of a eukaryotic genome. *Nature* **431**, 99-104.

Harris, M. A., Clark, J., Ireland, A., Lomax, J., Ashburner, M., Foulger, R., Eilbeck, K., Lewis, S., Marshall, B., Mungall, C., Richter, J., Rubin, G. M., Blake, J. A., Bult, C., Dolan, M., Drabkin, H., Eppig, J. T., Hill, D. P., Ni, L., Ringwald, M., Balakrishnan, R., Cherry, J. M., Christie, K. R., Costanzo, M. C., Dwight, S. S., Engel, S., Fisk, D. G., Hirschman, J. E., Hong, E. L., Nash, R. S., Sethuraman, A., Theesfeld, C. L., Botstein, D., Dolinski, K., Feierbach, B., Berardini, T., Mundodi, S., Rhee, S. Y., Apweiler, R., Barrell, D., Camon, E., Dimmer, E., Lee, V., Chisholm, R., Gaudet, P., Kibbe, W., Kishore, R., Schwarz, E. M., Sternberg, P., Gwinn, M., Hannick, L., Wortman, J., Berriman, M., Wood, V., de la Cruz, N., Tonellato, P., Jaiswal, P., Seigfried, T., and White, R. (2004). The Gene Ontology (GO) database and informatics resource. *Nucleic Acids Res* **32 Database issue**, D258-61.

Israel, D. A., Salama, N., Arnold, C. N., Moss, S. F., Ando, T., Wirth, H. P., Tham, K. T., Camorlinga, M., Blaser, M. J., Falkow, S., and Peek, R. M., Jr. (2001a). *Helicobacter pylori* strain-specific differences in genetic content, identified by microarray, influence host inflammatory responses. *J Clin Invest* **107**, 611-20.

Israel, D. A., Salama, N., Krishna, U., Rieger, U. M., Atherton, J. C., Falkow, S., and Peek, R. M., Jr. (2001b). *Helicobacter pylori* genetic diversity within the gastric niche of a single human host. *Proc Natl Acad Sci U S A* **98**, 14625-30.

Jaffe, J. D., Stange-Thomann, N., Smith, C., DeCaprio, D., Fisher, S., Butler, J., Calvo, S., Elkins, T., FitzGerald, M. G., Hafez, N., Kodira, C. D., Major, J., Wang, S., Wilkinson, J., Nicol, R., Nusbaum, C., Birren, B., Berg, H. C., and Church, G. M. (2004). The complete genome and proteome of Mycoplasma mobile. *Genome Res* **14**, 1447-61.

Karlin, S., Mrazek, J., and Gentles, A. J. (2003). Genome comparisons and analysis. *Curr Opin Struct Biol* **13**, 344-52.

Kellis, M., Patterson, N., Endrizzi, M., Birren, B., and Lander, E. S. (2003). Sequencing and comparison of yeast species to identify genes and regulatory elements. *Nature* **423**, 241-54.

Kothapalli, R., Yoder, S. J., Mane, S., and Loughran, T. P., Jr. (2002). Microarray results: how accurate are they? *BMC Bioinformatics* **3**, 22.

Kuipers, E. J., and Grool, T. A. (2001). The dynamics of gastritis. *Curr Gastroenterol Rep* **3**, 509-15.

Kunz, G. M., Jr., and Chan, D. W. (2004). The use of laser capture microscopy in proteomics research--a review. *Dis Markers* **20**, 155-60.

Li, C., and Wong, W. (2001a). Model-based analysis of oligonucleotide arrays: model validation, design issues and standard error application. *Genome Biol* **2**, RESEARCH0032.

Li, C., and Wong, W. H. (2001b). Model-based analysis of oligonucleotide arrays: expression index computation and outlier detection. *Proc Natl Acad Sci U S A* **98**, 31-6.

Li, C., and Wong, W. H. (2003). DNA-Chip Analyzer (dChip). In The analysis of gene expression data: methods and software (G. Parmigiani, E. S. Garret, R. Irizarry and S. L. Zeger, eds.). Springer, New York.

Mirnics, K., and Pevsner, J. (2004). Progress in the use of microarray technology to study the neurobiology of disease. *Nat Neurosci* **7**, 434-9.

Mueller, A., O'Rourke, J., Grimm, J., Guillemin, K., Dixon, M. F., Lee, A., and Falkow, S. (2003). Distinct gene expression profiles characterize the histopathological stages of disease in Helicobacter-induced mucosa-associated lymphoid tissue lymphoma. *Proc Natl Acad Sci U S A* **100**, 1292-7.

Myles, M. H., Livingston, R. S., Livingston, B. A., Criley, J. M., and Franklin, C. L. (2003). Analysis of gene expression in ceca of *Helicobacter hepaticus*-infected A/JCr mice before and after development of typhlitis. *Infect Immun* **71**, 3885-93.

Niehus, E., Gressmann, H., Ye, F., Schlapbach, R., Dehio, M., Dehio, C., Stack, A., Meyer, T. F., Suerbaum, S., and Josenhans, C. (2004). Genome-wide analysis of transcriptional hierarchy and feedback regulation in the flagellar system of *Helicobacter pylori*. *Mol Microbiol* **52**, 947-61.

Player, A., Barrett, J. C., and Kawasaki, E. S. (2004). Laser capture microdissection, microarrays and the precise definition of a cancer cell. *Expert Rev Mol Diagn* **4**, 831-40.

Ramaswamy, S., and Golub, T. R. (2002). DNA microarrays in clinical oncology. *J Clin Oncol* **20**, 1932-41.

Ramljak, D., Jones, A. B., Diwan, B. A., Perantoni, A. O., Hochadel, J. F., and Anderson, L. M. (1998). Epidermal growth factor and transforming growth factor-alpha-associated

overexpression of cyclin D1, Cdk4, and c-Myc during hepatocarcinogenesis in *Helicobacter hepaticus*-infected A/JCr mice. *Cancer Res* **58**, 3590-7.

Raychaudhuri, S., Stuart, J. M., and Altman, R. B. (2000). Principal components analysis to summarize microarray experiments: application to sporulation time series. *Pac Symp Biocomput*, 455-66.

Russo, G., Claudio, P. P., Fu, Y., Stiegler, P., Yu, Z., Macaluso, M., and Giordano, A. (2003). pRB2/p130 target genes in non-small lung cancer cells identified by microarray analysis. *Oncogene* **22**, 6959-69.

Salaun, L., Linz, B., Suerbaum, S., and Saunders, N. J. (2004). The diversity within an expanded and redefined repertoire of phase-variable genes in *Helicobacter pylori*. *Microbiology* **150**, 817-30.

Schena, M., Shalon, D., Davis, R. W., and Brown, P. O. (1995). Quantitative monitoring of gene expression patterns with a complementary DNA microarray. *Science* **270**, 467-70.

Smith, L. I. (2002). Principal Component Analysis, p. Computer vision class tutorial. Carnegie Mellon University, Pittsburgh, Pennsylvania.

Solnick, J. V., Hansen, L. M., Salama, N. R., Boonjakuakul, J. K., and Syvanen, M. (2004). Modification of *Helicobacter pylori* outer membrane protein expression during experimental infection of rhesus macaques. *Proc Natl Acad Sci U S A* **101**, 2106-11.

Spellman, P. T., Sherlock, G., Zhang, M. Q., Iyer, V. R., Anders, K., Eisen, M. B., Brown, P. O., Botstein, D., and Futcher, B. (1998). Comprehensive identification of cell cycle-regulated genes of the yeast Saccharomyces cerevisiae by microarray hybridization. *Mol Biol Cell* **9**, 3273-97.

Stegmaier, K., Ross, K. N., Colavito, S. A., O'Malley, S., Stockwell, B. R., and Golub, T. R. (2004). Gene expression-based high-throughput screening(GE-HTS) and application to leukemia differentiation. *Nat Genet* **36**, 257-63.

Su, A. I., Cooke, M. P., Ching, K. A., Hakak, Y., Walker, J. R., Wiltshire, T., Orth, A. P., Vega, R. G., Sapinoso, L. M., Moqrich, A., Patapoutian, A., Hampton, G. M., Schultz, P. G., and Hogenesch, J. B. (2002). Large-scale analysis of the human and mouse transcriptomes. *Proc Natl Acad Sci U S A* **99**, 4465-70.

Suerbaum, S., Josenhans, C., Sterzenbach, T., Drescher, B., Brandt, P., Bell, M., Droge, M., Fartmann, B., Fischer, H. P., Ge, Z., Horster, A., Holland, R., Klein, K., Konig, J., Macko, L., Mendz, G. L., Nyakatura, G., Schauer, D. B., Shen, Z., Weber, J., Frosch, M., and Fox, J. G. (2003). The complete genome sequence of the carcinogenic bacterium *Helicobacter hepaticus*. *Proc Natl Acad Sci U S A* **100**, 7901-6.

Suerbaum, S., Smith, J. M., Bapumia, K., Morelli, G., Smith, N. H., Kunstmann, E., Dyrek, I., and Achtman, M. (1998). Free recombination within *Helicobacter pylori*. *Proc Natl Acad Sci U S A* **95**, 12619-24.

Tamayo, P., Slonim, D., Mesirov, J., Zhu, Q., Kitareewan, S., Dmitrovsky, E., Lander, E. S., and Golub, T. R. (1999). Interpreting patterns of gene expression with self-organizing maps: methods and application to hematopoietic differentiation. *Proc Natl Acad Sci U S A* **96**, 2907-12.

Tatusov, R. L., Natale, D. A., Garkavtsev, I. V., Tatusova, T. A., Shankavaram, U. T., Rao, B. S., Kiryutin, B., Galperin, M. Y., Fedorova, N. D., and Koonin, E. V. (2001). The COG database: new developments in phylogenetic classification of proteins from complete genomes. *Nucleic Acids Res* **29**, 22-8.

Thompson, L. J., Danon, S. J., Wilson, J. E., O'Rourke, J. L., Salama, N. R., Falkow, S., Mitchell, H., and Lee, A. (2004). Chronic *Helicobacter pylori* infection with Sydney strain 1 and a newly identified mouse-adapted strain (Sydney strain 2000) in C57BL/6 and BALB/c mice. *Infect Immun* **72**, 4668-79.

Van Gelder, R. N., von Zastrow, M. E., Yool, A., Dement, W. C., Barchas, J. D., and Eberwine, J. H. (1990). Amplified RNA synthesized from limited quantities of heterogeneous cDNA. *Proc Natl Acad Sci U S A* **87**, 1663-7.

Welford, S. M., Gregg, J., Chen, E., Garrison, D., Sorensen, P. H., Denny, C. T., and Nelson, S. F. (1998). Detection of differentially expressed genes in primary tumor tissues using representational differences analysis coupled to microarray hybridization. *Nucleic Acids Res* **26**, 3059-65.

Woo, Y., Affourtit, J., Daigle, S., Viale, A., Johnson, K., Naggert, J., and Churchill, G. (2004). A comparison of cDNA, oligonucleotide, and Affymetrix GeneChip gene expression microarray platforms. *J Biomol Tech* **15**, 276-84.

Yaffe, M. B., and Smerdon, S. J. (2004). The use of in vitro peptide-library screens in the analysis of phosphoserine/threonine-binding domain structure and function. *Annu Rev Biophys Biomol Struct* **33**, 225-44.

Yamasaki, R., Yokota, K., Okada, H., Hayashi, S., Mizuno, M., Yoshino, T., Hirai, Y., Saitou, D., Akagi, T., and Oguma, K. (2004). Immune response in *Helicobacter pylori*-induced low-grade gastric-mucosa-associated lymphoid tissue (MALT) lymphoma. *J Med Microbiol* **53**, 21-9.

Yauk, C. L., Berndt, M. L., Williams, A., and Douglas, G. R. (2004). Comprehensive comparison of six microarray technologies. *Nucleic Acids Res* **32**, e124.

## Chapter 3

## Hepatic temporal gene expression profiling in *Helicobacter hepaticus* infected A/JCr mice

A version of this chapter has been previously published and is reprinted here with the permission of the publisher:

Boutin SR, Rogers AB, Shen Z, Fry RC, Love JA, Nambiar PR, Suerbaum S, Fox JG. (2004). Hepatic Temporal Gene Expression Profiling in *Helicobacter hepaticus*-Infected A/JCr Mice. *Toxicol Pathol* **32**, 678-93.

**Abstract**

*Helicobacter hepaticus* infection of A/JCr mice is a model of infectious liver cancer. We monitored hepatic global gene expression profiles in *H. hepaticus* infected and control male A/JCr mice at 3 months, 6 months, and 1 year of age using an Affymetrix-based oligonucleotide microarray platform on the premise that a specific genetic expression signature at isolated time points would be indicative of disease status. Model based expression index comparisons generated by dChip yielded consistent profiles of differential gene expression for *H. hepaticus* infected male mice with progressive liver disease versus uninfected control mice within each age group. Linear discriminant analysis and principal component analysis allowed segregation of mice based on combined age and lesion status, or age alone. Up-regulation of putative tumor markers correlated with advancing hepatocellular dysplasia. Transcriptionally down-regulated genes in mice with liver lesions included those related to peroxisome proliferator, fatty acid, and steroid metabolism pathways. In conclusion, transcriptional profiling of hepatic genes documented gene expression signatures in the livers of *H. hepaticus* infected male A/JCr mice with chronic progressive hepatitis and preneoplastic liver lesions, complemented the histopathological diagnosis, and suggested molecular targets for the monitoring and intervention of disease progression prior to the onset of hepatocellular neoplasia.

## Introduction

Microbial causes of enterohepatic cancer are well known. *Helicobacter pylori* infection is the single greatest risk factor for gastric adenocarcinoma and has been classified a class I carcinogen by the World Health Organization (Fox *et al.* 2003a). Liver cancer in humans is associated with hepatitis B and C virus infection. Similarly, *Helicobacter* spp. may potentiate inflammation and risk of hepatocellular carcinoma (HCC) in humans with or without viral hepatitis. (Ponzetto *et al.* 2000). Infection-associated inflammation is widely recognized as a contributor to human HCC and cholangiocarcinoma (Avenaud *et al.* 2000; Fox *et al.* 1998a; Nilsson *et al.* 2001)

*Helicobacter hepaticus* is associated with chronic hepatitis and HCC in A/JCr and other susceptible mouse strains, including AxB recombinant inbred mice, B6C3F1 mice and B6AF1 mice (Fox *et al.* 1994; Fox *et al.* 1996b; Hailey *et al.* 1998; Ihrig *et al.* 1999; Ward *et al.* 1994). A/JCr mice infected with *H. hepaticus* develop necrogranulomatous lobular and/or lymphocytic portal hepatitis. Male mice are more susceptible to hepatitis and tumors than females. For reasons that are not clear, only a subset of *H. hepaticus* infected male mice are affected (Fox *et al.* 1996b). In the present study, we monitored by microarray analysis chronological changes in hepatic gene expression due to *H. hepaticus* induced chronic hepatitis in the preneoplastic phase. We compared gene expression profiles in *H. hepaticus* infected male A/JCr mice with severe liver disease to uninfected mice and to infected non-diseased mice at 3 months, 6 months, and 1 year of age. Unique gene expression signatures obtained from the microarray analysis allowed us to segregate *H. hepaticus* infected diseased liver from *H. hepaticus* infected disease-free livers and uninfected controls. Furthermore, the gene expression profiles allowed segregation of liver

profiles based on age of the mice. This study provides for the first time a chronological transcriptional characterization of a microbially induced progressive inflammation of the liver resulting in preneoplastic liver lesions.

## Materials and methods

### Animals

Thirty-six *Helicobacter*-free female A/JCr mice (National Cancer Institute, Frederick, MD) were bred to 18 males, and pregnant dams were divided into groups. Dams received $10^7$ colony-forming units *H. hepaticus* or vehicle only by gastric gavage every 48 hours for 3 doses at conception (confirmed by vaginal plug visualization) or beginning midway (day 10) through pregnancy. Pups received a similar bacterial or sham inoculum regimen at 3 or 12 weeks postnatally. Assessment of transplacental bacterial or antigenic exposure was not performed. Offspring were euthanatized by $CO_2$ inhalation at 3, 6, or 12 months of age. A total of 117 mice were evaluated: 33 at 3 months, 41 at 6 months, and 43 at 12 months. Animals were maintained in a facility certified by the Association for the Assessment and Accreditation of Laboratory Animal Care in compliance with the National Academy of Sciences' *Guide for the Care and Use of Laboratory Animals*, and all protocols were approved by the Massachusetts Institute of Technology (MIT) Committee on Animal Care.

*Helicobacter hepaticus* infection

*H. hepaticus* type strain ATCCC 51449 was grown on TSA 5% sheep blood agar (Remel, Lenexa, KS) under microaerobic conditions ($N_2$, $H_2$ and $CO_2$; 90:5:5) for two days and transferred with a sterile applicator to 1.5 ml of Brucella broth and 30% glycerol. This was immediately deposited into 150 ml of Brucella broth in a flask, enclosed in an BBL GasPak 100 polycarbonate anaerobic jar (Becton Dickison Microbiology Systems, Cockeysville, MD) under microaerobic conditions, and placed on a PsychroTherm incubator-shaker table (New Brunswick Scientific Co., Edison N.J.) at 30 RPM at 37°C overnight. Approximately $10^8$ bacteria/ml were placed in phosphate buffered saline (PBS) for one dose. Bacterial count was confirmed by a reading of 1.0 at 660 nm on a DuPro 640 spectrophotometer (Beckman Coulter, Fullerton, CA). Bacterial viability, motility, and morphology were confirmed by phase-contrast microscopy.

Histopathology

At necropsy, ileocecocolic junction and two sagittal sections of each liver lobe (median, caudate, left, and right) were collected for histopathology. Tissues were immersion fixed overnight in 10% neutral-buffered fromalin (VWR Scientific, West Chester, PA) and Prefer (Anatech, Ltd., Battle Creek, MI). Fixed tissues were processed and embedded by routine histologic methods, sectioned at 4 μm, and stained with hematoxylin and eosin (H&E). The 8 liver sections representing replicate samples from each lobe were examined by a veterinary pathologist blinded to sample identity and graded on a 0-4 scale for lobular histologic activity (lobular hepatitis), portal activity (portal and/or interface hepatitis), and staged on the same scale for fibrosis using

criteria established by Scheuer (Ferrell 2002; Scheuer *et al.* 2002). Additionally, dysplastic progression was scored using criteria adapted from published schemes for the terminology of rodent and human liver lesions: (0) normal, (1) foci of cellular alteration or dysplastic foci, (2) nodules of cellular alteration or low grade dysplastic nodules, (3) high grade dysplastic nodules or focal well differentiated HCC, and (4) multifocal and/or moderately differentiated HCC (Bannasch *et al.* 2001; IWP 1995).

Special stains, immunohistochemistry, and morphometric analysis

Selected liver sections were stained by the Warthin-Starry stain for visualization of bacteria, or diastase periodic acid-Schiff or Perl's iron for demonstration of activated macrophages. Formalin- and Prefer-fixed liver sections were subjected to standard microwave heat-induced epitope retrieval and immunostained for cell phenotype markers or specific biomolecules using mouse monoclonal or rabbit polyclonal primary antibodies according to previous methods (Erdman *et al.* 2003c; Fox *et al.* 2003b). For mouse primary antibodies the ARK kit was used (DAKO, Carpinteria, CA), a system that employs prelabeled same-species antibodies to overcome labeling of endogenous immunoglobulins, a strategy proven as well in other settings (Rogers *et al.* 2002). Rabbit primary antibodies were labeled with biotinylated goat anti-rabbit IgG (Sigma). Cell phenotypes and other biomolecules demonstrated included T cells (rabbit anti-CD3, Sigma), B cells (CD45R/B220) and the mitosis marker Ki-67 (BD Pharmingen, San Diego, CA), macrophages (F4/80, Caltag Laboratories, Burlingame, CA), iNOS (NOS2) and COX-2 (PGH2; Santa Cruz Biotechnology, Santa Cruz, CA), and the apoptosis marker cleaved caspase-3 (Cell Signaling Technology, Beverly, MA). Diaminobenzidine (DAB) or Vector VIP was used

as chromogen, and tissues were counterstained with Gill's hematoxylin. Morphometric analysis of immunohistochemically stained tissue sections was performed by a comparative pathologist using IPLab 3.6 software for Macintosh (Scanalytics, Inc., Fairfax, VA) according to previously described methods (Fox *et al.* 2003b).

Liver Samples

Samples were sections of the left liver lobe of A/JCr mice (*Mus musculus*). Sections of the liver were used for histology and total RNA isolation. Total RNA was used for microarray and quantitative real-time fluorogenic PCR assays. Mouse liver was aseptically removed immediately after $CO_2$ euthanasia and placed in an individual cryogenic vial (Corning, NY). The cryogenic vial was immediately placed in the vapor phase of liquid nitrogen. At the end of the necropsy for the total experiment, the cryogenic vials were transferred to an -80°C freezer.

Representative samples at 3, 6, and 12 months from 6 male mice were selected for microarray analysis based on known infection status and presence or absence of hepatitis as demonstrated by histopathology. Biological replicates representing 2 uninfected mice, 2 infected mice without significant liver lesions, and 2 infected mice with severe hepatitis were analyzed at each time point. Samples for microarray analysis were selected from groups of pups born to dams inoculated during pregnancy with subsequent *H. hepaticus* inoculation of pups at 3 weeks postnatally. *H. hepaticus* infected litter- and cagemates with and without hepatitis were chosen for direct comparison whenever possible.

RNA isolation and quality assessment

The standard protocols followed were per Affymetix's instructions (Genechip® Expression Analysis Technical Manual 701021 Rev 4). Briefly, total RNA was isolated from two sections (each approximately 35 mg) of flash frozen liver using Trizol (Invitrogen, Carlsbad, CA) as per manufacturer's instructions. The RNA pellet was resuspended in 100 ul of RNAse free water. The RNeasy Clean-up kit (Qiagen, Valencia, CA) was utilized per manufacturer's instructions resulting in 30 ul total RNA sample. The total RNA concentration and 260/280 ratio was evaluated on a NanoDrop ND-1000 UV-Vis Spectrophotomter (NanoDrop Technologies, Rockland, DE). Only samples with a 260/280 ratio greater than 1.9 were further processed. An aliquot of 1 ul from each of the samples was diluted to be within the dynamic range of the Agilent RNA 6000 Nano Labchip kit (Agilent, Palo Alto, CA), with a target of 100 ng. The Nano Labchip protocol was followed as per manufacturer's instructions and was placed on an Agilent 2100 Bioanalyzer (Agilent, Palo Alto, CA) for evaluation. Samples with the highest concentration, only two distinct 18S and 28 S peaks, and no evidence of degradation were further processed. To obtain 15 μg of total RNA for first strand cDNA synthesis, samples were sometimes combined and placed on a spin-vacuum to obtain the necessary concentration (1.66 μg/μl) and volume (9 μl). Six hundred units of SuperScript II reverse transcriptase were used for the first strand cDNA synthesis reaction. Half of the samples were prepared at the Division of Comparative Medicine at MIT and the other half of the samples were prepared at the Whitehead Institute (JAL) for comparison. The second strand DNA synthesis, the clean-up of the double-stranded cDNA, the synthesis of the biotin-labeled cRNA, and the clean-up of the biotin-labeled cRNA were per Affymetrix instructions. The Genechip® Sample Clean-up module was used

for the clean-up steps of the double-stranded cDNA and the biotin-labeled cRNA. Quantification of the cRNA was evaluated on the NanoDrop. Samples were used for hybridization only if 20 μg of cRNA were obtained in an individual sample or by combining samples.

Array design

Affymetrix Murine Genome Arrays U74Av2. (Affymetrix, Santa Clara, CA) Array size: Standard Format. Feature size 20 μm. Sensitivity: 1:100,000. See www.affymetrix.com for the probe sequences or reference sequence from which the probe was derived. Microarrays were hybridized overnight, washed in a fluidics station, and scanned using the GeneArray® scanner per manufacturer's instructions (Affymetrix, Santa Clara, CA). The U74Av2 oligonucleotide array contained ~6000 functionally characterized gene sequences (Unigene Murine Database, Build 74) and a similar number of expressed sequence-tagged (EST) clusters. There were 16-20 pairs of 25-mer oligonucletide probes per sequence, with a sensitivity of ~1:100,000. Control sequences on the microarray included *bioB, bioC, bioD,* and *cre,* and house-keeping genes considered were actin, GAPDH, and hexokinase.

Hybridization

Fragmentation, hybridization, washing, staining, and scanning were done according to the Affymetrix protocol. Briefly, reagent preparation included 12X MES stock (1.22M MES, 0.89M [$Na^+$]) and 2X hybridization buffer (1X hybridization buffer: 100mM MES, 1M [$Na^+$], 20 mM EDTA, .01% Tween 20). The hybridization cocktail components and final concentrations consisted of fragmented cDNA (.05 μg/μl), control oligonucleotide B2 (50 pM), 20X eukaryotic

hybridization controls *bioB, bioC, bioD,* and *cre* (1.5, 5, 25, 100 pM, respectively), herring sperm DNA (.1 mg/ml), acetylated BSA (.5 mg/ml), 1X hybridization buffer with a final volume of 300 µl. The GeneChip array was filled with 250 µl of the hybridization cocktail and hybridized for 16 hours, rotated at 60 RPM, and maintained at 45°C.

Reagents prepared for washing and staining included a non-stringent wash buffer (6X SSPE, .01% Tween 20), a stringent wash buffer (100 mM MES, 0.1 M [$Na^+$], 0.01% Tween 20), and a 2X stain buffer (1X: 100 mM MES, 1M [$Na^+$], 0.05% Tween 20). The wash procedure was carried out in an Affymetrix Fluidics Station 400 controlled by Affymetrix Microarray Suite 5.0 software resident on a personal computer. The fluidics station first went through a priming step and subsequently did the washing and staining by a software protocol designed for the Affymetrix Murine Genome Array U74Av2.

Measurements

The microarrays were scanned using the GeneArray® scanner per manufacturer's instructions (Affymetrix, Santa Clara, CA). The quality control algorithms for eliminating an array are based on recommendations in both the Affymetrix and dChip software packages.

Normalization

For dChip software, a invariant-set normalization method is used (Li and Hung Wong 2001; Li and Wong 2001). Briefly, the expectation is that a probe of a non-differentially expressed gene in two arrays will have similar intensity ranks in two separate arrays. The ranks are calculated

separately in the two arrays. Although it is unknown which genes are non-differentially expressed, an iterative procedure is used to determine rank differences with an empirically derived threshold for inclusion. All arrays are normalized, except the baseline array, to the common baseline array with median intensity.

Data analysis

Two software packages were utilized for data analysis, dChip (Li and Hung Wong 2001; Li and Wong 2001) and Affymetrix Microarray Suite 5.0. Microarray Suite 5.0 was used to generate a cell intensity file (*.cel). The *.cel file and the perfect match model (PM) were used for the dChip analysis and is the data presented. The dChip software is model based, and generates a "model based expression index" (MBEI) and a standard error. The software utilizes the response characteristics of individual probe sets. Unless otherwise specified, default settings were used. Comparison analysis, hierarchical clustering, linear discriminant analysis (LDA), and principal component analysis (PCA) within dChip were performed. Comparison analysis used the default setting of 1.2 fold change, positive or negative. For hierarchical clustering, default settings were used, the distance metric was 1-correlation and the linkage was centroid.

Quantitative real-rime flurogenic PCR (Taqman)

To confirm microarray data, quantitative real-time flurogenic PCR was utilized. Assay-on-Demand gene expression kits (Applied Biosystems, Foster City, CA) were used to quantitate cytochrome P450 4a14 (Cyp4a14), interferon γ-induced GTPase (Igtp), H19 fetal liver mRNA

(H19), hydroxysteroid dehydrogenase-5, delta<5>-3-beta (Hsd3b5), CD5 antigen-like (Cd5l) (formerly known as apoptosis inhibitor 6), trefoil factor 3, intestinal (Tff3) genes were normalized against the expression of glyceraldehyde 3 phosphate dehydrogenase (Gapdh) as the housekeeping standard. Two μg of total RNA from the uninfected and infected A/JCr mouse liver samples was reverse-transcribed to single strand cDNA using the Superscript Reverse Transcriptase II (Invitrogen, Carlsbad, CA) protocol. The single strand cDNA from the reverse transcriptase reaction was amplified by real-time quantitative flourogenic PCR. Eighty microliters of 1X TE was added to the 20 ul reaction volume. The Taqman protocol was per manufacturer's instructions for the Applied Biosystems 7700 Sequence Detection System except that 25ul total volume was used. The reaction consisted of the Taqman Universal 2X PCR Master Mix (12.5 ul), 5 ul of the cDNA/1XTE solution, 20X target (1.25 ul) and 6.25 ul of water. That RNA expression level fold changes were calculated as described by the Taqman protocol.

**Results**

Histopathology

Inflammatory lesions in mice infected with *H. hepaticus* followed one of two courses, resulting in necrogranulomatous lobular and/or lymphocytic portal hepatitis. In cases of lobular hepatitis, necroinflammatory lesions consisted primarily of Kupffer cells and recruited macrophages surrounding and infiltrating foci of spotty or confluent hepatocellular necrosis (Fig. 1a), resulting in translobular coagulative necrosis in severe cases. Neutrophils and lymphocytes made a minority contribution to lobular lesions. Larger lesions were evident grossly as round white foci

up to 2 mm diameter. Lobular lesions were often but not always situated near terminal hepatic venules. Acidophil bodies were mildly increased in number in mice with lobular hepatitis, though not always located near inflammatory foci.

Portal hepatitis consisted primarily of lymphocytoid cells forming expansile nodular lesions, either in conjunction with lobular lesions or comprising the main disease process. Uncomplicated portal hepatitis was most common in females. Because bacteria were rarely identified in portal regions, it is possible these lesions developed due to circulating antigens or cytokines from the lower bowel. Lobular necrogranulomatous lesions were evident at all sampled timepoints, whereas chronic portal inflammation was not fully developed until 12 months of age. Especially in conjunction with lobular lesions, portal mononuclear infiltrates disrupted the hepatic limiting plate, resulting in interface hepatitis (Fig. 1b). Lymphocytoid cells filled and expanded reactive portal lymphatic vessels, and in larger lesions surrounded and infiltrated bile ductules inducing epithelial loss, hypertrophy, and atypia (Fig. 1b). Expansile aggregates sometimes were organized into follicles consistent with "tertiary lymphoid tissue" (Fig. 1c) (Shomer *et al.* 2003). Unlike the case of *H. hepaticus* infection in mice with targeted immune mutations (Erdman *et al.* 2003b; Erdman *et al.* 2003c; Tomczak *et al.* 2003a; Young *et al.* 2004) but in agreement with previous studies utilizing A/JCr mice (Whary *et al.* 2001; Whary *et al.* 1998), inflammation of the cecum and colon (typhlocolitis) in these

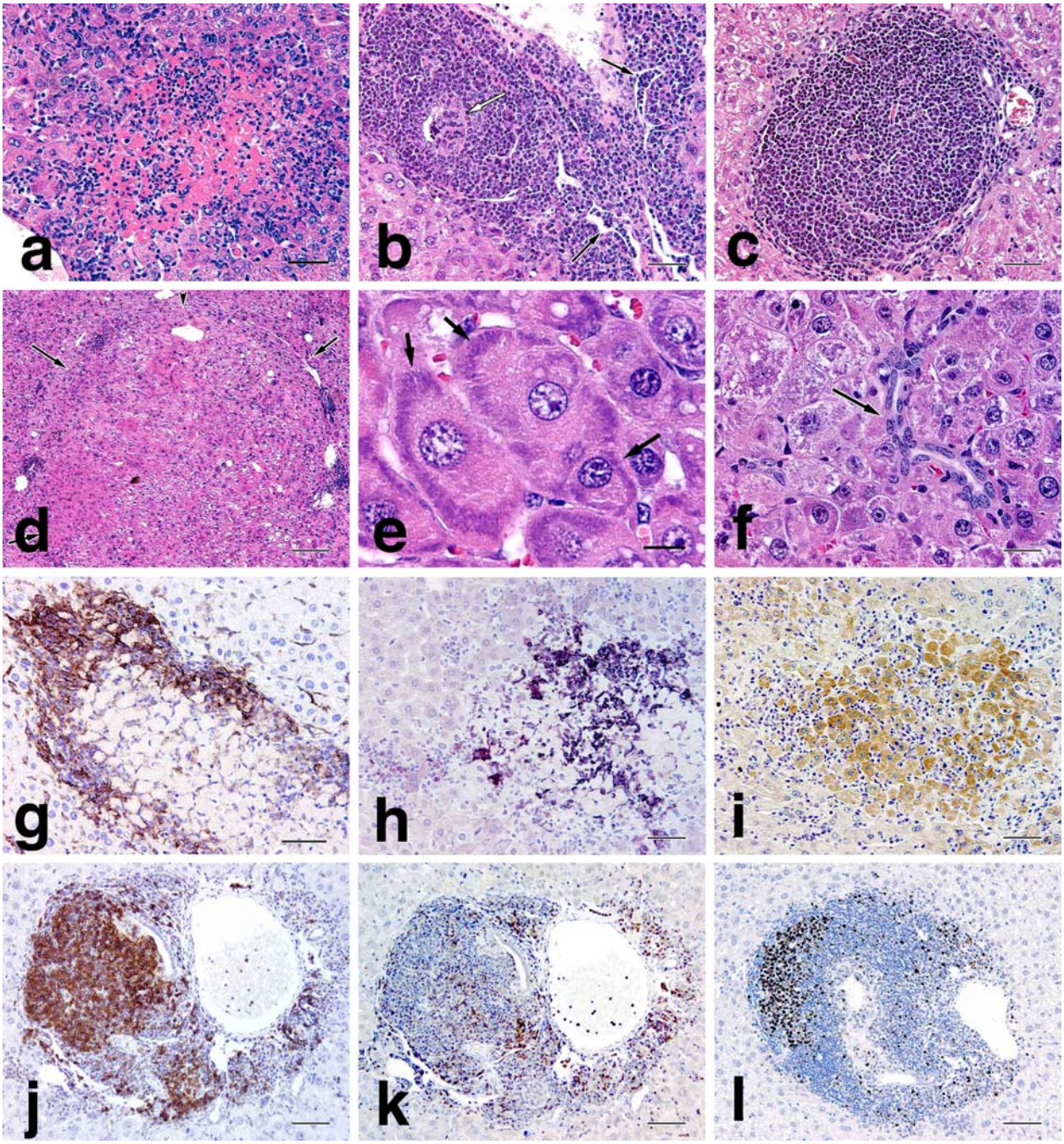


**Figure 1.** Histopathology of *H. hepaticus* induced liver disease. (**a**) Lobular hepatitis with infiltrating leukocytes and coagulative necrosis. (**b**) Portal and interface hepatitis with dilated lymphatics containing many mononuclear cells (black arrows); leukocytes surround and infiltrate a reactive bile ductule (white arrow). (**c**) Portal tertiary lymphoid follicle. (**d**) Dysplastic nodule (arrows). **(e)** Tigroid cells in focus of cellular alteration; note radial subplasmalemmal striations (arrows). (**f**) Oval cell hyperplasia with pseudocholangiole formation (arrow) in dysplastic nodule. (**g**) F4/80$^{+}$ macrophages surrounding and infiltrating a sheet of hepatocytes undergoing coagulative necrosis. Lobular necroinflammatory focus with upregulated expression of (**h**) iNOS in inflammatory cells and (**i**) COX-2 in intralesional hepatocytes. Portal tertiary lymphoid tissue with (**j**) CD45R/B220$^{+}$ follicular B cell aggregates , and (**k**) individually dispersed CD3$^{+}$ T cells. (**l**) Intrahepatic lymphoid expansion with abundant Ki-67$^{+}$ nuclei in portal tertiary lymphoid follicle (IHC). H&E (a—f), immunohistochemistry (g—l); bar ~100 μm (a, c, g, j—l), 50 μm (b, h, i), 250 μm (d), 10 μm (e), 25 μm (f).

immunocompetent animals was generally mild, with inflammation scores typically in the range of 0.5--1 out of 4. Typhlocolitis was limited to mice infected at or before 3 weeks of age, but was not present in all animals, and there were no statistically significant differences between groups. Although morphologic changes were mild, microarray experiments have shown that lower bowel colonization of A/JCr mice with *H. hepaticus* induces prominent transcriptional responses (Myles *et al.* 2003).

At 12 months of age, male mice with severe lobular hepatitis exhibited dysplastic and proliferative lesions similar to those previously documented (Bannasch *et al.* 2001; Canella *et al.* 1996; Fox *et al.* 1998b; Fox *et al.* 1996c; Hailey *et al.* 1998; Haseman *et al.* 1998; Rice 1995; Ward *et al.* 1996a; Ward *et al.* 1996b). Foci of cellular alteration or dysplastic foci were multifocal, and often merged imperceptibly into adjacent zones of more normal hepatocytes. In some instances expansile dysplastic nodules were sharply delineated from surrounding less affected lobules (Fig. 1d). Inflammation was concentrated at the perimeter of dysplastic nodules. Foci of cellular alteration, putative precursors to HCC (Bannasch *et al.* 1985; Bannasch *et al.* 2001) were of the clear cell, eosinophilic, or basophilic-tigroid (Fig. 1e) phenotype, often comingled. Hepatocellular atypia was manifest as marked anisocytosis and anisokaryosis, structural and tinctorial pleomorphism, irregular cytoplasmic vacuolation and molding, aberrent multinucleation, and nuclear clearing with bizarre chromatin patterns. Oval cell hyperplasia, with occasional pseudocholangiole formation (Fig. 1f), was common within foci of cellular alteration.

Special stains and immunohistochemistry

Confirmation of the primarily granulomatous nature of lobular necroinflammatory lesions was provided by F4/80 immunohistochemistry (Fig. 1g). As described in human viral hepatitis, activated macrophages containing diastase-resistant PAS-positive material were present in some inflammatory lesions (Ferrell 2002). In contrast, phagocytes with accumulated iron were extremely rare. Argyrophilic spiral bacteria, some undergoing longitudinal fission, were readily identified in bile canaliculi of Warthin-Starry-stained liver sections near histologically active lobular lesions, but were rare near portal tracts. In agreement with PCR results, organisms were absent in uninfected mice, and very rarely visualized in Warthin-Starry stained liver sections from mice lacking lobular inflammation. Immunohistochemical demonstration of iNOS and COX-2 was limited to necroinflammatory lesions; however, the cell populations expressing each of these proteins were different. iNOS was demonstrated almost exclusively within inflammatory cells (Fig. 1h), while COX-2 was upregulated in intralesional hepatocytes (Fig. 1i). Scattered acidophil bodies and some leukocytes, but not sheets of hepatocytes within zones of coagulative necrosis, contained cleaved caspase-3.

Morphometric analysis

Observational quantitation of lesions in liver sections proved problematic due to variable densities of leukocellular aggregation, and confluence of adjoining inflammatory foci. We therefore applied morphometric analysis to 5 affected and 2 control immunohistochemically stained livers from the 12-month timepoint in order to determine percent area occupied by

specific cell subsets within a defined region of interest (Fox et al. 2003a). We examined ten left lobe fields per mouse under the 10X ocular objective (0.61mm$^2$/field). In mice with lobular and/or portal hepatitis (histologic activity ≥2), the median hepatic tissue area comprised of leukocyte-common antigen CD45$^+$ white blood cells was 4%. One liver with severe disease contained 9% leukocytes, and when leukocytes were combined with zones of coagulative necrosis 25% of the most affected lobe was effaced. Portal tertiary lymphoid nodules contained a median of 72% CD45$^+$ leukocytes, the remaining tissue being comprised of resident portal arterioles, bile ductules, lymphatic channels, and connective tissue (portal venules were excluded from the manually defined region of interest). Among the inflammatory cells, 45% displayed the B cell marker CD45R/B220 (Fig. 1j), 7% were CD3$^+$ T cells (Fig. 1k), and 3% were identified as F4/80$^+$ professional antigen-presenting cells (macrophages ± dendritic cells). Unlabeled portal tertiary lymphoid tissue included arterioles and bile ducts as well as presumptive NK cells, scattered granulocytes, and other cells unrecognized by our antibody panel. Within tertiary lymphoid nodules, B cells were aggregated into follicular structures (Fig. 1j) while T cells (Fig. 1k) and antigen-presenting cells were more widely dispersed. In portal tracts where bile ducts were surrounded and transmigrated by leukocytes, ductular epithelium exhibited atrophy, hypertrophy, and decreased cytokeratin expression. Scattered throughout portal tertiary lymphoid tissue, and focally concentrated at the periphery, were many actively proliferating cells attesting to intrahepatic lymphoid expansion (Fig. 1l). The Ki-67 labeling index per 10X field was >100 in tertiary lymphoid tissue. Increased cell proliferation was also evident in foci of cellular alteration and dysplastic nodules, with a Ki-67 labeling index of 7 hepatocyte nuclei per 10X field, versus <1 in normal hepatic lobules ($P$<0.0001).

Microarray results overview

Certain clusters of gene expression (Tables I and II), gene categories (Table III), and protein domains (Table IV) persisted throughout the 12 month experimental period, while other clusters arose at 6 months or at 12 months. (Gene categories and protein domains are standardized vocabulary defined by the Gene Ontology consortium (http://www.geneontology.org)). A Venn diagram (Figure 2) presents this scenario in a simplified form for illustrative purposes. Tables III and IV are color coded to represent the 3 month (red), 6 month (blue), and 12 month (green) time points. Group 1 represents all the genes, gene categories, and protein domains exhibited at 3, 6, and 12 months. It contains many signatures of an acute-phase response which persisted over 12 months. Group 2 represents most, but not all, of the Group 1 clusters, plus new genes, gene categories, and protein domains at 6 months. Group 2 encompasses biological processes of both the acute immune response of Group 1, plus a more mature or chronic immune response. Table V and VI lists genes within the Gene Ontology category corresponding to the immune response and the pathogen response. Group 3 again intersects most of Group 1 and Group 2, but new entries indicate tubulin, microtubule, cytoskeletal, peroxisome, scavenger, and structural and proliferative activity. Table VII lists specific genes in the Gene Ontology categories of cell proliferation, growth, and death. Genes expressed during fetal development or imprinted genes are also evident in Group 3.

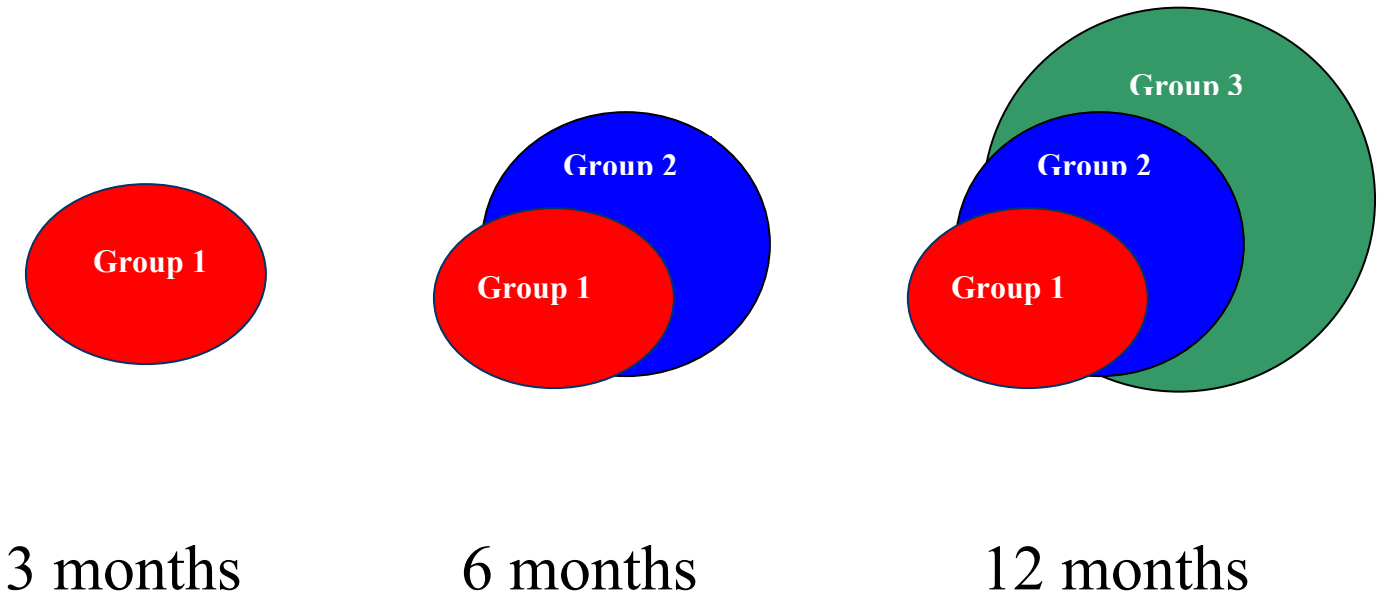


**Figure 2.** Simplified Venn diagram representation of clusters of hepatic differential gene expression, gene categories, and protein domains arising during the course of the *H. hepaticus* experimental infection of male A/JCr mice. Group 1 figuratively represents the acute phase of lobular hepatitis observed histologically throughout the course of the experiment due to persistent infection. Group 2 intersects Group 1 and additionally represents the maturation of inflammatory response and the portal hepatitis first recognized at 6 months which became progressively more severe. Group 3 intersects Group 1 and Group 2 and additionally represents tubulin, microtuble, scavenger, peroxisome, and structural gene categories, plus genes suggestive of hepatic pre-neoplasia.

Genes up-regulated and down-regulated

Age matched *H. hepaticus* infected mice with progressive disease, exhibiting altered gene expression as defined by dChip software with default settings (Li and Wong 2001), yielded 188 differentially expressed genes at 3 months, 401 at 6 months, and 678 at 12 months. Immune response genes, including the acute phase response, histocompatibility, macrophage, T and B cell development, and complement represented most of the up-regulated genes at 3 months (Table I). These genes continued to be up-regulated throughout the 12 month experiment. The acute phase lipocalin family and serum amyloid family are represented in this group. At 6 months, there was a further increase in expression of these genes plus new differential expression levels of genes suggestive of further inflammatory response and repair including chemokine ligands (such as lymphocyte attracting chemokines Cxcl9 and Cxc13), chemokine receptors of the CC motif, ADAM family members, lysozyme, procollagen, cellular retinol binding protein (Lepreux *et al.* 2004), and detoxification enzymes. At 12 months post *H hepaticus* infection, new genes up-regulated represented more structurally related genes and more detoxification genes including tubulin, growth factors, carriers, and cytochrome P450 genes. Genes historically linked to neoplasia and up-regulated in the 12 month group included H19, intestinal trefoil factor 3, the ras family, and Jun-B. Up-regulated genes predominated over down-regulated genes at all time points for *H. hepaticus* infected A/J mice with hepatic lesions. Interestingly, the vast majority of down-regulated genes were at 12 months (Table II). Down-regulated genes at 12 months were associated with steroid hormones, heme metabolism, and sodium/bile acid co-transport (Fraser *et al.* 2003; Jung *et al.* 2004). There was a consistent segregation of the most highly up-regulated and select down-regulated genes for *H. hepaticus* infected mice with lesions. Genes up-

regulated or down-regulated at 12 months, along with their corresponding values at 3 and 6 months are exhibited in Tables I and II, respectively.

**Table I.** Genes with up-regulated transcription in the livers of of *H. hepaticus* infected male A/JCr mice with severe disease versus sham-infected age-matched controls (fold increase).

| **Gene** | **3 months** | **6 months** | **12 months** |
|---|---|---|---|
| lipocalin 2 | 7.91 | 46.72 | 30.27 |
| T-cell specific GTPase | 9.26 | 22.37 | 24.96 |
| trefoil factor 3, intestinal | * | 8.4 | 20.09 |
| ubiquitin D | 1.96 | 21.04 | 15.36 |
| Ia-associated invariant chain | 3.18 | 11.9 | 15.06 |
| histocompatibility 2, class II antigen A, alpha | 3.75 | 13.98 | 10.5 |
| tubulin, beta 2 | * | * | 7.4 |
| chemokine (C-X-C motif) ligand 13 | * | 4.61 | 5.99 |
| apoptosis inhibitor 6 | 2.38 | 4.77 | 5.99 |
| glycoprotein 49 A | * | 3.04 | 5.69 |
| cathepsin S | 2.35 | 4.24 | 5.38 |
| insulin-like growth factor binding protein 1 | * | * | 5.31 |
| ADP-ribosyltransferase 2a | 3.37 | 5.47 | 5.07 |
| chemokine (C-X-C motif) ligand 9 | 2.16 | 17.3 | 5.05 |
| procollagen, type IV, alpha 1 | * | 2.08 | 5.04 |
| immunoglobulin kappa chain variable 28 (V28) | * | * | 4.93 |
| CD53 antigen | 1.84 | 3.82 | 4.92 |
| Fc receptor, IgE, high affinity I, gamma polypeptide | * | 5.82 | 4.79 |
| phospholipase A2 group VII (platelet-activating factor acetylhydrolase, plasma) | * | 4.02 | 4.71 |
| chemokine (C-C) receptor 5 | * | 5.33 | 4.7 |
| complement component 1, q subcomponent, beta polypeptide | 1.91 | 4.6 | 4.69 |
| proteosome (prosome, macropain) subunit, beta type 8 (large multifunctional protease 7) | 3.7 | 5.93 | 4.59 |
| complement component 1, q subcomponent, alpha polypeptide | 1.81 | 4.33 | 4.09 |
| expressed sequence AU046135 | * | 2.88 | 3.82 |
| glycoprotein 49 B | * | * | 3.81 |
| lysozyme | * | 5.82 | 3.79 |
| leukocyte specific transcript 1 | 1.68 | 4.54 | 3.78 |
| complement component 1, q subcomponent, c polypeptide | 1.79 | 4.15 | 3.71 |

**Table 1 (continued)**

| Gene | 3 months | 6 months | 12 months |
|---|---|---|---|
| cytochrome P450, 2b9, phenobarbitol inducible, type a | * | * | 3.62 |
| serum amyloid A 3 | 2.21 | 15.37 | 3.6 |
| H19 fetal liver mRNA | * | * | 3.56 |
| proteoglycan, secretory granule | * | 3.02 | 3.52 |
| protein tyrosine phosphatase, non-receptor type substrate 1 | * | 3.43 | 3.51 |
| cytochrome P450, 2b13, phenobarbitol inducible, type c | * | * | 3.46 |
| serum amyloid A 2 | 5.14 | 2.22 | 3.29 |
| ESTs, Moderately similar to hypothetical protein FLJ11127 (Homo sapiens) (H.sapiens) | * | 3.54 | 3.28 |
| Mus musculus, Similar to hypothetical protein FLJ20509, clone IMAGE:3489119, mRNA, partial cds | * | * | 3.27 |
| ESTs, Weakly similar to RIKEN cDNA 0610011E17 (Mus musculus) (M.musulus) | * | * | 3.21 |
| histocompatibility 2, T region locus 17 | 2.11 | 2.85 | 3.19 |
| CD52 antigen | 2 | 4.71 | 3.17 |
| lectin, galactose binding, soluble 3 | * | 5.28 | 3.14 |
| TAP binding protein | 1.64 | 3.42 | 3.14 |
| signal transducer and activator of transcription 1 | 2.57 | 5.75 | 3.11 |
| proteosome (prosome, macropain) subunit, beta type 9 (large multifunctional protease 2) | 3.77 | 6.28 | 3.1 |
| chemokine (C-X-C motif) ligand 1 | * | 4 | 3.1 |
| Cluster Incl M17790:Serum amyloid A pseudogene /cds=(0,251) /gb=M17790 /gi=200920 /ug=Mm.56949 /len=252 | 4.22 | 13.87 | 3.06 |
| macrophage receptor with collagenous structure | 6.49 | * | 3 |
| C-type (calcium dependent, carbohydrate recognition domain) lectin, superfamily member 13 | 1.43 | * | 2.99 |
| RIKEN cDNA 2310057H16 gene | * | * | 2.96 |
| lymphocyte antigen 6 complex, locus A | 6.45 | 5.38 | 2.95 |
| histocompatibility 2, T region locus 10 | 2.14 | 2.99 | 2.95 |
| guanylate nucleotide binding protein 2 | 2.55 | 7.62 | 2.91 |
| expressed sequence AI854770 | 1.7 | 2.28 | 2.9 |

**Table 1 (continued)**

| Gene | 3 months | 6 months | 12 months |
|---|---|---|---|
| macrophage expressed gene 1 | 2.45 | 3.79 | 2.84 |
| ADAM-like, decysin 1 | * | 2.11 | 2.83 |
| interferon gamma inducible protein, 47 kDa | 1.83 | 2.92 | 2.81 |
| retinol binding protein 1, cellular | * | 2.74 | 2.8 |
| hydroxyacid oxidase (glycolate oxidase) 3 | * | * | 2.72 |
| expressed sequence AW112010 | 2.02 | 2.84 | 2.68 |
| tubulin, beta 3 | * | * | 2.68 |
| tubulin, beta 5 | * | * | 2.67 |
| CREBBP/EP300 inhibitory protein 1 | * | 2.24 | 2.63 |
| retinoic acid early transcript gamma | * | 1.69 | 2.63 |
| carbon catabolite repression 4 homolog (S. cerevisiae) | * | 2.03 | 2.6 |
| paired-Ig-like receptor A1 | * | 3.24 | 2.6 |
| vascular cell adhesion molecule 1 | 4.06 | 4.64 | 2.59 |
| histocompatibility 2, class II, locus Mb1 | 2.95 | 5.94 | 2.59 |
| histocompatibility 2, class II antigen E beta | 2.44 | 5.06 | 2.53 |
| transporter 2, ATP-binding cassette, sub-family B (MDR/TAP) | 1.76 | 3.1 | 2.52 |
| orosomucoid 2 | * | 1.94 | 2.52 |
| protamine 2 | 2.08 | * | 2.52 |
| solute carrier family 4 (anion exchanger), member 4 | * | * | 2.49 |
| glutathione S-transferase, mu 2 | * | 2.3 | 2.48 |
| cystatin B | * | 2.96 | 2.48 |
| Cluster Incl U38967:Prothymosin beta | 1.56 | 2.88 | 2.48 |
| reticulon 4 | 1.9 | 2.88 | 2.48 |
| cytochrome b-245, alpha polypeptide | 1.53 | 3.04 | 2.47 |
| lipoprotein lipase | * | * | 2.44 |
| intercellular adhesion molecule | * | 2.19 | 2.44 |
| IQ motif containing GTPase activating protein 1 | * | 2.11 | 2.42 |
| amyloid beta (A4) precursor protein-binding, family B, member 1 interacting protein | * | 2.52 | 2.4 |
| lymphocyte antigen 6 complex, locus E | 2.01 | 2.92 | 2.36 |
| myristoylated alanine rich protein kinase C substrate | * | 1.91 | 2.34 |

**Table 1 (continued)**

| Gene | 3 months | 6 months | 12 months |
|---|---|---|---|
| histocompatibility 2, D region locus 1 | 1.73 | 2.64 | 2.31 |
| fibrinogen-like protein 2 | 2.21 | 4.3 | 2.31 |
| lipoprotein lipase | * | * | 2.31 |
| intracisternal A particles | * | 1.95 | 2.3 |
| TAP binding protein | 1.64 | 3.42 | 2.3 |
| MARCKS-like protein | * | 1.96 | 2.28 |
| lipopolysaccharide binding protein | 1.71 | 2 | 2.27 |
| circadian locomoter output cycles kaput | * | * | 2.27 |
| eukaryotic translation initiation factor 1A | * | * | 2.26 |
| interferon gamma induced GTPase | 2.86 | 3.97 | 2.26 |
| mitogen activated protein kinase kinase kinase 1 | * | * | 2.24 |
| ribosomal protein L7 | * | * | 2.23 |
| secreted phosphoprotein 1 | * | * | 2.21 |
| chloride intracellular channel 1 | * | 2.56 | 2.2 |
| decorin | * | * | 2.17 |
| annexin A1 | * | 1.98 | 2.16 |
| expressed sequence AW547365 | * | * | 2.16 |
| transporter 1, ATP-binding cassette, sub-family B (MDR/TAP) | 1.84 | 2.99 | 2.15 |
| long chain fatty acyl elongase | -1.46 | * | 2.14 |
| acidic (leucine-rich) nuclear phosphoprotein 32 family, member A | * | * | 2.14 |
| lymphocyte antigen 86 | 1.58 | 2.39 | 2.13 |
| CD9 antigen | * | 1.93 | 2.12 |
| ADP-ribosylation-like factor 6 interacting protein 5 | * | * | 2.1 |
| polymerase (DNA directed), gamma | * | * | 2.1 |
| hypothetical protein MGC47434 | * | * | 2.08 |
| properdin factor, complement | 1.42 | 2.92 | 2.07 |
| B-cell translocation gene 1, anti-proliferative | * | * | 2.06 |
| erythroid differentiation regulator | * | * | 2.06 |
| tubulin, alpha 6 | * | * | 2.06 |
| annexin A5 | * | 2.39 | 2.03 |
| guanylate nucleotide binding protein 3 | 3.03 | 6.67 | 2.03 |
| chemokine (C-X-C motif) ligand 1 | * | 4 | 2.02 |
| flavin containing monooxygenase 3 | * | * | 2 |
| dystroglycan 1 | * | * | 2 |

**Table II**. Genes with down-regulated transcription in the livers of of *H. hepaticus* infected male A/JCr mice with severe disease versus sham-infected controls (fold decrease).

| Gene | 3 months | 6 months | 12 months |
|---|---|---|---|
| hydroxysteroid dehydrogenase-5, delta<5>-3-beta | -3.32 | -13.47 | -28 |
| aminolevulinic acid synthase 1 | * | * | -5.45 |
| D site albumin promoter binding protein | * | * | -5.37 |
| cytochrome P450, 7b1 | * | -2.09 | -4.68 |
| thyroid hormone responsive SPOT14 homolog (Rattus) | * | * | -3.94 |
| metallothionein 1 | +4.3 | +2.14 | -3.59 |
| kidney expressed gene 1 | * | * | -3.57 |
| cytochrome P450, 7b1 | * | * | -3.36 |
| RIKEN cDNA 2410041F14 gene | * | * | -2.99 |
| epidermal growth factor receptor | * | * | -2.97 |
| expressed sequence AI467657 | * | * | -2.88 |
| G0/G1 switch gene 2 | * | * | -2.83 |
| homocysteine-inducible, endoplasmic reticulum stress-inducible, ubiquitin-like domain member 1 | * | * | -2.78 |
| sialyltransferase 9 (CMP-NeuAc:lactosylceramide alpha-2,3-sialyltransferase) | +2.24 | * | -2.78 |
| Cluster Incl V00722:Mouse gene for beta-1-globin | * | * | -2.65 |
| sulfotransferase-related protein SULT-X1 | * | * | -2.64 |
| eleven-nineteen lysine-rich leukemia gene | * | -1.94 | -2.58 |
| ubiquitin specific protease 2 | * | * | -2.56 |
| serine (or cysteine) proteinase inhibitor, clade E, member 2 | * | * | -2.53 |
| expressed sequence AI266885 | +1.51 | | -2.5 |
| period homolog 2 (Drosophila) | * | * | -2.39 |
| solute carrier family 10 (sodium/bile acid cotransporter family), member 1 | * | * | -2.36 |
| MAP kinase-interacting serine/threonine kinase 2 | * | * | -2.35 |
| glucose-6-phosphatase, transport protein 1 | * | * | -2.24 |
| expressed sequence C77405 | * | * | -2.24 |
| amiloride-sensitive sodium channel | * | * | -2.23 |
| hemoglobin, beta adult major chain | * | * | -2.21 |
| angiopoietin-like 4 | * | * | -2.19 |
| pre-B-cell colony-enhancing factor | +1.51 | +1.58 | -2.18 |
| P450 (cytochrome) oxidoreductase | * | * | -2.17 |
| peroxisomal delta3, delta2-enoyl-Coenzyme A isomerase | * | -1.61 | -2.14 |
| DnaJ (Hsp40) homolog, subfamily A, member 1 | * | * | -2.11 |
| epidermal growth factor receptor | * | * | -2.1 |
| BCL2/adenovirus E1B 19 kDa-interacting protein 1, NIP3 | * | * | -2.03 |
| elastase 1, pancreatic | -1.43 | -1.85 | -2.01 |
| colony stimulating factor 2 receptor, beta 1, low-affinity (granulocyte-macrophage) | * | * | -2.01 |
| interleukin 1 receptor, type I | +1.82 | * | -2 |

Gene ontology clusters

Gene ontology (www.geneontology.org) describes gene products in three structured controlled vocabularies related to biological process, cellular components, and molecular functions. Microarray analysis generated multiple biological process ontology clusters for hepatic lesions of *H. hepaticus* infected A/JCr mice at all three time points (Table III). There were several biological processes involved over the entire 12 month time period pertaining to an active infection including gene products associated with the defense response, immune response, acute phase response, antigen presentation and processing, MHC receptor activity, lysosomes, and others represented in red print in Table III. At 6 months post *H. hepaticus* infection, the 3 month inflammatory biological processes were maintained and a chemokine activity cluster was added. Gene products associated with electron transport and lipid transport demonstrated increased activity (Table III, blue print). At 12 months, new clusters of biological processes indicated gene products involved with structural change, increased signal transduction, and peroxisome organization (Table III, green print).

**Table III: Gene Ontology Clusters**

Gene Categories at 3, 6, 12 months

Endoplasmic reticulum (3,6,12)

Cytosol (3,6,12)

Defense response (3,6,12)

Acute-phase response (3,6,12)

Immune response (3,6,12)

Cell surface (3,6,12)

Membrane (3,6,12)

Integral to membrane (3,6,12)

Antigen presentation, endogenous antigen (3,6,12)

Antigen presentation, exogenous antigen (3,6,12)

Antigen processing, endogenous antigen via MHC class I (3,6,12)

Antigen processing, exogenous antigen via MHC class II (3,6,12)

MHC Class I receptor activity (3,6,12)

MHC class II receptor activity (3,6,12)

Extracellular space (3,6,12)

Lysosome (3,6,12)

Plasma membrane (3,6,12)

Monooxygenase activity (3,6,12)

Oxidoreductase activity (3,6,12)

Complement activation (3,6)

External side of plasma membrane (3,6)

Antigen presentation, exogenous antigen via MHC class II (3,6)

Complement activation /classical pathway (3,6)

Peptidase activity (3,6)

Mitochondrion (3,12)

GTPase (3)

Microsome (3)

Chemokine activity (6,12)

Electron transport (6,12)

Integral to plasma membrane (6,12)

Lipid transporter activity (6,12)

Inflammatory response (6)

Extracellular (6)

Catalytic activity (6)

GTPase activity (12)

GTP binding (12)

Microtubule (12)

Carboxylic ester hydrolase activity (12)

Microtubule-based process (12)

Microtubule-based movement (12)

Serine esterase activity (12)

Peroxisome organization and biogenesis (12)

Scavenger receptor activity (12)

Structural molecule activity (12)

Structural constituent of cytoskeleton (12)

Signal transduction (12)

Transporter activity (12)

Structural constituent of ribosome (12)

Protein domain clusters

Protein domain clusters produced via microarray analysis indicated regulatory proteins and systems involved during *H. hepaticus* pathogenesis (Table IV). These domains often mediate interactions of regulatory protein construction or have enzymatic activity (Pawson and Nash 2003). As with the gene ontology clusters, some protein domain clusters were involved throughout the 12 month experimental period and were immunoglobulin related (Table IV, red print). The immunoglobulin C-type protein domain involvement began at 6 months, as did chemokine and serum amyloid protein interactions (Table IV, green print). At 12 months, structural activity promoted by tubulin domains was evident (Table IV, blue print).

**Table IV: Protein Domain Clusters**

**Protein Domains**

ATP/GTP-binding site motif A (P-loop) (3,6,12)

Immunoglobulin/major histocompatibility complex (3,6,12)

Immunoglobulin-like (3,6,12)

Serum Amyloid A protein (6)

Small chemokine, interleukin 8 like (6)

Immunoglobulin, C-type (6,12)

Small chemokine, C-X-C subfamily (6,12)

Tubulin family (12)

Tyrosine protein kinase, active site (12)

Immune response gene expression

The individual genes members of the immune response biological process and their differential response at 3, 6, and 12 months are presented in Table V. Four hundred sixteen genes are members of this gene ontology biological process category. Table V genes include individual histocompatibility, chemokine, serum amyloid, and complement, and confirm the gene category clusters and protein domain clusters results.

**Table V**. Gene Ontology category: Immune Response. Genes with up-regulated transcription in the livers of of *H. hepaticus* infected male A/JCr mice with severe disease versus sham-infected age-matched controls (fold increase).

| Symbol | Gene | 3 months | 6 months | 12 months |
|---|---|---|---|---|
| Ii | Ia-associated invariant chain | 3.18 | 11.9 | 15.06 |
| H2-Aa | histocompatibility 2, class II antigen A, alpha | 3.75 | 13.98 | 10.5 |
| Cxcl13 | chemokine (C-X-C motif) ligand 13 | * | 4.61 | 5.99 |
| Cxcl9 | chemokine (C-X-C motif) ligand 9 | 2.16 | 17.3 | 5.05 |
| Igk-V8 | immunoglobulin kappa chain variable 8 (V8) | * | * | 4.93 |
| Pla2g7 | phospholipase A2, group VII (platelet-activating factor acetylhydrolase, plasma) | * | 4.02 | 4.71 |
| C1qb | complement component 1, q subcomponent, beta polypeptide | 1.91 | 4.6 | 4.69 |
| Psmb8 | proteosome (prosome, macropain) subunit, beta type 8 (large multifunctional protease 7) | 3.7 | 5.93 | 4.59 |
| C1qa | complement component 1, q subcomponent, alpha polypeptide | 1.81 | 4.33 | 4.1 |
| C1qg | complement component 1, q subcomponent, gamma polypeptide | 1.79 | 4.15 | 3.71 |
| Saa3 | serum amyloid A 3 | 2.21 | 15.37 | 3.6 |
| Saa2 | serum amyloid A 2 | 5.14 | 12.87 | 3.29 |
| Cxcl1 | chemokine (C-X-C motif) ligand 1 | * | 4 | 3.1 |
| Psmb9 | proteosome (prosome, macropain) subunit, beta type 9 (large multifunctional protease 2) | 3.77 | 6.28 | 3.1 |
| H2-T10 | histocompatibility 2, T region locus 10 | 2.14 | 2.99 | 2.95 |
| Gbp2 | guanylate nucleotide binding protein 2 | 2.55 | 7.62 | 2.91 |
| H2-DMb1 | histocompatibility 2, class II, locus Mb1 | 2.95 | 5.94 | 2.59 |
| H2-Eb1 | histocompatibility 2, class II antigen E beta | 2.44 | 5.06 | 2.53 |
| Tap2 | transporter 2, ATP-binding cassette, sub-family B (MDR/TAP) | 1.76 | 3.1 | 2.53 |
| Orm2 | orosomucoid 2 | * | 2.92 | 2.52 |
| H2-D1 | histocompatibility 2, D region locus 1 | 1.73 | 2.64 | 2.3 |
| Tap1 | transporter 1, ATP-binding cassette, sub-family B (MDR/TAP) | 1.84 | 2.99 | 2.16 |
| Ly86 | lymphocyte antigen 86 | 1.58 | 2.39 | 2.13 |
| Pfc | properdin factor, complement | 1.42 | 2.92 | 2.07 |
| Il1rn | interleukin 1 receptor antagonist | * | * | 2.05 |
| Gbp3 | guanylate nucleotide binding protein 3 | 3.03 | 6.67 | 2.03 |

Pathogen response gene expression

The Gene Ontology pathogen response biological process category consists of 241 genes and is a sub-category of the immune response. The individual genes and their differential response at 3, 6, and 12 months are presented in Table VI. This pattern of individual chemokine, immunoglobulin, acute phase, and complement genes change expression putatively due to *H. hepaticus* infection.

**Table VI**. Gene Ontology category: Pathogen Response. Genes with up and down regulated transcription in the livers of of *H. hepaticus* infected male A/JCr mice with severe disease versus sham-infected controls (fold increase/decrease).

| Symbol | Gene | 3 months | 6 months | 12 months |
|---|---|---|---|---|
| Cxcl13 | chemokine (C-X-C motif) ligand 13 | * | 4.61 | 5.99 |
| Cxcl9 | chemokine (C-X-C motif) ligand 9 | 2.16 | 17.3 | 5.05 |
| Igk-V8 | immunoglobulin kappa chain variable 8 (V8) | * | * | 4.93 |
| Pla2g7 | phospholipase A2, group VII (platelet-activating factor acetylhydrolase, plasma) | * | 4.02 | 4.71 |
| C1qb | complement component 1, q subcomponent, beta polypeptide | 1.91 | 4.6 | 4.69 |
| C1qa | complement component 1, q subcomponent, alpha polypeptide | 1.81 | 4.33 | 4.1 |
| C1qg | complement component 1, q subcomponent, gamma polypeptide | 1.79 | 4.15 | 3.71 |
| Saa3 | serum amyloid A 3 | 2.21 | 15.37 | 3.6 |
| Saa2 | serum amyloid A 2 | 5.14 | 12.87 | 3.29 |
| Cxcl1 | chemokine (C-X-C motif) ligand 1 | * | 4 | 3.1 |
| Orm2 | orosomucoid 2 | * | 2.92 | 2.52 |
| Ly86 | lymphocyte antigen 86 | 1.58 | 2.39 | 2.13 |
| | | | | |
| Dnaja1 | DnaJ (Hsp40) homolog, subfamily A, member 1 | * | * | -2.11 |
| Herpud1 | homocysteine-inducible, endoplasmic reticulum stress-inducible, ubiquitin-like domain member 1 | * | * | -2.78 |

Cell proliferation, growth, and death

Gene ontology categories suggestive of pre-neoplasia were investigated and included cell proliferation, cell growth, and cell death (Table VII). Some of the genes, as would be expected, suggest inflammatory cell turnover. Other genes do not necessarily fit into the inflammatory category including two oncogenes, the Kirsten rat sarcoma oncogene 2 (K-ras) and the Jun-B oncogene, that were slightly up-regulated 12 months post infection.

**Table VII**. Gene Ontology category: Cell Proliferation, Growth, and Death. Genes with up and down regulated transcription in the livers of of *H. hepaticus* infected male A/JCr mice with severe disease versus sham-infected controls (fold increase/decrease).

| Symbol | Gene | 3 months | 6 months | 12 months |
|---|---|---|---|---|
| Cxcl1 | chemokine (C-X-C motif) ligand 1 | * | 4 | 3.1 |
| Tgfa | transforming growth factor alpha | * | * | 2.9 |
| Prm2 | protamine 2 | 2.08 | -1.62 | 2.52 |
| Polg | polymerase (DNA directed), gamma | * | * | 2.1 |
| Btg1 | B-cell translocation gene 1, anti-proliferative | * | * | 2.06 |
| Cdkn1a | cyclin-dependent kinase inhibitor 1A (P21) | 2.95 | 2.96 | 1.95 |
| Nfkbia | nuclear factor of kappa light chain gene enhancer in B-cells inhibitor, alpha | * | 1.39 | 1.92 |
| Ahr | aryl-hydrocarbon receptor | * | * | 1.9 |
| Kras2 | Kirsten rat sarcoma oncogene 2, expressed | * | * | 1.69 |
| Macf1 | microtubule-actin crosslinking factor 1 | * | * | 1.54 |
| Ccnd1 | cyclin D1 | 1.69 | 3.21 | 1.53 |
| Ifnar2 | interferon (alpha and beta) receptor 2 | * | * | 1.51 |
| Gas2 | growth arrest specific 2 | * | * | 1.46 |
| Stat6 | signal transducer and activator of transcription 6 | * | * | 1.44 |
| Junb | Jun-B oncogene | * | * | 1.3 |
| | | | | |
| Cul4a | cullin 4A | * | * | -1.42 |
| Gspt2 | G1 to phase transition 2 | * | * | -1.45 |
| Nfix | nuclear factor I/X | * | * | -1.62 |
| Ches1 | checkpoint suppressor 1 | * | * | -1.67 |
| Fgf1 | fibroblast growth factor 1 | * | -1.71 | -1.71 |
| G0s2 | G0/G1 switch gene 2 | * | * | -2.83 |
| Egfr | epidermal growth factor receptor | * | * | -2.97 |

* No Differential Expression

Microarray Model Validation

Microarray results were tightly correlated ($r>0.99$ for controls and $r>0.97$ for mice with lesions) between biological replicates (individual mouse liver per array) (Figure. 3A). There was a moderate correlation between infected male mice that did not develop significant disease and uninfected controls (Figure 3C). In contrast, the correlation lessened substantially ($r<0.79$) between infected mice that developed severe disease and uninfected controls (Figure.3D). These results confirm that histologic assessment of lesion severity is reflected by global gene expression profile alterations, represented by all the genes not on the linear scatterplot as seen in Figure 3D. These genes have differential expression as compared to the controls in Figure 3A.

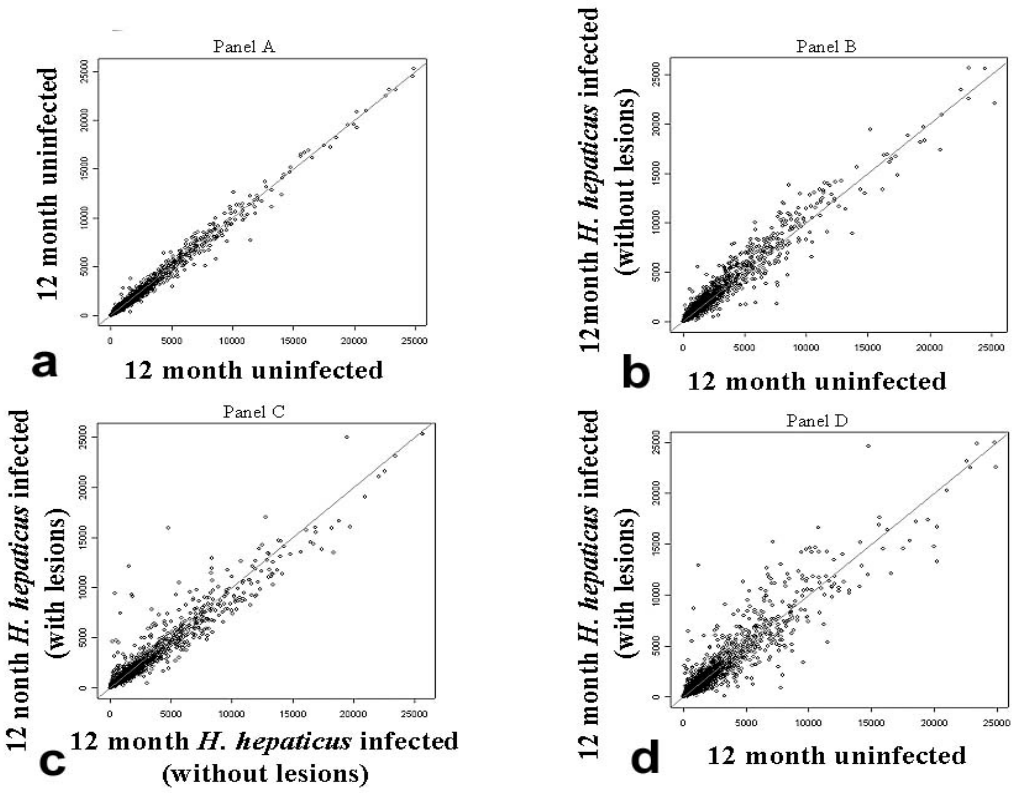


**Figure 3.** Scatterplots highlighting variable degrees of correlation between microarray results from different groups of male A/JCr mice at 12 months. (a) High correlation between biological replicates ($r>0.99$). (b) *H. hepaticus*-infected mice that did not develop disease are better correlated with sham-infected controls ($r>0.97$) (c) than with infected diseased mice. (d). Marked discorrelation between infected mice with disease and sham-infected controls ($r<0.79$)

Differential gene expression for aging

The experimental design enabled comparisons of transcription profiles due to aging. Aging control mice yielded 402 differentially expressed genes at 6 months versus 3 months, 675 at 12 months versus 3 months, and 437 at 12 months versus 6 months. Although a large number of genes were associated with aging, the magnitude of hepatic expression differences was small (–6 to +10). Additional aging results are presented under linear discriminant analysis and principal component analysis.

Hierarchical clustering

Hierarchical clustering allowed age-matched A/JCr mice pairs with lesions to be differentiated from controls. The dChip option of combined hierarchical clustering of mouse microarray samples and genes produced very similar 'heatmap' patterns between mouse microarray sample pairs within 6 groups, with each group displaying a different pattern (Figure 4). The increasing intensity of red (green) in the heatmap indicates an increasing (decreasing) expression level. The mice groups are labeled at the top of each column of the heatmap and consisted of the following pairs of arrays: (1) 3 month controls (3u1, 3u2) (u: uninfected) (2) 6 month controls (6u1, 6u2) (3) 12 month controls (12u1, 12u2) (4) 3 month *H. hepaticus* infected A/J mice with lesions (3L1, 3L2) (L: lesions) (5) 6 month *H. hepaticus* infected A/J mice with lesions (6L1, 6L2) (6) 12 month *H. hepaticus* infected A/J mice with lesions (12L1, 12L2) (Figure 4).

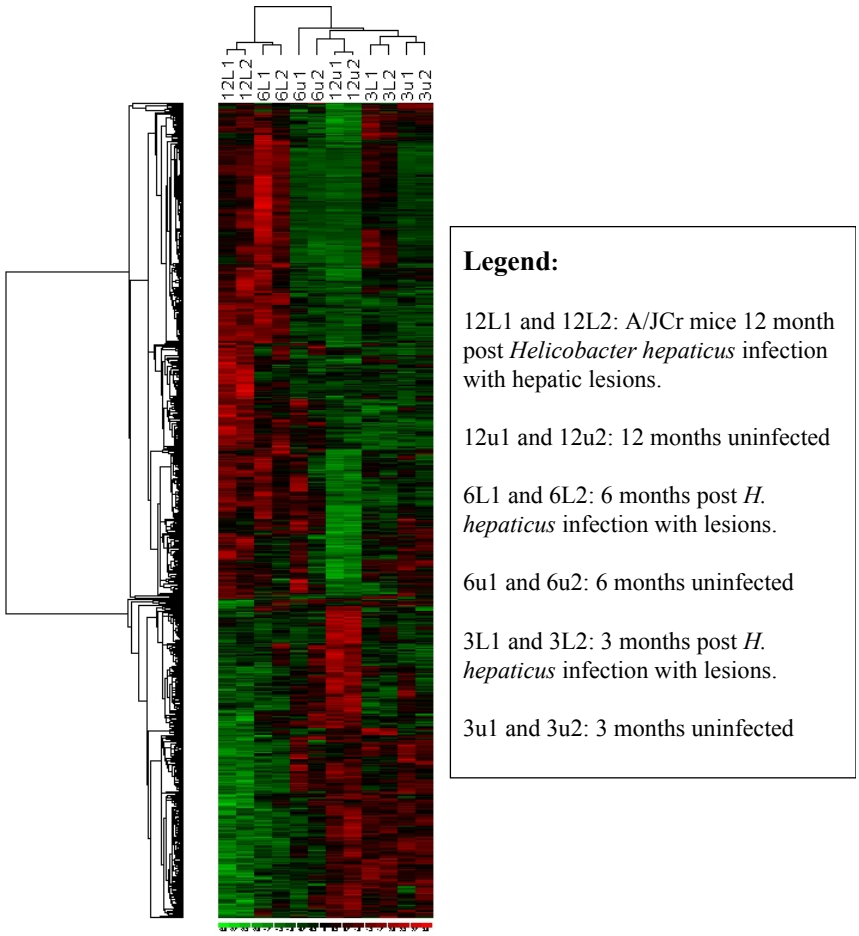


**Figure 4.** Hierarchical clustering and two dimensional dendrogram. Columns represent individual A/JCr mice and rows represent genes. Every 2 columns represent the same group with a total of 6 groups. Columns exhibiting similar patterns are representative of groups of mice based on age and lesion status. The A/JCr mice illustrated are *H. hepaticus* infected with lesions and age matched uninfected controls.

Linear discriminant analysis and principal component analysis

Linear discriminant analysis also differentiated between controls and *H. hepaticus* infected A/J mice with hepatic lesions (Figure 5). The control mice and the mice with hepatic lesions occupied opposite sides of the plot. Principal component analysis provided even more powerful classification of A/JCr mice groups. This algorithm produced regions of different ages for controls and for age groups of *H. hepaticus* infected A/J mice with lesions (Figure 6). However, these clear demarcations occurred only when the analysis omitted the transcription profile data for infected mice without lesions. Therefore, the LDA and PCA did not clearly differentiate the infection status of the mice when the livers were histologically normal at 3 and 6 months, but did indicate differences at 12 months post infection (data not shown).

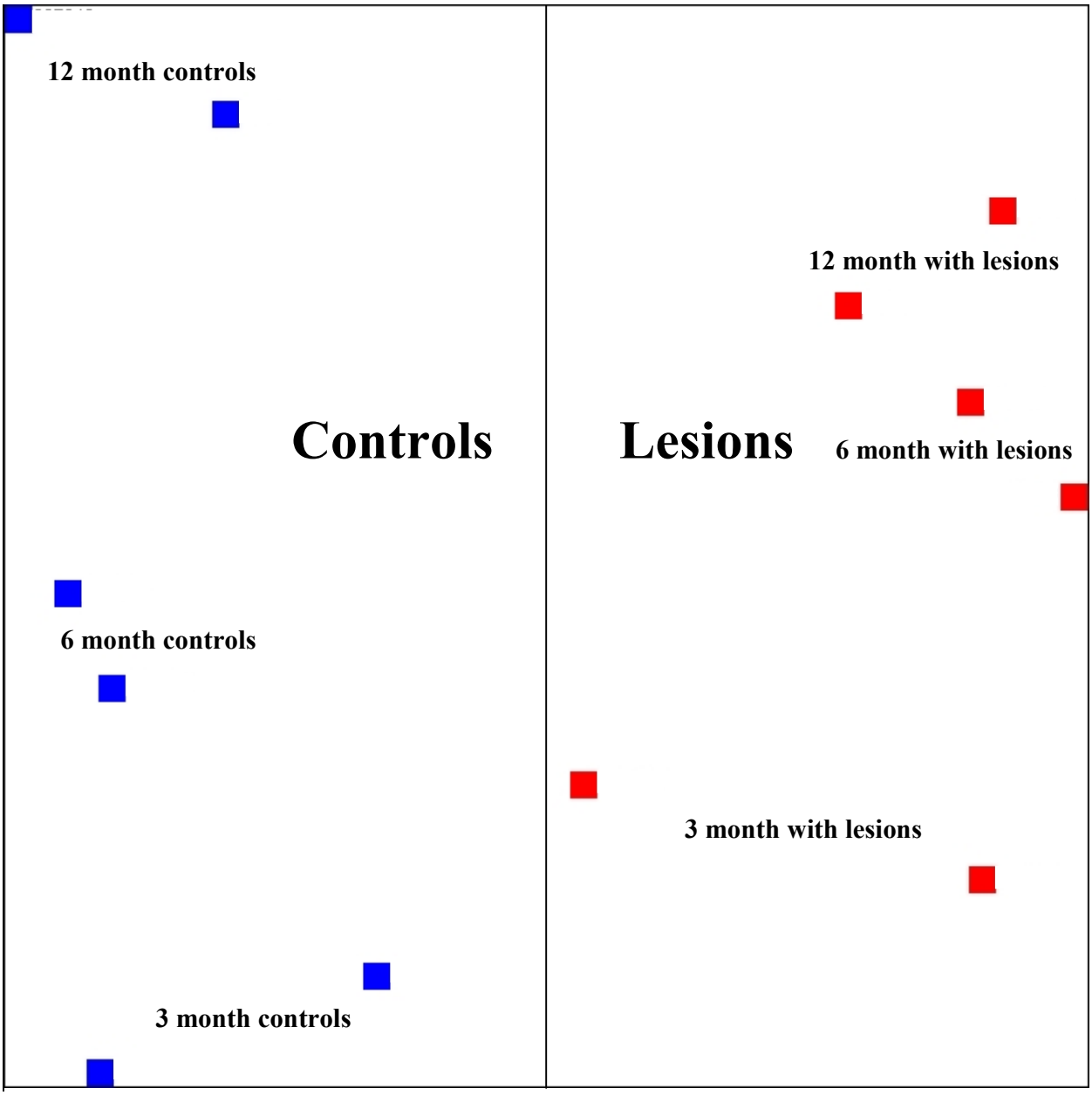


**Figure 5.** Linear discriminant analysis demonstrating differentiation of the 6 groups by lesion status. Each box represents an A/JCr mouse. Note the mice on different sides of the plot. The A/JCr mice illustrated are *H. hepaticus* infected with lesions and age matched controls.

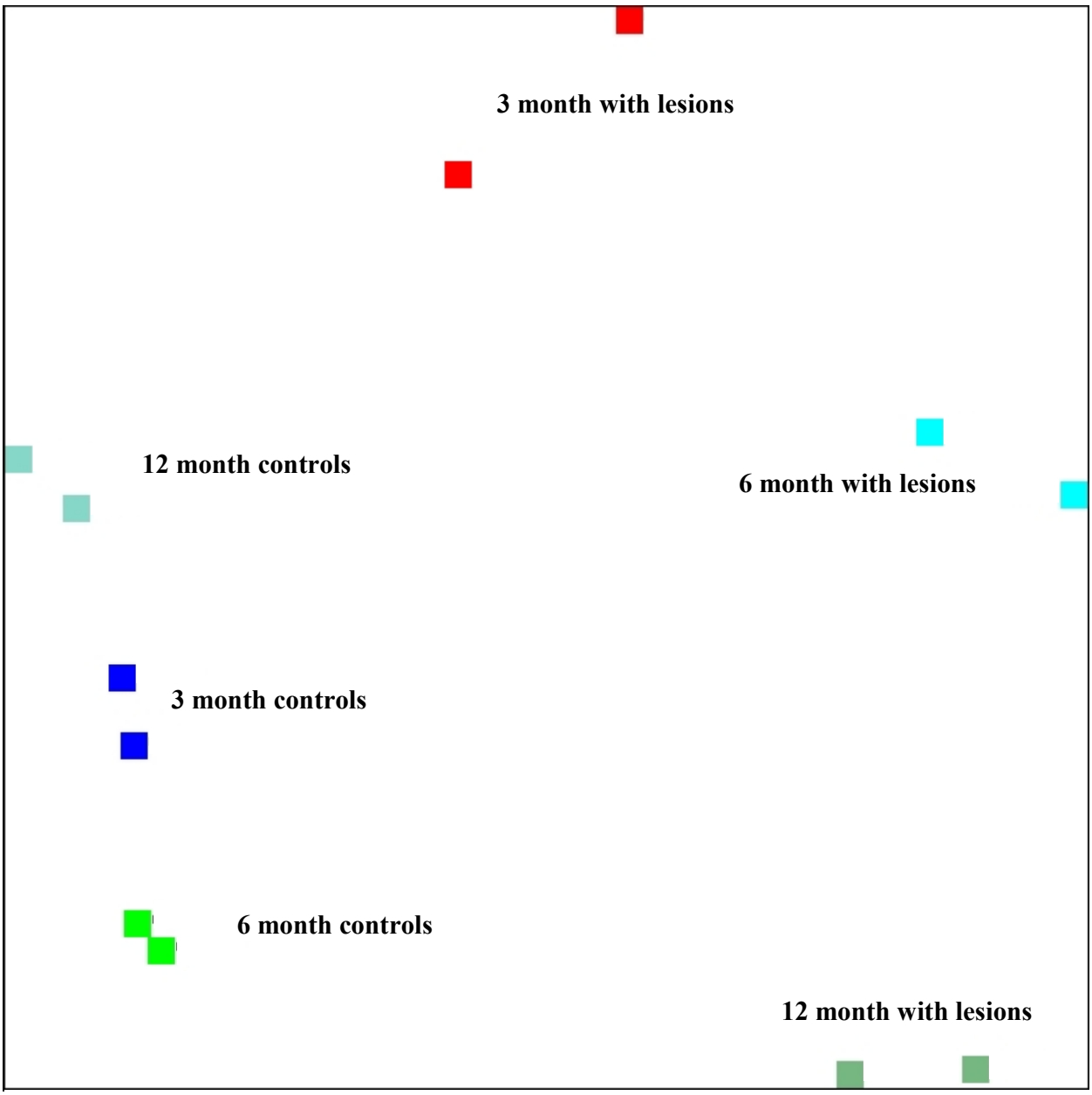


**Figure 6.** Principal component analysis demonstrating differentiation of the groups by age and lesion status. Each box represents an A/JCr mouse. Note the mice are clustered in separate regions. The A/JCr mice illustrated are *H. hepaticus* infected with lesions and age matched controls.

Microarray result verification by quantitative real time RT-PCR

The Assay on Demand results validated the Affymetrix microarray values except for 2 data points where fold changes were less than 2 for both methods (Figure 7).

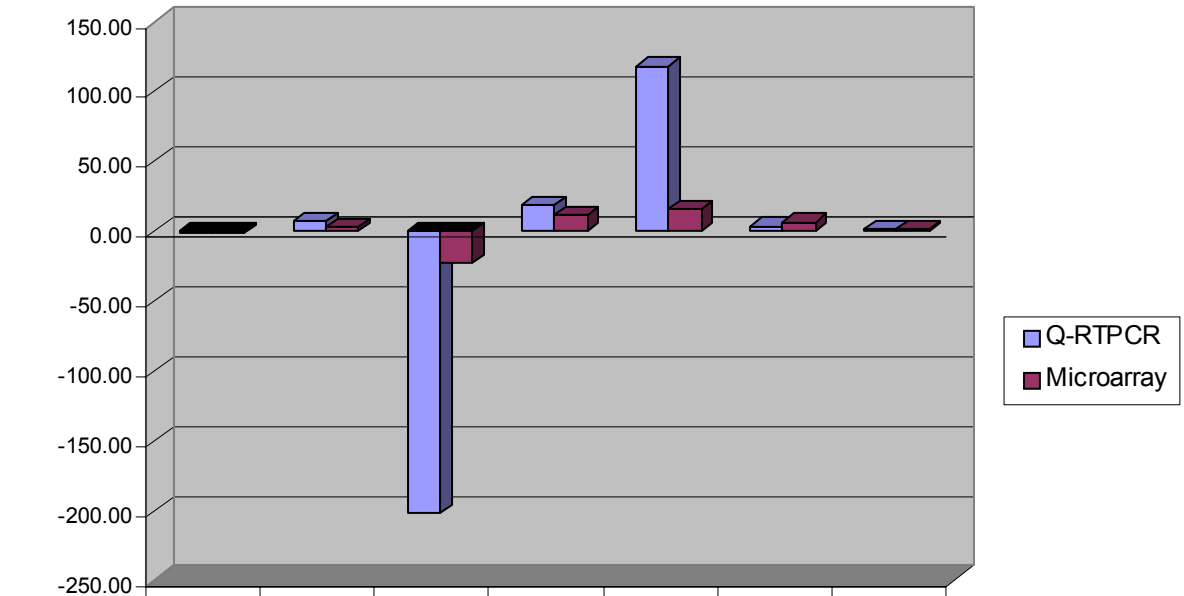


| | Cyp4a14 | H19 | Hsd3b5 | Ubd | Tff3 | Api6 | Igtp |
|---|---|---|---|---|---|---|---|
| Q-RTPCR | -1.78 | 6.99 | -201.55 | 18.70 | 118.19 | 3.71 | 1.26 |
| Microarray | -1.28 | 3.14 | -23.25 | 11.58 | 16.28 | 6.53 | 2.05 |

**Figure 7.** Microarray (Affymetrix) result validation with RT-PCR (Assay on Demand). Rank invariant normalization to a baseline microarray was used for the microarray results (dChip). Normalization to GAPDH is used for the quantitative real time RT-PCR.

**Discussion**

Microarray analysis of the livers of *H. hepaticus* infected A/JCr mice demonstrated reproducible changes in global transcription profiles at 3, 6, and 12 months that were indicative of the progressive liver disease illustrated by histopathology. The progressive severity of hepatitis and dysplasia in infected mice was associated with an increasing number of differentially expressed genes and a specific transcription profile. The gene expression signature of age matched controls and age matched infected mice with lesions could be differentiated from each other utilizing hierarchical clustering and principal component analysis. Whether the hepatic transcription profile can be used to identify the age at infection, the time post-infection, and the temporal course of the molecular pathogenesis will require additional study. The gene expression signature complements histopathology and PCR techniques and aids in diagnosis and prognosis for this experimental infection. Whether another strain of *H. hepaticus,* a different liver pathogen, or other liver insult yields a unique gene expression signature over time in various strains of mice is under investigation. Recent studies indicate a specific gene signature for virally induced HCC (Iizuka *et al.* 2004). Many of the same differentially expressed genes in mice infected with *H. hepaticus* have also been documented in other models of murine hepatic injury and hepatic tumor promotion (Graveel *et al.* 2001; Meyer *et al.* 2003; Nyska *et al.* 1997) . Some studies suggest the transcription profile of a small set of highly up-regulated or down-regulated genes are indicative of a particular disease while other studies indicate even very modest changes in a larger set of genes and pathways are suggestive of a specific disease (Etzioni *et al.* 2003; Mootha *et al.* 2003a).

Genes associated with neoplasia and proliferation

Two putative tumor markers, H19 fetal liver mRNA and intestinal trefoil factor 3 (Table I), were increasingly up-regulated over time in mice with progressive hepatocellular dysplasia. The product of the H19 gene is considered a non-messenger polyadenylated RNA molecule (Brannan *et al.* 1990). H19 has putative regulatory roles in normal development, hepatocyte proliferation, and in oncogenesis (Kaplan *et al.* 2003; Yamamoto *et al.* 2004). H19 shares the non-protein coding property with a rapidly growing number of novel transcripts, and recent experiments indicate that as much as an order of magnitude more chromosomal DNA is transcribed than accounted for by currently predicted and characterized exons (Kapranov *et al.* 2002). H19 is an imprinted gene with maternal allele expression. Loss of imprinting is a recognized human cancer risk, including genes H19, insulin-like growth factor 2 (Igf2), and cyclin dependent kinase inhibitor 1C (p57, KIP, CDK1NC) (Brannan and Bartolomei 1999; Kaplan *et al.* 2003; Vernucci *et al.* 2000). H19 and Igf2 are reciprocally imprinted, with Igf2 being expressed from the paternal allele (Vernucci *et al.* 2000). Igf2 is an anti-apoptotic factor associated with hepatocarcinogenesis, and is putatively activated and regulated by H19 (Vernucci *et al.* 2000). Although Igf2 up-regulation was not observed at 12 months by microarray analysis, there was nearly 2-fold down-regulation of the Igf2 receptor (Table II), and an inverse relationship has been observed between epidermal growth factor and its cognate receptor in mice infected with *H. hepaticus* (Ramljak *et al.* 1998). Insulin-like growth factor 1 (Igf1) is an acute phase protein that is decreased in plasma serum levels during systemic responses to inflammation (Gabay and Kushner 1999). Insulin-like growth factor binding protein 1 (Igfbp1) (Table I) was highly up-regulated in *H. hepaticus* infected A/JCr mice at 12 months with liver lesions and foci of altered

hepatocytes. Igfbp1 binds both Igf1 and Igf2 with high affinity. Igfbp1 putatively functions as a critical survival factor in the liver by suppressing the level and activation of specific proapoptotic factors via its regulation of integrin-mediated signaling (Leu *et al.* 2003). Igf1 is important in fetal growth and development (along with Igf2, the imprinted gene described above). Igf1 is expressed predominantly in the liver, and targeted gene knockout results in embryonic lethality in mice (Le Roith *et al.* 1999; Scharf *et al.* 2001; Yakar *et al.* 1999). Intestinal trefoil factor 3 is associated with enterohepatic inflammation, gastric cancer, colon cancer, pancreatic cancer, and breast cancer (Al-azzeh *et al.* 2002; Katoh 2003; Khan *et al.* 2003; Kimura *et al.* 2002; Leung *et al.* 2002; Rodrigues *et al.* 2003). This factor promotes epithelial cell migration and mucosal restitution during inflammation, and is differentially expressed in primary biliary cirrhosis (Kimura *et al.* 2002).

Cyclin D1 is overexpressed in many human and murine tumors (Hinds *et al.* 1994; Hinds and Weinberg 1994; Parker *et al.* 2003). Cyclin D1 (Ccnd1) affects G1 and was slightly up-regulated. Cyclin-dependent kinase inhibitor 1A (p21) (Cdkn1a) was also slightly up-regulated (Table VII). It maintains the G2 checkpoint and, after DNA damage, can arrest cells in G2. Cytolethal distending toxin (CDT) in several *Helicobacter* spp. including *H. hepaticus* causes cell cycle arrest in the G2/M phase resulting in cell distension in selected cell culture lines (Taylor *et al.* 2003; Young *et al.* 2000). An isogenic mutant of *H. hepaticus* lacking CDT activity when inoculated into C57BL/6 IL-$10^{-/-}$ produced less inflammatory bowel disease (IBD) when compared to its wild type counter part (Young *et al.* 2004). In another isogenic CDT mutant study, wild type *Campylobacter jejeuni* infected NF-κB deficient mice exhibited a moderately severe gastritis and proximal duodenitis at 4 months post infection while *C. jejeuni*

CDT mutant infected NF-κB deficient mice were consistently cleared of *C. jejeuni* at 4 months post infection. These results suggest CDT plays a role in inflammation and potentially participates in avoiding the immune response (Fox *et al.* 2004).

In addition to CDT's possible role in inflammation, dChip analysis indicates cytoskeletal organization effects by *H. hepaticus*, possibly in part due to CDT activity in the liver. Protein domain clusters associated with tubulin (Table III) and gene category clusters associated with structural constituents of the cytoskeleton, structural molecule movement, and microtubules are evident at 12 months (Table IV). CDT reportedly damages DNA via its CdtB subunit, a homologue of mammalian type I Dnase. CDT has putative nuclear localization signals and may induce apoptosis through activation of caspase 2 and caspase 7 (Lara-Tejero and Galan 2000; McSweeney and Dreyfus 2004; Ohara *et al.* 2004). Caspase 3 and caspase 2 were slightly upregulated in this study, but caspase 7 was not.

Two oncogenes, K-ras and Jun-B, were slightly upregulated at 12 months post *H. hepaticus* infection. The ras family, K-ras, N-ras, and H-ras are guanine nucleotide binding proteins involved in cell proliferation, differentiation, and survival (Chan *et al.* 2004). K-ras mediates cytokine signaling in formation of E-cadherin based adherens junctions in hepatocyte development(Matsui *et al.* 2002). Jun-B suppresses cell proliferation through its inhibition of activation protein transcription factor (AP-1), however overexpression of Jun-B putatively perpetuates undifferentiated cancers (Song *et al.* 2004). LPS from gram negative bacteria induces AP-1, but there was no differential expression of any of the sub-units of the AP-1 complex in this study. Mutations and increased expression in these genes have been reported in

myeloproliferative disease, colon cancer, breast cancer, prostate cancer, and metastases to the liver (Chan *et al.* 2004; Edwards *et al.* 2003; Frasor *et al.* 2003; Matsui *et al.* 2002; Palmer *et al.* 2003; Selvamurugan *et al.* 2004; Song *et al.* 2004). Although K-ras mutations have been reported in chemically induced hepatocellular carcinoma in the A/J mouse (Bai *et al.* 2003), K-ras, H-ras, and N-ras mutations have not been reported in A/J mice infected with *H. hepaticus* (Diwan *et al.* 1997; Sipowicz *et al.* 1997b). These data, indicating that *H. hepaticus* is non-genotoxic, are further documentation that *H. hepaticus* is acting as a tumor promoter.

Genes associated with inflammation

Chronic inflammation is a risk factor for cancer, and acute-phase proteins indicative of ongoing inflammation persisted at high levels over time in *H. hepaticus* -infected male mice with progressive disease (Gabay and Kushner 1999; Rogers and Fox 2004). One acute-phase protein, lipocalin 2 (Table I), was prominently up-regulated in the liver as a result of *H. hepaticus* infection. Lipocalin 2 is highly expressed in hepatocellular carcinoma via genotoxic or peroxisomal mechanisms (Meyer *et al.* 2003) and the lipocalin family is expressed in other forms of cancer including pancreatic, colorectal, and ovarian (Bartsch and Tschesche 1995; Bratt 2000; Furutani *et al.* 1998; Nielsen *et al.* 1996). Lipocalin 2 (Lpn2, uterocalin, 24p3, NGAL, SIP24) was discovered as a secreted, inducible protein from BALB/c 3T3 cells (Nilsen-Hamilton *et al.* 1982) and later identified as a product of mouse 24p3 mRNA and as an acute-phase protein (Liu and Nilsen-Hamilton 1995). Lipocalin 2 in the Gene Ontology system is considered a transporter. Reported roles of lipocalin 2 include mucosal immunity, epithelial development in the kidney, signaling, transport of non-transferrin-bound iron, chaperoning, apoptosis, retinol

transport, prostaglandin synthesis, and male scent expression (Cavaggioni and Mucignat-Caretta 2000; Devireddy *et al.* 2001; Tong *et al.* 2003; Xu and Venge 2000; Yang *et al.* 2003). Other lipocalins, up-regulated in this study include orosomucoid and retinol-binding protein. Other acute-phase proteins were up-regulated in *H. hepaticus* infected male A/JCr mice with severe disease. For example, serum amyloid A (Tables IV and V) is a hallmark indicator of active inflammation, and putatively activates neutrophils in addition to direct antimicrobial properties (Hatanaka *et al.* 2003; Ribeiro *et al.* 2003). Also up-regulated was properdin factor (Table V), a member of the alternative complement pathway of the innate immune system which binds to microbial surfaces. Ceruloplasmin, a plasma metalloprotein, binds copper and is involved in transferrin peroxidation. Haptoglobin protects against microbial growth by binding hemoglobin and preventing microbial access to iron (Eaton *et al.* 1982). Hemopexin binds heme and transports it to the liver for iron recovery.

Genes associated with Cytochrome P450

As seen in other rodent and human studies of hepatic injury, *H. hepaticus* infection in male A/JCr resulted in altered expression of several members of the cytochrome P450 (CYP) family. At 3 months, CYP2c37, 4a10, and 4a14 were down-regulated (Table II) while CYP2b10 was up-regulated (Table I). At 6 months, CYP2c37, 4a10, 4a14, 51, and 7b1 were down-regulated (Table II). At 12 months, the previously listed group remained down-regulated (Table II) while CYP2b9, 2b10, and 2b13 were up-regulated (Table I). Phenobarbital also up-regulates Cyp2b10 (Rivera-Rivera *et al.* 2003; Yoshinari *et al.* 2003). Phenobarbital promotes hepatic tumors initiated by compounds such as N-nitrosodiethylamine (NDMA) (Thirunavukkarasu and

Sakthisekaran 2003). These data are consistent with the hypothesis that *H. hepaticus* is a tumor promoter in the mouse liver initiated by NDMA (Diwan *et al.* 1997; Sipowicz *et al.* 1997b). Members of the cytochrome P450 family are integral to detoxification, and play key roles in steroid, lipid, and bile acid metabolism. Reactive oxygen species are postulated to contribute to DNA damage and tumorigenesis, and electrophilic cytochrome P450 molecules are a major source of these highly reactive radicals (Bondy and Naderi 1994). Oxidative DNA damage including increased 8-hydroxydeoxyguanosine adducts have been reported in *H. hepaticus* infected A/JCr mice, along with alterations in glutathione S-transferase and CYP2a5 (Chomarat *et al.* 1997; Sipowicz *et al.* 1997a). It has been noted, however, that CYP2a5 induction may not be dependent on oxidative damage alone given reactive oxygen species are also produced in liver injury caused by LPS which results in CYP2a5 down-regulation (Bautista and Spitzer 1990). This cumulative data suggests *H. hepaticus* infection has genotoxic and non-genotoxic effects and may be a complete carcinogen.

Genes associated with steroids

The male predominance of HCC in humans suggests sex steroid involvement but epidemiological studies of serum levels have been controversial (Kuper *et al.* 2001; Tanaka *et al.* 2000). Therapeutic trials of steroid receptor inhibitors on patients with diagnosed HCC yielded mixed results (Nowak *et al.* 2004). One gene prominently and consistently down-regulated (Table II) in *H. hepaticus* infected male A/JCr mice with severe hepatitis and preneoplastic liver lesions was hydroxysteroid dehydrogenase-5, delta<5>-3-beta (Hsd3b5). This 3-ketosteroid reductase gene, expressed only in the male mouse liver after puberty, reduces

dihydrotestosterone to the relatively inactive 3β,17β-androstanediol, in preparation for conjugation and elimination (Payne *et al.* 1997). Hsd3b5 is also down-regulated in the liver of mice exposed to peroxisome proliferators and genotoxins (Wong and Gill 2002; Wong *et al.* 2002).

Genes associated with aging

Splicing factor 3b subunit 1 (Sf3b1), a subunit of the spliceosome complex; peroxisome proliferation activated receptor alpha (Ppara), a transcription factor involved in regulation of fatty acid oxidation, glycerol metabolism, and amino acid metabolism in the liver (Kersten *et al.* 2001; Patsouris *et al.* 2004); pre-B cell colony enhancing factor 1 (Pbef1), a growth factor for early stage B cells and recently identified as an inflammatory cytokine affecting neutrophil apoptosis(Jia *et al.* 2004); and D site albumin promoter binding protein (Dbp), a liver enriched transcription factor, were up-regulated greater than 5 fold at 12 months of age versus 3 months of age. Syndecan (Sdc4), a heparan sulfate proteoglycan promotes focal adhesion and stress fibers and delays healing and impairs angiogenesis when deleted in mice (Echtermeyer *et al.* 2001; Keum *et al.* 2004); and tubulin beta 2 (Tubb2) were down-regulated by 5 fold. Although there were few genes substantially up-regulated or down-regulated with aging, the principal component analysis graph spatially clustered regions of age groups at 3, 6, and 12 months in the A/JCr mouse. Aging may be associated with slight but coordinated changes in gene expression over time, implying that co-regulated groups of genes or pathways may be modified more predictably as a group pattern change rather than individual gene changes. Future analysis should examine this approach (Mootha *et al.* 2003b). For example, aging is associated with an increased

level of inflammation, and the present analysis confirms inflammation-associated genes being differentially expressed, but few individual genes change substantially over the course of 12 months. It is interesting to note that some genes such as insulin-like growth factor binding protein 1 (Igfbp1), apoptosis inhibitor 6 (now named CD5 antigen-like (Cd5l)), lysozyme (Lyzs), complement component 1 subcomponents (C1qa, C1qb, C1qg), tubulin beta 2 (Tubb2), Ia associated invariant chain (Ii), lipoprotein lipase (Lp1), and vascular cell adhesion molecule (Vcam1) are up-regulated due to *H. hepaticus* related lesions but are down-regulated with aging. In the aggregate, however, aging down-regulates more genes than it up-regulates in this study and others (Cao *et al.* 2001).

Similar studies analyzing gene expression in H. hepaticus infected A/JCr mice

*H. hepaticus* initially colonizes the lower bowel before migrating to the liver. Although infection generally results in minimal-to-moderate inflammation in the lower bowel in immunocompetent mice, this murine pathogen induces severe typhlocolitis and lower bowel cancer in mutant mice with targeted immune dysfunctions (Erdman *et al.* 2003a; Rogers and Fox 2004; Tomczak *et al.* 2003b). In an *H. hepaticus* infection study in A/JCr mice, a cDNA array consisting of 1176 genes demonstrated 31 up-regulated and 2 down-regulated genes in the cecum at 3 months post-infection (Myles *et al.* 2003). Some up-regulated genes in common in both studies at the 3 month time point included Ia associated invariant chain (Ii), interferon gamma inducible protein (Ifi47), and chemokine (CXC motif) ligand 9 (Cxcl9), and several different serum amyloid A components. Opioid receptor sigma 1 (Oprs1) was slightly up-regulated at 12 months in the present study. Continued study of host responses to *H. hepaticus* in the lower bowel may help

identify factors responsible for protection or susceptibility to typhlocolitis as well as *H. hepaticus* translocation to the liver.

Hepatic proliferation is a key component of the development of HCC in the livers of mice infected with *H. hepaticus* (Fox *et al.* 1996a; Hailey *et al.* 1998). In agreement with a previous study of *H. hepaticus* infection in 6-18 month old mice, we documented increased transcription of cyclin D1 and decreased epidermal growth factor receptor 2 in mice with progressive hepatic disease (Ramljak *et al.* 1998). However, our microarray results did not confirm previously reported differences in other genes including c-myc, cyclin-dependent kinase 4, hepatocyte growth factor, and transforming growth factor-α (Ramljak *et al.* 1998). Further studies are required to determine the contribution of different cell proliferation pathways related to tumorigenesis and their transcriptional, translational, and post-translational regulatory mechanisms.

Summary

In summary, we characterized time-dependent gene expression signatures in the *H. hepaticus* infected A/J mouse liver with progressively severe liver disease. Transcription profiles in the livers of *H. hepaticus* infected male A/JCr mice exhibiting liver lesions yield a consistent ranking of differentially expressed genes. Importantly, the bimodal distribution of disease severity in infected male mice, as demonstrated by histopathology, corresponds with global hepatic gene expression differences. The reasons for the variable *H. hepaticus* colonization density and disease susceptibility in males, however, remain unexplained. There was an

increased number of genes exhibiting differential expression for aging mice, in both *H. hepaticus* infected A/JCr mice and controls. Two putative tumor markers, intestinal trefoil factor 3 and H19 fetal liver mRNA were up-regulated in progressively dysplastic livers. Further investigations will determine if the gene expression signature of a target organ is diagnostic of a specific pathogen and whether there is prognostic value in data derived from this type of analysis. Global gene expression profiling by microarray analysis will continue to play an important role in elucidating molecular events in pre-neoplasia and cancer induced by microbial agents.

**References**


Al-azzeh, E., Dittrich, O., Vervoorts, J., Blin, N., Gott, P., and Luscher, B. (2002). Gastroprotective peptide trefoil factor family 2 gene is activated by upstream stimulating factor but not by c-Myc in gastrointestinal cancer cells. *Gut* **51**, 685-90.

Avenaud, P., Marais, A., Monteiro, L., Le Bail, B., Bioulac Sage, P., Balabaud, C., and Megraud, F. (2000). Detection of *Helicobacter* species in the liver of patients with and without primary liver carcinoma. *Cancer* **89**, 1431-9.

Bai, F., Nakanishi, Y., Takayama, K., Pei, X. H., Inoue, K., Harada, T., Izumi, M., and Hara, N. (2003). Codon 64 of K-ras gene mutation pattern in hepatocellular carcinomas induced by bleomycin and 1-nitropyrene in A/J mice. *Teratog Carcinog Mutagen* **Suppl 1**, 161-70.

Bannasch, P., Benner, U., Enzmann, H., and Hacker, H. J. (1985). Tigroid cell foci and neoplastic nodules in the liver of rats treated with a single dose of aflatoxin B1. *Carcinogenesis* **6**, 1641-8.

Bannasch, P., Nehrbass, D., and Kopp-Schneider, A. (2001). Significance of hepatic preneoplasia for cancer chemoprevention. *IARC Sci Publ* **154**, 223-40.

Bartsch, S., and Tschesche, H. (1995). Cloning and expression of human neutrophil lipocalin cDNA derived from bone marrow and ovarian cancer cells. *FEBS Lett* **357**, 255-9.

Bautista, A. P., and Spitzer, J. J. (1990). Superoxide anion generation by in situ perfused rat liver: effect of in vivo endotoxin. *Am J Physiol* **259**, G907-12.

Bondy, S. C., and Naderi, S. (1994). Contribution of hepatic cytochrome P450 systems to the generation of reactive oxygen species. *Biochem Pharmacol* **48**, 155-9.

Brannan, C. I., and Bartolomei, M. S. (1999). Mechanisms of genomic imprinting. *Curr Opin Genet Dev* **9**, 164-70.

Brannan, C. I., Dees, E. C., Ingram, R. S., and Tilghman, S. M. (1990). The product of the H19 gene may function as an RNA. *Mol Cell Biol* **10**, 28-36.

Bratt, T. (2000). Lipocalins and cancer. *Biochim Biophys Acta* **1482**, 318-26.

Canella, K. A., Diwan, B. A., Gorelick, P. L., Donovan, P. J., Sipowicz, M. A., Kasprzak, K. S., Weghorst, C. M., Snyderwine, E. G., Davis, C. D., Keefer, L. K., Kyrtopoulos, S. A., Hecht, S. S., Wang, M., Anderson, L. M., and Rice, J. M. (1996). Liver tumorigenesis by *Helicobacter hepaticus*: considerations of mechanism. *In Vivo* **10**, 285-92.

Cao, S. X., Dhahbi, J. M., Mote, P. L., and Spindler, S. R. (2001). Genomic profiling of short- and long-term caloric restriction effects in the liver of aging mice. *Proc Natl Acad Sci U S A* **98**, 10630-5.

Cavaggioni, A., and Mucignat-Caretta, C. (2000). Major urinary proteins, alpha(2U)-globulins and aphrodisin. *Biochim Biophys Acta* **1482**, 218-28.

Chan, I. T., Kutok, J. L., Williams, I. R., Cohen, S., Kelly, L., Shigematsu, H., Johnson, L., Akashi, K., Tuveson, D. A., Jacks, T., and Gilliland, D. G. (2004). Conditional expression of oncogenic K-ras from its endogenous promoter induces a myeloproliferative disease. *J Clin Invest* **113**, 528-38.

Chomarat, P., Sipowicz, M. A., Diwan, B. A., Fornwald, L. W., Awasthi, Y. C., Anver, M. R., Rice, J. M., Anderson, L. M., and Wild, C. P. (1997). Distinct time courses of increase in cytochromes P450 1A2, 2A5 and glutathione S-transferases during the progressive hepatitis associated with *Helicobacter hepaticus*. *Carcinogenesis* **18**, 2179-90.

Devireddy, L. R., Teodoro, J. G., Richard, F. A., and Green, M. R. (2001). Induction of apoptosis by a secreted lipocalin that is transcriptionally regulated by IL-3 deprivation. *Science* **293**, 829-34.

Diwan, B. A., Ward, J. M., Ramljak, D., and Anderson, L. M. (1997). Promotion by *Helicobacter hepaticus*-induced hepatitis of hepatic tumors initiated by N-nitrosodimethylamine in male A/JCr mice. *Toxicol Pathol* **25**, 597-605.

Eaton, J. W., Brandt, P., Mahoney, J. R., and Lee, J. T., Jr. (1982). Haptoglobin: a natural bacteriostat. *Science* **215**, 691-3.

Echtermeyer, F., Streit, M., Wilcox-Adelman, S., Saoncella, S., Denhez, F., Detmar, M., and Goetinck, P. (2001). Delayed wound repair and impaired angiogenesis in mice lacking syndecan-4. *J Clin Invest* **107**, R9-R14.

Edwards, J., Krishna, N. S., Witton, C. J., and Bartlett, J. M. (2003). Gene amplifications associated with the development of hormone-resistant prostate cancer. *Clin Cancer Res* **9**, 5271-81.

Erdman, S. E., Poutahidis, T., Tomczak, M., Rogers, A. B., Cormier, K., Plank, B., Horwitz, B. H., and Fox, J. G. (2003a). CD4(+) CD25(+) Regulatory T Lymphocytes Inhibit Microbially Induced Colon Cancer in Rag2-Deficient Mice. *Am J Pathol* **162**, 691-702.

Erdman, S. E., Poutahidis, T., Tomczak, M., Rogers, A. B., Cormier, K., Plank, B., Horwitz, B. H., and Fox, J. G. (2003b). CD4+ CD25+ regulatory T lymphocytes inhibit microbially induced colon cancer in Rag2-deficient mice. *Am J Pathol* **162**, 691-702.

Erdman, S. E., Rao, V. P., Poutahidis, T., Ihrig, M. M., Ge, Z., Feng, Y., Tomczak, M., Rogers, A. B., Horwitz, B. H., and Fox, J. G. (2003c). CD4(+)CD25(+) regulatory lymphocytes require interleukin 10 to interrupt colon carcinogenesis in mice. *Cancer Res* **63**, 6042-50.

Etzioni, R., Urban, N., Ramsey, S., McIntosh, M., Schwartz, S., Reid, B., Radich, J., Anderson, G., and Hartwell, L. (2003). The case for early detection. *Nat Rev Cancer* **3**, 243-52.

Ferrell, L. D., Theise, N. D., and Scheuer, P. J. (2002). Acute and chronic viral hepatitis. In In Pathology of the Liver (A. D. B. R. N. M. MacSween, B. C. Portmann, K. G. Ishak, P. J. Scheuer and P. P. Anthony, ed., pp. . 313-362. Churchill Livingstone, London.

Fox, J. G., Dewhirst, F. E., Shen, Z., Feng, Y., Taylor, N. S., Paster, B. J., Ericson, R. L., Lau, C. N., Correa, P., Araya, J. C., and Roa, I. (1998a). Hepatic *Helicobacter* species identified in bile and gallbladder tissue from Chileans with chronic cholecystitis. *Gastroenterology* **114**, 755-63.

Fox, J. G., Dewhirst, F. E., Tully, J. G., Paster, B. J., Yan, L., Taylor, N. S., Collins, M. J., Jr., Gorelick, P. L., and Ward, J. M. (1994). *Helicobacter hepaticus* sp. nov., a microaerophilic bacterium isolated from livers and intestinal mucosal scrapings from mice. *J Clin Microbiol* **32**, 1238-45.

Fox, J. G., Drolet, R., Higgins, R., Messier, S., Yan, L., Coleman, B. E., Paster, B. J., and Dewhirst, F. E. (1996a). *Helicobacter* canis isolated from a dog liver with multifocal necrotizing hepatitis. *J Clin Microbiol* **34**, 2479-82.

Fox, J. G., Li, X., Yan, L., Cahill, R. J., Hurley, R., Lewis, R., and Murphy, J. C. (1996b). Chronic proliferative hepatitis in A/JCr mice associated with persistent *Helicobacter hepaticus* infection: a model of *Helicobacter*- induced carcinogenesis. *Infect Immun* **64**, 1548-58.

Fox, J. G., MacGregor, J. A., Shen, Z., Li, X., Lewis, R., and Dangler, C. A. (1998b). Comparison of methods of identifying *Helicobacter hepaticus* in B6C3F1 mice used in a carcinogenesis bioassay. *J Clin Microbiol* **36**, 1382-7.

Fox, J. G., Rogers, A. B., Whary, M. T., Ge, Z., Taylor, N. S., Xu, S., Horwitz, B. H., and Erdman, S. E. (2004). Gastroenteritis in NF-kappaB-Deficient Mice Is Produced with Wild-Type Camplyobacter jejuni but Not with C. jejuni Lacking Cytolethal Distending Toxin despite Persistent Colonization with Both Strains. *Infect Immun* **72**, 1116-25.

Fox, J. G., Wang, T. C., Rogers, A. B., Poutahidis, T., Ge, Z., Taylor, N., Dangler, C. A., Israel, D. A., Krishna, U., Gaus, K., and Peek, R. M., Jr. (2003a). Host and microbial constituents influence *Helicobacter pylori*-induced cancer in a murine model of hypergastrinemia. *Gastroenterology* **124**, 1879-90.

Fox, J. G., Wang, T. C., Rogers, A. B., Poutahidis, T., Ge, Z., Taylor, N., Dangler, C. A., Israel, D. A., Krishna, U., Gaus, K., and Peek, R. M., Jr. (2003b). Host and microbial constituents influence *Helicobacter pylori*-induced cancer in a murine model of hypergastrinemia. *Gastroenterology* **124**, 1879-90.

Fox, J. G., Yan, L., Shames, B., Campbell, J., Murphy, J. C., and Li, X. (1996c). Persistent hepatitis and enterocolitis in germfree mice infected with *Helicobacter hepaticus*. *Infect Immun* **64**, 3673-81.

Fraser, D. J., Zumsteg, A., and Meyer, U. A. (2003). Nuclear receptors constitutive androstane receptor and pregnane X receptor activate a drug-responsive enhancer of the murine 5-aminolevulinic acid synthase gene. *J Biol Chem* **278**, 39392-401.

Frasor, J., Danes, J. M., Komm, B., Chang, K. C., Lyttle, C. R., and Katzenellenbogen, B. S. (2003). Profiling of estrogen up- and down-regulated gene expression in human breast cancer cells: insights into gene networks and pathways underlying estrogenic control of proliferation and cell phenotype. *Endocrinology* **144**, 4562-74.

Furutani, M., Arii, S., Mizumoto, M., Kato, M., and Imamura, M. (1998). Identification of a neutrophil gelatinase-associated lipocalin mRNA in human pancreatic cancers using a modified signal sequence trap method. *Cancer Lett* **122**, 209-14.

Gabay, C., and Kushner, I. (1999). Acute-phase proteins and other systemic responses to inflammation. *N Engl J Med* **340**, 448-54.

Graveel, C. R., Jatkoe, T., Madore, S. J., Holt, A. L., and Farnham, P. J. (2001). Expression profiling and identification of novel genes in hepatocellular carcinomas. *Oncogene* **20**, 2704-12.

Hailey, J. R., Haseman, J. K., Bucher, J. R., Radovsky, A. E., Malarkey, D. E., Miller, R. T., Nyska, A., and Maronpot, R. R. (1998). Impact of *Helicobacter hepaticus* infection in B6C3F1 mice from twelve National Toxicology Program two-year carcinogenesis studies. *Toxicol Pathol* **26**, 602-11.

Haseman, J. K., Hailey, J. R., and Morris, R. W. (1998). Spontaneous neoplasm incidences in Fischer 344 rats and B6C3F1 mice in two-year carcinogenicity studies: a National Toxicology Program update. *Toxicol Pathol* **26**, 428-41.

Hatanaka, E., Pereira Ribeiro, F., and Campa, A. (2003). The acute phase protein serum amyloid A primes neutrophils. *FEMS Immunol Med Microbiol* **38**, 81-84.

Hinds, P. W., Dowdy, S. F., Eaton, E. N., Arnold, A., and Weinberg, R. A. (1994). Function of a human cyclin gene as an oncogene. *Proc Natl Acad Sci U S A* **91**, 709-13.

Hinds, P. W., and Weinberg, R. A. (1994). Tumor suppressor genes. *Curr Opin Genet Dev* **4**, 135-41.

Ihrig, M., Schrenzel, M. D., and Fox, J. G. (1999). Differential susceptibility to hepatic inflammation and proliferation in AXB recombinant inbred mice chronically infected with *Helicobacter hepaticus*. *Am J Pathol* **155**, 571-82.

Iizuka, N., Oka, M., Yamada-Okabe, H., Hamada, K., Nakayama, H., Mori, N., Tamesa, T., Okada, T., Takemoto, N., Matoba, K., Takashima, M., Sakamoto, K., Tangoku, A., Miyamoto, T., Uchimura, S., and Hamamoto, Y. (2004). Molecular signature in three types of hepatocellular carcinoma with different viral origin by oligonucleotide microarray. *Int J Oncol* **24**, 565-74.

IWP (1995). Terminology of chronic hepatitis. International Working Party. *Am J Gastroenterol* **90**, 181-9.

Jia, S. H., Li, Y., Parodo, J., Kapus, A., Fan, L., Rotstein, O. D., and Marshall, J. C. (2004). Pre-B cell colony-enhancing factor inhibits neutrophil apoptosis in experimental inflammation and clinical sepsis. *J Clin Invest* **113**, 1318-27.

Jung, D., Hagenbuch, B., Fried, M., Meier, P. J., and Kullak-Ublick, G. A. (2004). Role of liver-enriched transcription factors and nuclear receptors in regulating the human, mouse, and rat NTCP gene. *Am J Physiol Gastrointest Liver Physiol* **286**, G752-61.

Kaplan, R., Luettich, K., Heguy, A., Hackett, N. R., Harvey, B. G., and Crystal, R. G. (2003). Monoallelic up-regulation of the imprinted H19 gene in airway epithelium of phenotypically normal cigarette smokers. *Cancer Res* **63**, 1475-82.

Kapranov, P., Cawley, S. E., Drenkow, J., Bekiranov, S., Strausberg, R. L., Fodor, S. P., and Gingeras, T. R. (2002). Large-scale transcriptional activity in chromosomes 21 and 22. *Science* **296**, 916-9.

Katoh, M. (2003). Trefoil factors and human gastric cancer (Review). *Int J Mol Med* **12**, 3-9.

Kersten, S., Mandard, S., Escher, P., Gonzalez, F. J., Tafuri, S., Desvergne, B., and Wahli, W. (2001). The peroxisome proliferator-activated receptor alpha regulates amino acid metabolism. *Faseb J* **15**, 1971-8.

Keum, E., Kim, Y., Kim, J., Kwon, S., Lim, Y., Han, I., and Oh, E. S. (2004). Syndecan-4 regulates localization, activity and stability of protein kinase C-alpha. *Biochem J* **378**, 1007-14.

Khan, Z. E., Wang, T. C., Cui, G., Chi, A. L., and Dimaline, R. (2003). Transcriptional regulation of the human trefoil factor, TFF1, by gastrin. *Gastroenterology* **125**, 510-21.

Kimura, Y., Leung, P. S., Kenny, T. P., Van De Water, J., Nishioka, M., Giraud, A. S., Neuberger, J., Benson, G., Kaul, R., Ansari, A. A., Coppel, R. L., and Gershwin, M. E. (2002). Differential expression of intestinal trefoil factor in biliary epithelial cells of primary biliary cirrhosis. *Hepatology* **36**, 1227-35.

Kuper, H., Mantzoros, C., Lagiou, P., Tzonou, A., Tamimi, R., Mucci, L., Benetou, V., Spanos, E., Stuver, S. O., and Trichopoulos, D. (2001). Estrogens, testosterone and sex hormone binding globulin in relation to liver cancer in men. *Oncology* **60**, 355-60.

Lara-Tejero, M., and Galan, J. E. (2000). A bacterial toxin that controls cell cycle progression as a deoxyribonuclease I-like protein. *Science* **290**, 354-7.

Le Roith, D., Karas, M., Yakar, S., Qu, B. H., Wu, Y., and Blakesley, V. A. (1999). The role of the insulin-like growth factors in cancer. *Isr Med Assoc J* **1**, 25-30.

Lepreux, S., Bioulac-Sage, P., Gabbiani, G., Sapin, V., Housset, C., Rosenbaum, J., Balabaud, C., and Desmouliere, A. (2004). Cellular retinol-binding protein-1 expression in normal and fibrotic/cirrhotic human liver: different patterns of expression in hepatic stellate cells and (myo)fibroblast subpopulations. *J Hepatol* **40**, 774-80.

Leu, J. I., Crissey, M. A., and Taub, R. (2003). Massive hepatic apoptosis associated with TGF-beta1 activation after Fas ligand treatment of IGF binding protein-1-deficient mice. *J Clin Invest* **111**, 129-39.

Leung, W. K., Yu, J., Chan, F. K., To, K. F., Chan, M. W., Ebert, M. P., Ng, E. K., Chung, S. C., Malfertheiner, P., and Sung, J. J. (2002). Expression of trefoil peptides (TFF1, TFF2, and TFF3) in gastric carcinomas, intestinal metaplasia, and non-neoplastic gastric tissues. *J Pathol* **197**, 582-8.

Li, C., and Hung Wong, W. (2001). Model-based analysis of oligonucleotide arrays: model validation, design issues and standard error application. *Genome Biol* **2**, RESEARCH0032.

Li, C., and Wong, W. H. (2001). Model-based analysis of oligonucleotide arrays: expression index computation and outlier detection. *Proc Natl Acad Sci U S A* **98**, 31-6.

Liu, Q., and Nilsen-Hamilton, M. (1995). Identification of a new acute phase protein. *J Biol Chem* **270**, 22565-70.

Matsui, T., Kinoshita, T., Morikawa, Y., Tohya, K., Katsuki, M., Ito, Y., Kamiya, A., and Miyajima, A. (2002). K-Ras mediates cytokine-induced formation of E-cadherin-based adherens junctions during liver development. *Embo J* **21**, 1021-30.

McSweeney, L. A., and Dreyfus, L. A. (2004). Nuclear localization of the Escherichia coli cytolethal distending toxin CdtB subunit. *Cell Microbiol* **6**, 447-58.

Meyer, K., Lee, J. S., Dyck, P. A., Cao, W. Q., Rao, M. S., Thorgeirsson, S. S., and Reddy, J. K. (2003). Molecular profiling of hepatocellular carcinomas developing spontaneously in acyl-CoA oxidase deficient mice: comparison with liver tumors induced in wild-type mice by a peroxisome proliferator and a genotoxic carcinogen. *Carcinogenesis* **24**, 975-84.

Mootha, V. K., Bunkenborg, J., Olsen, J. V., Hjerrild, M., Wisniewski, J. R., Stahl, E., Bolouri, M. S., Ray, H. N., Sihag, S., Kamal, M., Patterson, N., Lander, E. S., and Mann, M. (2003a). Integrated analysis of protein composition, tissue diversity, and gene regulation in mouse mitochondria. *Cell* **115**, 629-40.

Mootha, V. K., Lindgren, C. M., Eriksson, K. F., Subramanian, A., Sihag, S., Lehar, J., Puigserver, P., Carlsson, E., Ridderstrale, M., Laurila, E., Houstis, N., Daly, M. J., Patterson, N., Mesirov, J. P., Golub, T. R., Tamayo, P., Spiegelman, B., Lander, E. S., Hirschhorn, J. N., Altshuler, D., and Groop, L. C. (2003b). PGC-1alpha-responsive genes involved in oxidative phosphorylation are coordinately downregulated in human diabetes. *Nat Genet* **34**, 267-73.

Myles, M. H., Livingston, R. S., Livingston, B. A., Criley, J. M., and Franklin, C. L. (2003). Analysis of gene expression in ceca of *Helicobacter hepaticus*-infected A/JCr mice before and after development of typhlitis. *Infect Immun* **71**, 3885-93.

Nielsen, B. S., Borregaard, N., Bundgaard, J. R., Timshel, S., Sehested, M., and Kjeldsen, L. (1996). Induction of NGAL synthesis in epithelial cells of human colorectal neoplasia and inflammatory bowel diseases. *Gut* **38**, 414-20.

Nilsen-Hamilton, M., Hamilton, R. T., and Adams, G. A. (1982). Rapid selective stimulation by growth factors of the incorporation by BALB/C 3T3 cells of [35S]methionine into a glycoprotein and five superinducible proteins. *Biochem Biophys Res Commun* **108**, 158-66.

Nilsson, H. O., Mulchandani, R., Tranberg, K. G., and Wadstrom, T. (2001). *Helicobacter* species identified in liver from patients with cholangiocarcinoma and hepatocellular carcinoma. *Gastroenterology* **120**, 323-4.

Nowak, A., Findlay, M., Culjak, G., and Stockler, M. (2004). Tamoxifen for hepatocellular carcinoma. *Cochrane Database Syst Rev*, CD001024.

Nyska, A., Maronpot, R. R., Eldridge, S. R., Haseman, J. K., and Hailey, J. R. (1997). Alteration in cell kinetics in control B6C3F1 mice infected with *Helicobacter hepaticus*. *Toxicol Pathol* **25**, 591-6.

Ohara, M., Hayashi, T., Kusunoki, Y., Miyauchi, M., Takata, T., and Sugai, M. (2004). Caspase-2 and caspase-7 are involved in cytolethal distending toxin-induced apoptosis in Jurkat and MOLT-4 T-cell lines. *Infect Immun* **72**, 871-9.

Palmer, H. G., Sanchez-Carbayo, M., Ordonez-Moran, P., Larriba, M. J., Cordon-Cardo, C., and Munoz, A. (2003). Genetic signatures of differentiation induced by 1alpha,25-dihydroxyvitamin D3 in human colon cancer cells. *Cancer Res* **63**, 7799-806.

Parker, M. A., Deane, N. G., Thompson, E. A., Whitehead, R. H., Mithani, S. K., Washington, M. K., Datta, P. K., Dixon, D. A., and Beauchamp, R. D. (2003). Over-expression of cyclin D1 regulates Cdk4 protein synthesis. *Cell Prolif* **36**, 347-60.

Patsouris, D., Mandard, S., Voshol, P. J., Escher, P., Tan, N. S., Havekes, L. M., Koenig, W., Marz, W., Tafuri, S., Wahli, W., Muller, M., and Kersten, S. (2004). PPARalpha governs glycerol metabolism. *J Clin Invest* **114**, 94-103.

Pawson, T., and Nash, P. (2003). Assembly of cell regulatory systems through protein interaction domains. *Science* **300**, 445-52.

Payne, A. H., Abbaszade, I. G., Clarke, T. R., Bain, P. A., and Park, C. H. (1997). The multiple murine 3 beta-hydroxysteroid dehydrogenase isoforms: structure, function, and tissue- and developmentally specific expression. *Steroids* **62**, 169-75.

Ponzetto, A., Pellicano, R., Leone, N., Cutufia, M. A., Turrini, F., Grigioni, W. F., D'Errico, A., Mortimer, P., Rizzetto, M., and Silengo, L. (2000). *Helicobacter* infection and cirrhosis in hepatitis C virus carriage: is it an innocent bystander or a troublemaker? *Med Hypotheses* **54**, 275-7.

Ramljak, D., Jones, A. B., Diwan, B. A., Perantoni, A. O., Hochadel, J. F., and Anderson, L. M. (1998). Epidermal growth factor and transforming growth factor-alpha-associated overexpression of cyclin D1, Cdk4, and c-Myc during hepatocarcinogenesis in *Helicobacter hepaticus*-infected A/JCr mice. *Cancer Res* **58**, 3590-7.

Ribeiro, F. P., Furlaneto, C. J., Hatanaka, E., Ribeiro, W. B., Souza, G. M., Cassatella, M. A., and Campa, A. (2003). mRNA expression and release of interleukin-8 induced by serum amyloid A in neutrophils and monocytes. *Mediators Inflamm* **12**, 173-8.

Rice, J. M. (1995). *Helicobacter hepaticus*, a recently recognized bacterial pathogen, associated with chronic hepatitis and hepatocellular neoplasia in laboratory mice. *Emerg Infect Dis* **1**, 129-31.

Rivera-Rivera, I., Kim, J., and Kemper, B. (2003). Transcriptional analysis in vivo of the hepatic genes, Cyp2b9 and Cyp2b10, by intravenous administration of plasmid DNA in mice. *Biochim Biophys Acta* **1619**, 254-62.

Rodrigues, S., Attoub, S., Nguyen, Q. D., Bruyneel, E., Rodrigue, C. M., Westley, B. R., May, F. E., Thim, L., Mareel, M., Emami, S., and Gespach, C. (2003). Selective abrogation of the proinvasive activity of the trefoil peptides pS2 and spasmolytic polypeptide by disruption of the EGF receptor signaling pathways in kidney and colonic cancer cells. *Oncogene* **22**, 4488-97.

Rogers, A. B., and Fox, J. G. (2004). Inflammation and Cancer I. Rodent models of infectious gastrointestinal and liver cancer. *Am J Physiol Gastrointest Liver Physiol* **286**, G361-6.

Rogers, A. B., Mathiason, C. K., and Hoover, E. A. (2002). Immunohistochemical localization of feline immunodeficiency virus using native species antibodies. *Am J Pathol* **161**, 1143-51.

Scharf, J. G., Dombrowski, F., and Ramadori, G. (2001). The IGF axis and hepatocarcinogenesis. *Mol Pathol* **54**, 138-44.

Scheuer, P. J., Standish, R. A., and Dhillon, A. P. (2002). Scoring of chronic hepatitis. *Clin Liver Dis* **6**, 335-47, v-vi.

Selvamurugan, N., Kwok, S., and Partridge, N. C. (2004). Smad3 interacts with JunB and Cbfa1/Runx2 for transforming growth factor-beta1-stimulated collagenase-3 expression in human breast cancer cells. *J Biol Chem* **279**, 27764-73.

Shomer, N. H., Fox, J. G., Juedes, A. E., and Ruddle, N. H. (2003). *Helicobacter*-induced chronic active lymphoid aggregates have characteristics of tertiary lymphoid tissue. *Infect Immun* **71**, 3572-7.

Sipowicz, M. A., Chomarat, P., Diwan, B. A., Anver, M. A., Awasthi, Y. C., Ward, J. M., Rice, J. M., Kasprzak, K. S., Wild, C. P., and Anderson, L. M. (1997a). Increased oxidative DNA damage and hepatocyte overexpression of specific cytochrome P450 isoforms in hepatitis of mice infected with *Helicobacter hepaticus*. *Am J Pathol* **151**, 933-41.

Sipowicz, M. A., Weghorst, C. M., Shiao, Y. H., Buzard, G. S., Calvert, R. J., Anver, M. R., Anderson, L. M., and Rice, J. M. (1997b). Lack of p53 and ras mutations in *Helicobacter hepaticus*-induced liver tumors in A/JCr mice. *Carcinogenesis* **18**, 233-6.

Song, X., Tao, Y. G., Deng, X. Y., Jin, X., Tan, Y. N., Tang, M., Wu, Q., Lee, L. M., and Cao, Y. (2004). Heterodimer formation between c-Jun and Jun B proteins mediated by Epstein-Barr virus encoded latent membrane protein 1. *Cell Signal* **16**, 1153-62.

Tanaka, K., Sakai, H., Hashizume, M., and Hirohata, T. (2000). Serum testosterone:estradiol ratio and the development of hepatocellular carcinoma among male cirrhotic patients. *Cancer Res* **60**, 5106-10.

Taylor, N. S., Ge, Z., Shen, Z., Dewhirst, F. E., and Fox, J. G. (2003). Cytolethal distending toxin: a potential virulence factor for *Helicobacter* cinaedi. *J Infect Dis* **188**, 1892-7.

Thirunavukkarasu, C., and Sakthisekaran, D. (2003). Effect of dietary selenite on N-nitrosodiethylamine-induced and phenobarbital promoted multistage hepatocarcinogenesis in rat: reflection in some minerals. *Biomed Pharmacother* **57**, 416-21.

Tomczak, M. F., Erdman, S. E., Poutahidis, T., Rogers, A. B., Holcombe, H., Plank, B., Fox, J. G., and Horwitz, B. H. (2003a). NF-kappaB is required within the innate immune system to inhibit microflora-induced colitis and expression of IL-12 p40. *J Immunol* **171**, 1484-92.

Tomczak, M. F., Erdman, S. E., Poutahidis, T., Rogers, A. B., Holcombe, H., Plank, B., Fox, J. G., and Horwitz, B. H. (2003b). NF-kappaB is required within the innate immune system to inhibit microflora-induced colitis and expression of IL-12 p40. *J Immunol* **171**, 1484-92.

Tong, Z., Wu, X., and Kehrer, J. P. (2003). Increased expression of the lipocalin 24p3 as an apoptotic mechanism for MK886. *Biochem J* **372**, 203-10.

Vernucci, M., Cerrato, F., Besnard, N., Casola, S., Pedone, P. V., Bruni, C. B., and Riccio, A. (2000). The H19 endodermal enhancer is required for Igf2 activation and tumor formation in experimental liver carcinogenesis. *Oncogene* **19**, 6376-85.

Ward, J. M., Anver, M. R., Haines, D. C., Melhorn, J. M., Gorelick, P., Yan, L., and Fox, J. G. (1996a). Inflammatory large bowel disease in immunodeficient mice naturally infected with *Helicobacter hepaticus*. *Lab Anim Sci* **46**, 15-20.

Ward, J. M., Benveniste, R. E., Fox, C. H., Battles, J. K., Gonda, M. A., and Tully, J. G. (1996b). Autoimmunity in chronic active *Helicobacter* hepatitis of mice. Serum antibodies and expression of heat shock protein 70 in liver. *Am J Pathol* **148**, 509-17.

Ward, J. M., Fox, J. G., Anver, M. R., Haines, D. C., George, C. V., Collins, M. J., Jr., Gorelick, P. L., Nagashima, K., Gonda, M. A., Gilden, R. V., and et al. (1994). Chronic active hepatitis and associated liver tumors in mice caused by a persistent bacterial infection with a novel *Helicobacter* species. *J Natl Cancer Inst* **86**, 1222-7.

Whary, M. T., Cline, J., King, A., Ge, Z., Shen, Z., Sheppard, B., and Fox, J. G. (2001). Long-term colonization levels of *Helicobacter hepaticus* in the cecum of hepatitis-prone A/JCr mice are significantly lower than those in hepatitis-resistant C57BL/6 mice. *Comp Med* **51**, 413-7.

Whary, M. T., Morgan, T. J., Dangler, C. A., Gaudes, K. J., Taylor, N. S., and Fox, J. G. (1998). Chronic active hepatitis induced by *Helicobacter hepaticus* in the A/JCr mouse is associated with a Th1 cell-mediated immune response. *Infect Immun* **66**, 3142-8.

Wong, J. S., and Gill, S. S. (2002). Gene expression changes induced in mouse liver by di(2-ethylhexyl) phthalate. *Toxicol Appl Pharmacol* **185**, 180-96.

Wong, J. S., Ye, X., Muhlenkamp, C. R., and Gill, S. S. (2002). Effect of a peroxisome proliferator on 3 beta-hydroxysteroid dehydrogenase. *Biochem Biophys Res Commun* **293**, 549-53.

Xu, S., and Venge, P. (2000). Lipocalins as biochemical markers of disease. *Biochim Biophys Acta* **1482**, 298-307.

Yakar, S., Liu, J. L., Stannard, B., Butler, A., Accili, D., Sauer, B., and LeRoith, D. (1999). Normal growth and development in the absence of hepatic insulin-like growth factor I. *Proc Natl Acad Sci U S A* **96**, 7324-9.

Yamamoto, Y., Nishikawa, Y., Tokairin, T., Omori, Y., and Enomoto, K. (2004). Increased expression of H19 non-coding mRNA follows hepatocyte proliferation in the rat and mouse. *J Hepatol* **40**, 808-14.

Yang, J., Mori, K., Li, J. Y., and Barasch, J. (2003). Iron, lipocalin, and kidney epithelia. *Am J Physiol Renal Physiol* **285**, F9-18.

Yoshinari, K., Kobayashi, K., Moore, R., Kawamoto, T., and Negishi, M. (2003). Identification of the nuclear receptor CAR:HSP90 complex in mouse liver and recruitment of protein phosphatase 2A in response to phenobarbital. *FEBS Lett* **548**, 17-20.

Young, V. B., Knox, K. A., Pratt, J. S., Cortez, J. S., Mansfield, L. S., Rogers, A. B., Fox, J. G., and Schauer, D. B. (2004). In vitro and in vivo characterization of *Helicobacter hepaticus* cytolethal distending toxin mutants. *Infect Immun* **72**, 2521-7.

Young, V. B., Knox, K. A., and Schauer, D. B. (2000). Cytolethal distending toxin sequence and activity in the enterohepatic pathogen *Helicobacter hepaticus*. *Infect Immun* **68**, 184-91.

## Chapter 4

### The pathogenicity island in *Helicobacter hepaticus* mediates severity of hepatitis in A/JCr male mice

**Abstract**

*H. hepaticus* induces chronic hepatitis and hepatocellular carcinoma in the A/JCr mouse. A 70kb genomic island in *Helicobacter hepaticus* strain ATCC 51449 is a putative pathogenicity island (HHGI1). This low GC content region comprises genes HH0233-HH0302, and codes for three orthologs of a putative type IV secretion system (T4SS). A/JCr mice were experimentally infected with three naturally occurring strains of *H. hepaticus*; strain *H. hepaticus* ATCC 51449 strain (Hh3B1) isolated from A/JCr mice, MIT 96-1809 (HhNET) isolated from mice shipped from the Netherlands, and MIT-96-284 (HhG) isolated from mice acquired from Germany. HhNET and HhG lack an intact HHGI1 island and each exhibit other individual gene differences when compared to Hh3B1. HhNET infected male A/JCR mice exhibited a significantly lower prevalence of hepatic lesions at 6 months post infection (pi) than mice infected with Hh3B1 possessing the HHGI1 island. HhG also demonstrated a lower prevalence of hepatic lesions at 6 months pi. This variability in lesions was evident in male mice only. The inflammation scores in the liver of the *H. hepaticus* infected A/JCr mouse correlated with *H. hepaticus* liver colonization levels. The results suggest the presence or absence of the *H. hepaticus* 70 kb genomic island, a pathogenicity island, is a legitimate virulence determinant and predictor of severity of liver lesions in *H. hepaticus* infected A/JCr male mice.

**Introduction**

*Helicobacter hepaticus* causes chronic hepatitis and hepatocellular carcinoma in A/JCr mice (Fox *et al.* 1994; Fox *et al.* 1996a; Ward *et al.* 1994b) and typhlocolitis in susceptible mouse species as well as lower bowel cancer in 129S6 Rag 2-/- mice (129SG/SvEvTac-Rag2$^{tm1Fwa}$)(Erdman *et al.* 2003a; Erdman *et al.* 2003b; Rogers and Fox 2004). *H. hepaticus* is the best studied member of the enterohepatic *Helicobacter* species, a group of bacteria of increasing biomedical importance (Fox 2002; Rogers and Fox 2004; Solnick and Schauer 2001). The genome of *H. hepaticus* was recently sequenced and shares many genes with the gastric pathogen *H. pylori* and the enteric pathogen, *Campylobacter jejuni* (Suerbaum *et al.* 2003). Although *H. hepaticus* and *H. pylori* occupy different niches in the gastrointestinal tract, they both cause persistent infection in their respective hosts and have the potential to induce chronic inflammation which progresses to carcinoma. *C. jejuni*, the most frequent bacterial cause of human diarrhea, and *H. hepaticus* both inhabit the intestinal crypts of the lower bowel. *H. pylori* and *C. jejuni* possess numerous virulence factors, including a Type IV secretion system (Batchelor *et al.* 2004; Larsen *et al.* 2004; Poly *et al.* 2004). *C. jejuni* possesses invasion antigens (Cia proteins) and certain proteins with similarity to flagellar components contributing to secretion (Konkel *et al.* 2004; Song *et al.* 2004). The *H. pylori* genome contains a pathogenicity island (PAI) referred to as the *cag* PAI (Censini *et al.* 1996) (HP0520-HP0547 in *H. pylori* 26695; jhp0469-jhp0495 in *H. pylori* J99) and several other genes important for adherence to the gastric epithelium and persistent colonization. The presence of the *cag* PAI in *H. pylori* strains has been reported as a risk factor for atrophic gastritis and gastric cancer (Azuma *et al.* 2004; Backert *et al.* 2004; Blomstergren *et al.* 2004; Yang *et al.* 2004).

Pathogenicity islands reside in many other bacterial pathogens including *Escherichia col*i (Blum *et al.* 1994), *Shigella flexneri* (Rajakumar *et al.* 1997), *Yersinia pestis* (Buchrieser *et al.* 1998; Schubert *et al.* 1998), *Salmonella enterica* (Bajaj *et al.* 1995), *Vibrio cholerae* (Ogierman *et al.* 1997), *Staphylococcus aureus* (Lindsay *et al.* 1998), and *Haemophilus influenzae* (Martin *et al.* 1998). Bacterial secretion systems include Types I-V (T1SS, T2SS, T3SS, T4SS, and T5SS). The secretion systems consist of several different structural components to accommodate the variable biochemical composition of virulence factors (Remaut and Waksman 2004). Pathogenicity islands often possess one of these secretion systems for injecting virulence factors into the medium surrounding the bacteria or directly into cells.

Here we report histopathological changes in the liver of A/JCr mice infected with three different wild type (WT) strains of *H. hepaticus*. *H. hepaticus* type strain ATCC 51449 (Hh3B1) has an intact genomic island (HHGI1) and produced a lobular, necrogranulomatous hepatitis in all Hh3B1 infected male mice, whereas the other 2 WT strains, each possessing unique, individual partial deletions of HHGI1 (Suerbaum *et al.* 2003) were less virulent. One of these strains induced a significantly lower frequency of hepatitis and the other exhibited the same trend. Our results suggest that the 70 kb pathogenicity island in *H. hepaticus* 3B1 was, in part, responsible for the increased chronic, active hepatic inflammation seen in infected A/JCr mice versus mice infected with two strains of *H. hepaticus* lacking a large segment of HhPAI.

**Materials and methods**

Animals

Specific pathogen free male (n=34) and female (n=30) A/JCr mice that were viral antibody-free, free of pathogenic bacteria, parasites, and *Helicobacter*-free were purchased from the National Cancer Institute (NCI, Frederick, MD). Mice were maintained in an animal facility accredited by the Association for Assessment and Accreditation of Laboratory Animal Care, International (Rockville, MD). Mice were housed in 7.5 x 11.5 x 5 in. microisolator cages (Lab Products, Inc., Seaford, DE) on heat-treated hardwood bedding (Sanichips, PJ Murphy Inc., Montville, NJ), under environmental conditions of 22°C, 40 to 70% humidity, 15 nonrecirculated air changes/hour and a 12:12 h light: dark cycle. Pelleted diet (RMH 3000, Purina Mills Inc., Richmond, IN) and water produced by reverse-phase osmosis were provided ad libitum. Mice were euthanized by carbon dioxide asphyxiation at 3 months post-inoculation (one mouse from each cage; a total of 8 males and 8 females) and 6 months post-inoculation (Controls: 7 males, 4 females; Hh3B1: 6 males, 6 females; HhG: 6 males, 6 females; HhNET; 7 males, 6 females) (Table 1). Experimental use of animals was approved by the MIT Committee on Animal Care.

Bacteria

*H. hepaticus* strains ATCC 51449 (Hh3B1), MIT 96-284 (HhG), and MIT 96-1809 (HhNET) were utilized in this experiment. MIT 96-284 (HhG) and MIT 86-1809 (HhNET) were isolated at MIT from mice obtained from mouse colonies in Germany and the Netherlands, respectively. Strain differentiation was determined by DNA microarray hybridization (Suerbaum *et al.* 2003) and empty site polymerase chain reaction (PCR) utilizing the Expand Long Template PCR System (Roche, Indianapolis, IN) according to manufacturer's instructions. The empty site PCR

reaction was performed at the Suerbaum laboratory and utilized the primer set flanking the genomic island: fw 5'-ctaaatggctcatcaaccgg-3' which binds gene Hh0232 at position 221758-221777 and rv 5'-cacaaagtcatttgttgtgcc-3' and binds Hh0303 at position 294919-294938. No PCR product was obtained for Hh3B1 due to the 70kb length of HhPAI. PCR product obtained for HhNET was approximately 2.5 kilobases and for HhG was approximately 8 kb. The premix for each reaction was 5 ul buffer 2, 14 ul dNTP-mix, 2.5 ul of both primers (4 pmol/ul), 0.3 ul polymerase, 20.7 ul water added to 5 ul DNA. The cycling conditions were 94 °C for 5 minutes; 30 cycles at 94 °C for 1 minute, 55°C for 1 minute, 68 °C for 10 minutes; then 68 °C for 15 minutes. Additional standard PCR methods performed at MIT to verify strains utilized primers PCR1 (fw:5'-ggagcttcctcttgtatgcc-3'; rv: 5'-tacaaccctgcattttgcacc-3') binding to Hh0082, PCR2 (fw 5'-atcacttagattgacatagagc-3'; rv:5'-ataatccaaacaatgcaactcg-3') binding to Hh0236, and PCR3 (fw5'-gtgtttgattaactcctatccc-3'; rv:5'aaagaacggataactcatcgc-3') binding to Hh0298. All primer sequences were kindly provided by Suerbaum laboratory. The cycling conditions were: 94° C for 5 minutes; 30 cycles of 94° C for one minute, 55° C for one minute, 68° C for 1 minute; then 68° C for 15 minutes. *H. hepaticus* strains ATCC 51449 (Hh3B1) and MIT 96-1809 (HhNET) will generate a 461bp product and MIT 96-284 (HhG) will generate no product with primer PCR1. *H. hepaticus* strains ATCC 51449 (Hh3B1) generates a 461bp product and MIT 96-1809 (HhNET) and MIT 96-284 (HhG) will generate no product with primer PCR2. *H. hepaticus* strains ATCC 51449 (Hh3B1) and MIT 96-284 (HhG) will generate a 461bp product and MIT 96-1809 (HhNET) will generate no product with primer PCR3.

Bacterial inoculation

*H. hepaticus* strains ATCC 51449 (Hh3B1), MIT 96-284 (HhG), and MIT 96-1809 (HhNET) were cultured as previously described (Fox *et al.* 1994). Briefly, cultures were first grown on trypticase soy blood agar (Remel Laboratories, Lenexa, Kansas) at 37°C under microaerobic conditions in vented jars containing $N_2$, $H_2$, and $CO_2$ (80:10:10). After 48-72 hours, the cultures were inoculated into brucella broth containing 5% fetal calf serum and placed on a rotary shaker (New Brunswick Scientific, Edison, N.J.) at 130 rpm. After 48-72 hours, the culture was examined by phase microscopy for proper morphology and motility and Gram stained for detection of contaminants. The culture was centrifuged at 10,000 rpm (Microcentrifuge 235C; Fisher Scientific, Hampton, N. H.) for 20 minutes at 4°C. The pellet was resuspended in a solution of phosphate buffered saline (PBS) to approximately $10^8$ bacteria per ml as estimated by optical density ($OD_{600}$) (Fox *et al.* 1996a). At 10 weeks of age, mice (Hh3B1: 8 males, 8 females; HhG: 8 males, 8 females; HhNET; 9 males, 8 females) received 0.2 ml of fresh *H. hepaticus* inoculum, per dose, by oral gavage on three different days over a two week time period. Controls consisting of 9 males and 6 females received phosphate-buffered saline (PBS) alone (Table 1)

*Helicobacter hepaticus* isolation and colonization from feces, cecal contents, and cecum

Pooled fecal samples from all cages representative of all the experimental groups were cultured for *H. hepaticus* (Shames *et al.* 1995). DNA was extracted from the cecal contents using Qiagen DNA Stool Mini Kit #51504 (Qiagen, Valencia, CA) per manufacturer's instructions. DNA was extracted from paraffin-embedded cecal samples using EX-WAX DNA extraction kit (Chemicon International, Temecula, CA) per manufacturer's instructions.

*Helicobacter hepaticus* isolation and colonization from liver

*H. hepaticus* colonization in the liver for all 48 mice were assessed by real-time quantitative PCR using the PE Applied Biosystems Sequence Detection System (Model 7700, Applied Biosystems, Foster City, CA) as previously described (Ge *et al.* 2001). RNA and DNA were extracted from the liver using Trizol (Invitrogen, Carlsbad, CA) and RNA clean-up with RNeasy (Qiagen, Valencia, CA) following the manufacturer's protocol for the isolation of nucleic acids from tissue. Samples were separately probed with 18S rRNA-based primers for quantifying host DNA (Applied Biosystems) and with *H. hepaticus* primers complementary to a portion of the *H. hepaticus cdtB* gene as previously described (Ge *et al.* 2001). For quantitation, the PCR mix contained the following in duplicate 25 µl volumes: 5 µl template DNA, 12.5 µl of Universal Master Mix, 1.5 µl of cdtB probe and primer, and the balance DNAse-free dd$H_2O$. Thermocycling was performed at 50 °C for 2 minutes (min) and 95°C for 10 min, and then 40 repeats of 95°C for 15 seconds (sec) and 60°C for 60 sec. Seven *H. hepaticus* DNA standards including 2 femtograms (fg), 20 fg, 200 fg, 2 picograms (pg), 20 pg, 200 pg, and 2 nanograms (ng) , were used to generate a standard curve. The genome of *H. hepaticus* is 1.8 megabases with an approximate molecular weight (MW) of 845 x $10^6$ daltons (Suerbaum *et al.* 2003). One ng of *H. hepaticus* DNA is the equivalent of 1.18 x $10^6$ molecules (or bacteria). This relationship was used to estimate the number of *H. hepaticus* targets (genomes) per sample of liver (Ge *et al.* 2001).

Histopathology

Sagittal sections of each liver lobe (median, caudate, and left and right) were collected for histopathology. Tissues were immersion fixed overnight in 10% neutral-buffered formalin

(VWR Scientific, West Chester, PA). Fixed tissues were processed and embedded by routine histologic methods, sectioned at 5 μm, and stained with hematoxylin and eosin. The liver sections representing replicate samples from each lobe were examined by a board certified veterinary pathologist blinded to sample identity and graded on a 0—4 scale for lobular histologic activity, portal activity, and staged on the same scale for fibrosis using established criteria (Rogers *et al.* 2004; Scheuer 1991)

Dual fluorescence immunohistochemistry

To detect the predominant cellular infiltrate and evidence of reactive oxygen species, dual fluorescence immunohistochemistry with primary antibodies F4/80 and Nos2 was performed. Formalin fixed liver was deparaffinized and hydrated for antigen retrieval. The sequence of antibody applications and incubation times were as follows: avidin (Sigma, St. Louis, MO) for 5 minutes, biotin (Sigma, St. Louis, MO) for 5 minutes, primary antibodies Nos2 (Santa Cruz Biotech, Santa Cruz, CA) and F4/80 (Burlingame, CA) were combined at 1:100 for 30 minutes, biotinylated α rat (Sigma, St. Louis, MO) at 1:100 for 10 minutes, secondary antibody (SA)-fluorescein (FITC) at 1:100 for 5 minutes (green fluorochrome), biotin block for 1 minute, biotinylated α rabbit (Sigma, St. Louis, MO) at 1:1000 for 10 minutes, and (SA)-CY3™ (Sigma, St. Louis, MO) at 1:100 for 5 minutes (red fluorochrome). All the preceding antibody applications were followed by an phosphate buffered saline and Tween 20™ (Sigma, St. Louis, Mo) rinse: Slides were partially air-dried and cover slips with Vectorshield (Burlingame Lab, Burlingame, CA) with 4',6-Diamidino-2-phenylindole (DAPI) applied.

Statistical analysis

Analysis of hepatitis scores of all *H. hepaticus* infected A/JCr mouse groups and controls was performed by the Kruskal-Wallis nonparametric test and the Dunn's post test (GraphPad Prism, San Diego, CA). *H. hepaticus* colonization levels in the liver were obtained from quantitative real-time PCR and were analyzed by the same methods. Normalization of the *H. hepaticus* liver colonization data utilized the 18S rRNA levels in the total DNA content of the liver.

**Results**

Bacterial colonization in feces, cecal contents, and cecum

Each of the three strains of *H. hepaticus* was cultured from feces of 2 mice each from cages housing *H. hepaticus* infected mice at 12 weeks post infection, but *H. hepaticus* was not isolated from controls. The identity of the three strains at the start of the experiment, as well as *H. hepaticus* isolated from the feces of the experimental mice at 12 weeks post infection, was confirmed by PCR (Figure 1, Table 2). *H. hepaticus* colonization was detected in 36 of 37 infected mice via PCR of the cecum or cecal contents at 6 months post infection, but not from the 11 uninfected controls.

Bacterial copy number in liver

DNA from the liver of 48 mice necropsied at 6 months were tested for *H. hepaticus cdtB* by real-time quantitative PCR (Figure 2) (Ge *et al.* 2001). Serial dilutions of *H. hepaticus* DNA from 2 fg to 2 ng served as the positive control. *H. hepaticus* 3B1 ranking and median copy numbers in the male A/JCr mouse were consistently higher than the other two strains. Interestingly, one male mouse (03-6535) infected with the *H. hepaticus* HhNET strain and one male mouse

infected with strain HhG (03-6548) had high copy numbers and correspondingly severe composite hepatitis scores. For 6 of 8 composite hepatitis scores greater than or equal to 4.0, the *H hepaticus* copy numbers exceeded 1500. The maximum copy number measured was 23,300.

Histopathology

Sixteen mice representing each gender and all four groups were euthanized at 3 months post-infection. The mice exhibited varying degrees of lobular and portal hepatitis depending on *H. hepaticus* strain and gender. As expected, controls had no lesions while male mice infected with Hh3B1 had higher composite hepatitis index scores than other groups (Figure 3).

At 6 months post infection, all 6 male A/JCr mice infected with *H. hepaticus* ATCC 51449 (Hh3B1) developed severe liver disease resulting in necrogranulomatous lobular and/or lymphocytic portal hepatitis (Figures 4 and 5). The predominant cellular infiltrate of the lobular hepatitis was macrophages, and was accompanied by hepatocellular coagulative necrosis. Portal hepatitis was manifest as either well defined aggregates of mononuclear cells (chronic persistent hepatitis) or locally invasive lesions which disrupted the hepatic limiting plate (interface hepatitis). The results indicate a significant difference in hepatitis index (composite lobular hepatitis and portal hepatitis scores) between the Hh3B1 infected A/JCr mice versus controls ($p<.01$) and Hh3B1 versus HhNet ($p<.05$) (Figures 6 and 7). There is a trend, but not a significant difference, for Hh3B1 versus HhG. The male mice infected with MIT 96-284 (HhG) and MIT 96-1809 (HhNET) exhibited a bimodal histological index score as seen previously in a larger study of *H. hepaticus* 3B1 infection in A/J mice (Rogers et al, 2004). Four of six (4/6) HhG infected male A/JCr mice had minimal scores while two mice had moderate to severe hepatitis scores. Four of seven (4/7) HhNET infected A/JCr mice had minimal scores while

three mice had moderate to severe hepatitis scores. Sixteen of eighteen (16/18) female A/JCr mice in all three *H. hepaticus* infected groups had minimal hepatitis except for two mice (one Hh3B1 infected, one HhNET infected) where the hepatitis was judged moderate. The control mice had no or minimal hepatitis scores (Figures 6 and 7).

Dual fluorescence immunohistochemistry

Dual fluorescence immunohistochemistry confirmed that activated macrophages were the predominant cellular infiltrate in necrogranulomatous lobular hepatitis. The F4/80 primary antibody indicated the presence of macrophages and the Nos2 primary antibody indicated inducible nitric oxide synthase (iNOS) production. The dual fluorescence confirmed the presence of activated macrophages inducing iNOS within the foci of lobular hepatitis (Figure 8).

**Discussion**

*Helicobacter hepaticus* causes hepatocellular carcinoma in certain strains of mice, but the virulence factors responsible for this have not been identified (Fox *et al.* 1994; Fox *et al.* 1996a; Hailey *et al.* 1998; Ihrig *et al.* 1999; Ward *et al.* 1994a). The *H. hepaticus* strain ATCC 51449 *H. hepaticus* (Hh3B1) possesses a genomic island (HHGI1) hypothesized to play a key role in disease development (Suerbaum *et al.* 2003). To determine the importance of the putative PAI , we compared the wild type strain to two other strains, MIT 96-1809 (HhNET) isolated from mice originating in the Netherlands and MIT-96-284 (HhG) isolated from mice shipped from Germany; both of these strains lacked the genomic island (Suerbaum *et al.* 2003). In HhNET infected male A/JCR mice there was a significantly lower prevalence of hepatic lesions than Hh3B1 at 6 months post infection. Males exhibited more severe liver lesions than females. HhG

infected mice also had lower prevalence of hepatic lesions. Hepatitis scores greater than or equal to 2.5 generally corresponded with copy numbers of the *H. hepaticus* greater than 1500, with a maximum copy number of 22,300. However, there a large variance in *H. hepaticus* copy number did occur. Previous studies have demonstrated much larger copy numbers of *H. hepaticus* and more numerous and larger lobular lesions at 12 months post infection (Rogers *et al.* 2004). Nevertheless, in this experiment, all the *H. hepaticus* 3B1 infected male A/JCr mice had severe hepatic lesions at 6 months. The male A/JCr mice infected with the two HHGI1-defective *H. hepaticus* strains exhibited a bimodal distribution of hepatitis scores. This male predominance and bimodal distribution of lesions has been exhibited in other *H. hepaticus* 3B1 studies where there was a positive correlation of bacterial copy number to hepatitis score at 12 months post-inoculation (Rogers *et al.* 2004). Interestingly, this was the colony of mice where Hh3B1 was first isolated (Fox *et al.* 1994). This bimodal distribution was first noted in A/JCr mice naturally infected with *H. hepaticus* (Fox et al. 1996b)

As has been demonstrated in previous studies, the lobular hepatitis cellular infiltrate was predominantly macrophages (Rogers *et al.* 2004). In this study, we demonstrated that macrophages were activated as evidenced by iNOS protein synthesis (Figure 8). The reactive oxygen and nitrogen species generated by nitric oxide chemistry (this reads strange) increases cancer risk due to DNA mutation and DNA adducts (Dedon and Tannenbaum 2004). Results of several *in vitro* experiments show *H. pylori* induces iNOS expression in gastric epithelial cells (Kim *et al.* 2003; Perfetto *et al.* 2004). *H. pylori* infected iNOS$^{-/-}$ mice exhibit reduced apoptosis as compared to iNOS+/+ mice (Miyazawa *et al.* 2003). Also, recent studies with *H. felis*

infected iNOS$^{-/-}$ mice demonstrated significantly reduced gastritis scores relative to *H. felis* infected wild type mice at 32 weeks post infection (Ihrig *et al*., in press).

In summary, our findings demonstrate that A/JCr mice infected with two strains of *H. hepaticus* (HhG and HhNET), with large deletions in a 70kb genomic island as compared to ATCC 51449 (Hh3B1), exhibited a lower prevalence of hepatic lesions than Hh3B1 at 6 months post infection. The histologic index depended on *H. hepaticus* colonization levels and only male mice exhibited hepatic lesions with high histological indices. These results suggest that the HHGI1 plays a role in pathogenesis of liver disease in A/JCr male mice, and supports that this island represents a functional pathogenicity island. Additional infection studies are needed using isogenic mutants of *H. hepaticus* 3B1, lacking the HhPAI, to confirm these findings.

**Table 1** A/JCr mouse groups at inoculation and at 6 months post-infection. Eight males and eight females, two mice from each group, were euthanized at 3 months.

**Intial groups at inoculation**

| Groups | Males | Females |
|---|---|---|
| Control | 9 | 6 |
| Hh3B1 | 8 | 8 |
| HhG | 8 | 8 |
| HhNET | 9 | 8 |

**6 months post infection**

| Groups | Males | Females |
|---|---|---|
| Control | 7 | 4 |
| Hh3B1 | 6 | 6 |
| HhG | 6 | 6 |
| HhNET | 7 | 6 |

**Figure 1**. *H. hepaticus* strain identification via PCR prior to A/JCr mouse inoculation and after isolation from feces at 3 months post infection. Three primers, 83, 236, and 298 were utilized to differentiate *H. hepaticus* strains. Hh3B1 is in lane 1,5, and 9. HhG is in lane 2, 6, and 10. HhNET is in lane 3, 7, and 11. The gel exhibits the PCR primer products for each strain. The code for each strain is in Table 2.

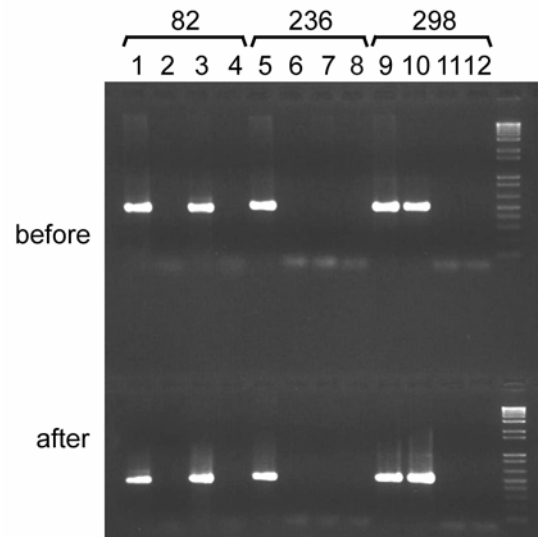


**Table 2** *H. hepaticus* strain differentiation via PCR. Primer combinations that produce bands (indicated by +) identify the individual strain.

| | **Primer** | 82 | 236 | 298 |
|---|---|---|---|---|
| **Group** | | | | |
| Hh3B1 | | + | + | + |
| HhG | | - | - | + |
| HhNET | | + | - | - |

**Figure 2.** *H. hepaticus* 3B1, HhG, and HhNET copy number in male A/JCr livers at 6 months.

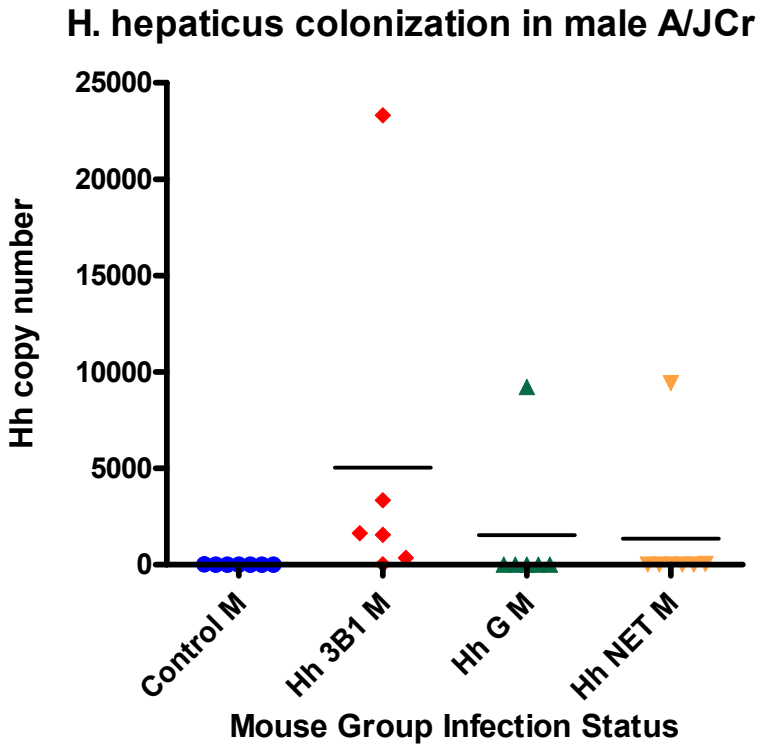

**Figure 3** Hepatitis index (combined lobular and portal hepatitis scores) of all groups of A/JCr mice infected with the type strain *H. hepaticus* 3B1 and two other wild type strains of *H. hepaticus* at 3 months post-inoculation.

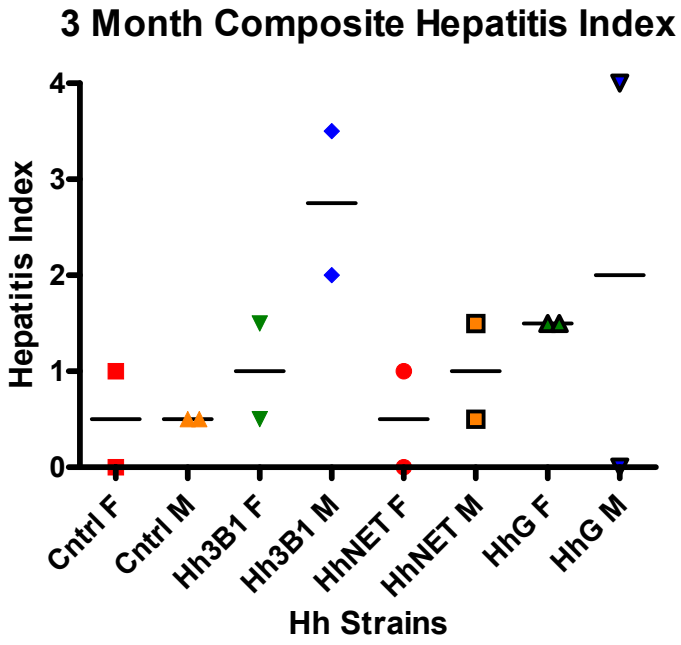

**Figure 4** Necrogranulomatous lobular hepatitis in an *H. hepaticus* 3B1 infected male A/JCr at 6 months post-inoculation. The predominant cellular infiltrate of the lobular hepatitis was macrophages, and was accompanied by hepatocellular coagulative necrosis. Magnification: 200X

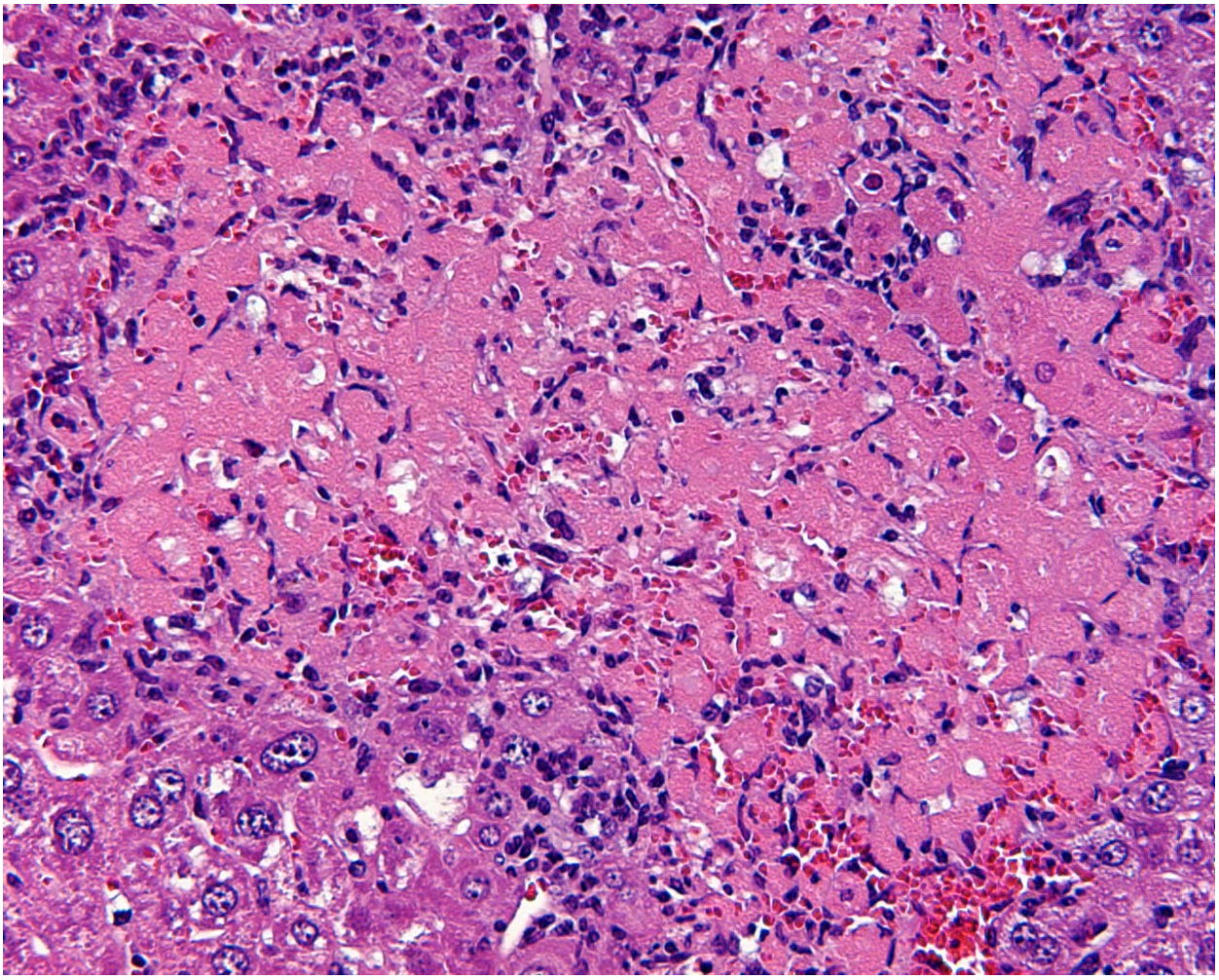

**Figure 5** Portal hepatitis in an *H. hepaticus* 3B1 infected male A/JCr mouse at 6 months post inoculation. Portal hepatitis was manifest as either well defined aggregates of mononuclear cells (chronic persistent hepatitis) or locally invasive lesions which disrupted the hepatic limiting plate (interface hepatitis). Magnification: 200X

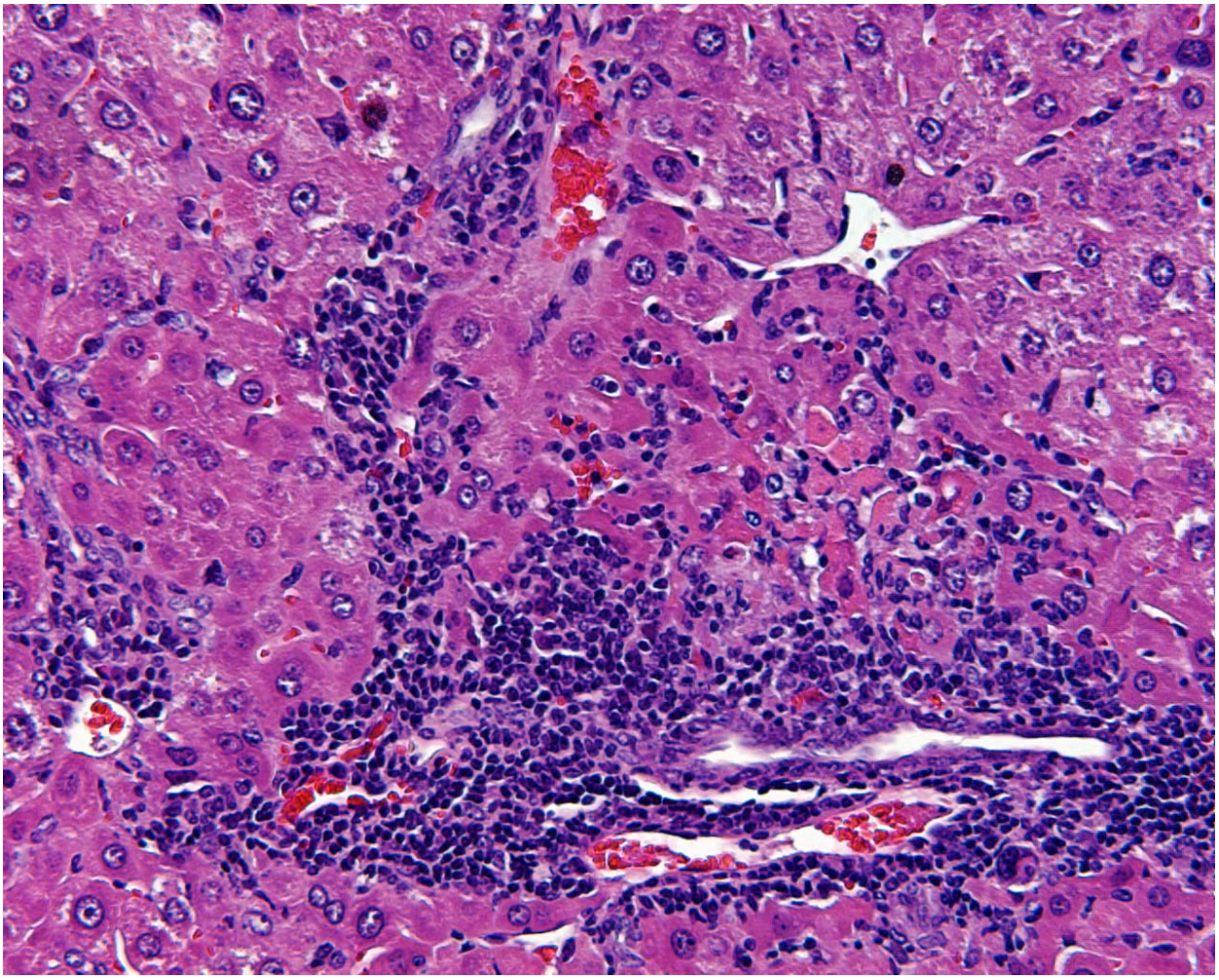

**Figure 6.** Hepatitis index (combined lobular and portal hepatitis scores) of all groups (both genders combined) of A/JCr mice infected with the type strain *H. hepaticus* 3B1 and two other wild type strains of *H. hepaticus* at 6 months post-inoculation. * Statistical significance ($p<.05$) versus control and HhNET, trend toward HhG

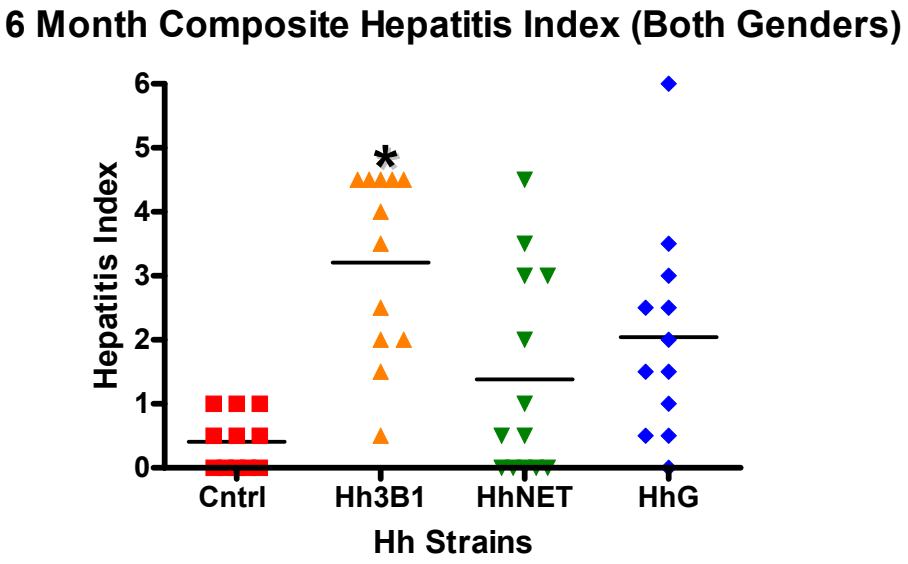

**Figure 7.** Hepatitis index (combined lobular and portal hepatitis scores) of all male groups of A/JCr mice infected with the type strain *H. hepaticus* 3B1 and two other wild type strains of *H. hepaticus* at 6 months post-inoculation. * Statistical significance ($p<.05$) versus control and HhNET, trend toward HhG

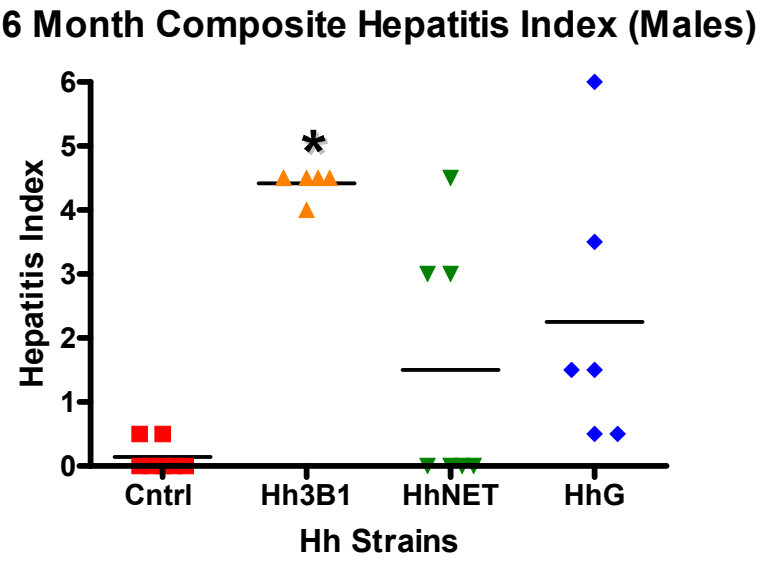

**Figure 8. Dual fluorescence immunohistochemistry.** The slide illustrates activated macrophages producing iNOS in necrogranulomatous lobular hepatitis. Colors: blue: nuclei; green: macrophages, red: iNOS, and yellow/orange: co-localization of iNOS and macrophage. Magnification: 400X

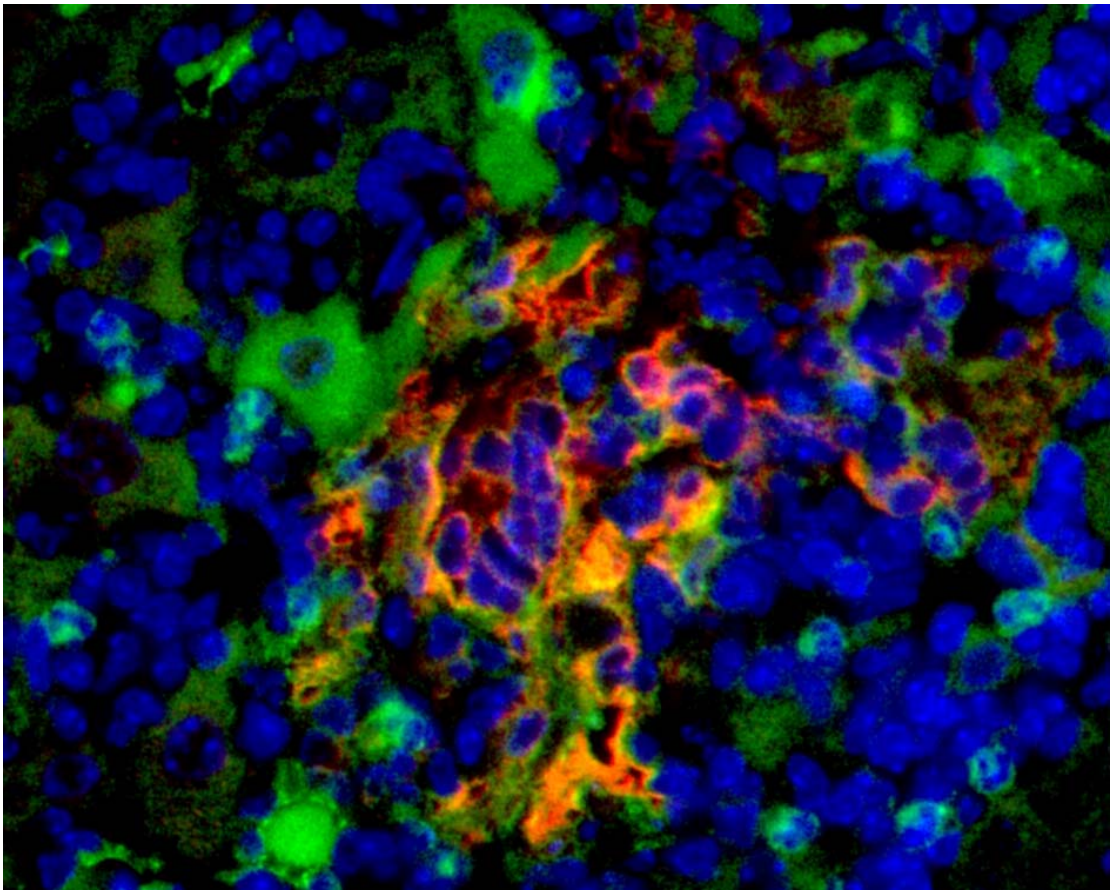

**REFERENCES**


Azuma, T., Yamakawa, A., Yamazaki, S., Ohtani, M., Ito, Y., Muramatsu, A., Suto, H., Yamazaki, Y., Keida, Y., Higashi, H., and Hatakeyama, M. (2004). Distinct diversity of the cag pathogenicity island among *Helicobacter pylori* strains in Japan. *J Clin Microbiol* **42**, 2508-17.

Backert, S., Schwarz, T., Miehlke, S., Kirsch, C., Sommer, C., Kwok, T., Gerhard, M., Goebel, U. B., Lehn, N., Koenig, W., and Meyer, T. F. (2004). Functional analysis of the cag pathogenicity island in *Helicobacter pylori* isolates from patients with gastritis, peptic ulcer, and gastric cancer. *Infect Immun* **72**, 1043-56.

Bajaj, V., Hwang, C., and Lee, C. A. (1995). hilA is a novel ompR/toxR family member that activates the expression of *Salmonella typhimurium* invasion genes. *Mol Microbiol* **18**, 715-27.

Batchelor, R. A., Pearson, B. M., Friis, L. M., Guerry, P., and Wells, J. M. (2004). Nucleotide sequences and comparison of two large conjugative plasmids from different *Campylobacter* species. *Microbiology* **150**, 3507-17.

Blomstergren, A., Lundin, A., Nilsson, C., Engstrand, L., and Lundeberg, J. (2004). Comparative analysis of the complete cag pathogenicity island sequence in four *Helicobacter pylori* isolates. *Gene* **328**, 85-93.

Blum, G., Ott, M., Lischewski, A., Ritter, A., Imrich, H., Tschape, H., and Hacker, J. (1994). Excision of large DNA regions termed pathogenicity islands from tRNA-specific loci in the chromosome of an *Escherichia coli* wild-type pathogen. *Infect Immun* **62**, 606-14.

Buchrieser, C., Prentice, M., and Carniel, E. (1998). The 102-kilobase unstable region of *Yersinia pestis* comprises a high-pathogenicity island linked to a pigmentation segment which undergoes internal rearrangement. *J Bacteriol* **180**, 2321-9.

Censini, S., Lange, C., Xiang, Z., Crabtree, J. E., Ghiara, P., Borodovsky, M., Rappuoli, R., and Covacci, A. (1996). cag, a pathogenicity island of *Helicobacter pylori*, encodes type I-specific and disease-associated virulence factors. *Proc Natl Acad Sci U S A* **93**, 14648-53.

Dedon, P. C., and Tannenbaum, S. R. (2004). Reactive nitrogen species in the chemical biology of inflammation. *Arch Biochem Biophys* **423**, 12-22.

Erdman, S. E., Poutahidis, T., Tomczak, M., Rogers, A. B., Cormier, K., Plank, B., Horwitz, B. H., and Fox, J. G. (2003a). CD4+ CD25+ regulatory T lymphocytes inhibit microbially induced colon cancer in Rag2-deficient mice. *Am J Pathol* **162**, 691-702.

Erdman, S. E., Rao, V. P., Poutahidis, T., Ihrig, M. M., Ge, Z., Feng, Y., Tomczak, M., Rogers, A. B., Horwitz, B. H., and Fox, J. G. (2003b). CD4(+)CD25(+) regulatory lymphocytes require interleukin 10 to interrupt colon carcinogenesis in mice. *Cancer Res* **63**, 6042-50.

Fox, J. G. (2002). The non-H *pylori Helicobacter*s: their expanding role in gastrointestinal and systemic diseases. *Gut* **50**, 273-83.

Fox, J. G., Dewhirst, F. E., Tully, J. G., Paster, B. J., Yan, L., Taylor, N. S., Collins, M. J., Jr., Gorelick, P. L., and Ward, J. M. (1994). *Helicobacter hepaticus* sp. nov., a microaerophilic bacterium isolated from livers and intestinal mucosal scrapings from mice. *J Clin Microbiol* **32**, 1238-45.

Fox, J. G., Li, X., Yan, L., Cahill, R. J., Hurley, R., Lewis, R., and Murphy, J. C. (1996a). Chronic proliferative hepatitis in A/JCr mice associated with persistent *Helicobacter hepaticus* infection: a model of *Helicobacter*- induced carcinogenesis. *Infect Immun* **64**, 1548-58.

Fox, J. G., Yan, L., Shames, B., Campbell, J., Murphy, J. C., and Li, X. (1996b). Persistent hepatitis and enterocolitis in germfree mice infected with *Helicobacter hepaticus*. *Infect Immun* **64**, 3673-81.

Ge, Z., White, D. A., Whary, M. T., and Fox, J. G. (2001). Fluorogenic PCR-based quantitative detection of a murine pathogen, *Helicobacter hepaticus*. *J Clin Microbiol* **39**, 2598-602.

Hailey, J. R., Haseman, J. K., Bucher, J. R., Radovsky, A. E., Malarkey, D. E., Miller, R. T., Nyska, A., and Maronpot, R. R. (1998). Impact of *Helicobacter hepaticus* infection in B6C3F1 mice from twelve National Toxicology Program two-year carcinogenesis studies. *Toxicol Pathol* **26**, 602-11.

Ihrig, M., Schrenzel, M. D., and Fox, J. G. (1999). Differential susceptibility to hepatic inflammation and proliferation in AXB recombinant inbred mice chronically infected with *Helicobacter hepaticus*. *Am J Pathol* **155**, 571-82.

Kim, J. M., Kim, J. S., Jung, H. C., Oh, Y. K., Chung, H. Y., Lee, C. H., and Song, I. S. (2003). *Helicobacter pylori* infection activates NF-kappaB signaling pathway to induce iNOS and protect human gastric epithelial cells from apoptosis. *Am J Physiol Gastrointest Liver Physiol* **285**, G1171-80.

Konkel, M. E., Klena, J. D., Rivera-Amill, V., Monteville, M. R., Biswas, D., Raphael, B., and Mickelson, J. (2004). Secretion of virulence proteins from *Campylobacter jejuni* is dependent on a functional flagellar export apparatus. *J Bacteriol* **186**, 3296-303.

Larsen, J. C., Szymanski, C., and Guerry, P. (2004). N-linked protein glycosylation is required for full competence in *Campylobacter jejuni* 81-176. *J Bacteriol* **186**, 6508-14.

Lindsay, J. A., Ruzin, A., Ross, H. F., Kurepina, N., and Novick, R. P. (1998). The gene for toxic shock toxin is carried by a family of mobile pathogenicity islands in *Staphylococcus aureus*. *Mol Microbiol* **29**, 527-43.

Martin, K., Morlin, G., Smith, A., Nordyke, A., Eisenstark, A., and Golomb, M. (1998). The tryptophanase gene cluster of *Haemophilus influenzae* type b: evidence for horizontal gene transfer. *J Bacteriol* **180**, 107-18.

Miyazawa, M., Suzuki, H., Masaoka, T., Kai, A., Suematsu, M., Nagata, H., Miura, S., and Ishii, H. (2003). Suppressed apoptosis in the inflamed gastric mucosa of *Helicobacter pylori*-colonized iNOS-knockout mice. *Free Radic Biol Med* **34**, 1621-30.

Ogierman, M. A., Fallarino, A., Riess, T., Williams, S. G., Attridge, S. R., and Manning, P. A. (1997). Characterization of the *Vibrio cholerae* El Tor lipase operon lipAB and a protease gene downstream of the hly region. *J Bacteriol* **179**, 7072-80.

Perfetto, B., Buommino, E., Canozo, N., Paoletti, I., Corrado, F., Greco, R., and Donnarumma, G. (2004). Interferon-gamma cooperates with *Helicobacter pylori* to induce iNOS-related apoptosis in AGS gastric adenocarcinoma cells. *Res Microbiol* **155**, 259-66.

Poly, F., Threadgill, D., and Stintzi, A. (2004). Identification of *Campylobacter jejuni* ATCC 43431-specific genes by whole microbial genome comparisons. *J Bacteriol* **186**, 4781-95.

Rajakumar, K., Sasakawa, C., and Adler, B. (1997). Use of a novel approach, termed island probing, identifies the *Shigella flexneri* she pathogenicity island which encodes a homolog of the immunoglobulin A protease-like family of proteins. *Infect Immun* **65**, 4606-14.

Remaut, H., and Waksman, G. (2004). Structural biology of bacterial pathogenesis. *Curr Opin Struct Biol* **14**, 161-70.

Rogers, A., Boutin, S., Whary, M., Sundina, N., Ge, Z., Cormier, K., and Fox, J. (2004). Progression of Chronic Hepatitis and Preneoplasia in *Helicobacter hepaticus*-Infected A/JCr Mice. *Toxicol Pathol* **32**, 668-77.

Rogers, A. B., and Fox, J. G. (2004). Inflammation and Cancer I. Rodent models of infectious gastrointestinal and liver cancer. *Am J Physiol Gastrointest Liver Physiol* **286**, G361-6.

Scheuer, P. J. (1991). Classification of chronic viral hepatitis: a need for reassessment. *J Hepatol* **13**, 372-4.

Schubert, S., Rakin, A., Karch, H., Carniel, E., and Heesemann, J. (1998). Prevalence of the "high-pathogenicity island" of *Yersinia* species among *Escherichia coli* strains that are pathogenic to humans. *Infect Immun* **66**, 480-5.

Shames, B., Fox, J. G., Dewhirst, F., Yan, L., Shen, Z., and Taylor, N. S. (1995). Identification of widespread *Helicobacter hepaticus* infection in feces in commercial mouse colonies by culture and PCR assay. *J Clin Microbiol* **33**, 2968-72.

Solnick, J. V., and Schauer, D. B. (2001). Emergence of diverse *Helicobacter* species in the pathogenesis of gastric and enterohepatic diseases. *Clin Microbiol Rev* **14**, 59-97.

Song, Y. C., Jin, S., Louie, H., Ng, D., Lau, R., Zhang, Y., Weerasekera, R., Al Rashid, S., Ward, L. A., Der, S. D., and Chan, V. L. (2004). FlaC, a protein of *Campylobacter jejuni* TGH9011 (ATCC43431) secreted through the flagellar apparatus, binds epithelial cells and influences cell invasion. *Mol Microbiol* **53**, 541-53.

Suerbaum, S., Josenhans, C., Sterzenbach, T., Drescher, B., Brandt, P., Bell, M., Droge, M., Fartmann, B., Fischer, H. P., Ge, Z., Horster, A., Holland, R., Klein, K., Konig, J., Macko, L., Mendz, G. L., Nyakatura, G., Schauer, D. B., Shen, Z., Weber, J., Frosch, M., and Fox, J. G. (2003). The complete genome sequence of the carcinogenic bacterium *Helicobacter hepaticus*. *Proc Natl Acad Sci U S A* **100**, 7901-6.

Ward, J. M., Anver, M. R., Haines, D. C., and Benveniste, R. E. (1994a). Chronic active hepatitis in mice caused by *Helicobacter hepaticus*. *Am J Pathol* **145**, 959-68.

Ward, J. M., Fox, J. G., Anver, M. R., Haines, D. C., George, C. V., Collins, M. J., Jr., Gorelick, P. L., Nagashima, K., Gonda, M. A., Gilden, R. V., and et al. (1994b). Chronic active hepatitis and associated liver tumors in mice caused by a persistent bacterial infection with a novel *Helicobacter* species. *J Natl Cancer Inst* **86**, 1222-7.

Yang, G. F., Deng, C. S., Xiong, Y. Y., Gong, L. L., Wang, B. C., and Luo, J. (2004). Expression of nuclear factor-kappa B and target genes in gastric precancerous lesions and adenocarcinoma: association with Helicobactor *pylori* cagA (+) infection. *World J Gastroenterol* **10**, 491-6.

# Chapter 5

## *Helicobacter hepaticus* pathogenicity island mediates RAW264.7 macrophage response

**Abstract**

*Helicobacter hepaticus* ATCC 51449 (Hh3B1) induces hepatocellular carcinoma (HCC) in A/JCr mice and colon cancer in certain immunodeficient lines of mice. Recent studies demonstrated the virulence of *H. hepaticus* to be bacterial strain dependent based on the possession of a 70kb genomic island. The genomic island, a putative pathogenicity island (HhPAI), consists of genes HH233-HH302 and components of a Type IV secretion system (T4SS). In order to characterize the differences in virulence between *H. hepaticus* strains isolated from mouse colonies from different regions of the world and isogenic mutants, *in vitro* experiments were performed. Since macrophages are the predominant inflammatory cell type in *H. hepaticus* induced lobular hepatitis, the location of progressively dysplastic lesions, and the development of HCC, the murine macrophage cell line RAW264.7 was utilized for *in vitro* infection studies. Hh3B1, possessing the HhPAI, induced significantly increased cytokine expression from murine macrophages as compared to an HhPAI isogenic mutant and one wild type strain lacking the HhPAI.

## Introduction

*Helicobacter hepaticus* induces hepatocellular carcinoma (HCC) in A/JCr mice and colon cancer in certain immunodeficient lines of mice (Erdman *et al.* 2003a; Erdman *et al.* 2003b; Fox *et al.* 1994; Fox *et al.* 1996; Ihrig *et al.* 1999; Ward *et al.* 1994). We recently demonstrated the virulence of *H. hepaticus* to be bacterial strain dependent based on the possession of a 70kb genomic island (Boutin et al, in preparation). In that study, the hepatitis of the A/JCr male mice infected with the type strain *H. hepaticus* ATC51449 (Hh3B1), possessing a genomic island (HHGI1), was more severe than two wild type strains lacking the HHGI1, at 6 months post inoculation. The genomic island, a putative pathogenicity island (HhPAI), consists of genes HH233-HH302. Hh3B1 was first isolated from in *H. hepaticus* infected A/JCr mice exhibiting HCC (Fox *et al.* 1994; Fox *et al.* 1996; Ward *et al.* 1994). Most of the PAI is absent in *H. hepaticus* MIT 96-1809 (HhNET) (Suerbaum *et al.* 2003). HhNET was isolated at MIT from murine samples obtained from mouse colonies in the Netherlands. HhNET and Hh3B1 contain gene differences in the rest of the genome as determined by DNA hybridization to a *H. hepaticus* microarray (Suerbaum *et al.* 2003).

In order to further characterize the differences in virulence between the *H. hepaticus* strains, *in vitro* experiments were performed. Since macrophages are the predominant inflammatory cell type in lobular hepatitis due to *H. hepaticus* infection as demonstrated by histopathology (Rogers *et al.* 2004) (Appendix 1) and microarray studies (Boutin *et al.* 2004) (Chapter 3), a murine macrophage cell line, RAW264.7, was chosen for

experiments. Macrophages are ubiquitous in normal tissues, as well as in cancers (Mantovani *et al.* 2003; Ohno *et al.* 2003; van Ravenswaay Claasen *et al.* 1992). The tumor microenvironment differs depending on tumor type and can influence the activation and differentiation of tumor-infiltrating monocytes generating macrophages with tumor-specific phenotypes (Lewis *et al.* 1999; Mantovani *et al.* 2003; Mantovani *et al.* 2004; Ohno *et al.* 2003). The activation and differentiation of macrophages can also depend on microbial stimuli, particularly the lipid A component of lipopolysaccharide (LPS) (Ulevitch *et al.* 2004; Ulevitch and Tobias 1999). There are other biochemical structures such as lipoproteins, flagellin, and peptidoglycans recognized by macrophage toll-like receptors and intracytoplasmic receptors (Li and Cherayil 2004; Viala *et al.* 2004). *H. hepaticus* LPS is recognized by toll-like receptor 4 whereas whole *H. hepaticus* is recognized by LPS toll-like receptor 2 as determined by cytokine response (Mandell *et al.* 2004). The expression of specific cytokine genes of a murine macrophage cell line in response to *H. hepaticus* allowed comparisons of these *in vitro* results to 3, 6, and 12 month microarray studies of *H. hepaticus* infected A/JCr mouse liver (Chapter 3) and an infection study with the Hh3B1, HhG, and HhNET at 6 months post-innoculation (Chapter 4).

In this study. we infected RAW264.7 murine macrophage cell cultures with two wild type strains (Hh3B1, HhNET) and an isogenic mutant strain (HhBac26) of *H. hepaticus*. One wild type strain, HhNET, lacks most of a putative PAI of *H. hepaticus*. The mutant strain lacks genes HH250-HH268 of the PAI. The goal was to test the hypothesis that HhNET was less virulent than Hh3B1 *in vivo* (Boutin et al, in preparation) due to the

absence of a type IV secretion system (T4SS). This was done by comparing the cytokine response of RAW264.7 murine macrophages to Hh3B1, HhNET, and HhBac26. Cytokines Cxcl4, Cxcl10, Cxcl1, Cxcl2, Ccl2, Ccl3 and Tnf were selected since they are up-regulated by macrophages in response to bacterial components (Burke and Lewis 2002; Mantovani *et al.* 2004; Moller *et al.* 2003). Hh3B1 possessing the HhPAI induced significantly increased cytokine expression from the murine macrophage cell line RAW 264.7 as compared to the wild type HhNET strain lacking the HhPAI, as well as the isogenic mutant HhBac26.

## Materials and methods

### Macrophage infection assay

All experiments utilized murine macrophage cell line RAW264.7 (ATCC: TIB-71) maintained in Dulbecco's Modified Eagle Medium (12800-058 Gibco/Invitrogen, Carlsbad, CA) supplemented with 3.7 g/L sodium bicarbonate (# 3506-01 Sigma, St. Louis, MO), 100 ml/L fetal calf serum (FCS) (#10082-147 Gibco/Invitrogen, Carlsbad, CA) at 37°C and 5% $CO_2$. Macrophages were seeded at 5.5 x $10^6$ cells per 25 $cm^2$ flask for the experiment and incubated for 24 hours at 37°C at 5% $CO_2$. After 24 hours, the medium was removed and replaced with medium without fetal calf serum. The cells were incubated an additional 24 hours prior to bacterial inoculation at a multiplicity of infection (MOI) of 0.1. The number of tissue culture flasks prepared allowed a minimum of three replicate flasks for each test group.

Bacterial inoculation

*H. hepaticus* strains ATCC 51449 (Hh3B1), MIT 96-1809 (HhNET), and isogenic mutant HhBac26 were utilized in this experiment. Genes HH0250-HH0268 are deleted in HhBac26. Both *H. hepaticus* strains and the isogenic mutant were cultured as previously described (Fox *et al.* 1994). Briefly, cultures were first grown on trypticase soy blood agar (Remel Laboratories, Lenexa, Kansas) at 37°C under microaerobic conditions in vented jars containing $N_2$, $H_2$, and $CO_2$ (80:10:10). After 72 hours, the bacteria were removed from the plates and resuspended in sterile phosphate buffered saline (PBS). The suspension was examined by phase microscopy for proper morphology, motility, and contaminants. A 50µl sample of the bacterial suspension was diluted 1:20 and a spectrophotometer (Beckman Coulter, Fullerton, CA) reading was performed at 660 nm to determine the number of bacteria. An optical density of 1.0 corresponds to approximately 3 x $10^9$ *H. hepaticus* /ml. The bacterial inoculum was prepared by diluting the bacterial suspension with PBS to obtain the desired multiplicity of infection (MOI).

Lipopolysaccharide (LPS) (LPS ECO55:B5 cat. # 62326 Sigma, St. Louis, MO) was used as a positive control. LPS was purified using hot phenol and water as previously reported (Hirschfeld *et al.* 2000).and prepared at a concentration of 100 ng/ml. The inoculation final concentration was 100ng LPS per 25 $cm^2$ cell culture flask.

MOI and exposure time were empirically determined and included MOI = 0.1, 1.0, and 10.0 at 4 and 24 hours. One ml of Trizol (Invitrogen, Carlsbad, CA) was pipetted into each flask for one minute and a sterile cell scraper (Becton Dickinson, Franklin Lakes,

NJ) was used to remove the cells. The cell/Trizol solution was stored at –80°C for subsequent RNA isolation.

RNA isolation and reverse transcription reaction

RNA and DNA were extracted from the RAW264.7 cells using Trizol (Invitrogen, Carlsbad, CA) for the isolation of nucleic acids from cell culture as specified by the manufacturer. Total RNA was further purified with RNeasy (Qiagen, Valencia, CA) following the manufacturer's protocol. All RNA samples used had a 260/280 ratio greater than 1.9. The Reverse Transcription reaction was performed according to manufacturer's instructions with the Superscript II system (Invitrogen, Carlsbad, CA) at a uniform total RNA concentration of 1μg per sample volume. Eighty microliters of TE was added to the resultant cDNA. For quantitation, real-time quantitative PCR was performed.

Gene expression measurements

Gene expression was assessed by real-time quantitative PCR using the PE Applied Biosystems Sequence Detection System per manufacturer's instructions (Model 7700, Applied Biosystems, Foster City, CA). For each replicate, the PCR mix contained the following in 25 μl volumes: 5 μl template DNA, 12.5 μl of Universal Master Mix, 1.5 μl of probe and primer, and the balance DNAse-free dd$H_2O$. Thermocycling was performed at 50 °C for 2 minutes (min) and 95°C for 10 min, and then 40 repeats of 95°C for 15 seconds (sec) and 60°C for 60 sec. Control samples were probed with 18S rRNA-based

primers (Applied Biosystems, Foster City, CA) for quantifying host RAW cell RNA for normalization calculations. The Taqman® Gene Expression system probes and primers utilized were cytokines Cxcl4, Cxcl10, Cxcl1, Cxcl2, Ccl2, Ccl3 and Tnf (Applied Biosystems, Foster City, CA).

Normalization

Normalization and fold change calculations for cytokine expression values were calculated by the comparative $C_T$ method as recommended in User Bulletin #2: ABI Prism 7700 Sequence Detection System (Applied Biosystems, Foster City, CA). Reference samples for normalization were assessed by 18S Taqman Gene Expression (Applied Biosystems, Foster City, CA)

Statistical analysis

The $\Delta C_T$ value was determined by subtracting the average 18S $C_T$ value from a average positive control, cytokine, or LPS value. The standard deviation of $\Delta C_T$ is the square root of the sum of the squares of the standard deviations of the individual $C_T$ values. The standard deviation of $\Delta\Delta C_T$ is the same as the standard deviation of $\Delta C_T$. Analysis of $\Delta\Delta C_T$ scores from all *H. hepaticus* infected RAW264.7 groups and positive and negative controls was performed by One Way Analysis of Variance and Dunnett's post test.

## Results

The RAW264.7 murine macrophage cell line was exposed to the type strain Hh3B1 which contains the HhPAI, a wild type strain HhNET lacking the PAI, and an isogenic mutant HhBac26 with genes HH0250-HH0268 deleted. The MOI was 0.1 and the exposure time was 24 hours.

Quantitative real time RT-PCR

HhBac26 (isogenic mutant of HhPAI) did not elicit a cytokine increase for any cytokine tested. Hh3B1 (with HhPAI) and LPS produced a significant increase ($p<.05$) of cytokine level versus control for Cxcl2, Ccl2, Ccl3, and Tnf (Figure 1). The average fold changes for these cytokines are shown in Table 1. Hh3B1, HhNET (without HhPAI), and LPS induced a significant increase of Cxcl4 versus control ($p<.05$). Only LPS produced a significant Cxcl1 response ($p<.01$), while no treatment exhibited significant differences for Cxcl10. The results indicate cytokine increases for 4 out of 6 cytokines tested due to the presence of the HhPAI.

## Discussion

*H. hepaticus* virulence factors may reside on the 70kb genomic island HHGI1, a putative *H. hepaticus* pathogenicity island (HhPAI) contained in the type strain *H. hepaticus* ATCC 51449 strain (Hh3B1). HHGI1 encodes three basic components of a T4SS and

other virulence protein homologs (Suerbaum *et al.* 2003). Our experiments demonstrate a significant difference in selected cytokine responses of the murine macrophage cell line RAW264.7 (ATCC: TIB-71) when infected by Hh3B1 versus control but not HhNET or HhBac26 versus control (Figure 1). Wild type strain MIT 96-1809 (HhNET) has most of the HhPAI deleted and isogenic mutant strain HhBac26 has a partial deletion of the HhPAI. The RAW264.7/*H. hepaticus* infection experiments were performed at an MOI=0.1 for 24 hours. Previous *in vivo* studies of different wild type strains of *H. hepaticus* in the A/JCr mouse have demonstrated the type strain *H. hepaticus* ATCC 51449 strain (Hh3B1), which contains the HhPAI, to be more virulent than two other strains MIT 96-1809 (HhNET) and MIT-96-284 (HhG) which lack most of the HhPAI (Chapter 4). These data support the hypothesis that HhNET and HhG are less virulent due to the lack of a T4SS and other virulence components. Hh3B1 produced both more severe hepatitis scores and a higher frequency of hepatitis than HhG and HhNET (Chapter 4).

Previous microarray studies of chronic active hepatitis and dysplasia of *H. hepaticus* infected A/JCr mice at 3, 6, and 12 months post-infection demonstrated a consistent grouping of inflammation associated genes exhibiting differential expression (Chapter 3). The cytokines and cytokine receptors in hepatic tissue were up-regulated more than 2 fold in those studies included Cxcl9, Cxcl10, Cxcl13, and Ccr5. Interestingly, macrophages have recently been categorized by activation and polarization phenotypes as M1, M2a, M2b, and M2c, analogous to the Th1 and Th2 lymphocytes (Mantovani *et al.* 2004). Cxcl9 and Cxcl10 produced by monocytes bind receptor Cxcr3 on natural killer

(NK) and Th1 cells in a polarizing Type 1 response, and Cxcr3 and Ccr5 are also expressed on polarized Type I T cells (Mantovani *et al.* 2004). Cxcl13, formerly known as B cell activating cytokine, also binds with Cxcr5 on B cells.

In this study, *H. hepaticus* 3B1 and LPS, but not HhNET or HhBac26, significantly increased the expression of Ccl2, Ccl3, Ccl4, Cxcl2, and Tnf of RAW264.7 murine macrophages versus controls. These macrophages are from a BALB/c mouse cell line, a mouse strain susceptible to Hh3B1 infection and a Th2 dominant strain. LPS increased the expression of an additional cytokine, Cxcl1. Interestingly, Cxc10 did not show a significantly different expression level with Hh3B1 at an MOI=0.1 or LPS at 100 ng/ul. Ccl2 is a proinflammatory cytokine and binds to Ccr2 on monocytes, NK cells, basophils, immature dendritic cells, activated T cells, and B cells. Ccl3 and Ccl4 are also pro-inflammatory cytokines produced by macrophages and bind to Ccr5 on monocytes, macrophages, Th1 cells, activated T cells and NK cells. Ccl3 also binds to Ccr1 on monocytes, macrophages, immature dendritic cells, and NK cells (Mantovani *et al.* 2004). Interestingly, while Tnf was upregulated in RAW264.7 BALB/c murine macrophages at 24 hours, it was not differentially expressed in the liver of *H. hepaticus* infected A/JCr mice at 3, 6, and 12 months.

Since the HhPAI isogenic mutant HhBac26 lacked an increased cytokine response in RAW264.7 for all cytokines tested, the HhPAI presumably influences this outcome. HhNET also lacks the HhPAI and did not exhibit an increased cytokine response for 4/6 cytokines, adding further support to the contribution of the HhPAI as a virulence factor.

The one cytokine that was increased for HhNET could imply that other genes outside the HhPAI, and not in Hh3B1 or HhBac26, could also influence the macrophage response. The HhPAI was demonstrated to affect virulence in both the *in vivo* experiments of Chapter 4 and the *in vitro* experiments in this chapter. Whether the PAI will affect HCC in A/JCr mice is an on-going investigation.

In summary, our findings demonstrate that RAW264.7 murine macrophages infected with the type strain Hh3B1 possessing the HhPAI exhibited a significantly higher cytokine response than HhNET and mutant HhBac26 at an MOI=0.1 and 24 hours post infection. Both HhNET and HhBac26 have large deletions in the HhPAI. These results suggest that the HhPAI plays a role in pathogenesis.

**Table 1** Summary of fold change versus controls for significantly increased cytokine responses induced by the type strain *H. hepaticus* 3B1 possessing the HhPAI. Fold changes for the positive control LPS, HhNET (without HhPAI), and the isogenic mutant HhBac26 are also listed.

| **Cxcl2** | **Average Fold Change** |
|---|---|
| Hh3B1 | 68.59 |
| HhNET | 5.54 |
| HhBac26 | 0.88 |
| LPS | 897.64 |

| **Ccl2** | **Average Fold Change** |
|---|---|
| Hh3B1 | 59.03 |
| HhNET | 4.72 |
| HhBac26 | 0.36 |
| LPS | 116.97 |

| **Ccl3** | **Average Fold Change** |
|---|---|
| Hh3B1 | 9.26 |
| HhNET | 1.82 |
| HhBac26 | 0.15 |
| LPS | 44.63 |

| **Tnf** | **Average Fold Change** |
|---|---|
| Hh3B1 | 7.71 |
| HhNET | 2.62 |
| HhBac26 | 0.47 |
| LPS | 5.66 |

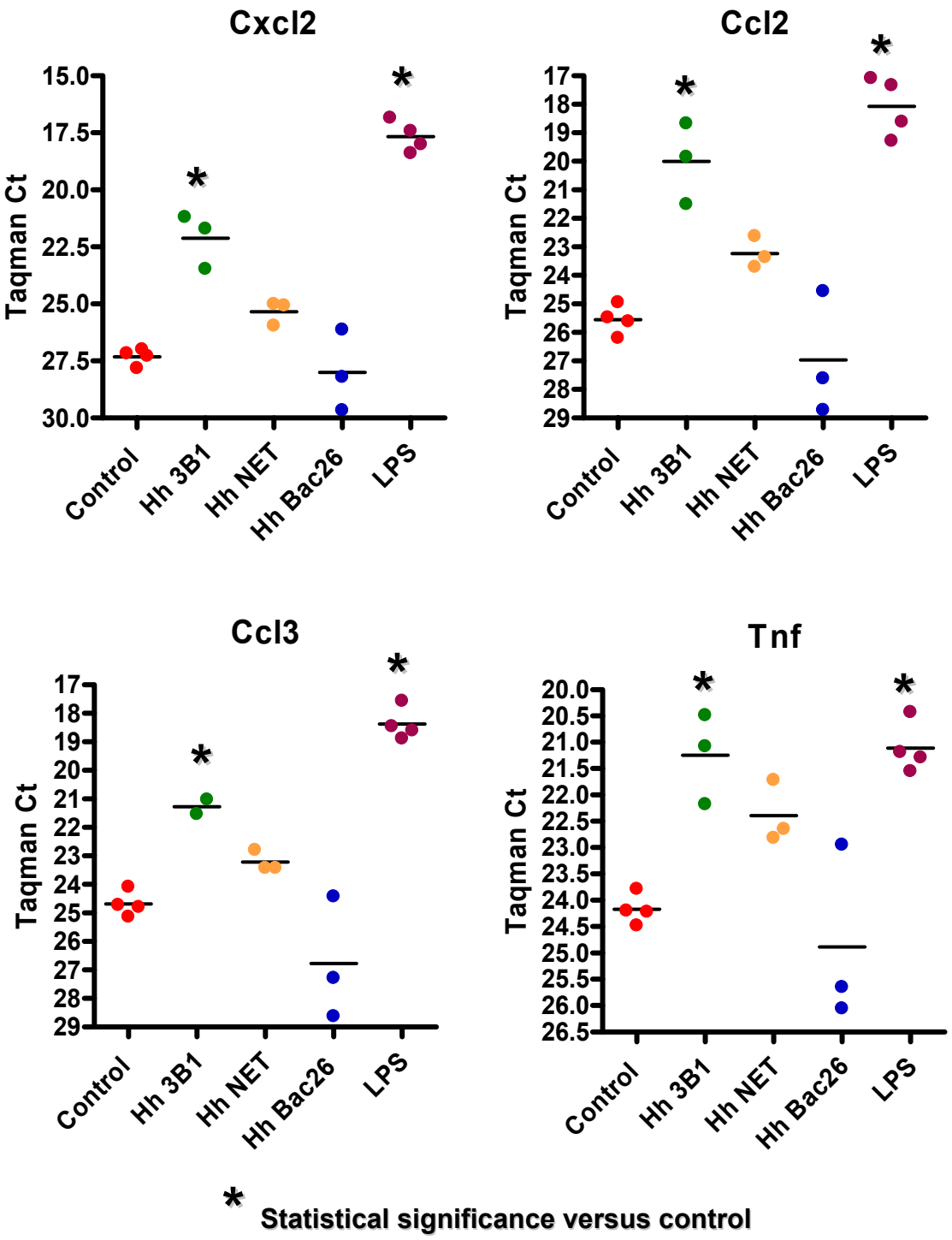


**Figure 1** Macrophage cell line RAW264.7 infection assay. The graph illustrates type *H. hepaticus* strain Hh3B1, possessing the HhPAI, and LPS induced a significantly increased response versus control for the cytokines exhibited. The *H. hepaticus* strains are at an MOI=0.1 and exposure time of 24 hours. The HhBac26 HhPAI isogenic mutant did not differ from controls for all cytokines measured.

**References**


Boutin, S., Rogers, A., Shen, Z., Fry, R., Love, J., Nambiar, P., Suerbaum, S., and Fox, J. (2004). Hepatic Temporal Gene Expression Profiling in *Helicobacter hepaticus*-Infected A/JCr Mice. *Toxicol Pathol* **32**, 678-93.

Burke, B., and Lewis, C. E. (2002). *The macrophage*. Oxford University Press, Oxford ; New York.

Erdman, S. E., Poutahidis, T., Tomczak, M., Rogers, A. B., Cormier, K., Plank, B., Horwitz, B. H., and Fox, J. G. (2003a). CD4+ CD25+ regulatory T lymphocytes inhibit microbially induced colon cancer in Rag2-deficient mice. *Am J Pathol* **162**, 691-702.

Erdman, S. E., Rao, V. P., Poutahidis, T., Ihrig, M. M., Ge, Z., Feng, Y., Tomczak, M., Rogers, A. B., Horwitz, B. H., and Fox, J. G. (2003b). CD4(+)CD25(+) regulatory lymphocytes require interleukin 10 to interrupt colon carcinogenesis in mice. *Cancer Res* **63**, 6042-50.

Fox, J. G., Dewhirst, F. E., Tully, J. G., Paster, B. J., Yan, L., Taylor, N. S., Collins, M. J., Jr., Gorelick, P. L., and Ward, J. M. (1994). *Helicobacter hepaticus* sp. nov., a microaerophilic bacterium isolated from livers and intestinal mucosal scrapings from mice. *J Clin Microbiol* **32**, 1238-45.

Fox, J. G., Li, X., Yan, L., Cahill, R. J., Hurley, R., Lewis, R., and Murphy, J. C. (1996). Chronic proliferative hepatitis in A/JCr mice associated with persistent *Helicobacter hepaticus* infection: a model of *Helicobacter*- induced carcinogenesis. *Infect Immun* **64**, 1548-58.

Hirschfeld, M., Ma, Y., Weis, J. H., Vogel, S. N., and Weis, J. J. (2000). Cutting edge: repurification of lipopolysaccharide eliminates signaling through both human and murine toll-like receptor 2. *J Immunol* **165**, 618-22.

Ihrig, M., Schrenzel, M. D., and Fox, J. G. (1999). Differential susceptibility to hepatic inflammation and proliferation in AXB recombinant inbred mice chronically infected with *Helicobacter hepaticus*. *Am J Pathol* **155**, 571-82.

Lewis, J. S., Lee, J. A., Underwood, J. C., Harris, A. L., and Lewis, C. E. (1999). Macrophage responses to hypoxia: relevance to disease mechanisms. *J Leukoc Biol* **66**, 889-900.

Li, Q., and Cherayil, B. J. (2004). Toll-like receptor 4 mutation impairs the macrophage TNFalpha response to peptidoglycan. *Biochem Biophys Res Commun* **325**, 91-6.

Mandell, L., Moran, A. P., Cocchiarella, A., Houghton, J., Taylor, N., Fox, J. G., Wang, T. C., and Kurt-Jones, E. A. (2004). Intact gram-negative *Helicobacter pylori*,

*Helicobacter felis*, and *Helicobacter hepaticus* bacteria activate innate immunity via toll-like receptor 2 but not toll-like receptor 4. *Infect Immun* **72**, 6446-54.

Mantovani, A., Schioppa, T., Biswas, S. K., Marchesi, F., Allavena, P., and Sica, A. (2003). Tumor-associated macrophages and dendritic cells as prototypic type II polarized myeloid populations. *Tumori* **89**, 459-68.

Mantovani, A., Sica, A., Sozzani, S., Allavena, P., Vecchi, A., and Locati, M. (2004). The chemokine system in diverse forms of macrophage activation and polarization. *Trends Immunol* **25**, 677-86.

Moller, A. S., Ovstebo, R., Westvik, A. B., Joo, G. B., Haug, K. B., and Kierulf, P. (2003). Effects of bacterial cell wall components (PAMPs) on the expression of monocyte chemoattractant protein-1 (MCP-1), macrophage inflammatory protein-1alpha (MIP-1alpha) and the chemokine receptor CCR2 by purified human blood monocytes. *J Endotoxin Res* **9**, 349-60.

Ohno, S., Suzuki, N., Ohno, Y., Inagawa, H., Soma, G., and Inoue, M. (2003). Tumor-associated macrophages: foe or accomplice of tumors? *Anticancer Res* **23**, 4395-409.

Rogers, A., Boutin, S., Whary, M., Sundina, N., Ge, Z., Cormier, K., and Fox, J. (2004). Progression of Chronic Hepatitis and Preneoplasia in *Helicobacter hepaticus*-Infected A/JCr Mice. *Toxicol Pathol* **32**, 668-77.

Suerbaum, S., Josenhans, C., Sterzenbach, T., Drescher, B., Brandt, P., Bell, M., Droge, M., Fartmann, B., Fischer, H. P., Ge, Z., Horster, A., Holland, R., Klein, K., Konig, J., Macko, L., Mendz, G. L., Nyakatura, G., Schauer, D. B., Shen, Z., Weber, J., Frosch, M., and Fox, J. G. (2003). The complete genome sequence of the carcinogenic bacterium *Helicobacter hepaticus*. *Proc Natl Acad Sci U S A* **100**, 7901-6.

Ulevitch, R. J., Mathison, J. C., and Correia Jda, S. (2004). Innate immune responses during infection. *Vaccine* **22 Suppl 1**, S25-30.

Ulevitch, R. J., and Tobias, P. S. (1999). Recognition of gram-negative bacteria and endotoxin by the innate immune system. *Curr Opin Immunol* **11**, 19-22.

van Ravenswaay Claasen, H. H., Kluin, P. M., and Fleuren, G. J. (1992). Tumor infiltrating cells in human cancer. On the possible role of CD16+ macrophages in antitumor cytotoxicity. *Lab Invest* **67**, 166-74.

Viala, J., Chaput, C., Boneca, I. G., Cardona, A., Girardin, S. E., Moran, A. P., Athman, R., Memet, S., Huerre, M. R., Coyle, A. J., DiStefano, P. S., Sansonetti, P. J., Labigne, A., Bertin, J., Philpott, D. J., and Ferrero, R. L. (2004). Nod1 responds to peptidoglycan delivered by the *Helicobacter pylori* cag pathogenicity island. *Nat Immunol* **5**, 1166-74.

Ward, J. M., Anver, M. R., Haines, D. C., and Benveniste, R. E. (1994). Chronic active hepatitis in mice caused by *Helicobacter hepaticus*. *Am J Pathol* **145**, 959-68.

## Chapter 6

## Summary

This thesis reported on studies of the molecular pathogenesis of *Helicobacter hepaticus* induced liver disease. *H. hepaticus* is a model organism of the enterohepatic *Helicobacter* spp., and the cause of hepatocellular carcinoma (HCC) in A/JCr mice. The experiments focused on 3 areas: (1) the gene signature of the A/JCr male mouse hepatic transcriptional response to infection by the *H. hepaticus* type strain ATCC 51448 (Hh3B1) at 3, 6, and 12 months post-inoculation; (2) the A/JCr mouse hepatic histopathological response and corresponding hepatic colonization levels to infection by 3 *H. hepaticus* wild type strains. Two of the strains (HhNET and HhG) lacked a putative pathogenicity island (PAI) containing components of a type IV secretions system (T4SS) present in the third strain, Hh3B1; and (3) the *in vitro* cytokine response of the murine macrophage, the predominant inflammatory cell in lobular hepatitis, after 24 hour exposure to Hh3B1, HhNET, and HhBac26. Hh3B1 contains the PAI, Hh NET lacks the PAI, and HhBac26 is an isogenic mutant with a partial deletion of the PAI, including components of the T4SS.

The results of the experiments demonstrated: (1) a definitive gene expression signature of lesions induced by *H. hepaticus* infection at 3, 6, and 12 months post inoculation. It also suggested a potential hepatic gene signature for *H. hepaticus* infection in male mice not exhibiting lesions. This will require further study. (2) a significant difference in virulence among the 3 wild type strains of *H. hepaticus*, providing additional evidence of the existence of a PAI in Hh3B1. Hh3B1 hepatic colonization levels trended higher than

HhG and HhNET; and (3) the macrophage response of selected cytokines is significantly increased versus controls by exposure to Hh3B1, as compared to HhNET and HhBac26 versus controls. This again provides evidence of a PAI and T4SS in Hh3B1.

The molecular mechanisms of *H. hepaticus* induced HCC remains unclear. *H. hepaticus* possesses characteristics of both a tumor promoter and tumor initiator, and may indeed be a complete carcinogen. The prototypical non-genotoxic carcinogen that promotes HCC in rodents is phenobarbital. It activates the orphan nuclear receptor constitutive active/adrostane receptor (CAR) and results in differential expression in the liver of some cytochrome P450 genes in common with *H. hepaticus* infection. CAR deficient mice do not exhibit HCC after diethylnitrosamine initiation and phenobarbital promotion. Future *H. hepaticus* experimental infections of CAR deficient mice would test the hypothesis of shared pathways of *H. hepaticus* and phenobarbital in the molecular pathogenesis of HCC.

The reasons for male predominance of *H. hepaticus* induced chronic, active inflammation progressing to HCC are also unknown. Investigations are underway to determine the effect that *H. hepaticus* has on steroid hormones and cholesterol, biomolecules with many shared biochemical pathways. Further investigation of enterohepatic *Helicobacter* species is important, because increasing evidence suggests a definitive role in human enterohepatic disease. This would not be a surprising result, given the paradigm of *H. pylori*.

*Toxicologic Pathology*, 32:668–677, 2004

ISSN: 0192-6233 print / 1533-1601 online
DOI: 10.1080/01926230490524247

# Progression of Chronic Hepatitis and Preneoplasia in *Helicobacter hepaticus*-Infected A/JCr Mice

ARLIN B. ROGERS, SAMUEL R. BOUTIN, MARK T. WHARY, NATALIYA SUNDINA, ZHONGMING GE, KATHLEEN CORMIER, AND JAMES G. FOX

*Division of Comparative Medicine, Massachusetts Institute of Technology, Cambridge, Massachusetts 02139, USA*

ABSTRACT

*Helicobacter hepaticus* infection induces sustained inflammation and carcinoma of the liver in A/JCr mice, and serves as a model of human cancers associated with viral hepatitis and *H. pylori* chronic gastritis. Here we describe the pathogenesis of premalignant disease in A/JCr mice infected with *H. hepaticus*. We inoculated dams intragestationally and/or pups postnatally, and evaluated offspring at 3, 6, or 12 months. Mice infected at or before 3 weeks of age, but not at 12 weeks, developed disease. Male mice were most affected, but expressed a bimodal pattern of susceptibility. Males exhibited lobular necrogranulomatous and interface (chronic active) hepatitis, while females usually developed intraportal (chronic persistent) hepatitis. Portal inflammation was slowly progressive, with tertiary lymphoid nodule development by 12 months. Hepatic bacterial load and preneoplastic lesions, including clear and tigroid cell foci of cellular alteration, were correlated with lobular hepatitis severity. No extrahepatic surrogate disease marker reliably predicted individual hepatitis grade. In conclusion, gender and bacterial exposure timing are key determinants of *H. hepaticus* disease outcomes. Intrahepatic inflammation is driven by local signals characterized by a vigorous but nonsterilizing immune response. Continued study of chronic hepatitis progression may reveal therapeutic targets to reduce the risk of hepatocellular carcinoma.

*Keywords*. Liver diseases; hepatitis, animal; *Helicobacter* infections; mice, inbred A; hepatocellular carcinoma.

## INTRODUCTION

Hepatocellular carcinoma (HCC), which usually arises in a setting of chronic hepatitis, is the third leading cause of human cancer deaths worldwide (Shibuya et al., 2002). Most patients diagnosed with HCC are seropositive for hepatitis B virus, hepatitis C virus, or both (Waris, 2003). Men develop HCC at more than 3 times the rate of women regardless of inciting cause, suggesting that perturbations of sexually dimorphic metabolic pathways predispose to tumorigenesis (Kew, 2002). Complex interactions between host and pathogen in human infectious liver cancer, especially in early disease, are difficult to evaluate. Animal models can be used to help unravel pathogenetic mechanisms in the progression from hepatitis to malignancy (Rogers and Fox, 2004). Whereas liver cancer in humans and murine models has been extensively investigated, fewer studies have characterized in detail the chronic inflammation which predisposes to carcinogenesis.

*Helicobacter hepaticus* infection of A/JCr and other susceptible mice induces chronic hepatitis and hepatocellular tumors (Fox et al., 1994; Ward et al., 1994b). *H. hepaticus* is the prototype enterohepatic *Helicobacter* species, and closely related organisms are now known to commonly infect humans and a wide array of animals (Fox et al., 1996a, 1996b; Fox, 1998; Solnick and Schauer, 2001; Garcia et al., 2002). *H. pylori* infection is the leading cause of human gastric cancer (Fox et al., 2003b), and hepatobiliary *Helicobacter* spp. have been implicated as liver tumor promoters in people, either alone or superimposed on viral hepatitis (Fox et al., 1998a; Nilsson et al., 2000; Ponzetto et al., 2000; Dore et al., 2002; Fan et al., 2002; Fukuda et al., 2002; Leong and Sung, 2002; Matsukura et al., 2002). In mice, enterohepatic *Helicobacter* spp. promote chemically initiated liver tumors (Diwan et al., 1997), and are the only infectious pathogens known to act as complete hepatocarcinogens. Thus, *H. hepaticus* infection provides a uniquely valuable rodent model for exploring basic mechanisms underlying inflammation-associated liver cancer. Although the carcinogenic potential of *H. hepaticus* infection in susceptible mouse strains has been proven (Fox et al., 1996a; Hailey et al., 1998; Ward et al., 1994b), disease progression in the premalignant period has received less attention. In this report we characterize the pathogenesis of chronic hepatitis and preneoplasia over a 12-month period in A/JCr mice exposed to *H. hepaticus* at different stages of antenatal, neonatal, and/or postnatal development. Clinicopathologic findings correlated well with global transcriptome changes in the liver (Boutin et al., 2004). An ancillary aim was to evaluate the influence of the timing of *H. hepaticus* exposure on subsequent disease expression and progression. Increased understanding of preneoplastic events in this murine model of inflammation-associated HCC will enhance our knowledge of basic mechanisms in human hepatitis and liver cancer, and may elucidate novel targets for therapeutic intervention prior to the onset of malignancy.

Address correspondence to: Arlin B. Rogers, Comparative Pathology Laboratory 16-849, Division of Comparative Medicine, Massachusetts Institute of Technology, Cambridge, Massachusetts 02139, USA; e-mail: abr@mit.edu

Abbreviations: HCC, hepatocellular carcinoma; spp. and sp., species; WBC, white blood cells; ANOVA, analysis of variance; ALP, alkaline phosphatase; AST, aspartate aminotransferase; ALT, alanine aminotransferase; IU/L, international units per liter; Ig, immunoglobulin; ELISA, enzyme-linked immunosorbent assay; TNF-$\alpha$, tumor necrosis factor-$\alpha$; PCR, polymerase chain reaction; rRNA, ribosomal RNA; bp, base pairs; $\mu$m, micrometers; iNOS, inducible nitric oxide synthase; COX-2, cyclooxygenase-2; DAB, 3,3'-diaminobenzidine; $\mu$g, microgram; SEM, standard error of the mean.

TABLE 1.—Group designations by time of *H. hepaticus* inoculation in pregnant dams and/or offspring, and proportion of affected male (M) and female (F) offspring with histologic activity scores ≥2 and/or dysplasia ≥1.

| Group | *H. hepaticus* in dams at conception | *H. hepaticus* in dams at 10 days postconception | *H. hepaticus* in pups at 3 weeks of age | *H. hepaticus* in pups at 12 weeks of age | Lobular ± portal hepatitis (affected/total) | Portal hepatitis only* (affected/total) | Dysplasia* (affected/total) |
|---|---|---|---|---|---|---|---|
| 1 | − | − | − | − | M: 0/8<br>F: 0/6 | M: 0/2<br>F: 0/2 | M: 0/2<br>F: 0/2 |
| 2 | + | − | − | − | M: 6/9<br>F: 0/6 | M: 0/3<br>F: 2/2 | M: 2/3<br>F: 0/2 |
| 3 | − | + | − | − | M: 3/8<br>F: 0/6 | M: 0/2<br>F: 0/2 | M: 1/2<br>F: 0/2 |
| 4 | − | − | + | − | M: 2/9<br>F: 0/6 | M: 1/3<br>F: 2/2 | M: 0/3<br>F: 0/2 |
| 5 | + | − | + | − | M: 5/10<br>F: 0/7 | M: 0/3<br>F: 1/3 | M: 1/3<br>F: 0/3 |
| 6 | − | + | + | − | M: 4/10<br>F: 1/5 | M: 0/3<br>F: 0/2 | M: 0/3<br>F: 0/2 |
| 7 | − | − | − | + | M: 0/4<br>F: 0/3 | M: 0/2<br>F: 0/3 | M: 0/2<br>F: 0/3 |
| 8 | + | − | − | + | M: 4/6<br>F: 0/4 | M: 1/3<br>F: 1/2 | M: 3/3<br>F: 0/2 |
| 9 | − | + | − | + | M: 2/6<br>F: 0/3 | M: 1/3<br>F: 0/2 | M: 2/3<br>F: 0/2 |

*12-month time point only.

## METHODS

### *Study Design*

Thirty-six *helicobacter*-free female A/JCr mice (National Cancer Institute, Frederick, MD) were bred to 18 males, and pregnant dams were divided into groups. Dams received $10^7$ colony-forming units *H. hepaticus* or vehicle only by gastric gavage every 48 hours for 3 doses at conception (confirmed by vaginal plug visualization) or beginning midway (day 10) through pregnancy. Pups received a similar bacterial or sham inoculum regimen at 3 or 12 weeks postnatally (Table 1). Assessment of transplacental bacterial or antigenic exposure was not performed. Offspring were euthanatized by $CO_2$ inhalation at 3, 6, or 12 months of age. A total of 117 mice were evaluated: 33 at 3 months, 41 at 6 months, and 43 at 12 months. Animals were maintained in a facility certified by the Association for the Assessment and Accreditation of Laboratory Animal Care in compliance with the National Academy of Sciences' *Guide for the Care and Use of Laboratory Animals*, and all protocols were approved by the Massachusetts Institute of Technology (MIT) Committee on Animal Care.

### *Hemogram and Serum Chemistry*

Hemograms were performed in-house according to standard protocols. Serum from mice collected at 3 and 6 months of age was separated from packed cells by centrifugation and sent to a reference laboratory (Idexx Laboratories, North Grafton, MA) for serum biochemical analysis including alkaline phosphatase (ALP), direct and indirect bilirubins, cholesterol, γ-glutamyl transferase, aspartate aminotransferase (AST), alanine aminotransferase (ALT), albumin, and globulin. Hemogram and serum chemistry value differences between groups were assessed by 1 way analysis of variance (ANOVA), followed by Dunnett's pairwise posttest using Prism 3.0cx software for Macintosh (GraphPad, San Diego, CA).

### *Antibody and Restimulated Splenocyte Cytokine Titers*

*H. hepaticus*-specific serum $IgG_1$ and $IgG_{2a}$ titers were determined by ELISA using a previously described method (Whary et al., 2000). Spleens were aseptically collected, dissociated, maintained in primary culture, and exposed to sterile-filtered whole bacterial *H. hepaticus* sonicate or medium only. Supernatants were collected at 48 hours' poststimulation and assayed for tumor necrosis factor-α (TNF-α) and interferon-γ by ELISA as previously described (Whary et al., 1998). Statistical analyses were performed by ANOVA or unpaired t test using the statistical package of Microsoft Excel (Seattle, WA). Fecal pellets were emulsified in protease inhibitor (Sigma, St. Louis, MO), debris separated by centrifugation, and supernatant analyzed for anti-*H. hepaticus* IgA titers by ELISA as described (Whary et al., 1998).

### *DNA PCR*

DNA was extracted from feces and frozen liver sections using a commercial kit (DNeasy Tissue Kit, Qiagen, Carlsbad, CA). Nested DNA PCR was performed using genus-specific primers in the first round that amplify a ~1200 base-pair (bp) sequence in the 16S rRNA gene using a previously described protocol (Fox et al., 1996b). Ten percent of first-round product was amplified in a second round using *H. hepaticus*-specific primers to amplify a 417 bp product nested within the first round amplicon (Fox et al., 1998b). Samples positive for bacterial DNA by nested PCR, as well as uninfected negative controls, were quantitated by real-time fluorogenic PCR (TaqMan) according to a previously described protocol (Ge et al., 2001).

### *Histopathology*

At necropsy, ileocecocolic junction and 2 sagittal sections of each liver lobe (median, caudate, left, and right) were collected for histopathology. Tissues were immersion fixed overnight in 10% neutral-buffered fromalin (VWR Scientific, West Chester, PA) and Prefer (Anatech, Ltd., Battle Creek, MI). Fixed tissues were processed and embedded by routine histologic methods, sectioned at 4 μm, and stained with hematoxylin and eosin (H&E). The 8 liver sections representing replicate samples from each lobe were examined by a veterinary pathologist blinded to sample identity and

graded on a 0–4 scale for lobular histologic activity (lobular hepatitis), portal activity (portal and/or interface hepatitis), and staged on the same scale for fibrosis using criteria established by Scheuer (Ferrell et al., 2002; Scheuer et al., 2002).

Additionally, dysplastic progression was scored using criteria adapted from published schemes for the terminology of rodent and human liver lesions: (0) normal, (1) foci of cellular alteration or dysplastic foci, (2) nodules of cellular alteration or low grade dysplastic nodules, (3) high-grade dysplastic nodules or focal well differentiated HCC, and (4) multifocal and/or moderately differentiated HCC (IWP, 1995; Bannasch et al., 2001). Statistical comparison of mean histologic activity scores by ANOVA was not possible because the bimodal distribution in infected males produced large standard deviations (see Results). Therefore, we categorized by the presence or absence of moderate-to-severe hepatitis (defined as lobular or portal histologic activity $\geq 2$ in any lobe; Table 1) and performed contingency table analyses. Contingency tables were assessed by Fisher's exact test using Prism software as described before.

### *Special Stains, Immunohistochemistry, and Morphometric Analysis*

Selected liver sections were stained by the Warthin-Starry stain for visualization of bacteria, or diastase periodic acid-Schiff or Perl's iron for demonstration of activated macrophages. Formalin- and Prefer-fixed liver sections were subjected to standard microwave heat-induced epitope retrieval and immunostained for cell phenotype markers or specific biomolecules using mouse monoclonal or rabbit polyclonal primary antibodies according to previous methods (Erdman et al., 2003a; Fox et al., 2003b). For mouse primary antibodies the ARK kit was used (DAKO, Carpinteria, CA), a system that employs prelabeled same-species antibodies to overcome labeling of endogenous immunoglobulins, a strategy proven in other settings (Rogers et al., 2002). Rabbit primary antibodies were labeled with biotinylated goat anti-rabbit IgG (Sigma). Cell phenotypes and other biomolecules included T cells (rabbit anti-CD3, Sigma), B cells (CD45R/B220) and the mitosis marker Ki-67 (BD Pharmingen, San Diego, CA), macrophages (F4/80, Caltag Laboratories, Burlingame, CA), iNOS (NOS2) and COX-2 (PGH2; Santa Cruz Biotechnology, Santa Cruz, CA), and the apoptosis marker cleaved caspase-3 (Cell Signaling Technology, Beverly, MA). Diaminobenzidine (DAB) or Vector VIP was used as chromogen, and tissues were counterstained with Gill's hematoxylin. Morphometric analysis of immunohistochemically stained tissue sections was performed using IPLab 3.6 software for Macintosh (Scanalytics, Inc., Fairfax, VA) according to previously described methods (Fox et al., 2003a).

## RESULTS

### *Hemogram and Serum Chemistry*

Offspring infected with *H. hepaticus* had higher mean white blood cell (WBC) counts than uninfected controls at 3 months of age. Statistical analysis by ANOVA revealed significant ($p < 0.05$) differences between infected and uninfected groups at 3 months for WBC and absolute lymphocyte counts, but not for other leukocytes (Figure 1). There were no significant differences in mean WBC counts between infected and uninfected groups at 6 months (Figure 1) or 12 months, demonstrating that circulating leukocytosis returned to background levels between 2 and 5 months postinoculation. At no collection point were there significant differences in erythrocyte parameters or platelet counts. Increased serum levels of ALT and AST were evident in some groups of infected mice, but not others (Figure 2).

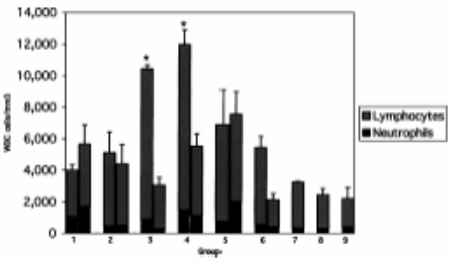


FIGURE 1.—Circulating white blood cell counts (WBC) in uninfected (group 1) versus *H. hepaticus*-infected mice (groups 2–9, Table 1) at 3 and 6 months (leukocytes other than neutrophils and lymphocytes comprised <2% of WBC). *$p < 0.05$ versus controls.

Mean combined ALT and AST levels in infected versus uninfected mice were 55 vs. 29 IU/L ($p = 0.11$) and 198 vs. 80 IU/L ($p = 0.06$), respectively. There was no difference in ALP levels between infected and uninfected mice (91 vs. 100 IU/L, respectively; $p = 0.40$) or any other analyte in the liver panel. In summary, serum chemistry demonstrated that cellular damage associated with *H. hepaticus* infection was inconsistent and limited to hepatocytes. Whereas mean serum aminotransferase levels tended to be increased in groups of infected mice, there was no correlation with liver lesion severity in individual animals as determined by histopathology.

### *Antibody and Restimulated Splenocyte Cytokine Titers*

All mice infected with *H. hepaticus* developed and maintained moderate to high antigen-specific mucosal IgA responses detected in fecal extracts, as well as serum $IgG_1$ and $IgG_{2a}$ responses (Figure 3). Whereas there was no correlation between IgA titers and inoculation protocol or hepatitis grade, mucosal IgA levels were higher in infected females than males, especially at 12 months ($p = 0.007$; Figure 3). There were no significant differences in serum antibody responses between infected groups in chronic disease. Serum antibody levels peaked at 6 months ($p < 0.001$) but did not correlate with gender or severity of hepatitis. From the 3-month to 6-month time point, $IgG_{2a}$ levels increased proportionately more than $IgG_1$, and between 6 and 12 months, $IgG_1$ levels decreased to a greater extent than $IgG_{2a}$ (Figure 3). Restimulated splenocyte interferon-$\gamma$ and TNF-$\alpha$ responses (not shown) were not significantly different between infected and uninfected mice, nor was there any correlation with gender, inoculation protocol, or hepatitis severity.

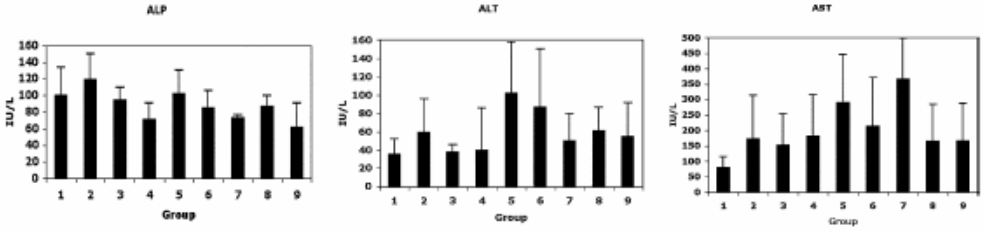


FIGURE 2.—Composite 3- and 6-month mean serum chemistry enzyme values (±SD) for alkaline phosphatase (ALP), alanine aminotransferase (ALT), and aspartate aminotransferase (AST) in groups of uninfected and *H. hepaticus*-infected mice as shown in Table 1.

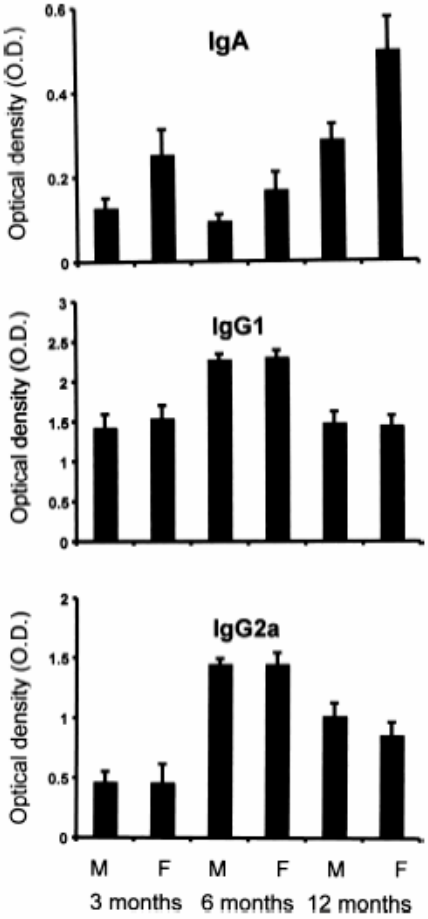


FIGURE 3.—*H. hepaticus*-specific mucosal (fecal) IgA, serum $IgG_1$, and $IgG_{2a}$ titers in infected male and female mice at 3, 6, and 12 months.

*PCR*

All infected mice were positive, and all control mice were negative, for *H. hepaticus* in feces following a single round of standard DNA PCR. A direct correlation emerged in liver samples between nonquantitative nested bacterial DNA PCR, quantitative fluorogenic DNA PCR (TaqMan), and lobular histologic activity (described next), especially among male mice at the 12-month collection point (Figure 4). At 12-months the mean number of copies of bacterial DNA per $\mu$g host DNA in mice with a positive first round standard PCR signal was $1.3 \times 10^6$ in males and $3.4 \times 10^3$ in females (Figure 4). In nearly all instances, samples requiring 2 rounds of nested PCR to demonstrate signal were below the sensitivity threshold of the single-round fluorogenic assay. The median histologic activity grade of male mice with a positive first round standard DNA PCR signal was 3, versus 1 in males without first-round signal ($p < 0.001$; Figure 4). The difference was less striking in females (2 versus 1), but still approached statistical significance ($p = 0.09$; Figure 4). Thus, detection of intrahepatic bacterial DNA after one round of standard DNA PCR was associated with high bacterial load and severe hepatitis, especially in male mice at 12 months. Retrospective PCR-based analysis of archived mouse liver sections has proven useful for identifying *H.*

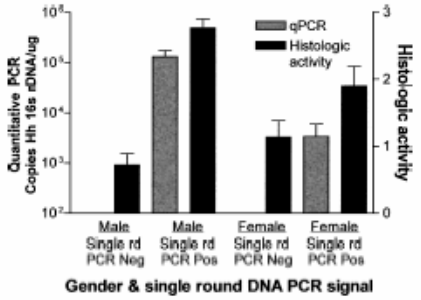


FIGURE 4.—Correlation of hepatic bacterial load demonstrated by quantitative fluorogenic PCR (qPCR, TaqMan; grey bars) with hepatitis severity (histologic activity; black bars) in *H. hepaticus*-infected mice stratified by signal presence or absence using single-round standard DNA PCR.

*hepaticus* as a confounding factor in mouse carcinogenesis studies (Malarkey et al., 1997).

*Histopathology*

Inflammatory lesions in mice infected with *H. hepaticus* followed one of two courses, resulting in necrogranulomatous lobular and/or lymphocytic portal hepatitis. These histologic presentations correlated with descriptions of human "chronic active" and "chronic persistent" hepatitis, though such terminology is falling from favor (Brunt, 2000). In cases of lobular hepatitis, necroinflammatory lesions consisted primarily of Küpffer cells and recruited macrophages surrounding and infiltrating foci of spotty or confluent hepatocellular necrosis (Figure 5a), resulting in translobular coagulative necrosis in severe cases. Neutrophils and lymphocytes made a minority contribution to lobular lesions. Larger lesions were evident grossly as round white foci up to 2 mm diameter. Lobular lesions were often but not always situated near terminal hepatic venules. Acidophil bodies were mildly increased in number in mice with lobular hepatitis, though not always located near inflammatory foci. Fibrosis was not a prominent feature of disease.

Portal hepatitis consisted primarily of lymphocytoid cells forming expansile nodular lesions, either in conjunction with lobular lesions or comprising the main disease process. Uncomplicated portal hepatitis was most common in females. Because bacteria were rarely identified in portal regions, it is possible these lesions developed due to circulating antigens or cytokines from the lower bowel. Lobular necrogranulomatous lesions were evident at all sampled timepoints, whereas chronic portal inflammation was not fully developed until 12 months of age. Especially in conjunction with lobular lesions, portal mononuclear infiltrates disrupted the hepatic limiting plate, resulting in interface hepatitis (Figure 5b). Lymphocytoid cells filled and expanded reactive portal lymphatic vessels, and in larger lesions surrounded and infiltrated bile ductules inducing epithelial loss, hypertrophy, and atypia (Figure 5b). Expansile aggregates sometimes were organized into follicles consistent with "tertiary lymphoid tissue" (Figure 5c) (Shomer et al., 2003). Unlike the case of *H. hepaticus* infection in mice with targeted immune mutations (Erdman et al., 2003a, 2003b; Tomczak et al., 2003; Young et al., 2004), but in agreement with previous studies utilizing A/JCr mice (Whary et al., 1998, 2001), inflammation of the cecum and colon (typhlocolitis) in these immunocompetent animals was generally mild, with inflammation scores typically in the range of 0.5–1 out of 4. Typhlocolitis was limited to mice infected at or before 3 weeks of age, but was not present in all animals, and there were no statistically significant differences between groups. Although morphologic changes were mild, microarray experiments have shown that lower bowel colonization of A/JCr mice with *H. hepaticus* induces prominent transcriptional responses (Myles et al., 2003).

At 12 months of age, male mice with severe lobular hepatitis exhibited dysplastic and proliferative lesions similar to those previously documented (Ward et al., 1994a, 1994b; Rice, 1995; Canella et al., 1996; Fox et al., 1996a, 1998; Hailey et al., 1998; Haseman et al., 1998; Bannasch et al., 2001). Foci of cellular alteration or dysplastic foci were multifocal, and often merged imperceptibly into adjacent zones of more normal hepatocytes. In some instances expansile dysplastic nodules were sharply delineated from surrounding less affected lobules (Figure 5d). Inflammation was concentrated at the perimeter of dysplastic nodules. Foci of cellular alteration, putative precursors to HCC (Bannasch et al., 1985, 2001), were of the clear cell, eosinophilic, or basophilic-tigroid (Figure 5e) phenotype, often comingled. Hepatocellular atypia was manifest as marked anisocytosis and anisokaryosis, structural and tinctorial pleomorphism, irregular cytoplasmic vacuolation and molding, aberrent multinucleation, and nuclear clearing with bizarre chromatin patterns. Oval cell hyperplasia, with occasional pseudocholangiole formation (Figure 5f), was common within foci of cellular alteration.

*Special Stains and Immunohistochemistry*

Confirmation of the primarily granulomatous nature of lobular necroinflammatory lesions was provided by F4/80 immunohistochemistry (Figure 5g). As described in human viral hepatitis, activated macrophages containing diastase-resistant PAS-positive material were present in some inflammatory lesions (Ferrell et al., 2002). In contrast, phagocytes with accumulated iron were extremely rare. Argyrophilic spiral bacteria, some undergoing longitudinal fission, were readily identified in bile canaliculi of Warthin–Starry-stained liver sections near histologically active lobular lesions, but were rare near portal tracts. In agreement with PCR results, organisms were absent in uninfected mice, and very rarely visualized in Warthin–Starry-stained liver sections from mice lacking lobular inflammation. Immunohistochemical demonstration of iNOS and COX-2 was limited to necroinflammatory lesions; however, the cell populations expressing each of these proteins were different. iNOS was demonstrated almost exclusively within inflammatory cells (Figure 5h), while COX-2 was up-regulated in intralesional hepatocytes (Figure 5i). Scattered acidophil bodies and some leukocytes, but not sheets of hepatocytes within zones of coagulative necrosis, contained cleaved caspase-3.

*Morphometric Analysis*

Observational quantitation of lesions in liver sections proved problematic due to variable densities of leukocellular aggregation, and confluence of adjoining inflammatory foci. We therefore applied morphometric analysis to 5 affected and 2 control immunohistochemically stained livers from the 12-month time point in order to determine percent area occupied by specific cell subsets within a defined region of interest (Fox et al., 2003a). We examined 10 left lobe fields per mouse under the 10X objective (0.61 $mm^2$/field). In mice with lobular and/or portal hepatitis (histologic activity $\geq 2$), the median hepatic tissue area comprised of leukocyte-common antigen $CD45^+$ white blood cells was 4%. One liver with severe disease contained 9% leukocytes, and when leukocytes were combined with zones of coagulative necrosis 25% of the most affected lobe was effaced. Portal tertiary lymphoid nodules contained a median of 72% $CD45^+$ leukocytes, the remaining tissue being comprised of resident portal arterioles, bile ductules, lymphatic channels, and connective tissue (portal venules were excluded from the manually defined region of interest).

Among the inflammatory cells, 45% displayed the B cell marker CD45R/B220 (Figure 5j), 7% were $CD3^+$ T cells

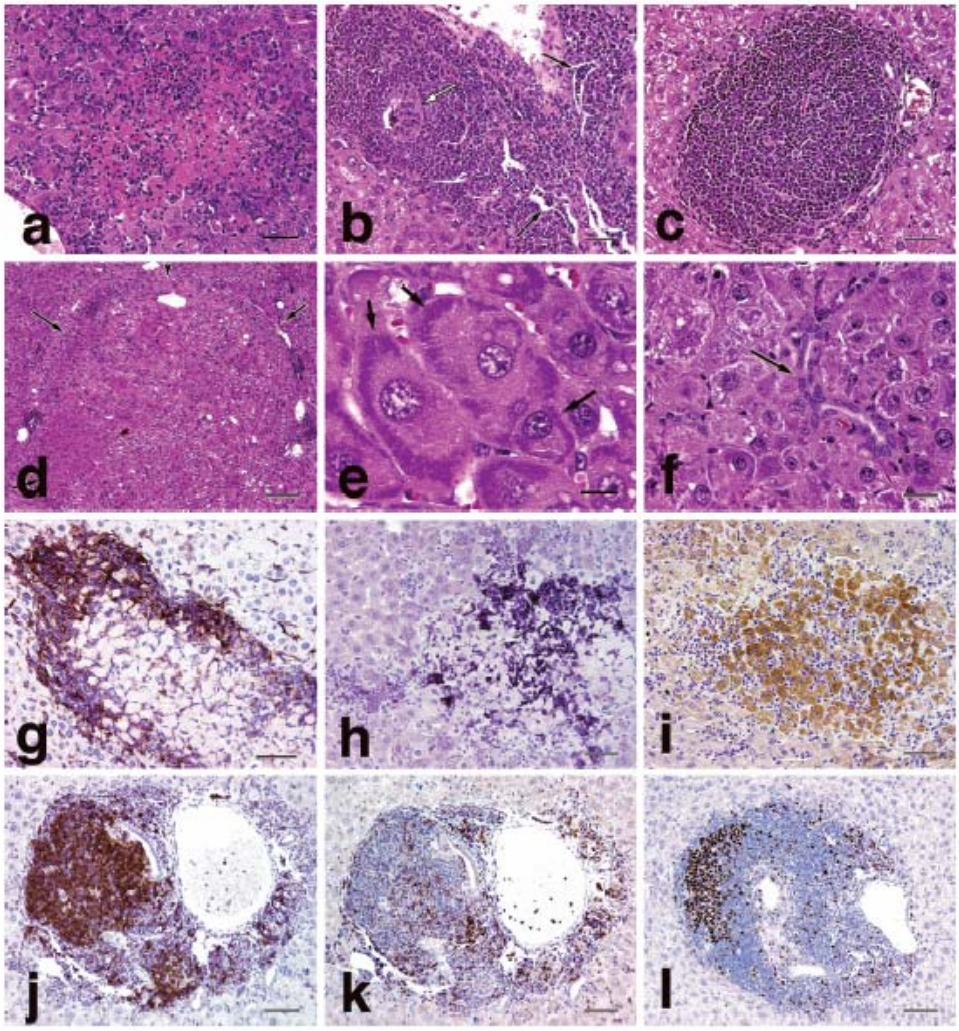


FIGURE 5.—Histopathology of *H. hepaticus*-induced liver disease. (a) Lobular hepatitis with infiltrating leukocytes and coagulative necrosis. (b) Portal and interface hepatitis with dilated lymphatics containing many mononuclear cells (black arrows); leukocytes surround and infiltrate a reactive bile ductule (white arrow). (c) Portal tertiary lymphoid follicle. (d) Dysplastic nodule (arrows). (e) Tigroid cells in focus of cellular alteration; note radial subplasmalemmal striations (arrows). (f) Oval cell hyperplasia with pseudocholangiole formation (arrow) in dysplastic nodule. (g) F4/80$^+$ macrophages surrounding and infiltrating a sheet of hepatocytes undergoing coagulative necrosis. Lobular necroinflammatory focus with up-regulated expression of (h) iNOS in inflammatory cells and (i) COX-2 in intralesional hepatocytes. Portal tertiary lymphoid tissue with (g) CD45R/B220$^+$ follicular B cell aggregates, and (h) individually dispersed CD3$^+$ T cells. (k) Intrahepatic lymphoid expansion with abundant Ki-67$^+$ nuclei in portal tertiary lymphoid follicle (IHC). H&E (a–f), immunohistochemistry (g–l); bar ~100 $\mu$m (a, c, g, j–l), 50 $\mu$m (b, h, i), 250 $\mu$m (d), 10 $\mu$m (e), 25 $\mu$m (f).

(Figure 5k), and 3% were identified as F4/80+ professional antigen-presenting cells (macrophages ± dendritic cells). Unlabeled portal tertiary lymphoid tissue included arterioles and bile ducts as well as presumptive NK cells, scattered granulocytes, and other cells unrecognized by our antibody panel. Within tertiary lymphoid nodules, B cells were aggregated into follicular structures (Figure 5j) while T cells (Figure 5k) and antigen-presenting cells were more widely dispersed. In portal tracts where bile ducts were surrounded and transmigrated by leukocytes, ductular epithelium exhibited atrophy, hypertrophy, and decreased cytokeratin expression. Scattered throughout portal tertiary lymphoid tissue, and focally concentrated at the periphery, were many actively proliferating cells attesting to intrahepatic lymphoid expansion (Figure 5l). The Ki-67 labeling index per X10 field was 104 in tertiary lymphoid tissue. Increased cell proliferation was also evident in foci of cellular alteration and dysplastic nodules, with a Ki-67 labeling index of 7 hepatocyte nuclei per X10 field, versus <1 in normal hepatic lobules ($p < 0.0001$).

*Statistical Analysis of Disease Distribution*

We categorized mice with lobular histologic activity ≥2 as having *lobular hepatitis* even though most also demonstrated significant portal inflammation. The assignment of *portal hepatitis* was reserved for those with histologic activity ≥2 exclusively in portal regions (Table 1). In agreement with previous studies (Ward et al., 1994b; Fox et al., 1996a; Whary et al., 1998), these experiments demonstrated a significantly higher risk of lobular hepatitis in male mice. Among groups infected with *H. hepaticus* at 3 weeks of age or earlier, 44% of males (24/54) but only 3% of females (1/37) developed lobular hepatitis ($p < 0.0001$; Figure 6a). In contrast, males and females were at equal risk for portal hepatitis at the 12-month time point (6/19 and 6/14, respectively; $p = 0.75$; Figure 6a).

When combined, a distinct bimodal distribution pattern of histologic activity scores emerged among males, with clustering of groups at the upper and lower ends of the spectrum attributable to lobular activity, while female hepatitis scores presented a Guassian distribution with most of the higher scores representing portal activity (Figure 6b). The "all-or-none" phenomenon in males resulted in large standard deviations, necessitating contingency table analyses (see Methods). Pattern analyses of male mice with and without lobular hepatitis revealed no correlations based on sibling status or cage distribution. No mice in the group infected at 12 weeks of age developed significant hepatitis ($p = 0.02$). Thus, early exposure to *H. hepaticus* was essential to induce disease.

Inflammatory lesion severity was highly variable between liver lobes in mice with disease, and even in focally severe cases some lobes were usually spared. Therefore, microscopic evaluation of all liver lobes was essential to rule out hepatitis. Among the 46 mice with moderate-to-severe hepatitis at any time point, a median of 2 (±1) out of 4 liver lobes demonstrated a histologic activity grade ≥2. Inflammatory foci were randomly distributed between and within lobes, presumably reflecting bacterial migration patterns. Likewise, there was no consistent intralobular lesion distribution, although pericentral foci were common. All male mice at the 12-month time point with lobular hepatitis scores ≥2 also exhibited putatively preneoplastic foci or nodules of altered hepatocytes, and no mice in any other group had such lesions ($p < 0.0001$). Thus, there was a strong association between necrogranulomatous lobular hepatitis and early tumorigenic progression in male mice infected with *H. hepaticus*, as described in older literature linking human "chronic aggressive hepatitis" with risk of hepatocellular carcinoma (Brunt, 2000).

## DISCUSSION

In this report we characterize in detail the progression of chronic hepatitis and dysplasia in the premalignant phase of a mouse model of infectious liver cancer. We show that early exposure to *H. hepaticus* is required for disease susceptibility. Male mice are more prone to severe disease than females, but only a subset of males are affected. Disease severity correlates directly with intrahepatic bacterial load. Taken together, our results demonstrate that chronic hepatitis is driven by a vigorous but nonsterilizing immune response to *H. hepaticus*.

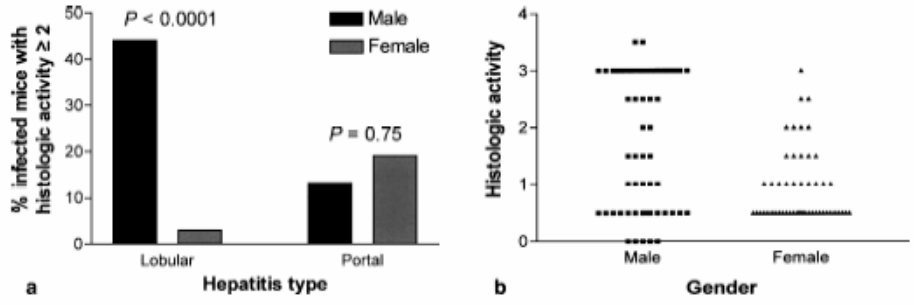


FIGURE 6.—Histologic activity comparison between infected male and female mice. (a) *H. hepaticus*-infected male mice demonstrate increased risk of lobular hepatitis versus female mice, while portal hepatitis risk is equal between genders. (b) Combined hepatitis scores demonstrate hourglass-shaped distribution in males, indicating bimodal expression of disease susceptibility attributable to lobular hepatitis, versus lower and more normally distributed hepatitis scores in females attributable to portal hepatitis.

These findings were confirmed by microarray analysis documenting progressive transcriptome changes over time (Boutin et al., 2004). It has been proposed that autoimmunity, especially to heat shock protein 70, may contribute to hepatocellular damage in *H. hepaticus* infection (Ward et al., 1996). Systemic and extrahepatic surrogate disease markers including complete blood count, serum chemistry values, circulating and mucosal antibody titers, and restimulated splenocyte cytokine responses, fail to predict hepatitis severity in individual animals, suggesting that intrahepatic inflammation is governed by local signals. *H. hepaticus* persists as a lifelong infection in the cecum and colon of mice. An important question requiring further study is whether bacterial containment in mice that do not develop hepatic disease occurs at the level of the large bowel, the liver, or both. Higher fecal IgA titers could help explain relative resistance to liver disease in female versus male mice, but the absence of correlation between fecal IgA titer and hepatitis severity implies that other factors must also be involved. Likewise in humans, serology is useful for the diagnosis of *H. pylori* infection, but is a generally poor predictor of gastric disease severity (Strauss et al., 1990).

An ancillary aim of this study was to test the hypothesis that dams infected with *H. hepaticus* during specific gestational stages would produce pups vulnerable to exacerbated liver disease, especially if offspring were inoculated with high doses of bacteria postnatally. This hypothesis was disproven. There were no significant differences between groups exposed to *H. hepaticus* at or before 3 weeks of age, regardless of intragestational maternal infection protocol. In contrast, a significant resistance to disease was exhibited by mice first inoculated at 12 weeks of age. Thus, *H. hepaticus* exposure early in life is essential for disease. The finding of putative preneoplastic lesions but not carcinoma at 12 months concurs with other studies of natural and experimental *H. hepaticus* infection, wherein documentation of tumors prior to 15 months of age is exceedingly rare (Ward et al., 1994a, 1994b; Fox et al., 1996a; Hailey et al., 1998; Avenaud et al., 2003).

Premalignant liver lesions were restricted to male mice with lobular necrogranulomatous hepatitis, and included poorly circumscribed zones of hepatocellular dysplasia, foci of cellular alteration, and dysplastic nodules. Altered hepatocytes were of the clear cell, eosinophilic, or basophilic-tigroid variety. We have observed hepatocellular carcinomas containing cells of each of these phenotypes in mice infected with *H. hepaticus* for 18 months ((Fox et al., 1996a) and unpublished observations). Tigroid hepatocytes, characterized ultrastructurally by orderly stacks of dilated endoplasmic reticulum cisternae richly decorated with ribosomes, were first described in rats used in chemical carcinogenicity studies (Bannasch et al., 1985). Their physiometabolic origin is uncertain, but they belong to the lineage of basophilic hepatocytes that in rats represent a high risk for malignant transformation (Bannasch and Schroeder, 2002). To our knowledge, this is the first published report of tigroid hepatocytes in mice. Morphologic consistency with rat tigroid cells was independently verified (P. Bannasch, personal communication). It is possible that small numbers of tigroid cells may have been overlooked in other mouse studies. Alternatively, the combination of bacterial strain, inoculation protocol, and environment may have uniquely predisposed to tigroid cell formation in our setting. Further investigation will be required to determine whether tigroid cells in mice behave similar to those in rats.

In humans and rodents, hepatocellular carcinoma is more prevalent in males than in females (Kew, 2002). In the case of hepatitis-associated tumorigenesis, influence of androgens on immune function may be operative. Androgens dampen certain T-cell functions, with the overall effect of reducing Type I and enhancing Type II cytokine responses (Kelley and Duggan, 2003; NIH, 2003). In addition to effects on the immune system, androgens may act directly as tumor promoters in the liver. Men have higher rates of HCC than women even in the absence of underlying hepatitis. Likewise, male-predominant HCC is described in noninflammatory rodent transgenic viral (Lerat et al., 2002; Okuda et al., 2002), constitutive proto-oncogene (Santoni-Rugiu et al., 1999), and chemical carcinogenesis models (Takahashi et al., 2002). We and others are actively investigating mechanisms underlying sexual dimorphism in hepatocellular carcinogenesis.

In summary, we have shown that early exposure to *H. hepaticus* is required to produce disease in A/JCr mice. Inflammation severity and intrahepatic bacterial load are positively correlated, suggesting that disease is driven by vigorous but ultimately ineffectual immunity. As with human viral hepatitis, extrahepatic surrogate disease markers are poorly predictive of histologic grade in individuals. Males develop more severe disease than females, but, for reasons unexplained, express a bimodal pattern of susceptibility. Failure of sibling status or cage distribution patterns to predict phenotypic outcomes suggests that disease susceptibility is polyfactorial. Advancing knowledge of disease pathogenesis in A/JCr mice infected with *Helicobacter hepaticus* will help illuminate our basic understanding of infectious liver cancer.

## ACKNOWLEDGMENTS

We thank Nancy Taylor for coordination of laboratory studies, Jennifer Cline, Noel Radwanski, Michele DeMarco, Vivian Ng, and Jeff Bajko for assistance with animal procedures, Ernie Smith and Erinn Stefanich for histologic processing, Charlotte Corcoran, Ellen Buckley, and Kaye Ivatts for clinical assays, and Peter Bannasch for helpful consultation.

## REFERENCES

Avenaud, P., Le Bail, B., Mayo, K., Marais, A., Fawaz, R., Bioulac-Sage, P., and Megraud, F. (2003). Natural history of *Helicobacter hepaticus* infection in conventional A/J mice, with special reference to liver involvement. *Infect Immun* 71, 3667–72.

Bannasch, P., Benner, U., Enzmann, H., and Hacker, H. J. (1985). Tigroid cell foci and neoplastic nodules in the liver of rats treated with a single dose of aflatoxin B1. *Carcinogenesis* 6, 1641–8.

Bannasch, P., Nehrbass, D., and Kopp-Schneider, A. (2001). Significance of hepatic preneoplasia for cancer chemoprevention. *IARC Sci Publ* 154, 223–40.

Bannasch, P., and Schroeder, C. H. (2002). 2. Tumours and tumour-like lesions of the liver and biliary tract: aetiology, epidemiology and pathology. In Pathology of the Liver (R. N. M. MacSween, A. D. Burt, B. C. Portman, K. G. Ishak, P. J. Scheuer and P. P. Anthony, eds.), pp. 777–826. Churchill Livingstone, London.

Boutin, S. R., Rogers, A. B., Shen, Z., Fry, R. C., Nambiar, P. R., Suerbaum, S., and Fox, J. G. (2004). Temporal gene expression profiling of hepatic genes

in *Helicobacter hepaticus* infected A/JCr mice: a model of progressive liver disease. *Toxicol Pathol* 32, 678–693.

Brunt, E. M. (2000). Grading and staging the histopathological lesions of chronic hepatitis: the Knodell histology activity index and beyond. *Hepatology* 31, 241–6.

Canella, K. A., Diwan, B. A., Gorelick, P. L., Donovan, P. J., Sipowicz, M. A., Kasprzak, K. S., Weghorst, C. M., Snyderwine, E. G., Davis, C. D., Keefer, L. K., Kyrtopoulos, S. A., Hecht, S. S., Wang, M., Anderson, L. M., and Rice, J. M. (1996). Liver tumorigenesis by *Helicobacter hepaticus*: considerations of mechanism. *In Vivo* 10, 285–92.

Diwan, B. A., Ward, J. M., Ramljak, D., and Anderson, L. M. (1997). Promotion by *Helicobacter hepaticus*-induced hepatitis of hepatic tumors initiated by *N*-nitrosodimethylamine in male A/JCr mice. *Toxicol Pathol* 25, 597–605.

Dore, M. P., Realdi, G., Mura, D., Graham, D. Y., and Sepulveda, A. R. (2002). *Helicobacter* infection in patients with HCV-related chronic hepatitis, cirrhosis, and hepatocellular carcinoma. *Dig Dis Sci* 47, 1638–43.

Erdman, S. E., Poutahidis, T., Tomczak, M., Rogers, A. B., Cormier, K., Plank, B., Horwitz, B. H., and Fox, J. G. (2003a). CD4(+) CD25(+) Regulatory T lymphocytes inhibit microbially induced colon cancer in Rag2-deficient mice. *Am J Pathol* 162, 691–702.

Erdman, S. E., Rao, V. P., Poutahidis, T., Ihrig, M. M., Ge, Z., Feng, Y., Tomczak, M., Rogers, A. B., Horwitz, B. H., and Fox, J. G. (2003b). CD4(+)CD25(+) regulatory lymphocytes require interleukin 10 to interrupt colon carcinogenesis in mice. *Cancer Res* 63, 6042–50.

Fan, X. G., Peng, X. N., Huang, Y., Yakoob, J., Wang, Z. M., and Chen, Y. P. (2002). Helicobacter species ribosomal DNA recovered from the liver tissue of chinese patients with primary hepatocellular carcinoma. *Clin Infect Dis* 35, 1555–7.

Ferrell, L. D., Theise, N. D., and Scheuer, P. J. (2002). Acute and chronic viral hepatitis. In Pathology of the Liver (R. N. M. MacSween, A. D. Burt, B. C. Portmann, K. G. Ishak, P. J. Scheuer and P. P. Anthony, eds.), pp. 313–362. Churchill Livingstone, London.

Fox, J. (1998). Enterohepatic *Helicobacters*: natural and experimental models. *Ital J Gastroenterol Hepatol* 30 Suppl 3, S264–9.

Fox, J. G., Dewhirst, F. E., Shen, Z., Feng, Y., Taylor, N. S., Paster, B. J., Ericson, R. L., Lau, C. N., Correa, P., Araya, J. C., and Roa, I. (1998a). Hepatic *Helicobacter* species identified in bile and gallbladder tissue from Chileans with chronic cholecystitis. *Gastroenterology* 114, 755–63.

Fox, J. G., Dewhirst, F. E., Tully, J. G., Paster, B. J., Yan, L., Taylor, N. S., Collins, M. J., Jr., Gorelick, P. L., and Ward, J. M. (1994). *Helicobacter* hepaticus sp. nov., a microaerophilic bacterium isolated from livers and intestinal mucosal scrapings from mice. *J Clin Microbiol* 32, 1238–45.

Fox, J. G., Li, X., Yan, L., Cahill, R. J., Hurley, R., Lewis, R., and Murphy, J. C. (1996a). Chronic proliferative hepatitis in A/JCr mice associated with persistent *Helicobacter hepaticus* infection: a model of *Helicobacter*-induced carcinogenesis. *Infect Immun* 64, 1548–58.

Fox, J. G., MacGregor, J. A., Shen, Z., Li, X., Lewis, R., and Dangler, C. A. (1998b). Comparison of methods of identifying *Helicobacter hepaticus* in B6C3F1 mice used in a carcinogenesis bioassay. *J Clin Microbiol* 36, 1382–7.

Fox, J. G., Rogers, A. B., Ihrig, M., Taylor, N. S., Whary, M. T., Dockray, G., Varro, A., and Wang, T. C. (2003a). *Helicobacter pylori*-associated gastric cancer in INS-GAS mice is gender specific. *Cancer Res* 63, 942–50.

Fox, J. G., Wang, T. C., Rogers, A. B., Poutahidis, T., Ge, Z., Taylor, N., Dangler, C. A., Israel, D. A., Krishna, U., Gaus, K., and Peek, R. M., Jr. (2003b). Host and microbial constituents influence *Helicobacter pylori*-induced cancer in a murine model of hypergastrinemia. *Gastroenterology* 124, 1879–90.

Fox, J. G., Yan, L., Shames, B., Campbell, J., Murphy, J. C., and Li, X. (1996b). Persistent hepatitis and enterocolitis in germfree mice infected with *Helicobacter hepaticus*. *Infect Immun* 64, 3673–81.

Fukuda, K., Kuroki, T., Tajima, Y., Tsuneoka, N., Kitajima, T., Matsuzaki, S., Furui, J., and Kanematsu, T. (2002). Comparative analysis of *Helicobacter* DNAs and biliary pathology in patients with and without hepatobiliary cancer. *Carcinogenesis* 23, 1927–31.

Garcia, A., Erdman, S. E., Xu, S., Feng, Y., Rogers, A. B., Schrenzel, M. D., Murphy, J. C., and Fox, J. G. (2002). Hepatobiliary inflammation, neoplasia, and argyrophilic bacteria in a ferret colony. *Vet Pathol* 39, 173–9.

Ge, Z., White, D. A., Whary, M. T., and Fox, J. G. (2001). Fluorogenic PCR-based quantitative detection of a murine pathogen, Helicobacter hepaticus. *J Clin Microbiol* 39, 2598–602.

Hailey, J. R., Haseman, J. K., Bucher, J. R., Radovsky, A. E., Malarkey, D. E., Miller, R. T., Nyska, A., and Maronpot, R. R. (1998). Impact of Helicobacter hepaticus infection in B6C3F1 mice from twelve National Toxicology Program two-year carcinogenesis studies. *Toxicol Pathol* 26, 602–11.

Haseman, J. K., Hailey, J. R., and Morris, R. W. (1998). Spontaneous neoplasm incidences in Fischer 344 rats and B6C3F1 mice in two-year carcinogenicity studies: a National Toxicology Program update. *Toxicol Pathol* 26, 428–41.

IWP. (1995). Terminology of nodular hepatocellular lesions. International Working Party. *Hepatology* 22, 983–93.

Kelley, J. R., and Duggan, J. M. (2003). Gastric cancer epidemiology and risk factors. *J Clin Epidemiol* 56, 1–9.

Kew, M. C. (2002). Epidemiology of hepatocellular carcinoma. *Toxicology* 181–182, 35–8.

Leong, R. W., and Sung, J. J. (2002). Review article: *Helicobacter* species and hepatobiliary diseases. *Aliment Pharmacol Ther* 16, 1037–45.

Lerat, H., Honda, M., Beard, M. R., Loesch, K., Sun, J., Yang, Y., Okuda, M., Gosert, R., Xiao, S. Y., Weinman, S. A., and Lemon, S. M. (2002). Steatosis and liver cancer in transgenic mice expressing the structural and nonstructural proteins of hepatitis C virus. *Gastroenterology* 122, 352–65.

Malarkey, D. E., Ton, T. V., Hailey, J. R., and Devereux, T. R. (1997). A PCR-RFLP method for the detection of *Helicobacter hepaticus* in frozen or fixed liver from B6C3F1 mice. *Toxicol Pathol* 25, 606–12.

Matsukura, N., Yokomuro, S., Yamada, S., Tajiri, T., Sundo, T., Hadama, T., Kamiya, S., Naito, Z., and Fox, J. G. (2002). Association between *Helicobacter bilis* in bile and biliary tract malignancies: *H. bilis* in bile from Japanese and Thai Patients with benign and malignant diseases in the biliary tract. *Jpn J Cancer Res* 93, 842–7.

Myles, M. H., Livingston, R. S., Livingston, B. A., Criley, J. M., and Franklin, C. L. (2003). Analysis of gene expression in ceca of Helicobacter hepaticus-infected A/JCr mice before and after development of typhlitis. *Infect Immun* 71, 3885–93.

NIH (2003). National Institutes of Health Consensus Development Conference Statement Management of Hepatitis C: 2002 June 10–12, 2002. *HIV Clin Trials* 4, 55–75.

Nilsson, H. O., Taneera, J., Castedal, M., Glatz, E., Olsson, R., and Wadstrom, T. (2000). Identification of *Helicobacter pylori* and other *Helicobacter* species by PCR, hybridization, and partial DNA sequencing in human liver samples from patients with primary sclerosing cholangitis or primary biliary cirrhosis. *J Clin Microbiol* 38, 1072–6.

Okuda, M., Li, K., Beard, M. R., Showalter, L. A., Scholle, F., Lemon, S. M., and Weinman, S. A. (2002). Mitochondrial injury, oxidative stress, and antioxidant gene expression are induced by hepatitis C virus core protein. *Gastroenterology* 122, 366–75.

Ponzetto, A., Pellicano, R., Leone, N., Cutufia, M. A., Turrini, F., Grigioni, W. F., D'Errico, A., Mortimer, P., Rizzetto, M., and Silengo, L. (2000). *Helicobacter* infection and cirrhosis in hepatitis C virus carriage: is it an innocent bystander or a troublemaker? *Med Hypotheses* 54, 275–7.

Rice, J. M. (1995). *Helicobacter hepaticus*, a recently recognized bacterial pathogen, associated with chronic hepatitis and hepatocellular neoplasia in laboratory mice. *Emerg Infect Dis* 1, 129–31.

Rogers, A. B., and Fox, J. G. (2004). Inflammation and cancer. I. Rodent models of infectious gastrointestinal and liver cancer. *Am J Physiol Gastrointest Liver Physiol* 286, G361–6.

Rogers, A. B., Mathiason, C. K., and Hoover, E. A. (2002). Immunohistochemical localization of feline immunodeficiency virus using native species antibodies. *Am J Pathol* 161, 1143–51.

Santoni-Rugiu, E., Jensen, M. R., Factor, V. M., and Thorgeirsson, S. S. (1999). Acceleration of c-myc-induced hepatocarcinogenesis by Co-expression of transforming growth factor (TGF)-alpha in transgenic mice is associated with TGF-beta1 signaling disruption. *Am J Pathol* 154, 1693–700.

Scheuer, P. J., Standish, R. A., and Dhillon, A. P. (2002). Scoring of chronic hepatitis. *Clin Liver Dis* 6, 335–47, v–vi.

Shibuya, K., Mathers, C. D., Boschi-Pinto, C., Lopez, A. D., and Murray, C. J. (2002). Global and regional estimates of cancer mortality and incidence by site: II. Results for the global burden of disease 2000. *BMC Cancer* 2, 37.

Shomer, N. H., Fox, J. G., Juedes, A. E., and Ruddle, N. H. (2003). *Helicobacter*-induced chronic active lymphoid aggregates have characteristics of tertiary lymphoid tissue. *Infect Immun* 71, 3572–7.

Solnick, J. V., and Schauer, D. B. (2001). Emergence of diverse *Helicobacter* species in the pathogenesis of gastric and enterohepatic diseases. *Clin Microbiol Rev* 14, 59–97.

Strauss, R. M., Wang, T. C., Kelsey, P. B., Compton, C. C., Ferraro, M. J., Perez-Perez, G., Parsonnet, J., and Blaser, M. J. (1990). Association of *Helicobacter pylori* infection with dyspeptic symptoms in patients undergoing gastroduodenoscopy. *Am J Med* 89, 464–9.

Takahashi, M., Dinse, G. E., Foley, J. F., Hardisty, J. F., and Maronpot, R. R. (2002). Comparative prevalence, multiplicity, and progression of spontaneous and vinyl carbamate-induced liver lesions in five strains of male mice. *Toxicol Pathol* 30, 599–605.

Tomczak, M. F., Erdman, S. E., Poutahidis, T., Rogers, A. B., Holcombe, H., Plank, B., Fox, J. G., and Horwitz, B. H. (2003). NF-$\kappa\beta$ is required within the innate immune system to inhibit microflora-induced colitis and expression of IL-12 p40. *J Immunol* 171, 1484–92.

Ward, J. M., Anver, M. R., Haines, D. C., and Benveniste, R. E. (1994a). Chronic active hepatitis in mice caused by *Helicobacter hepaticus*. *Am J Pathol* 145, 959–68.

Ward, J. M., Benveniste, R. E., Fox, C. H., Battles, J. K., Gonda, M. A., and Tully, J. G. (1996). Autoimmunity in chronic active *Helicobacter hepatitis* of mice. Serum antibodies and expression of heat shock protein 70 in liver. *Am J Pathol* 148, 509–17.

Ward, J. M., Fox, J. G., Anver, M. R., Haines, D. C., George, C. V., Collins, M. J., Jr., Gorelick, P. L., Nagashima, K., Gonda, M. A., Gilden, R. V., Tully, J. G., Russell, R. J., Benveniste, R. E., Paster, B. J., Dewhirst, F. E., Donovan, J. C., Anderson, L. M., and Rice, J. M. (1994b). Chronic active hepatitis and associated liver tumors in mice caused by a persistent bacterial infection with a novel *Helicobacter* species. *J Natl Cancer Inst* 86, 1222–7.

Waris, G. (2003). Regulatory mechanisms of viral hepatitis B and C. *J Biosci* 28, 311–21.

Whary, M. T., Cline, J., King, A., Ge, Z., Shen, Z., Sheppard, B., and Fox, J. G. (2001). Long-term colonization levels of *Helicobacter hepaticus* in the cecum of hepatitis-prone A/JCr mice are significantly lower than those in hepatitis-resistant C57BL/6 mice. *Comp Med* 51, 413–7.

Whary, M. T., Cline, J. H., King, A. E., Hewes, K. M., Chojnacky, D., Salvarrey, A., and Fox, J. G. (2000). Monitoring sentinel mice for *Helicobacter hepaticus*, *H. rodentium*, and *H. bilis* infection by use of polymerase chain reaction analysis and serologic testing. *Comp Med* 50, 436–43.

Whary, M. T., Morgan, T. J., Dangler, C. A., Gaudes, K. J., Taylor, N. S., and Fox, J. G. (1998). Chronic active hepatitis induced by *Helicobacter hepaticus* in the A/JCr mouse is associated with a Th1 cell-mediated immune response. *Infect Immun* 66, 3142–8.

Young, V. B., Knox, K. A., Pratt, J. S., Cortez, J. S., Mansfield, L. S., Rogers, A. B., Fox, J. G., and Schauer, D. B. (2004). In vitro and in vivo characterization of *Helicobacter hepaticus* cytolethal distending toxin mutants. *Infect Immun* 72, 2521–7.

# Global gene expression profiling: a complement to conventional histopathologic analysis of neoplasia

**Prashant R. Nambiar, Samuel R. Boutin, Rajiv Raja and Daniel W. Rosenberg**

*Division of Comparative Medicine, Massachusetts Institute of Technology (PRN, SRB), Arcturus Bioscience Inc., Mountain View, CA (RR), and Center for Molecular Medicine, University of Connecticut Health Center, CT (DWR)*

**Running title:** Global expression profiling in neoplasia

**Key words:** cancer; gene expression; laser-capture microdissection; microarray, review, veterinary, RNA linear amplification

**Corresponding author address**: Dr. P.R.Nambiar, Division of Comparative Medicine, Massachusetts Institute of Technology, 77, Massachusetts Avenue, Cambridge, MA-02139 (USA)Tel: 617-2539441; Fax: 617-2521882; email: nambiar@mit.edu

***Abstract***

Transcriptional profiling of entire tumors has yielded considerable insight into the molecular mechanisms of heterogeneous cell populations within different types of neoplasms. The data thus acquired can be further refined by microdissection methods that enable the analyses of sub-populations of neoplastic cells. Separation of the various components of a neoplasm- i.e., stromal cells, inflammatory infiltrates, and blood vessels- has been problematic, primarily because of a paucity of tools for accurate microdissection. The advent of laser-capture microdissection combined with powerful tools of linear amplification of RNA and high throughput microarray-based assays have allowed the transcriptional mapping of intricate and highly complex networks within pure populations of neoplastic cells. Using this approach, specific "molecular signatures" can be assigned to tumors of distinct or even similar histomorphology, thereby aiding the desired objective of pattern recognition, tumor classification, and prognostication. This review highlights the potential benefits of global gene expression profiling of tumor cells as a complement to conventional histopathologic analyses.

## ***Introduction***

Although the virtual explosion in the development of new molecular biological tools during the past decade has greatly expanded our understanding of the genetics and pathophysiology of tumorigenesis, histopathology remains the most reliable tool (the 'gold standard') for definitive diagnosis and classification of tumors. Classification of cancers has relied primarily upon morphological characteristics of the tumor, including tumor size, lymph node status, histology, and more recently, expression of specific markers associated with clinical course.[26] Traditionally, pathologists build up a relational database correlating histopathology of tumors with available patient data, such as recurrence rates, infiltrative nature, metastatic or non-metastatic behavior, post-surgical survival, and treatment response. These subjective measurements of cell morphology and behavior are ultimately combined to provide the framework for diagnostic, prognostic, and therapeutic decisions. However, our ability to predict tumor behavior based solely on histopathology remains elusive at best.

In tumors that follow a multistage model of progression, such as cancers of the colon or breast, only a subset of precancerous lesions progress to malignancy. For example, human colorectal cancer (CRC) is characterized by pathologically defined stages including the formation of preneoplastic aberrant crypt foci (ACF), pre-invasive adenomas, and carcinomas.[34,53,72] However, a significant percentage of ACF and adenomas do not progress to metastatic tumors.[49,53,92] In the case of CRC, *TGF-□ type II receptor* mutations and microsatellite instability are generally associated with a better

prognosis, whereas allelic losses of chromosomes 8q and 18q are often considered markers of poor prognosis.[127,133] Unfortunately, there are no reliable markers that can unequivocally distinguish the malignant potential of such lesions.[72] Therefore, it is of critical importance to develop robust methodology that may provide the means to stratify risk potential of specific precursor lesions. Such an approach can be extended to other forms of cancer. For example, human breast tumors typically progress through a pre-malignant atypical ductal hyperplasia, followed by pre-invasive ductal carcinomas *in situ*, culminating in invasive ductal carcinoma.[5,26,68] Although markers such as the estrogen receptor, her2/neu, PCNA, and VEGF have provided some utility in predicting the clinical course of the disease, they do not allow sufficient stratification of patients into groups that would benefit from a particular course of therapy.[26] Gene expression profiling using microarray technology has greatly improved our ability to classify tumors by generating unique molecular fingerprints that have delineated tumor subtypes.[29,54,95,97]

In this review, we discuss the potential benefits of global gene expression profiling of tumor cells as a complement to conventional histopathologic analyses. It is argued that such a combined approach will further enhance our understanding of the molecular pathogenesis of neoplasia. It should also be emphasized that the same principle/technology can be applied to the study of non-neoplastic diseases, including infectious and autoimmune diseases.

***1) Gene expression profiling***

Genes under epigenetic and transcriptional regulation produce their various forms of coding and non-coding RNA molecules. All of these RNA molecules with their differentially regulated synthesis, and degradation, form hierarchical systems, which function through topologically complex and interactive pathways that ultimately determine organ, tissue, and cell function. An aggregate effect of the complex multitude of molecular aberrations that control gene transcription may ultimately contribute to tumor phenotype. Traditional techniques that focus on a single gene or a limited composite of genes may limit our view of these complex interactions. Several global approaches, such as differential hybridization, subtractive hybridization, differential display, and serial analysis of gene expression have been developed with a goal towards identifying differentially expressed genes in normal and diseased tissues.[61]

Each of these methods suffer from inherent limitations, such as requiring large amounts of RNA, and being labor intensive.[61] Since its development in the mid-1990s, microarray technology has gained considerable interest in the scientific field. Microarray technology enables a snapshot of the entire cellular transcriptome on a single microarray chip, furnishing investigators with a global perspective of the complex interactions among thousands of genes simultaneously.[25,100] Microarray technology conveys a gene expression "fingerprint" that potentially characterizes a specific physiologic or pathologic state of an organ, tissue, or cell, thereby allowing the establishment of new subtypes of previously recognized diseases with prognostic correlations.[13,17,62,95] In fact, the RNA profile obtained from microarrays is a static representation of the biological state of the

sample, and yields the highest information and throughput of any classification assay.[29] Thus, microarray technology can be a powerful ancillary tool by allowing the identification of gene signature in tumor cells that in turn may provide important etiological and diagnostic clues. Using this experimental approach, studies utilizing microarrays and other technologies are now focusing on the dynamic behavior of neoplasia as a consequence of therapeutic intervention.[29,48]

***2) Laser-capture microdissection (LCM)***

Data output from microarray experiments is a direct reflection of the input RNA, which is dependent on the cellular composition of the particular tumor. Solid tumors are generally comprised of a heterogeneous mixture of tumor cells, including stromal tissue, inflammatory cells, blood vessels, and necrotic tissue. Therefore, if the goal of the microarray experiment is to analyze genetic changes within pure populations of cancer cells, isolation of RNA from complex tissues (i.e., grossly dissected tumors) may compromise the usefulness of the expression profiles thus generated. Furthermore, expression profiles from whole tumors may vary considerably between samples, a result of differences in the relative proportions of cell types present within each tumor specimen.

The confounding influence of cell heterogeneity can be resolved by applying methods that achieve high-resolution separation of cells based on morphology or fluorescent markers. Techniques such as flow cytometry/cell sorting and the use of affinity-labeled magnetic beads allow separation of sub-populations of cells from a complex mixture of

cells. However, these approaches are not necessarily practical for solid tissues. A relatively new technology, LCM directly addresses the issue of cell heterogeneity since it allows precise identification of cells by light microscopy followed by microdissection and harvesting of pure populations of cells.[15,30] Microdissection was initially performed by manually scraping an area of interest from a glass slide using needles. Later, this process was mechanized by the use of micromanipulators.[39,102,118] These techniques were fraught with errors and were labor-intensive. The first laser-assisted microdissection method was published in 1992[104] following which there has been a tremendous advancement in this technology. Several different types of LCM systems are available, providing the investigator with the ability to procure pure population of cells for further genetic analyses and global gene expression profiling.

Thus, coupling LCM to microarray technology impart the investigator with a sophisticated tool for obtaining genetic information from individual populations of cells. By using these combined approaches, it is now possible to correlate variations in gene expression with specific histologic stages of disease, an approach that may ultimately shed new light on the etiopathogenesis of cancer.[83,108] Most notably, the advent of LCM allows the rapid, reliable, and accurate procurement of pure populations of cells from specific putative, preneoplastic lesions. These technological advancements thus provide the opportunity to perform molecular genetic analysis at early time points during the tumorigenic process.[15]

(a) LCM tissue preparation:

Careful tissue preparation is critical to the successful outcome of subsequent molecular-based applications. A robust method that consistently yields high quality RNA for microarray analysis is to freeze quickly the tissues in a cryoprotectant media such as OCT. Both RNA and DNA of good quality can be extracted from such specimens for most downstream molecular-based applications. The frozen tissue sections are fixed briefly in 75% ethanol and stained rapidly with a modified hematoxylin-eosin staining procedure (http://dir.nichd.nih.gov/lcm/LCMTAP.htm). It should be noted that conventional immunohistochemistry could also be performed on these tissue sections, thereby enabling the visualization and capture of immuno-stained cells. Similarly, fluorescently-labeled cells can be visualized and microdissected by fluorescence-equipped LCM systems for downstream applications.[35]

The final dehydration steps with ethanol and incubation with xylene are critically important for successful dissection. Samples with residual moisture will be subject to hydrostatic forces that make it difficult to separate the microdissected tissue from the glass slide. Furthermore, fixatives such as formalin extensively cross-link RNA, DNA and proteins, thereby limiting analysis of nucleic acids.[76] However, DNA from formalin-fixed tissues is amenable to downstream applications such as direct sequence analysis for mutations and loss of heterozygosity studies. Alternatively, newer fixation protocols, such as ethanol fixation or the recently developed HOPE fixative, have been developed that allow preservation of tissue morphology and RNA quality.[85] A comprehensive list of standard protocols for tissue preparation and staining of both frozen and formalin-fixed

tissues is provided elsewhere (http://dir.nichd.nih.gov/lcm/LCMTAP.htm). It should be cautioned that all of the solutions that are used for staining must be RNAse and DNAse free, and must be replaced periodically. For optimal microdissection and guarantee extraction of high quality RNA, the entire work area and reagents must be maintained within an "RNAse-free zone".

(b) LCM methodology:

After the stained histologic section is visualized under a conventional light microscope, the region of interest is either transferred to a thermoplastic polymer film using a low energy infrared laser pulse, or cut with a high-energy ultraviolet laser and catapulted into a tube. Although, these two systems use slightly different technologies for procuring the cells, the end-result is the same. In this review, we will describe the thermoplastic film system as an example. In the thermoplastic film system, the area of film that absorbs the laser energy expands and adheres to the underlying cells (Fig. 1A). The laser pulse typically lasts several hundred microseconds to two milliseconds, and the transient heat generated in the film is rapidly dissipated through the glass slide heat sink, leaving the biomolecules undamaged.[75] When the device coated with the film is lifted off the tissue section, the tissue shears at the edges of its attachment to the polymer, leaving all of the untargeted area still attached to the glass slide (Fig. 1B). The exact morphology of the transferred cells is maintained and held on the transfer film (Fig. 1B). The device with the film is then mated to tubes with appropriate buffers to obtain DNA/RNA or proteins for subsequent experiments. Subsequent molecular analyses are not affected by the

microdissection process, as LCM typically creates only minimal chemical bonds with the targeted tissue.[118]

Thus, LCM aids in the analysis of cellular function in complex organs by separation of morphologically or histochemically identifiable subunits that can be subsequently analyzed using array-based experiments.[108] The inception of the Cancer Genome Anatomy Project (CGAP), sponsored by the National Center for Biotechnology Information, has been instrumental in the development and implementation of LCM technology. The CGAP goal is to establish an exhaustive and high quality database of genes expressed by normal, preneoplastic, and neoplastic human tissues. LCM has provided a particularly useful experimental tool for this project because of its fine resolution with respect to cellular dissection. At the CGAP website, an exhaustive library of partially sequenced clones has been generated using microdissected normal, preneoplastic, and neoplastic tissues.[6,67,82,87,88,99,101,105,130] In fact, the ability to study global gene expression at the cellular level with LCM has been demonstrated through studies reported in the fields of breast cancer[26,68] and colon cancer.[77]

***3) Linear amplification (LA) of RNA***

The ability to study global gene expression at a cellular level using laser-capture microscopy (LCM) is often compromised by the limited yield of RNA extracted from the low numbers of captured cells. This is especially true in the study of focal preneoplastic lesions. The developments of experimental strategies to amplify RNA thus become imperative. Since the publication of the original method,[123] several approaches have been

developed to amplify RNA in a linear fashion without creating an inherent bias in transcript levels.[27,52,118,125] These methods are largely based on the T7 RNA polymerase system. Briefly, LA technology consists of three distinct phases: first strand synthesis, second strand synthesis, and *in vitro* transcription. During first strand synthesis, mRNA within the total cellular RNA is converted to cDNA using a reverse transcriptase enzyme and a DNA primer that contains an oligo-dT and a T7 promoter sequence (Fig. 1C). Following first strand synthesis (conversion of mRNA to cDNA), the resultant single-stranded cDNA is converted to double-stranded cDNA utilizing DNA polymerase and a second exogenous (degenerate) primer. This double-stranded cDNA contains a T7 promoter site that will be recognized by T7 RNA polymerase to generate thousands of copies of each transcript during the *in vitro* transcription phase. The amplified RNA generated is in the antisense orientation and usually represents several hundred bases of the 3' region of the parent mRNA. The antisense RNA (aRNA) generated after one round of amplification can be used as template for another round of amplification as described above to yield a further 1,000 to 3,000 fold amplification (Fig. 1C). Thus, a 1 to 9 million-fold amplification of the native mRNA population can be attained through two rounds of amplification. Successful amplification can be verified by ultraviolet spectrophotometry, gel electrophoresis, or commercially available lab-on-a-chip technology.

Linear amplification of RNA enables the generation of 30 to 100 micrograms of aRNA from 500 picograms to 10 nanograms of total cellular RNA or 50 to 1000 cells. Unlike other amplification techniques such as polymerase chain reaction (PCR), an advantage of

LA is its high fidelity.[66,123,125] The relative proportions of rare as well as abundant transcripts within the native mRNA pool are maintained throughout the amplification process. Reproducibility and linearity of LA have been verified and well-documented in the literature and in commercial protocols.[27,50,52,118]

Amplifying RNA from certain cell types (e.g., enterocytes) may pose a particular challenge because these cells contain only a very low proportion of mRNA within their total cellular RNA (less than 0.5 percent). These limitations can be further accentuated when analyzing preneoplastic lesions that contain only limited numbers of cells. One way to address this challenge is to prepare serial sections of a tissue specimen from which the same lesion is laser-captured, followed by pooling of extracted RNA before LA.

Recently, non-uniform quality of the amplified aRNA as a result of inter-protocol variability of LA was described..[52] These differences may potentially impair direct comparisons of results between research groups that use different amplification strategies. Therefore, to facilitate the comparison of expression data, it was recommended to use a "standard reverse transcription reaction" for small-sample-transcriptome profiling experiments as part of the Minimal Information about a Microarray Experiment (MIAME) set of standards that has been established for microarray-based experiments (see details in microarray section).[52] Use of commercial kits for LA may address these issues of standardization.

***4) Microarray***

In this section, we will describe the critical components of a successful microarray experiment, including microarray platforms, data collection, analysis, and visualization. The two most commonly used array-based platforms are oligonucleotide and cDNA (complimentary DNA) arrays. It is important to note that in the microarray literature, a "target" is usually defined as the synthesized oligonucleotide or cloned cDNA sequences anchored to the glass slide, while the "probe" is the labeled RNA or cDNA from the experimental sample. Oligonucleotide arrays have shorter target sequences (typically between 25-60 base pairs) and are manufactured commercially by several methods including photolithography, ink-jet printing, and spotting pens.[12,36,46,118] Targets typically consist of a single long oligomer, or multiple shorter oligomers per gene. Increasing the target density of oligomer arrays allows a greater density of genes per array. The advantages of oligonucleotide arrays are a higher target density and greater specificity relative to cDNA arrays.[12,64] Cross platform comparisons of microarrays have revealed discrepancies in results necessitating buyer discretion.[31,116,118]

In cDNA arrays, discrete DNA sequences (PCR products of 500-5000 base pairs) representing specific sets of genes are spotted on a chemically coated glass microscope slide using spotting pens.[28] The large size of the target cDNA sequences provides extensive complementarity for hybridization, generally producing positive signals under most experimental conditions. However, there are several disadvantages to the cDNA platform. The large size of the targets may result in cross-hybridization between genes that share varying degrees of homology, raising the possibility of generating spurious

results. This may be especially problematic for high throughput studies that involve the analyses of hundreds, or even thousands of samples. Furthermore, denatured target sequences may re-anneal, potentially affecting the interaction of the probe and its target sequence.[66]

Oligonucleotide and cDNA arrays can be hybridized with either the test and reference samples simultaneously on the same array, or separately on different arrays, depending on the manufacturer's specifications. The mRNA isolated from test and control samples are processed to yield cDNA molecules that are labeled with fluorescent dyes. Oligomer arrays utilize one or two fluorescent dyes of a specific wavelength allowing their signals to be clearly distinguished. The one dye method allows array-to-array comparisons, with one array usually serving as the reference/control array. The two-dye method allows comparisons within arrays, and typically compares expression profiles of two samples on the same array. The most popular fluorescent dyes used to label, test and reference samples are Cyanine-3 (green) and Cyanine-5 (red). After hybridization, slides are scanned using a confocal scanner that illuminates every spot and measures fluorescence intensity for each dye. These signal intensity measurements determine the relative abundance of the mRNA species within the test sample relative to the control/reference. Fig. 2 depicts the flow chart of the microarray schema for the two-dye/channel or one-dye/channel microarray scenarios. Briefly, cyanine-5 (red) labeled cDNA/aRNA from the test sample is mixed with cyanine-3 (green) labeled cDNA/ aRNA from the reference (control) sample, and is hybridized to a microarray (Fig. 2A). The hybridized microarray is scanned under two channels and the raw fluorescence intensity under each channel is

calculated. Because two-color microarrays are based on the principle of competitive hybridization between two samples, the expression level of a particular gene (spot) in a test sample relative to the reference sample (red versus green) is measured by evaluating the relative fluorescent intensities in each channel. Higher magnification of a hybridized microarray slide (Fig. 2A) demonstrates a wide array of colors (between the red and green spectrum) that correspond to multiple genes (spots). For example, a yellow spot indicates comparable expression level for a particular gene in both test and reference samples (i.e., red + green = yellow), while a redder or greener spot indicates greater number of mRNA transcripts for that gene in the sample labeled with cyanine-5 and cyanine-3, respectively. Lack of color (black) at a specific gene spot indicated lack of that specific mRNA transcript in both test and control samples (Fig. 2A). In one-color hybridization, test and reference samples are labeled with the same fluorophore and hybridized to separate arrays; scanned under the appropriate channel and the ratios of fluorescent intensity in the test and reference arrays are computed to generate the relative gene expression level (Fig. 2B).

After the array hybridization phase of the study is completed, image acquisition, analysis, normalization, modeling, and identification of differentially expressed genes are required. An integral component to microarray-based experiments is the increasingly sophisticated software tools that provide relatively robust image visualization and analysis.

(a) Image analysis:

Image analysis software facilitates acquisition of raw signal data from each spot. A high quality image is critical as it enhances the efficacy of the microarray experiment and decreases the need for manipulation of the acquired data. A final signal value is ultimately dependent upon several important variables including spot features (location, orientation, size, and shape), uniformity of composition of the oligomer/cDNA, dye biases, resolution of the scanner, and chip alignment. Algorithms taking into account the spatial distribution, cumulative signal, and number of pixels that collectively represent each oligomer/cDNA determine the ultimate signal intensity level. If there are multiple oligomers representing an individual gene in a microarray, further processing is done, and signal to noise thresholds are utilized to determine the presence or absence of expression for that particular gene. For example, an algorithm could determine the presence or absence of gene expression based on the average signal level of a number of oligomer probes representing a gene versus the background signal level of the chip surface. The smallest copy number of sample cDNA that can be detected determines sensitivity, while specificity is decided by the amount of cross-hybridization between oligomers. Thus, image analysis entails identification of internal standards and removal of ambiguous and poor quality spots. The remaining high quality, signal level data is stored permanently for further analysis or for comparison in other experiments. This is especially important for reference controls in experiments.[58,109] Details of image acquisition and data pre-processing have been extensively reviewed elsewhere.[58,109]

(b) Data normalization:

The next step in data analysis is normalization of the signal data acquired from multiple array experiments. The normalization process is inherent to a successful microarray analysis because the amount of RNA initially processed or the cDNA/aRNA applied to the array(s) is often unequal. Furthermore, differences in hybridization kinetics and labeling/detection efficiencies are important issues inherent to replicate or multiple microarray experiments. The ultimate aim of data normalization is to efficiently remove bias between each individual microarray experiment.[129] Less sophisticated normalization strategies using house-keeping genes are being replaced by more complex approaches. The currently used normalization strategies are often dependent on the microarray technology utilized, and have been reviewed elsewhere.[14,59,91,109,129] Commonly used normalization approaches include non-linear smoothing, data transformation for altering the signal distribution, non-parametric, parametric and mixed methods.[14,59,91,109,129]

(c) Data Analysis:

Further processing of normalized data allows reduction of additive and multiplicative error in microarray comparisons, as illustrated by the "model based expression index." This is a statistical model that is generated to allow probe level analysis on multiple arrays.[59] The microarray data obtained with a small number of experimental cases and a large number of genes do not conform to "classical biostatistics," which is usually characterized by large number of experimental cases and a small number of variables. Conventional statistical analyses provide the probability (p) that a difference in gene expression occurred by chance.[121] For example, a significant p-value of 0.01 is

significant in the context of small number of test genes. However, during expression analysis of 10,000 genes, a p-value of 0.01 indicates that 1% (100 genes) of the genes will show a difference between test and control samples by chance and not because of actual biological differences (type I statistical error). Therefore, there is a need to eliminate as many false positive and false negative results as possible. To address this issue of "false discovery rate" (FDR), Tusher et al.[121] developed a novel statistical method specifically for microarray analysis, referred to as significance analysis of microarrays (SAM). They were successful in using FDR to identify non-significant genes by analyzing permutations of the measurements. SAM also allows filtering of genes that are above or below a user-defined fold-change (delta value). This is especially important, as there is a constant danger in microarray analysis of not including genes that are minimally altered, but highly relevant.

The next important step in the analysis of the voluminous data set is pattern recognition. Pattern recognition algorithms are loosely classified into two categories: "unsupervised or clustering" (implying no *a priori* classification of data) and "supervised or classification" (using data from known *a priori* classifications and applying predictors from these data to new data). A hybrid of these two approaches is also commonly utilized.[109] These algorithms may recognize a pattern in the data that correlates with a disease or a previously unrecognized subtype of a disease, thus complementing histopathologic classification. A cornucopia of algorithmic terms exists, including hierarchical and non-hierarchical clustering, K-means clustering, self-organizing maps, principal component analysis, one and two dimensional dendrograms, heat-maps, linear discriminant analysis,

support vector machines, decision trees, and neural networks. In summary, although statistical tools are constantly evolving to analyze microarray data, the ultimate aim is to develop a specific and universally accepted analytic approach for disease diagnosis and prognosis.

(d) Data presentation:

The final step in microarray experiments is presentation of data. This is extremely important because of the voluminous nature of the data set. Most commonly, expression data from microarray experiments can be pictorially summarized within a two-dimensional table, in which each row represents a single gene, and each column represents the expression levels of the entire set of genes within a single sample. A color scale correlates color intensity to gene expression. This approach allows easy visualization of the gene expression data in an intuitive manner, thereby allowing a global perspective on the transcriptome for multiple samples (see example in section 7).

Although microarray technology has the potential to analyze the entire transcriptome, the only limiting factor is the number of target elements present on the array. However, with the genome sequences of human, mouse, rat, and dog now completed, construction of arrays that represent the entire genome is now feasible. Thus, expression profiles of the entire genome (transcriptome) can be probed on a single array and the acquired data can be then superimposed on the genome sequence of the species that is being studied, thereby providing a new kind of genomic map. For example, if a subset of genes is deregulated (upregulated/downregulated) in a test sample, and a subset of these genes can

be localized within a specific chromosomal locus, chromosomal segment aberration (duplication/deletion) can be suspected. This can be verified by comparative gene hybridization (CGH) analysis or array CGH. Similarly, based on the knowledge of known transcriptional targets, deregulation of a subset of genes may also suggest a defect within a particular control element (transcription factor, tumor suppressor genes, protooncogenes, etc.). Thus, by carefully examining patterns of global gene expression, it may be possible to identify potential genetic aberrations. Such bioinformatics approaches are now feasible because of the efforts of the Gene Ontology (GO) Consortium. The GO Consortium (http://www.geneontology.org) is a work-in-progress for obtaining consistent descriptions of gene products, lists of protein domains, pathways, and respective chromosomes. The GO consortium also provides a standardized vocabulary for gene product attributes, including biological processes, cellular components, and molecular function.

One major criticism of microarray technology is the lack of uniformity of microarray data between experiments and across platforms.[12,43,118] In an attempt to standardize microarray data acquired from different academic and commercial platforms, the Microarray Gene Expression Data (MGED) Society has advocated the use of a set of minimum standards for each microarray experiment.[7,16,58] The standards are available at the Minimal Information about a Microarray Experiment (MIAME) website (http://www.mged.org/Workgroups/MIAME/miame.html). While lack of standardization may be less of an issue with experiments using commercial microarrays, documentation of experimental parameters and software analysis is essential for experimental

replication. For customized arrays, compliance with MIAME is now a prerequisite for publication of microarray data in many peer-reviewed journals.

***5) Post-array experiments***

An important requirement of microarray technology is the careful validation of test results using complementary quantitative methods. The expression changes observed in multiple gene sets are usually validated by reverse transcriptase PCR (RT-PCR), quantitative real time PCR (QRT-PCR), Northern analysis, or *in situ* hybridization.[20,21]

The relationship between the expressed levels of mRNA and protein is non-linear in many cases, especially because protein levels are often affected by post-translational modifications.[57,74] Therefore, data acquired from gene expression studies should be used cautiously in formulation of hypotheses and drawing conclusions pertaining to gene function. For these reasons, the field of proteomics is gaining significant traction as an important adjunct to transcriptome profiling. Direct mass spectrometric and two-dimensional PAGE analyses are widely used techniques that can be used in parallel with expression profiling.[57,74] In addition, immunohistochemistry (IHC) can also be used to independently confirm cell-type specific expression of proteins in tissues. In fact, the gaining of popularity of tissue microarrays for IHC allows a high throughput validation of microarray targets at the protein level.[113,120,122]

***6) Special considerations for overcoming inherent limitations***

A drawback of the technology described above that combines laser-capture microdissection-linear amplification (LCM-LA) and microarray is the absolute requirement for frozen tissue sections. This limitation is especially problematic from a clinical perspective, where the availability of fresh-frozen specimens may be limiting. However, recent technical advances in LCM-LA have enabled the extension of this approach to formalin-fixed, paraffin embedded tissue sections.[69]

The potential for RNA degradation is another important issue that must be considered. RNA degradation is important in LCM-LA experiments because the microdissected cells (few hundreds to thousands) are much fewer in comparison to conventional tissue/cell culture samples. However, this complication can be addressed by keeping the time required for tissue harvesting and tissue preservation (i.e., snap freezing) minimum. This is especially important while studying tissues with high levels of endogenous RNAses, such as the pancreas and gastrointestinal tract. Fortunately, one can minimize RNA degradation with the use of RNAse inhibitors and denaturants during the extraction procedures and subsequent amplification reactions, while taking extreme care to control for contamination in the work area. Another disadvantage of this technology is the cost. Technical advances will hopefully bring down the cost and provide the possibility of retrospective analyses of tumor tissues. This will greatly expand the utility of this approach within the clinical setting.

***7) Molecular profiling of cancerous and precancerous lesions in humans and laboratory animals***

During the past decade, numerous microarray-based studies have attempted to identify unique patterns of gene expression that can be used to assist in patient classification, treatment, and prognosis. For example, among patients with diffuse large B-cell lymphoma, therapeutic response is typically non-uniform.[3,4,29] However, it was not possible to distinguish between these two populations of patients.[3,4] Microarray-based experiments were able to identify unique gene expression signatures among 'responders' and 'non-responders', thereby aiding the classification of these patient subgroups with distinct prognosis.[3,4] A similar approach was successful in distinguishing acute myeloid leukemia (AML) from acute lymphoblastic leukemia (ALL) in humans.[40] In this study, unique gene expression profiles (class predictor sets) were established by microarray analysis for known cases of AML and ALL. These class predictor sets were then used to successfully classify unknown leukemic blood samples.[40] Similarly, microarray studies in human melanoma cell lines have successfully identified subsets of genes that play an important role in growth rate, contact inhibition, and metastasis.[25] Microarray experiments on primary solid tumors (for example, breast cancer) have also reinforced the use of genetic signatures to classify tumor subtypes.[37,87,96,111] Advances in gene expression-based tumor classification have also been documented in lung,[38] liver,[55,84,106] prostate,[19,130] ovaries,[126] colon,[132,134] skin (melanoma),[22] and brain.[65,94,96]

Alterations in the gene expression profiles of human colon tumors using oligonucleotide and customized cDNA microarrays were recently reported.[6,82] Molecular changes that

occur concurrently with the adenoma-carcinoma progression sequence in human colorectal cancer were monitored by expression profiling of early colonic adenomas and late adenocarcinomas.[62] The resultant set of unique discriminatory genes that were differentially expressed in adenomas and carcinomas of the colon were used as an objective, highly sensitive and specific diagnostic scoring system ("molecular diagnosis score"). Using this molecular diagnosis score, the authors correctly predicted whether the unknown samples were adenomas or adenocarcinomas. Similarly, in another study, primary non-metastatic and metastatic (to liver) human colon adenocarcinomas were compared by microarray analysis.[60] Several putative metastasis genes (*PRDX4*, *CKS2*, *MAGED2*, and EST BF696304) were subsequently identified. Distinct gene expression profiles within areas of dysplasia in colonic adenomas that were likely to be involved in progression from the adenoma to carcinoma stage were reported using LCM-microarray approach.[56] Recently, differences in global expression profiles between cancers arising from the left and right colon were established, followed by near perfect molecular classification of human colonic adenocarcinomas that were positive or negative for lymph node metastasis.[133] Interestingly, this classification was derived without previous pathological information, and based entirely on gene expression data.

In early microarray studies utilizing heterogeneous cell populations of tumors, the need to identify gene expression in pure population of cells was complicated by several technical issues. These included the issue of total RNA quantity needed for microarray assays, lack of linear amplification (LA) schemes to obtain the necessary amount of RNA, and a method to capture the cells of interest with intact RNA. Significant technical advances

in microdissection of complex tissues, particularly with the development of laser-capture microdissection-linear amplification (LCM-LA), provide the investigator with the ability to undertake array-based expression analysis using *in vivo*-derived genetic material originating from histologically complex tissue. The LCM-LA approach has been used successfully to analyze gene expression profiles in several different cancers, including carcinomas of the cervix, colon, breast, ovary, prostate, and esophagus.[67,82,88,105,107]

The combination of LCM-LA and microarray technologies has allowed the generation of epithelial-specific, *in situ* gene expression profiles of premalignant, preinvasive, and invasive stages of breast cancer.[68] Results demonstrated significant gene alterations at the earliest phenotypically recognized stage of progression of breast cancer (atypical ductal hyperplasia). However, these changes were maintained throughout the later stages of progression (ductal carcinoma *in situ* and invasive ductal carcinoma) without any unique discriminatory signature profiles segregating the precancerous lesions. Their results implied that different stages of progression are most likely clonal in origin and confirmed the putative malignant nature of these lesions. The authors were thus able to study the molecular relationship between morphologically distinct stages of breast cancer progression within an individual patient and between multiple patients.[68] Evaluation of estrogen receptor (ER)-positive invasive breast cancers from patients treated with adjuvant tamoxifen by LCM-LA, allowed the identification of a simple two-gene expression ratio of *HOXB13*:*Il17BR* from the entire microarray data set.[69] This ratio was utilized to accurately predict tumor recurrence in the setting of tamoxifen therapy and identify individuals at risk for tumor recurrence. This finding was especially important

because approximately 40% of patients with ER-positive breast cancers do not respond to therapy and can even become resistant to tamoxifen resulting in disease progression. This ratio proved more powerful than the currently used clinicopathological features, such as tumor stage, grade, ERBB2, and EGFR protein expression.

Using a similar approach, our laboratory recently demonstrated the ability to segregate preneoplastic colon lesions of similar histology, but divergent risk potential from two mouse strains that are differentially susceptible to the colonotropic carcinogen, azoxymethane (AOM).[80] AOM-induced preneoplastic aberrant crypt foci (ACF) from two strains of mice (A/J and AKR/J) were subjected to LCM-LA. Colonic epithelia from saline treated animals were similarly processed for use as reference controls. The amplified RNA was subsequently labeled with fluorescent dyes and hybridized to a 15K microarray slide with 4,992 gene elements represented in triplicate. The array slides were scanned and the raw fluorescence intensities were calculated. The data was processed and subjected to normalization and the ratios of the lesion to the normal saline-treated colons were determined for each strain for subsequent comparisons across the strains. The similarity in expression profiles between the control colons from A/J and AKR/J strains allowed comparison of lesions to each other. The scatter-plot of fluorescent gene intensities shown in Fig.3 demonstrates a simple way of inter-sample comparisons. For example, the expression profiles of two histologically similar microadenomas from A/J mouse colon, were highly correlated (Fig. 3A). As expected, the expression profile between histologically dissimilar samples remained skewed (Fig. 3B). Furthermore, using the unsupervised method of clustering (centroid algorithm), we identified several

subsets of genes that were distinct between ACF of similar histomorphology across the two strains with variable risk. The dendrogram (relationship tree) in Fig. 4 shows a subset of genes that were mostly up-regulated (red) in A/J and down-regulated (green) or unchanged (black) in AKR/J dysplastic ACF. The mathematical relationships between lesions are computed on the basis of the overall gene expression patterns, and the length of the branches of the dendrogram is inversely proportional to the similarities in the samples with respect to gene expression level. Thus, the dendrogram in Fig. 4 shows clear segregation of dysplastic ACF from the two mouse strains, and this was exclusively based on the unique gene expression profiles. These data imply that lesions of similar morphologies may have distinct molecular signatures that ultimately determine their biological outcome.[80] In the same model, microarray approach was used to study the functionality of two important tumor-suppressor pathways, p53 and TGF-β.[41,77] We demonstrated that despite high levels of p53 protein in AOM-induced colon tumors in A/J mice, microarray analysis of a panel of transcriptional targets of *p53* gene were found to be non-regulated, providing further evidence for inactivation of the p53 pathway, independent of mutational inactivation.[77] Similarly, lack of activation of the TGF-β pathway was demonstrated in AOM-induced murine colonic tumors.[41]

In summary, LCM-LA technology in human and rodent tissues has begun to yield significant benefits. Studies that focus on identification of unique gene expression signatures in tumors may now complement the subjective, histomorphologic phenotype. Expression profiles can be of prognostic significance when specific signatures are

compared to available patient data such as rate of recurrence, metastasis, patient survival, response to therapy, etc.

***8) Gene expression analysis in veterinary medicine***

High throughput expression analysis has great potential in the field of veterinary oncology to advance our knowledge of tumor biology and enhance the quality of life of affected animals. Unfortunately, the use of microarrays in the veterinary field has been limited by two main factors: lack of availability of species-specific microarrays and the high cost of analysis. The availability of human, mouse, and rat genomes allow manufacture of microarrays specific for these species. Fortunately, the sequencing of the genomes of other domestic animals such as the pig, sheep, cat, and cow is on-going (http://www.ncbi.nlm.nih.gov/Genomes/index.html).[81,115] For example, the *Canis familiaris* genome (based on the boxer dog) was recently sequenced at high resolution, and is publicly available (http://www.ncbi.nlm.nih.gov/genome/guide/dog). The entire genomes of the beagle and the standard poodle were sequenced privately, and a canine microarray is commercially available based on the privately licensed sequence. As a result, there has been an increase in the use of microarray-based technology in the veterinary field, most of which has been in the study of non-neoplastic diseases.

Canine specific cDNA microarray comprised of 60-cardiovascular related genes was developed to study expression profiles of myocytes during myocardial ischemia and necrosis.[8] Approximately 50% of the genes including E*cto-5'-nucleotidase*, *Endothelin-1*, *PAI-1*, and AT receptors were found to have an altered expression under conditions of

ischemia.[8] The ability of microarray analysis to evaluate simultaneously the expression patterns of the entire transcriptome has resulted in several attempts to increase the number of probe sets represented on these custom-built canine microarrays. A larger canine cDNA array consisting of 12,473 genes was recently designed to identify subsets of genes that are transcriptionally regulated by hepatocyte growth factor in a commonly used canine renal epithelial cell line.[10]

a) Cross-species hybridization studies:

Because currently available microarrays for domestic animals are capable of probing relatively few genes, cross-species hybridization strategies have been used to increase the number of represented genes. One group designed a custom canine array consisting of 13,729 canine genes and 9,045 human-derived probe sets.[45] This array was employed to identify biomarkers of acute phase response in the liver following administration of lipopolysaccharide to dogs. To maximize cross-species hybridization efficiency, the human-derived probes were designed for the more homologous terminal end of the coding region relative to the canine probes that were designed for the non-homologous 3' UTR region.

A similar cross-hybridization microarray experiment was performed using a high-density human oligonucleotide microarray to evaluate gene expression patterns of bovine monocyte-derived macrophages incubated with *Mycobacterium avium* subsp. *paratuberculosis*.[128] In another study, specific gene expression profiles in mitogen stimulated and unstimulated bovine peripheral blood mononuclear cells (PBMC) were

evaluated using a bovine specific cDNA array comprised of genes involved in immune, endocrine, and inflammatory responses.[117] Using this experimental system, the authors demonstrated similar gene expression patterns in ovine and porcine PBMC, thereby advocating the use of the cross-species hybridization strategy.

Although cross-species hybridization has merit in the veterinary field, especially with only limited availability of species-specific microarrays, a serious limitation is that only homologous genes across species will produce positive signals. Interpretation of negative results may thus be complicated and may be due to the absence of cross-species hybridization to non-homologous probe sets.

To overcome the disadvantages associated with these cross-species hybridization experiments, several investigators have custom designed bovine microarrays comprised of few hundred to several thousand bovine-specific probe sets to study multiple aspects of mammary gland development, pregnancy associated changes in multiple organs, and immune-endocrine axis.[11,44,71,114,131]

(b) Current and future applications in veterinary oncology:

Despite recent articles describing the use of microarray in bovine and canine species, high throughput microarray technology has only rarely been applied to the study domestic animal neoplasms. Recently, an array comparative genome hybridization (CGH) approach was utilized to evaluate gene copy number changes in canine lymphoma.[119] The array CGH is a powerful technique that allows high resolution

molecular karyotyping and has encouraged further development in veterinary oncology. However, array CGH based technology cannot be used to perform gene expression analyses. Interestingly, the converse has been demonstrated in humans by using cDNA gene arrays for CGH analysis.[47,63,110,122] Such an approach allowed direct correlation between mRNA transcripts and amplification/deletion of genes at the genomic DNA level.[47,63,110] For example, CGH using cDNA microarrays identified several novel genes, whose over-expression was attributable to gene amplification in human breast cancer.[47] Such approaches allowing simultaneous evaluation of both the transcriptome and the genome, are critical in gaining insights to multiple diseases.

In the veterinary oncology literature, techniques such as immunohistochemistry (IHC) and *in situ* hybridization (ISH) are typically used to complement traditional histomorphologic analysis. Commonly used markers include cell surface molecules (for immunophenotyping), intermediate filaments (to ascertain histogenesis), proteins involved in cell proliferation (PCNA, Ki-67, and AgNOR), cell cycle (cyclin D1, p21, and p27), growth stimuli (c-Myc, K-ras, and β-catenin), growth inhibition (p53 and Rb), apoptosis (caspase-3 and Bcl2), and vascularization (VEGF and bFGF).[93] Although IHC and ISH have been useful in prognostication to some extent, their reductionist nature precludes a global perspective on the neoplastic cell state.

As clearly described above, the application of high throughput, microarray technology may allow for evaluation of complex multidimensional cell circuits and greatly hasten the discovery of potential biomarkers of prognostic significance. There are numerous

examples of neoplasia in the veterinary field that are potential candidates for such high throughput analysis. Although it is beyond the scope of this review article to present an exhaustive set of examples, there are several key examples of tumors where grade or histologic features correlate with survival, metastatic rate, disease-free interval, and/or speed of local recurrence. These examples include canine cutaneous mast cell tumors (MCT), lymphoid tumors, canine histiocytic diseases, hemangiosarcomas, mammary gland carcinomas, and vaccine site-sarcoma (VSS).

The long term tumor behavior of MCT is dependent upon the subjective histomorphologic classification scheme.[86,112] Grade II and III tumors have worse prognosis than grade I. However, there is approximately 50-60% discordance in the tumor grade between experienced pathologists, resulting in reproducibility issues.[112] Using molecular markers such as AgNOR, PCNA, Ki-67, c-kit, and p53 have been attempted to predict biological behavior of MCT in terms of recurrence, metastasis, and survival.[1,112] Similarly, in the example of canine histiocytic diseases (cutaneous histiocytosis, systemic histiocytosis, splenic histiocytosis, and malignant histiocytosis), there are marked differences in prognosis and outcome. Diagnosis is often based on organ involvement and microscopic features.[2,70] The use of microarray-generated profiles in these examples may provide clues for ascertaining histogenesis of the tumors, yield multiple biomarkers that might be useful in predicting risk, response to treatment, and remission rates. This might prove to be a valuable supplement to histology that may provide additional objectivity to the current histomorphologic classification scheme.

Using an immunophenotyping approach (by IHC), differentiation of feline lymphoid tumors that were non-responsive and responsive to chemotherapy was unsuccessful.[24] Application of microarray technology to such neoplasms may enable identification of the inherent genetic difference between the non-responders and responders. In canine lymphosarcoma, identification of cell lineages (immunophenotyping) has prognostic significance; dogs with B cell lymphosarcoma have a better prognosis than those with T cell neoplasms.[103] Significant differences in prognosis between B- and T-cell subtypes of canine lymphomas were demonstrated in a recent study.[89] Definitive diagnoses and predictive outcome in such cases are dependent upon histomorphology and/or cytochemical stains. However, these are often limited by the availability of antibodies and can yield equivocal results. Similarly, differentiation of hemangioma and hemangiosarcoma in any species can be difficult, especially when based on biopsy or cytologic examination, as these can be confounded by excessive hemorrhage, inflammation and inadequate sampling.[23] Canine mammary tumors are challenging for clinicians and pathologists because of complex histologic classification, low specificity of cytologic diagnosis, and unpredictable biologic behavior.[135] Several studies in canine mammary tumors have attempted to investigate the correlation between histologic invasiveness (stage) and proliferation markers such as AgNOR and Ki-67 with some success.[98] In all of the above examples, use of microarray-based technology may allow identification of unique signature profiles that aid in molecular classification of these neoplasms with an ultimate aim of accurate diagnosis and/or prognosis.

Feline VSS has been an important neoplasm of cats that has been epidemiologically linked to feline leukemia virus and feline rabies vaccines.[78,79] Despite extensive research in the field in the last decade, etiopathogenesis of VSS is largely speculative and circumstantial. Application of microarray technology may allow comparison of VSS to non-vaccine site sarcomas and thereby allow valuable insights into the pathogenesis of VSS.

In summary, there does not seem to be a paucity of appropriate diseases in veterinary medicine to which this technology can be successfully applied. The microarray approach has the potential to yield robust panel of markers for specific conditions; and such newly discovered markers can be tested in tissues by the more practical and inexpensive tools (such as IHC or PCR-based assays) to assist the veterinary clinician. Despite these apparent applications, it is important to highlight that the use of microarrays in diagnostic human oncology is still in its infancy, and microarrays are even further away from practical application in veterinary oncology.

(c) Comparative oncology:

Application of microarray to study animal neoplasms has gained impetus with recent establishment of the comparative oncology program at the National Institutes of Health (http://ccr.nci.nih.gov/resources/cop/). The primary goal of this program is to characterize and validate comparative models for use in pre-clinical trials, including companion animals to obtain a broader understanding of the etiopathogenesis and treatment of cancer. Companion animals are being used as animal models because they

share similar environmental risk factors as their human owners and in some cases, have similar tumor histology.[42] For these reasons, it is important to know how similar or dissimilar many of these companion animal tumors are to their histological counterparts in humans. Apart from the detailed histomorphologic, IHC analysis of these "comparative animal tumors", microarray-based platforms add another dimension to the comparative oncology initiative. With a similar initiative taken by the American College of Veterinary Pathologists on lymphoid neoplasms and myeloproliferative disorders, application of microarray analysis can greatly benefit comparative veterinary oncology.

***9) Application in non-neoplastic diseases***

Despite the extensive application of laser-capture microdissection linear amplification (LCM-LA) technology to neoplasms, it must be emphasized that microarray studies are not necessarily restricted to the study of neoplastic diseases. A number of recent microarray studies have focused on infectious and autoimmune diseases, pharmacologic applications, and parasitology.[9,73,90] Microarray technology has been used to understand the complex genetic processes underlying the interaction between microorganisms and the host.[18] DNA microarray platforms have been utilized in the study of emerging infectious diseases to rapidly identify and characterize novel viruses.[124] Microarrays have been utilized to study various aspects of microbial pathogenesis, and have been especially useful in the identification and discovery of "pathogenicity genes."[32,33,51] Furthermore, microarrays have been tremendously useful in the testing of the "molecular Koch's postulates" for various virulence- and pathogenic trait-associated genes.[33] Microarrays have also been extremely useful in investigating the mechanisms of drug action and to

identify unique gene expression fingerprints that can predict adverse drug-associated reaction in patients.[32,33,51]

## ***10) Conclusions***

Pathology has been the cornerstone of diagnostic practice for more than a century. Subjective evaluation of cell morphology and behavior by pathologists is ultimately combined to provide the framework for diagnostic, prognostic and therapeutic decisions. Can rapidly developing molecular technology render pathologists obsolete? In our opinion, this is a highly unlikely scenario, at least in the near future. As the field continues to mature, microarray-based applications are likely to refine and tune the current tumor classifications, rendering further objectivity to the current subjective criteria of disease evaluation. Information that is being accumulated from thousands of microarray experiments will continue to provide a powerful and expanding database that will ultimately be compiled within a public repository, annotated and stored in accordance with Microarray Gene Expression Data (MGED) recommendations. Furthermore, laser-capture technology provides investigators with a superb dissection tool that can be used to procure samples for subsequent array-based genomic, transcriptional, and ultimately proteomic analyses, which can be combined to generate a unique tumor fingerprint. The compilation of such an exhaustive multi-dimensional and universally available database, combined with morphologic and clinical data will ultimately provide the research community with valuable new insights into infectious, autoimmune, and neoplastic diseases. Thus, it is of paramount importance for the veterinary field to remain at the forefront of this revolutionary approach and start by

creating appropriate tumor repositories to facilitate future multi-group and multi-disciplinary studies.

*Acknowledgements*

We wish to thank our grant support: NIH Grant CA 81248 and a grant from Robert Lee and Clara Guthrie Patterson Trust (DWR). We also wish to thank Drs. David B. Schauer, Laura Lemke, and James G. Fox for their valuable comments. We also wish to thank Elaine Robbins for technical help with the figures.

***References***


1 Abadie JJ, Amardeilh MA, Delverdier ME: Immunohistochemical detection of proliferating cell nuclear antigen and Ki-67 in mast cell tumors from dogs. J Am Vet Med Assoc **215:** 1629-1634, 1999

2 Affolter VK, Moore PF: Localized and disseminated histiocytic sarcoma of dendritic cell origin in dogs. Vet Pathol **39:** 74-83, 2002

3 Alizadeh AA, Eisen MB, Davis RE, Ma C, Lossos IS, Rosenwald A, Boldrick JC, Sabet H, Tran T, Yu X, Powell JI, Yang L, Marti GE, Moore T, Hudson J, Jr., Lu L, Lewis DB, Tibshirani R, Sherlock G, Chan WC, Greiner TC, Weisenburger DD, Armitage JO, Warnke R, Levy R, Wilson W, Grever MR, Byrd JC, Botstein D, Brown PO, Staudt LM: Distinct types of diffuse large B-cell lymphoma identified by gene expression profiling. Nature **403:** 503-511, 2000

4 Alizadeh AA, Staudt LM: Genomic-scale gene expression profiling of normal and malignant immune cells. Curr Opin Immunol **12:** 219-225, 2000

5 Allred DC, Mohsin SK, Fuqua SA: Histological and biological evolution of human premalignant breast disease. Endocr Relat Cancer **8:** 47-61, 2001

6 Alon U, Barkai N, Notterman DA, Gish K, Ybarra S, Mack D, Levine AJ: Broad patterns of gene expression revealed by clustering analysis of tumor and normal colon tissues probed by oligonucleotide arrays. Proc Natl Acad Sci U S A **96:** 6745-6750, 1999

7 Anonymous: Microarray standards at last. Nature **419:** 323, 2002

8 Asakura M, Takashima S, Asano Y, Honma T, Asanuma H, Sanada S, Shintani Y, Liao Y, Kim J, Ogita H, Node K, Minamino T, Yorikane R, Agai A, Kitamura S, Tomoike H, Hori M, Kitakaze M: Canine DNA array as a potential tool for combining physiology and molecular biology. Circ J **67:** 788-792, 2003

9 Aune TM, Maas K, Moore JH, Olsen NJ: Gene expression profiles in human autoimmune disease. Curr Pharm Des **9:** 1905-1917, 2003

10 Balkovetz DF, Gerrard ER, Jr., Li S, Johnson D, Lee J, Tobias JW, Rogers KK, Snyder RW, Lipschutz JH: Gene expression alterations during HGF-induced dedifferentiation of a renal tubular epithelial cell line (MDCK) using a novel canine DNA microarray. Am J Physiol Renal Physiol **286:** F702-710, 2004

11 Band MR, Olmstead C, Everts RE, Liu ZL, Lewin HA: A 3800 gene microarray for cattle functional genomics: comparison of gene expression in spleen, placenta, and brain. Anim Biotechnol **13:** 163-172, 2002

12 Barczak A, Rodriguez MW, Hanspers K, Koth LL, Tai YC, Bolstad BM, Speed TP, Erle DJ: Spotted long oligonucleotide arrays for human gene expression analysis. Genome Res **13:** 1775-1785, 2003

13 Basset DE, Jr, Eisen MB, Boguski MS: Gene expression informatics-it's all in your mine. Nat Genet (Suppl) **21:** 51-55, 1999

14 Bolstad BM, Irizarry RA, Astrand M, Speed TP: A comparison of normalization methods for high density oligonucleotide array data based on variance and bias. Bioinformatics **19:** 185-193, 2003

15 Bonner RF, Emmert-Buck M, Cole K, Pohida T, Chuaqui R, Goldstein S, Liotta LA: Laser capture microdissection: molecular analysis of tissue. Science **278:** 1481,1483, 1997
16 Brazma A, Hingamp P, Quackenbush J, Sherlock G, Spellman P, Stoeckert C, Aach J, Ansorge W, Ball CA, Causton HC, Gaasterland T, Glenisson P, Holstege FC, Kim IF, Markowitz V, Matese JC, Parkinson H, Robinson A, Sarkans U, Schulze-Kremer S, Stewart J, Taylor R, Vilo J, Vingron M: Minimum information about a microarray experiment (MIAME)-toward standards for microarray data. Nat Genet **29:** 365-371, 2001
17 Brown PO, Botstein D: Exploring the new world of the genome with DNA microarrays. Nat Genet **21:** 33-37, 1999
18 Bryant PA, Venter D, Robins-Browne R, Curtis N: Chips with everything: DNA microarrays in infectious diseases. Lancet Infect Dis **4:** 100-111, 2004
19 Bubendorf L, Kononen J, Koivisto P, Schraml P, Moch H, Gasser TC, Willi N, Mihatsch MJ, Sauter G, Kallioniemi OP: Survey of gene amplifications during prostate cancer progression by high-throughout fluorescence in situ hybridization on tissue microarrays. Cancer Res **59:** 803-806, 1999
20 Bustin SA: Absolute quantification of mRNA using real-time reverse transcription polymerase chain reaction assays. J Mol Endocrinol **25:** 169-193, 2000
21 Chuaqui RF, Bonner RF, Best CJ, Gillespie JW, Flaig MJ, Hewitt SM, Phillips JL, Krizman DB, Tangrea MA, Ahram M, Linehan WM, Knezevic V, Emmert-Buck MR: Post-analysis follow-up and validation of microarray experiments. Nat Genet **32** (Suppl)**:** 509-514, 2002
22 Clark EA, Golub TR, Lander ES, Hynes RO: Genomic analysis of metastasis reveals an essential role for RhoC. Nature **406:** 532-535, 2000
23 Clifford CA, Mackin AJ, Henry CJ: Treatment of canine hemangiosarcoma: 2000 and beyond. J Vet Intern Med **14:** 479-485, 2000
24 Dank G, Lucroy MD, Griffey SM, Gandour-Edwards R, Madewell BR: bcl-2 and MIB-1 labeling indexes in cats with lymphoma. J Vet Intern Med **16:** 720-725, 2002
25 DeRisi J, Penland L, Brown PO, Bittner ML, Meltzer PS, Ray M, Chen Y, Su YA, Trent JM: Use of a cDNA microarray to analyse gene expression patterns in human cancer. Nat Genet **14:** 457-460, 1996
26 Desai KV, Kavanaugh CJ, Calvo A, Green JE: Chipping away at breast cancer: insights from microarray studies of human and mouse mammary cancer. Endocr Relat Cancer **9:** 207-220, 2002
27 Dobson AT, Raja R, Abeyta MJ, Taylor T, Shen S, Haqq C, Pera RA: The unique transcriptome through day 3 of human preimplantation development. Hum Mol Genet **13:** 1461-1470, 2004
28 Duggan DJ, Bittner M, Chen Y, Meltzer P, Trent JM: Expression profiling using cDNA microarrays. Nat Genet **21:** 10-14, 1999
29 Ebert BL, Golub TR: Genomic approaches to hematologic malignancies. Blood **104:** 923-932, 2004
30 Emmert-Buck MR, Bonner RF, Smith PD, Chuaqui RF, Zhuang Z, Goldstein SR, Weiss RA, Liotta LA: Laser capture microdissection. Science **274:** 998-1001, 1996

31 Etienne W, Meyer MH, Peppers J, Meyer RA, Jr.: Comparison of mRNA gene expression by RT-PCR and DNA microarray. Biotechniques **36:** 618-626, 2004
32 Falkow S: Molecular Koch's postulates applied to bacterial pathogenicity--a personal recollection 15 years later. Nat Rev Microbiol **2:** 67-72, 2004
33 Falkow S: Molecular Koch's postulates applied to microbial pathogenicity. Rev Infect Dis **10** (Suppl 2)**:** S274-276, 1988
34 Fearon ER, Vogelstein B: A genetic model for colorectal tumorigenesis. Cell **61:** 759-767, 1990
35 Fend F, Kremer M, Quintanilla-Martinez L: Laser capture microdissection: methodical aspects and applications with emphasis on immuno-laser capture microdissection. Pathobiology **68:** 209-214, 2000
36 Fodor SP, Rava RP, Huang XC, Pease AC, Holmes CP, Adams CL: Multiplexed biochemical assays with biological chips. Nature **364:** 555-556, 1993
37 Fuller AP, Palmer-Toy D, Erlander MG, Sgroi DC: Laser capture microdissection and advanced molecular analysis of human breast cancer. J Mammary Gland Biol Neoplasia **8:** 335-345, 2003
38 Garber ME, Troyanskaya OG, Schluens K, Petersen S, Thaesler Z, Pacyna-Gengelbach M, van de Rijn M, Rosen GD, Perou CM, Whyte RI, Altman RB, Brown PO, Botstein D, Petersen I: Diversity of gene expression in adenocarcinoma of the lung. Proc Natl Acad Sci U S A **98:** 13784-13789, 2001
39 Going JJ, Lamb RF: Practical histological microdissection for PCR analysis. J Pathol **179:** 121-124, 1996
40 Golub TR, Slonim DK, Tamayo P, Huard C, Gaasenbeek M, Mesirov JP, Coller H, Loh ML, Downing JR, Caligiuri MA, Bloomfield CD, Lander ES: Molecular classification of cancer: class discovery and class prediction by gene expression monitoring. Science **286:** 531-537, 1999
41 Guda K, Giardina C, Nambiar P, Cui H, Rosenberg DW: Aberrant transforming growth factor-beta signaling in azoxymethane-induced mouse colon tumors. Mol Carcinog **31:** 204-213, 2001
42 Hansen K, Khanna C: Spontaneous and genetically engineered animal models; use in preclinical cancer drug development. Eur J Cancer **40:** 858-880, 2004
43 Hartman JLt, Garvik B, Hartwell L: Principles for the buffering of genetic variation. Science **291:** 1001-1004, 2001
44 Herath CB, Shiojima S, Ishiwata H, Katsuma S, Kadowaki T, Ushizawa K, Imai K, Takahashi T, Hirasawa A, Tsujimoto G, Hashizume K: Pregnancy-associated changes in genome-wide gene expression profiles in the liver of cow throughout pregnancy. Biochem Biophys Res Commun **313:** 666-680, 2004
45 Higgins MA, Berridge BR, Mills BJ, Schultze AE, Gao H, Searfoss GH, Baker TK, Ryan TP: Gene expression analysis of the acute phase response using a canine microarray. Toxicol Sci **74:** 470-484, 2003
46 Hughes TR, Mao M, Jones AR, Burchard J, Marton MJ, Shannon KW, Lefkowitz SM, Ziman M, Schelter JM, Meyer MR, Kobayashi S, Davis C, Dai H, He YD, Stephaniants SB, Cavet G, Walker WL, West A, Coffey E, Shoemaker DD, Stoughton R, Blanchard AP, Friend SH, Linsley PS: Expression profiling using microarrays fabricated by an ink-jet oligonucleotide synthesizer. Nat Biotechnol **19:** 342-347, 2001

47 Hyman E, Kauraniemi P, Hautaniemi S, Wolf M, Mousses S, Rozenblum E, Ringner M, Sauter G, Monni O, Elkahloun A, Kallioniemi OP, Kallioniemi A: Impact of DNA amplification on gene expression patterns in breast cancer. Cancer Res **62:** 6240-6245, 2002
48 Irish JM, Hovland R, Krutzik PO, Perez OD, Bruserud O, Gjertsen BT, Nolan GP: Single cell profiling of potentiated phospho-protein networks in cancer cells. Cell **118:** 217-228, 2004
49 Jass JR, Whitehall VL, Young J, Leggett BA: Emerging concepts in colorectal neoplasia. Gastroenterology **123:** 862-876, 2002
50 Kabbarah O, Pinto K, Mutch DG, Goodfellow PJ: Expression profiling of mouse endometrial cancers microdissected from ethanol-fixed, paraffin-embedded tissues. Am J Pathol **162:** 755-762, 2003
51 Kato-Maeda M, Gao Q, Small PM: Microarray analysis of pathogens and their interaction with hosts. Cell Microbiol **3:** 713-719, 2001
52 Kenzelmann M, Klaren R, Hergenhahn M, Bonrouhi M, Grone HJ, Schmid W, Schutz G: High-accuracy amplification of nanogram total RNA amounts for gene profiling. Genomics **83:** 550-558, 2004
53 Kobaek-Larsen M, Thorup I, Diederichsen A, Fenger C, Hoitinga MR: Review of colorectal cancer and its metastases in rodent models: comparative aspects with those in humans. Comp Med **50:** 16-26, 2000
54 Lapointe J, Li C, Higgins JP, van de Rijn M, Bair E, Montgomery K, Ferrari M, Egevad L, Rayford W, Bergerheim U, Ekman P, DeMarzo AM, Tibshirani R, Botstein D, Brown PO, Brooks JD, Pollack JR: Gene expression profiling identifies clinically relevant subtypes of prostate cancer. Proc Natl Acad Sci U S A **101:** 811-816, 2004
55 Lau WY, Lai PB, Leung MF, Leung BC, Wong N, Chen G, Leung TW, Liew CT: Differential gene expression of hepatocellular carcinoma using cDNA microarray analysis. Oncol Res **12:** 59-69, 2000
56 Lechner S, Muller-Ladner U, Renke B, Scholmerich J, Ruschoff J, Kullmann F: Gene expression pattern of laser microdissected colonic crypts of adenomas with low grade dysplasia. Gut **52:** 1148-1153, 2003
57 Lee PS, Shaw LB, Choe LH, Mehra A, Hatzimanikatis V, Lee KH: Insights into the relation between mrna and protein expression patterns: II. Experimental observations in Escherichia coli. Biotechnol Bioeng **84:** 834-841, 2003
58 Leung YF, Cavalieri D: Fundamentals of cDNA microarray data analysis. Trends Genet **19:** 649-659, 2003
59 Li C, Wong WH: Model-based analysis of oligonucleotide arrays: expression index computation and outlier detection. Proc Natl Acad Sci U S A **98:** 31-36, 2001
60 Li M, Lin YM, Hasegawa S, Shimokawa T, Murata K, Kameyama M, Ishikawa O, Katagiri T, Tsunoda T, Nakamura Y, Furukawa Y: Genes associated with liver metastasis of colon cancer, identified by genome-wide cDNA microarray. Int J Oncol **24:** 305-312, 2004
61 Liang APaP: Analysing differential expression in cancer. Nat Cancer Rev **3:** 869-876, 2003

62 Lin YM, Furukawa Y, Tsunoda T, Yue CT, Yang KC, Nakamura Y: Molecular diagnosis of colorectal tumors by expression profiles of 50 genes expressed differentially in adenomas and carcinomas. Oncogene **21:** 4120-4128, 2002
63 Linn SC, West RB, Pollack JR, Zhu S, Hernandez-Boussard T, Nielsen TO, Rubin BP, Patel R, Goldblum JR, Siegmund D, Botstein D, Brown PO, Gilks CB, van de Rijn M: Gene expression patterns and gene copy number changes in dermatofibrosarcoma protuberans. Am J Pathol **163:** 2383-2395, 2003
64 Lipschultz R: High density oligonucleotide array. Nat Genet **21:** 20-24, 1999
65 Ljubimova JY, Lakhter AJ, Loksh A, Yong WH, Riedinger MS, Miner JH, Sorokin LM, Ljubimov AV, Black KL: Overexpression of alpha4 chain-containing laminins in human glial tumors identified by gene microarray analysis. Cancer Res **61:** 5601-5610, 2001
66 Lockhart DJ, Dong H, Byrne MC, Follettie MT, Gallo MV, Chee MS, Mittmann M, Wang C, Kobayashi M, Horton H, Brown EL: Expression monitoring by hybridization to high-density oligonucleotide arrays. Nat Biotechnol **14:** 1675-1680, 1996
67 Lu J, Liu Z, Xiong M, Wang Q, Wang X, Yang G, Zhao L, Qiu Z, Zhou C, Wu M: Gene expression profile changes in initiation and progression of squamous cell carcinoma of esophagus. Int J Cancer **91:** 288-294, 2001
68 Ma XJ, Salunga R, Tuggle JT, Gaudet J, Enright E, McQuary P, Payette T, Pistone M, Stecker K, Zhang BM, Zhou YX, Varnholt H, Smith B, Gadd M, Chatfield E, Kessler J, Baer TM, Erlander MG, Sgroi DC: Gene expression profiles of human breast cancer progression. Proc Natl Acad Sci U S A **100:** 5974-5979, 2003
69 Ma XJ, Wang Z, Ryan PD, Isakoff SJ, Barmettler A, Fuller A, Muir B, Mohapatra G, Salunga R, Tuggle JT, Tran Y, Tran D, Tassin A, Amon P, Wang W, Enright E, Stecker K, Estepa-Sabal E, Smith B, Younger J, Balis U, Michaelson J, Bhan A, Habin K, Baer TM, Brugge J, Haber DA, Erlander MG, Sgroi DC: A two-gene expression ratio predicts clinical outcome in breast cancer patients treated with tamoxifen. Cancer Cell **5:** 607-616, 2004
70 Macy DW: Hematopoietic tumors. *In*: Small animal clinical oncology, eds. Withrow SJ, McEwen EG, 3 ed., pp. 667-672. W.B. Saunders, Philadelphia, 2001
71 Madsen SA, Chang LC, Hickey MC, Rosa GJ, Coussens PM, Burton JL: Microarray analysis of gene expression in blood neutrophils of parturient cows. Physiol Genomics **16:** 212-221, 2004
72 Markowitz SD, Dawson DM, Willis J, Willson JK: Focus on colon cancer. Cancer Cell **1:** 233-236, 2002
73 Meeusen EN, Piedrafita D: Exploiting natural immunity to helminth parasites for the development of veterinary vaccines. Int J Parasitol **33:** 1285-1290, 2003
74 Mehra A, Lee KH, Hatzimanikatis V: Insights into the relation between mRNA and protein expression patterns: I. Theoretical considerations. Biotechnol Bioeng **84:** 822-833, 2003
75 Mennis-Mikulowski A: High quality RNA from cells isolated by laser-capture microdissection. Biotechniques **33:** 176-179, 2002
76 Mies C: Molecular biological analysis of paraffin-embedded tissues. Hum Pathol **25:** 555-560, 1994

77 Nambiar PR, Giardina C, Guda K, Aizu W, Raja R, Rosenberg DW: Role of the alternating reading frame (P19)-p53 pathway in an in vivo murine colon tumor model. Cancer Res **62:** 3667-3674, 2002
78 Nambiar PR, Haines DM, Ellis JA, Kidney BA, Jackson ML: Mutational analysis of tumor suppressor gene p53 in feline vaccine site-associated sarcomas. Am J Vet Res **61:** 1277-1281, 2000
79 Nambiar PR, Jackson ML, Ellis JA, Chelack BJ, Kidney BA, Haines DM: Immunohistochemical detection of tumor suppressor gene p53 protein in feline injection site-associated sarcomas. Vet Pathol **38:** 236-238, 2001
80 Nambiar PR, Nakanishi M, Gupta R, Cheung E, Firouzi A, Ma X-J, Flynn C, Dong M, Guda K, Levine J, Raja R, Achenie L, Rosenberg DW: Genetic signatures of high-and low-risk aberrant crypt foci in a mouse model of sporadic colon cancer. Cancer Res **64:** 6394-6401, 2004
81 Nobis W, Ren X, Suchyta SP, Suchyta TR, Zanella AJ, Coussens PM: Development of a porcine brain cDNA library, EST database, and microarray resource. Physiol Genomics **16:** 153-159, 2003
82 Notterman DA, Alon U, Sierk AJ, Levine AJ: Transcriptional gene expression profiles of colorectal adenoma, adenocarcinoma, and normal tissue examined by oligonucleotide arrays. Cancer Res **61:** 3124-3130, 2001
83 Ohyama H, Zhang X, Kohno Y, Alevizos I, Posner M, Wong DT, Todd R: Laser capture microdissection-generated target sample for high-density oligonucleotide array hybridization. Biotechniques **29:** 530-536, 2000
84 Okabe H, Satoh S, Kato T, Kitahara O, Yanagawa R, Yamaoka Y, Tsunoda T, Furukawa Y, Nakamura Y: Genome-wide analysis of gene expression in human hepatocellular carcinomas using cDNA microarray: identification of genes involved in viral carcinogenesis and tumor progression. Cancer Res **61:** 2129-2137, 2001
85 Olert J, Wiedorn KH, Goldmann T, Kuhl H, Mehraein Y, Scherthan H, Niketeghad F, Vollmer E, Muller AM, Muller-Navia J: HOPE fixation: a novel fixing method and paraffin-embedding technique for human soft tissues. Pathol Res Pract **197:** 823-826, 2001
86 Patnaik AK, Ehler WJ, MacEwen EG: Canine cutaneous mast cell tumor: morphologic grading and survival time in 83 dogs. Vet Pathol **21:** 469-474, 1984
87 Perou CM, Jeffrey SS, van de Rijn M, Rees CA, Eisen MB, Ross DT, Pergamenschikov A, Williams CF, Zhu SX, Lee JC, Lashkari D, Shalon D, Brown PO, Botstein D: Distinctive gene expression patterns in human mammary epithelial cells and breast cancers. Proc Natl Acad Sci U S A **96:** 9212-9217, 1999
88 Perou CM, Sorlie T, Eisen MB, van de Rijn M, Jeffrey SS, Rees CA, Pollack JR, Ross DT, Johnsen H, Akslen LA, Fluge O, Pergamenschikov A, Williams C, Zhu SX, Lonning PE, Borresen-Dale AL, Brown PO, Botstein D: Molecular portraits of human breast tumours. Nature **406:** 747-752, 2000
89 Ponce F, Magnol JP, Ledieu D, Marchal T, Turinelli V, Chalvet-Monfray K, Fournel-Fleury C: Prognostic significance of morphological subtypes in canine malignant lymphomas during chemotherapy. Vet J **167:** 158-166, 2004
90 Prichard R, Tait A: The role of molecular biology in veterinary parasitology. Vet Parasitol **98:** 169-194, 2001

91 Quackenbush J: Microarray data normalization and transformation. Nat Genet **32** (Suppl)**:** 496-501, 2002
92 Renehan AG, O'Dwyer ST, Haboubi NJ, Potten CS: Early cellular events in colorectal carcinogenesis. Colorectal Dis **4:** 76-89, 2002
93 Rhind SM: Veterinary oncological pathology--current and future perspectives. Vet J **163:** 7-18, 2002
94 Rickman DS, Bobek MP, Misek DE, Kuick R, Blaivas M, Kurnit DM, Taylor J, Hanash SM: Distinctive molecular profiles of high-grade and low-grade gliomas based on oligonucleotide microarray analysis. Cancer Res **61:** 6885-6891, 2001
95 Russo G, Zegar C, Giordano A: Advantages and limitations of microarray technology in human cancer. Oncogene **22:** 6497-6507, 2003
96 Sallinen SL, Sallinen PK, Haapasalo HK, Helin HJ, Helen PT, Schraml P, Kallioniemi OP, Kononen J: Identification of differentially expressed genes in human gliomas by DNA microarray and tissue chip techniques. Cancer Res **60:** 6617-6622, 2000
97 Sanchez-Carbayo M, Cordon-Cardo C: Applications of array technology: identification of molecular targets in bladder cancer. Br J Cancer **89:** 2172-2177, 2003
98 Sarli G, Preziosi R, Benazzi C, Castellani G, Marcato PS: Prognostic value of histologic stage and proliferative activity in canine malignant mammary tumors. J Vet Diagn Invest **14:** 25-34, 2002
99 Sawiris GP, Sherman-Baust CA, Becker KG, Cheadle C, Teichberg D, Morin PJ: Development of a highly specialized cDNA array for the study and diagnosis of epithelial ovarian cancer. Cancer Res **62:** 2923-2928, 2002
100 Schena M: Genome analysis with gene expression microarrays. Bioessays **18:** 427-431, 1996
101 Schena M, Shalon D, Davis RW, Brown PO: Quantitative monitoring of gene expression patterns with a complementary DNA microarray. Science **270:** 467-470, 1995
102 Schutze K, Posl H, Lahr G: Laser micromanipulation systems as universal tools in cellular and molecular biology and in medicine. Cell Mol Biol (Noisy-le-grand) **44:** 735-746, 1998
103 Searcy G: The hematopoietic system. *In*: Thomson's special veterinary pathology, eds. McGavin MD, Carlton WW, Zachary JF, 3 ed., pp. 370-371. Mosby, St. Louis, 2001
104 Shibata D, Hawes D, Li ZH, Hernandez AM, Spruck CH, Nichols PW: Specific genetic analysis of microscopic tissue after selective ultraviolet radiation fractionation and the polymerase chain reaction. Am J Pathol **141:** 539-543, 1992
105 Shim C, Zhang W, Rhee CH, Lee JH: Profiling of differentially expressed genes in human primary cervical cancer by complementary DNA expression array. Clin Cancer Res **4:** 3045-3050, 1998
106 Shirota Y, Kaneko S, Honda M, Kawai HF, Kobayashi K: Identification of differentially expressed genes in hepatocellular carcinoma with cDNA microarrays. Hepatology **33:** 832-840, 2001

107 Shridhar V, Lee J, Pandita A, Iturria S, Avula R, Staub J, Morrissey M, Calhoun E, Sen A, Kalli K, Keeney G, Roche P, Cliby W, Lu K, Schmandt R, Mills GB, Bast RC, Jr., James CD, Couch FJ, Hartmann LC, Lillie J, Smith DI: Genetic analysis of early- versus late-stage ovarian tumors. Cancer Res **61:** 5895-5904, 2001
108 Simone NL, Bonner RF, Gillespie JW, Emmert-Buck MR, Liotta LA: Laser-capture microdissection: opening the microscopic frontier to molecular analysis. Trends Genet **14:** 272-276, 1998
109 Slonim DK: From patterns to pathways: gene expression data analysis comes of age. Nat Genet **32** (Suppl)**:** 502-508, 2002
110 Solinas-Toldo S, Lampel S, Stilgenbauer S, Nickolenko J, Benner A, Dohner H, Cremer T, Lichter P: Matrix-based comparative genomic hybridization: biochips to screen for genomic imbalances. Genes Chromosomes Cancer **20:** 399-407, 1997
111 Sorlie T, Perou CM, Tibshirani R, Aas T, Geisler S, Johnsen H, Hastie T, Eisen MB, van de Rijn M, Jeffrey SS, Thorsen T, Quist H, Matese JC, Brown PO, Botstein D, Eystein Lonning P, Borresen-Dale AL: Gene expression patterns of breast carcinomas distinguish tumor subclasses with clinical implications. Proc Natl Acad Sci U S A **98:** 10869-10874, 2001
112 Strefezzi Rde F, Xavier JG, Catao-Dias JL: Morphometry of canine cutaneous mast cell tumors. Vet Pathol **40:** 268-275, 2003
113 Su A: Large scale-analysis of the human and mouse transcriptomes. Proc Natl Acad Sci U S A **99:** 4465-4470, 2002
114 Suchyta SP, Sipkovsky S, Halgren RG, Kruska R, Elftman M, Weber-Nielsen M, Vandehaar MJ, Xiao L, Tempelman RJ, Coussens PM: Bovine mammary gene expression profiling using a cDNA microarray enhanced for mammary-specific transcripts. Physiol Genomics **16:** 8-18, 2003
115 Suchyta SP, Sipkovsky S, Kruska R, Jeffers A, McNulty A, Coussens MJ, Tempelman RJ, Halgren RG, Saama PM, Bauman DE, Boisclair YR, Burton JL, Collier RJ, DePeters EJ, Ferris TA, Lucy MC, McGuire MA, Medrano JF, Overton TR, Smith TP, Smith GW, Sonstegard TS, Spain JN, Spiers DE, Yao J, Coussens PM: Development and testing of a high-density cDNA microarray resource for cattle. Physiol Genomics **15:** 158-164, 2003
116 Tan PK, Downey TJ, Spitznagel EL, Jr., Xu P, Fu D, Dimitrov DS, Lempicki RA, Raaka BM, Cam MC: Evaluation of gene expression measurements from commercial microarray platforms. Nucleic Acids Res **31:** 5676-5684, 2003
117 Tao W, Mallard B, Karrow N, Bridle B: Construction and application of a bovine immune-endocrine cDNA microarray. Vet Immunol Immunopathol **101:** 1-17, 2004
118 Taylor TB, Nambiar PR, Raja R, Cheung E, Rosenberg DW, Anderegg B: Microgenomics: Identification of new expression profiles via small and single-cell sample analyses. Cytometry **59A:** 254-261, 2004
119 Thomas R, Fiegler H, Ostrander EA, Galibert F, Carter NP, Breen M: A canine cancer-gene microarray for CGH analysis of tumors. Cytogenet Genome Res **102:** 254-260, 2003
120 Torhost J: Tissue microarrays for rapid linking of molecular changes to clinical end points. Am J Pathol **159:** 2249-2256, 2001

121 Tusher VG, Tibshirani R, Chu G: Significance analysis of microarrays applied to the ionizing radiation response. Proc Natl Acad Sci U S A **98:** 5116-5121, 2001
122 van de Rijn M, Gilks CB: Applications of microarrays to histopathology. Histopathology **44:** 97-108, 2004
123 Van Gelder R: Amplified RNA synthesized from limited quantities of heterogeneous cDNA. Proc Natl Acad Sci U S A **87:** 1663-1667, 1990
124 Wang D, Urisman A, Liu YT, Springer M, Ksiazek TG, Erdman DD, Mardis ER, Hickenbotham M, Magrini V, Eldred J, Latreille JP, Wilson RK, Ganem D, DeRisi JL: Viral discovery and sequence recovery using DNA microarrays. PLoS Biol **1:** E2, 2003
125 Wang E, Miller LD, Ohnmacht GA, Liu ET, Marincola FM: High-fidelity mRNA amplification for gene profiling. Nat Biotechnol **18:** 457-459, 2000
126 Wang K, Gan L, Jeffery E, Gayle M, Gown AM, Skelly M, Nelson PS, Ng WV, Schummer M, Hood L, Mulligan J: Monitoring gene expression profile changes in ovarian carcinomas using cDNA microarray. Gene **229:** 101-108, 1999
127 Watanabe T, Wu TT, Catalano PJ, Ueki T, Satriano R, Haller DG, Benson AB, 3rd, Hamilton SR: Molecular predictors of survival after adjuvant chemotherapy for colon cancer. N Engl J Med **344:** 1196-1206, 2001
128 Weiss DJ, Evanson OA, Deng M, Abrahamsen MS: Gene expression and antimicrobial activity of bovine macrophages in response to Mycobacterium avium subsp. paratuberculosis. Vet Pathol **41:** 326-337, 2004
129 Wilson DL, Buckley MJ, Helliwell CA, Wilson IW: New normalization methods for cDNA microarray data. Bioinformatics **19:** 1325-1332, 2003
130 Xu J, Stolk JA, Zhang X, Silva SJ, Houghton RL, Matsumura M, Vedvick TS, Leslie KB, Badaro R, Reed SG: Identification of differentially expressed genes in human prostate cancer using subtraction and microarray. Cancer Res **60:** 1677-1682, 2000
131 Yao J, Burton JL, Saama P, Sipkovsky S, Coussens PM: Generation of EST and cDNA microarray resources for the study of bovine immunobiology. Acta Vet Scand **42:** 391-405, 2001
132 Zhang H, Yu CY, Singer B, Xiong M: Recursive partitioning for tumor classification with gene expression microarray data. Proc Natl Acad Sci U S A **98:** 6730-6735, 2001
133 Zhou W, Goodman SN, Galizia G, Lieto E, Ferraraccio F, Pignatelli C, Purdie CA, Piris J, Morris R, Harrison DJ, Paty PB, Culliford A, Romans KE, Montgomery EA, Choti MA, Kinzler KW, Vogelstein B: Counting alleles to predict recurrence of early-stage colorectal cancers. Lancet **359:** 219-225, 2002
134 Zou TT, Selaru FM, Xu Y, Shustova V, Yin J, Mori Y, Shibata D, Sato F, Wang S, Olaru A, Deacu E, Liu TC, Abraham JM, Meltzer SJ: Application of cDNA microarrays to generate a molecular taxonomy capable of distinguishing between colon cancer and normal colon. Oncogene **21:** 4855-4862, 2002
135 Zuccari DA, Santana AE, Cury PM, Cordeiro JA: Immunocytochemical study of Ki-67 as a prognostic marker in canine mammary neoplasia. Vet Clin Pathol **33:** 23-28, 2004

***Figures***

**Fig. 1. Microdissection and linear amplification process**. (A) The laser-capture microdissection process. An optical grade cap sits on top of a tissue section mounted on a conventional glass slide without a cover slip. The thin polymer film at the bottom of the cap is kept 12 microns above the tissue using concentric rails. The area of interest is then visualized through the microscope and the laser beam (red) is activated to dissect the cells. The thin polymer on the cap expands locally upon activation by the laser, contacts and subsequently adheres to the underlying tissue. On removal of the cap from the glass slide, the adherent tissue is detached from the adjoining section. The microdissected tissue attached to the cap is subjected to extraction buffers to harvest biomolecules. (B) Focal dysplastic aberrant crypt foci (ACF) from an azoxymethane treated A/J mouse colon before laser-capture, after capture, and within a cap after dissection. (C) Schematic representation of T7-polymerase-based linear amplification of RNA. Reproduced with permission from Arcturus Bioscience Inc., Mountain View, CA. Briefly, the mRNA undergoes 1st strand synthesis using an oligo-dT primer with a T7 promoter site (1st primer) which is then converted to a double stranded (ds) cDNA molecule using random hexamers (2nd primer). The purified ds cDNA is used as a template for an in vitro transcription reaction to generate multiple copies of antisense RNA (aRNA) which are complementary to the sequence of the original mRNA species. For a second round of amplification, the process is repeated using aRNA produced from the first round.

**Fig. 2. Schematic representation of a microarray experiment**. One- or two-color microarray procedures start with test and reference mRNA that undergo reverse transcription (RT) or linearly amplification to generate complimentary DNA (cDNA) or antisense RNA (aRNA), respectively. (A) For two-color microarray hybridization, samples are labeled with fluorescent dyes of two different excitation/emission wavelengths. The differentially labeled cDNA or aRNA are pooled and hybridized to a microarray. The relative fluorescence intensities for each spot (gene) from the test and reference samples are measured as a ratio using a dual channel confocal laser scanner. Higher magnification of a grid in a scanned hybridized array shows multiple gene spots with varying degree of hybridization, as depicted by colors between the red and green spectrum. (B) A single fluorescent dye is used in one-color microarray hybridization. The labeled cDNA or aRNA from each sample is separately hybridized to microarrays. Detection of the hybridization is made by a separate scan of each array using a confocal laser scanner. The relative abundance of mRNA for each gene between the two samples is measured by comparison of the absolute intensities for that gene between the two different normalized arrays.

**Fig. 3. Graphical representation of differential gene expression between two samples** by scatter-plot analysis. (A) Comparison of logarithm-transformed raw fluorescent gene intensities between two histologically similar, azoxymethane (AOM)-induced microadenomas microdissected from an A/J mouse colon, linearly amplified and hybridized onto a 15,000-element mouse cDNA array shows high correlation (r=0.93).

(B) Comparison of raw fluorescent intensities of genes between a microadenoma and normal appearing, adjacent crypts from an AOM-treated A/J mouse. Cells were microdissected, linearly amplified, and hybridized onto a 15,000-element cDNA array. The reduction in correlation coefficient (r=0.83) is consistent with samples that are histologically dissimilar.

**Fig. 4. Dendrogram and heat map of gene expression**. Levels of a subset of genes from three laser-captured, dysplastic aberrant crypt foci (ACF) from azoxymethane-treated A/J and AKR/J mouse strains, each, using Genesite software (BioDiscovery) are shown. The RNA from A/J and AKR/J strains were labeled with cyanine-5 and cyanine-3-labeled dUTP, respectively, during reverse transcription and hybridized to a cDNA array. Each row and column represents a gene and a lesion, respectively. Dendrograms or relationship trees are generated with software that evaluates the Pearson's correlation coefficient between same genes across different samples. The expression level of most of the genes in the A/J ACF are similar to each other (red=highly expressed) and distinct from the low (green) levels or no change (black) in AKR/J ACF. The generated dendrograms (note branches), based on this distinct expression profile, allow clear segregation of ACF in the two mouse strains. Color bar at the bottom correlates color-intensity to gene expression.

Figure 1

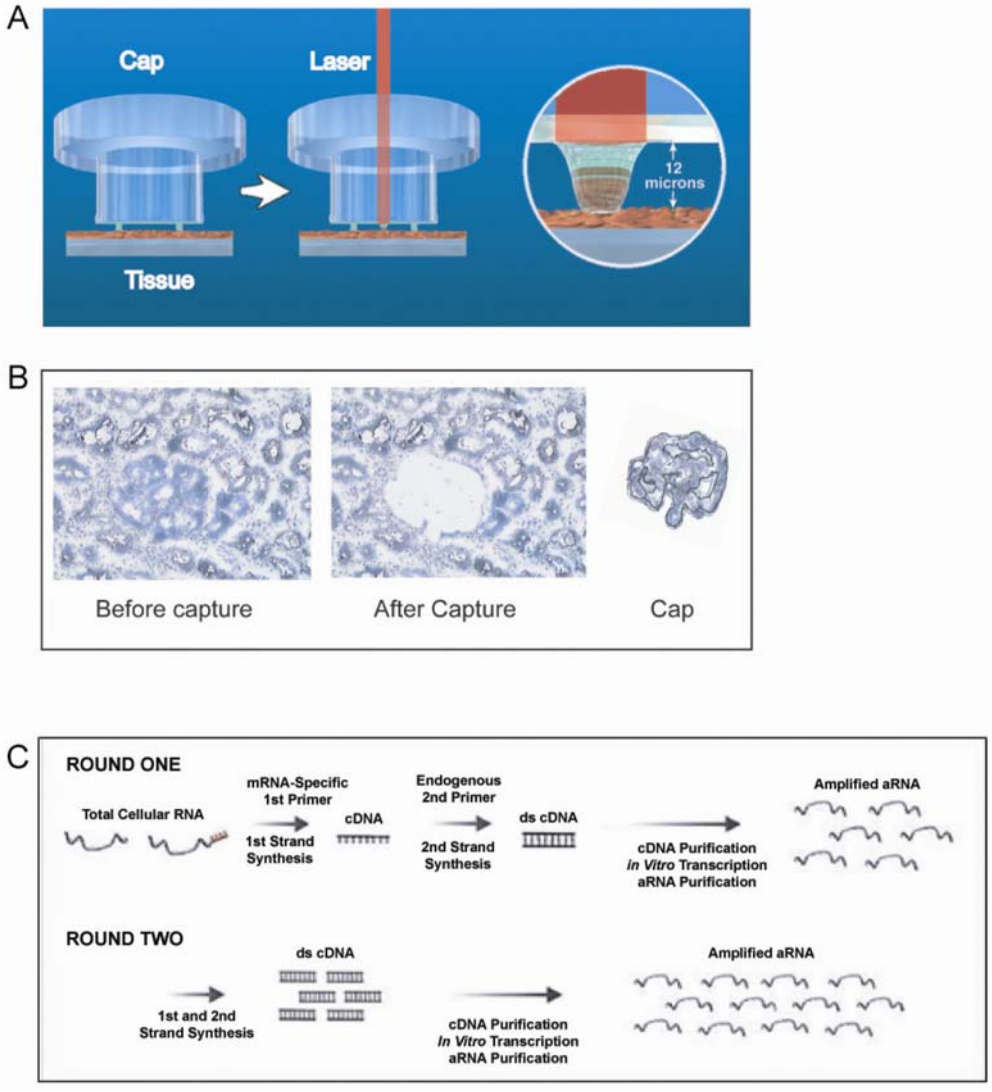
A
Cap
Laser
Tissue
12
microns
B
Before capture
After Capture
Cap
C
ROUND ONE
Total Cellular RNA
mRNA-Specific
1st Primer
1st Strand
Synthesis
cDNA
Endogenous
2nd Primer
2nd Strand
Synthesis
ds cDNA
cDNA Purification
In Vitro Transcription
aRNA Purification
Amplified aRNA
ROUND TWO
ds cDNA
1st and 2nd
Strand Synthesis
cDNA Purification
In Vitro Transcription
aRNA Purification
Amplified aRNA

Figure 2

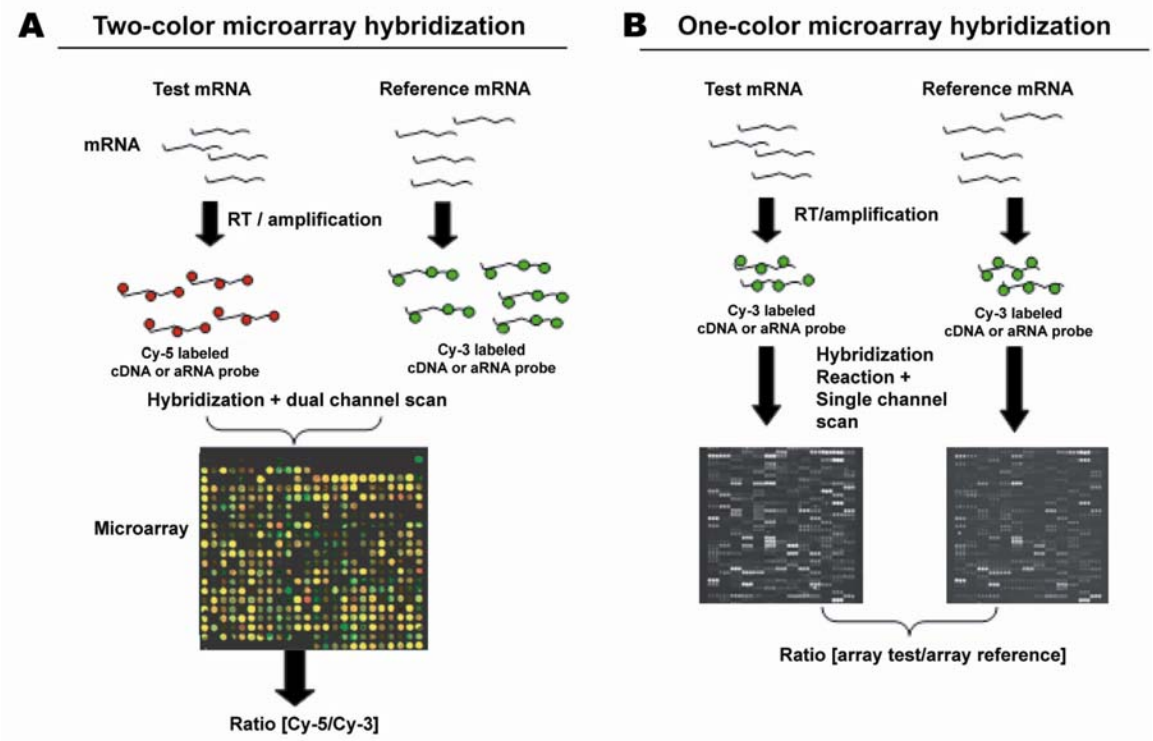
A
Two-color microarray hybridization
Test mRNA
Reference mRNA
mRNA
RT / amplification
Cy-5 labeled
cDNA or aRNA probe
Cy-3 labeled
cDNA or aRNA probe
Hybridization + dual channel scan
Microarray
Ratio [Cy-5/Cy-3]
B
One-color microarray hybridization
Test mRNA
Reference mRNA
RT/amplification
Cy-3 labeled
cDNA or aRNA probe
Cy-3 labeled
cDNA or aRNA probe
Hybridization
Reaction +
Single channel
scan
Ratio [array test/array reference]

Figure 3

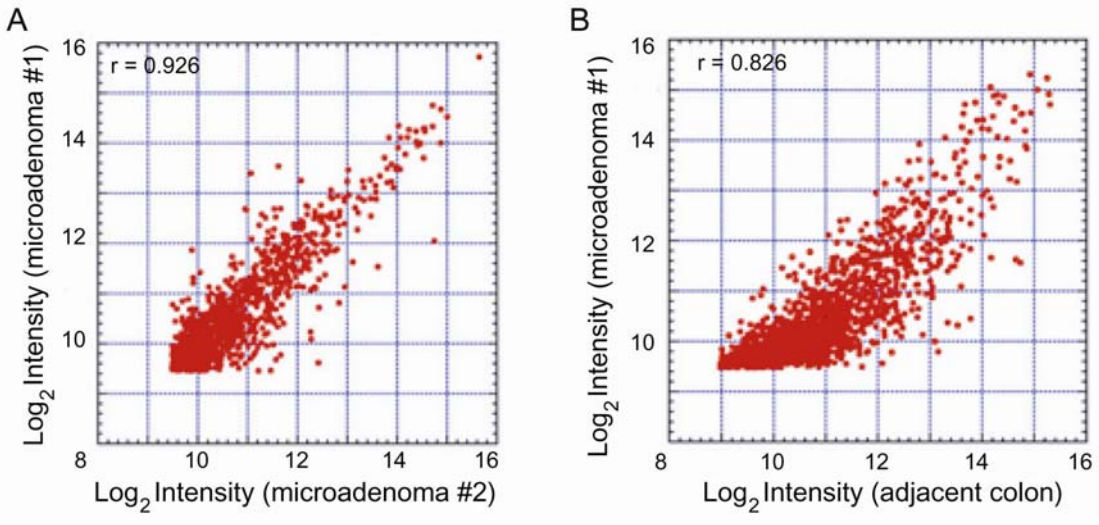
A
r = 0.926
Log2 Intensity (microadenoma #1)
Log2 Intensity (microadenoma #2)
8
10
12
14
16
B
r = 0.826
Log2 Intensity (microadenoma #1)
Log2 Intensity (adjacent colon)

Figure 4

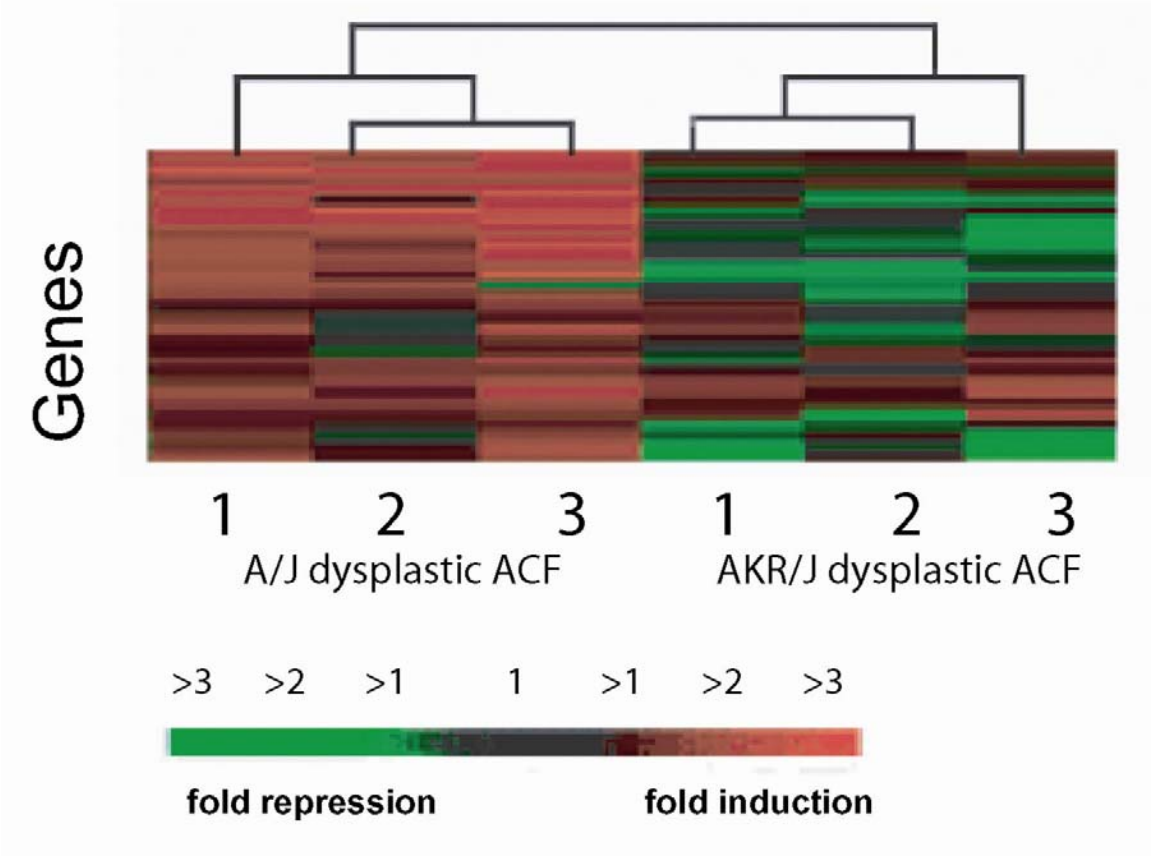
Genes
1
2
3
1
2
3
A/J dysplastic ACF
AKR/J dysplastic ACF
>3
>2
>1
1
>1
>2
>3
fold repression
fold induction

*Toxicologic Pathology*, 32:678–693, 2004

ISSN: 0192-6233 print / 1533-1601 online
DOI: 10.1080/01926230490524058

# Hepatic Temporal Gene Expression Profiling in *Helicobacter hepaticus*-Infected A/JCr Mice

SAMUEL R. BOUTIN,[1,2] ARLIN B. ROGERS,[1] ZELI SHEN,[1] REBECCA C. FRY,[3] JENNIFER A. LOVE,[4] PRASHANT R. NAMBIAR,[1] SEBASTIAN SUERBAUM,[5] AND JAMES G. FOX[1,2]

[1]*Division of Comparative Medicine, Massachusetts Institute of Technology, Cambridge, Massachusetts 02139, USA*
[2]*Division of Biological Engineering, Massachusetts Institute of Technology, Cambridge, Massachusetts 02139, USA*
[3]*Computational and Systems Biology Initiative, Massachusetts Institute of Technology, Cambridge, Massachusetts 02139, USA*
[4]*Whitehead Institute For Biomedical Research, Cambridge, Massachusetts 02139, USA*
[5]*Institute of Medical Microbiology and Hospital Epidemiology, Hannover Medical School, Hannover, Germany*

ABSTRACT

*Helicobacter hepaticus* infection of A/JCr mice is a model of infectious liver cancer. We monitored hepatic global gene expression profiles in *H. hepaticus* infected and control male A/JCr mice at 3 months, 6 months, and 1 year of age using an Affymetrix-based oligonucleotide microarray platform on the premise that a specific genetic expression signature at isolated time points would be indicative of disease status. Model based expression index comparisons generated by dChip yielded consistent profiles of differential gene expression for *H. hepaticus* infected male mice with progressive liver disease versus uninfected control mice within each age group. Linear discriminant analysis and principal component analysis allowed segregation of mice based on combined age and lesion status, or age alone. Up-regulation of putative tumor markers correlated with advancing hepatocellular dysplasia. Transcriptionally down-regulated genes in mice with liver lesions included those related to peroxisome proliferator, fatty acid, and steroid metabolism pathways. In conclusion, transcriptional profiling of hepatic genes documented gene expression signatures in the livers of *H. hepaticus* infected male A/JCr mice with chronic progressive hepatitis and preneoplastic liver lesions, complemented the histopathological diagnosis, and suggested molecular targets for the monitoring and intervention of disease progression prior to the onset of hepatocellular neoplasia.

*Keywords.* Microarray; hepatitis, chronic; carcinoma, hepatocellular; mice; inbred; *Helicobacter*.

## INTRODUCTION

Microbial causes of enterohepatic cancer are well known. ***Helicobacter pylori*** infection is the single greatest risk factor for gastric adenocarcinoma and has been classified a class I carcinogen by the World Health Organization (Fox et al., 2003). Liver cancer in humans is associated with hepatitis B and C virus infection. Similarly, ***Helicobacter*** spp. may potentiate inflammation and risk of hepatocellular carcinoma (HCC) in humans with or without viral hepatitis (Ponzetto et al., 2000). Infection-associated inflammation is widely recognized as a contributor to human HCC and cholangiocarcinoma (Fox et al., 1998; Avenaud et al., 2000; Nilsson et al., 2001).

***Helicobacter hepaticus*** is associated with chronic hepatitis and HCC in A/JCr and other susceptible mouse strains, including A × B recombinant inbred mice, B6C3F1 mice and B6AF1 mice (Fox et al., 1994, 1996b; Ward et al., 1994; Hailey et al., 1998; Ihrig et al., 1999). A/JCr mice infected with ***H. hepaticus*** develop necrogranulomatous lobular and/or lymphocytic portal hepatitis. Male mice are more susceptible to hepatitis and tumors than females. For reasons that are not clear, only a subset of ***H. hepaticus***-infected male mice are affected (Fox et al., 1996b). In the present study, we monitored by microarray analysis chronological changes in hepatic gene expression due to ***H. hepaticus***-induced chronic hepatitis in the preneoplastic phase. We compared gene expression profiles in ***H. hepaticus***-infected male A/JCr mice with severe liver disease to uninfected mice and to infected nondiseased mice at 3 months, 6 months, and 1 year of age. Unique gene expression signatures obtained from the microarray analysis allowed us to segregate ***H. hepaticus***-infected diseased liver from ***H. hepaticus***-infected disease-free livers and uninfected controls. Furthermore, the gene expression profiles allowed segregation of liver profiles based on age of the mice. This study provides for the first time a chronological transcriptional characterization of a microbially induced progressive inflammation of the liver resulting in preneoplastic liver lesions.

## MATERIALS AND METHODS

### *Animals*

Viral antibody free and ***Helicobacter*** free A/JCr mice were purchased from the National Cancer Institute. ***Helicobacter*** free status was confirmed by fecal PCR analysis as described elsewhere (Rogers et al., *Toxicologic Pathology*, this issue). Mice housing, food, water, bedding, lighting cycle and other environmental conditions, and euthanasia were as described (Rogers et al., *Toxicologic Pathology*, this issue) in an animal facility approved by the Association for the Assessment

Address correspondence to: James G. Fox, Director, Division of Comparative Medicine, Massachusetts Institute of Technology, 77 Massachusetts Avenue, 16-825, Cambridge, Massachusetts 02139, USA; e-mail: jgfox@mit.edu

Abbreviations: HCC, hepatocellular carcinoma; PCR, polymerase chain reaction; EST, expressed sequence-tagged; LDA, linear discriminant analysis; PCA, principal component analysis; FAH, foci of altered hepatocytes; CDT, cytolethal distending toxin; IBD, inflammatory bowel disease; AFP, Alpha-fetoprotein; CYP, cytochrome P450; HSD, hydroxysteroid dehydrogenase.

and Accreditation of Laboratory Animal Care, International (Rockville, MD). All experiments complied with the "Guide for the Care and Use of Laboratory Animals" prepared by the National Institutes of Health and were approved by the Committee on Animal Care at the Massachusetts Institute of Technology (MIT).

Helicobacter hepaticus *Infection*

The infection and bacterial colonization methods are discussed in detail elsewhere (Rogers et al., ***Toxicologic Pathology***, this issue). ***H. hepaticus*** type strain ATCCC 51488 was grown on TSA 5% sheep blood agar (Remel, Lenexa, KS) under microaerobic conditions ($N_2$, $H_2$, and $CO_2$; 90:5:5) for 2 days and transferred with a sterile applicator to 1.5 ml of Brucella broth. This was immediately deposited into 150 ml of Brucella broth in a flask, enclosed in an BBL GasPak 100 polycarbonate anaerobic jar (Becton Dickison Microbiology Systems, Cockeysville, MD) under microaerobic conditions, and placed on a PsychroTherm incubator-shaker table (New Brunswick Scientific Co., Edison NJ) at 30 RPM at 37°C overnight. Approximately $10^8$ bacteria/ml were placed in phosphate buffered saline (PBS) for one dose. Bacterial count was confirmed by a reading of 1.0 at 660 nm on a DuPro 640 spectrophotometer (Beckman Coulter, Fullerton, CA). Bacterial viability, motility, and morphology were confirmed by phase-contrast microscopy.

Helicobacter-free A/JCr mice were bred, and a subset of pregnant dams orally inoculated with ***Helicobacter hepaticus*** or vehicle only intragestationally as described elsewhere (Rogers et al., ***Toxicologic Pathology***, this issue). Additional groups were inoculated or rechallenged at 3-weeks or 12 weeks postnatally. Mice were euthanized by $CO_2$ inhalation at 3, 6, or 12 months of age. DNA was extracted from feces and frozen liver sections using a commercial kit (DNeasy Tissue Kit, Qiagen, Carlsbad, CA). Samples positive for ***H. hepaticus***-specific DNA by nested polymerase chain reaction (PCR), as well as uninfected negative controls, were quantitated by real-time fluorogenic PCR (TaqMan) as described (Rogers et al., ***Toxicologic Pathology***, this issue).

*Histopathology*

At necropsy, samples of each liver lobe were collected for histopathology. Lesions were evaluated histologically as described elsewhere (Rogers et al., ***Toxicologic Pathology***, this issue).

*Liver Samples*

Samples were sections of the left liver lobe of A/JCr mice (***Mus musculus***). Sections of the liver were used for histology and total RNA isolation. Total RNA was used for microarray and quantitative real-time fluorogenic PCR assays. Mouse liver was aseptically removed immediately after $CO_2$ euthanasia and placed in an individual cryogenic vial (Corning, NY). The cryogenic vial was immediately placed in the vapor phase of liquid nitrogen. At the end of the necropsy for the total experiment, the cryogenic vials were transferred to a −80°C freezer.

Representative samples at 3, 6, and 12 months from 18 male mice were selected for microarray analysis based on known infection status and presence or absence of hepatitis as demonstrated by histopathology. Biological replicates representing 2 uninfected mice, 2 infected mice without significant liver lesions, and 2 infected mice with severe hepatitis were analyzed at each time point. Samples for microarray analysis were selected from groups of pups born to dams inoculated during pregnancy with subsequent ***H. hepaticus*** inoculation of pups at 3 weeks postnatally (Rogers et al., ***Toxicologic Pathology***, this issue). ***H. hepaticus***-infected littermates and cagemates with and without hepatitis were chosen for direct comparison whenever possible.

*RNA Isolation and Quality Assessment*

The standard protocols followed were per Affymetix's instructions (Genechip Expression Analysis Technical Manual 701021 Rev 4). Briefly, total RNA was isolated from 2 sections (each approximately 35 mg) of flash frozen liver using Trizol (Invitrogen, Carlsbad, CA) as per manufacturer's instructions. The RNA pellet was resuspended in 100 ul of RNAse free water. The RNeasy Clean-up kit (Qiagen, Valencia, CA) was utilized per manufacturer's instructions resulting in 30 ul total RNA sample. The total RNA concentration and 260/280 ratio was evaluated on a NanoDrop ND-1000 UV-Vis Spectrophotomter (NanoDrop Technologies, Rockland, DE). Only samples with a 260/280 ratio greater than 1.9 were further processed. An aliquot of 1 ul from each of the samples was diluted to be within the dynamic range of the Agilent RNA 6000 Nano Labchip kit (Agilent, Palo Alto, CA), with a target of 100 ng. The Nano Labchip protocol was followed as per manufacturer's instructions and was placed on an Agilent 2100 Bioanalyzer (Agilent, Palo Alto, CA) for evaluation. Samples with the highest concentration, only 2 distinct 18 S and 28 S peaks, and no evidence of degradation were further processed.

To obtain 15 $\mu$g of total RNA for first strand cDNA synthesis, samples were sometimes combined and placed on a spin-vacuum to obtain the necessary concentration (1.66 $\mu$g/$\mu$l) and volume (9 $\mu$l). Six hundred units of SuperScript II reverse transcriptase were used for the first strand cDNA synthesis reaction. Half of the samples were prepared at the Division of Comparative Medicine at MIT and the other half of the samples were prepared at the Whitehead Institute (JAL) for comparison. The second strand DNA synthesis, the clean-up of the double-stranded cDNA, the synthesis of the biotin-labeled cRNA, and the clean-up of the biotin-labeled cRNA were per Affymetrix instructions. The Genechip Sample Clean-up module was used for the clean-up steps of the double-stranded cDNA and the biotin-labeled cRNA. Quantification of the cRNA was evaluated on the NanoDrop. Samples were used for hybridization only if 20 $\mu$g of cRNA were obtained in an individual sample or by combining samples.

*Array Design*

Affymetrix Murine Genome Arrays U74Av2. (Affymetrix, Santa Clara, CA) Array size: Standard Format. Feature size 20 $\mu$m. Sensitivity: 1:100,000. See ⟨www.affymetrix.com⟩ for the probe sequences or reference sequence from which the probe was derived. Microarrays were hybridized overnight, washed in a fluidics station, and scanned using the GeneArray scanner per manufacturer's instructions (Affymetrix, Santa Clara, CA). The U74Av2 oligonucleotide array contained ~6,000 functionally characterized gene sequences (Unigene

Murine Database, Build 74) and a similar number of expressed sequence-tagged (EST) clusters. There were 16–20 pairs of 25-mer oligonucletide probes per sequence, with a sensitivity of ~1:100,000. Control sequences on the microarray included *bioB*, *bioC*, *bioD*, and *cre*, and housekeeping genes considered were actin, GAPDH, and hexokinase.

*Hybridization*

Fragmentation, hybridization, washing, staining, and scanning were done according to the Affymetrix protocol. Briefly, reagent preparation included 12X MES stock (1.22 M MES, 0.89 M [$Na^+$]) and 2X hybridization buffer (1X hybridization buffer: 100 mM MES, 1 M [$Na^+$], 20 mM EDTA, 0.01% Tween 20). The hybridization cocktail components and final concentrations consisted of fragmented cDNA (.05 $\mu$g/$\mu$l), control oligonucleotide B2 (50 pM), 20X eukaryotic hybridization controls *bioB*, *bioC*, *bioD*, and *cre* (1.5, 5, 25, 100 pM, respectively), herring sperm DNA (.1 mg/ml), acetylated BSA (.5 mg/ml), 1X hybridization buffer with a final volume of 300 $\mu$l. The GeneChip array was filled with 250 $\mu$l of the hybridization cocktail and hybridized for 16 hours, rotated at 60 RPM, and maintained at 45°C.

Reagents prepared for washing and staining included a nonstringent wash buffer (6X SSPE, .01% Tween 20), a stringent wash buffer (100 mM MES, 0.1 M [$Na^+$], 0.01% Tween 20), and a 2X stain buffer (1X: 100 mM MES, 1 M [$Na^+$], 0.05% Tween 20). The wash procedure was carried out in an Affymetrix Fluidics Station 400 controlled by Affymetrix Microarray Suite 5.0 software resident on a personal computer. The fluidics station first went through a priming step and subsequently did the washing and staining by a software protocol designed for the Affymetrix Murine Genome Array U74Av2.

*Measurements*

The microarrays were scanned using the GeneArray scanner per manufacturer's instructions (Affymetrix, Santa Clara, CA). The quality control algorithms for eliminating an array are based on recommendations in both the Affymetrix and dChip software packages.

*Normalization*

For dChip software, an invariant-set normalization method is used (Li and Hung Wong, 2001a; Li and Wong, 2001b). Briefly, the expectation is that a probe of a nondifferentially expressed gene in 2 arrays will have similar intensity ranks in 2 separate arrays. The ranks are calculated separately in the two arrays. Although it is unknown which genes are nondifferentially expressed, an iterative procedure is used to determine rank differences with an empirically derived threshold for inclusion. All arrays are normalized, except the baseline array, to the common baseline array with median intensity.

*Data Analysis*

Two software packages were utilized for data analysis, dChip (Li and Hung Wong, 2001a; Li and Wong, 2001b) and Affymetrix Microarray Suite 5.0. Microarray Suite 5.0 was used to generate a cell intensity file (*.cel). The *.cel file and the perfect match model (PM) were used for the dChip analysis and is the data presented. The dChip software is model based, and generates a "model based expression index" (MBEI) and a standard error. The software utilizes the response characteristics of individual probe sets. Unless otherwise specified, default settings were used. Comparison analysis, hierarchical clustering, linear discriminant analysis (LDA), and principal component analysis (PCA) within dChip were performed. Comparison analysis used the default setting of 1.2-fold change, positive or negative. For hierarchical clustering, default settings were used, the distance metric was 1-correlation and the linkage was centroid.

*Quantitative Real-Time Flurogenic PCR (Taqman)*

To confirm microarray data, quantitative real-time flurogenic PCR was utilized. Assay-on-Demand gene expression kits (Applied Biosystems, Foster City, CA) were used to quantitate cytochrome P450 4a14 (Cyp4a14), interferon $\gamma$-induced GTPase (Igtp), H19 fetal liver mRNA (H19), hydroxysteroid dehydrogenase-5, delta(5)-3-beta (Hsd3b5), CD5 antigen-like (Cd5l) (formerly known as apoptosis inhibitor 6), trefoil factor 3, intestinal (Tff3) genes were normalized against the expression of glyceraldehyde 3 phosphate dehydrogenase (Gapdh) as the housekeeping standard. Two $\mu$g of total RNA from the uninfected and infected A/JCr mouse liver samples was reverse-transcribed to single strand cDNA using the Superscript Reverse Transcriptase II (Invitrogen, Carlsbad, CA) protocol. The single strand cDNA from the reverse transcriptase reaction was amplified by real-time quantitative flourogenic PCR. Eighty $\mu$l of 1X TE was added to the 20 $\mu$l reaction volume. The Taqman protocol was per manufacturer's instructions for the Applied Biosystems 7700 Sequence Detection System except that 25 $\mu$l total volume was used. The reaction consisted of the Taqman Universal 2X PCR Master Mix (12.5 ul), 5 ul of the cDNA/1XTE solution, 20X target (1.25 $\mu$l) and 6.25 $\mu$l of water. That RNA expression level fold changes were calculated as described by the Taqman protocol.

## RESULTS

*Histopathology*

Briefly, the lobular hepatitis appeared at 3 months and the severity of lobular hepatitis did not worsen noticeably over the 12-month observation period. The lobular hepatitis was comprised of Kupffer cells and recruited macrophages, and was accompanied by hepatocellular coagulative necrosis. Unlike the lobular hepatic lesions, portal hepatitis was progressive over the 12-month study period. Portal hepatitis was manifest as either well-defined aggregates of mononuclear cells or locally invasive lesions that disrupted the hepatic limiting plate. Known precursor lesions to hepatocellular carcinoma including clear and tigroid cell foci and nodules of altered hepatocytes were most evident at the 12-month time point in male mice with lobular hepatitis. *H. hepaticus* DNA levels and hepatic histologic activity were positively correlated in infected *H. hepaticus* A/JCr male mice at the 12-month time point. Complete histopathology results are presented elsewhere (Rogers et al., *Toxicologic Pathology*, this issue).

*Microarray Results Overview*

Certain clusters of gene expression (Tables 1 and 2), gene categories (Table 3), and protein domains (Table 4)

TABLE 1.—Genes with up-regulated transcription in the livers of *H. hepaticus*-infected male A/JCr mice with severe disease versus sham-infected age-matched controls (fold increase).

| Gene | 3 months | 6 months | 12 months | Gene | 3 months | 6 months | 12 months |
|---|---|---|---|---|---|---|---|
| Lipocalin 2 | 7.91 | 46.72 | 30.27 | Guanylate nucleotide binding protein 2 | 2.55 | 7.62 | 2.91 |
| T-cell specific GTPase | 9.26 | 22.37 | 24.96 | Expressed sequence AI854770 | 1.7 | 2.28 | 2.9 |
| Trefoil factor 3, intestinal | * | 8.4 | 20.09 | Macrophage expressed gene 1 | 2.45 | 3.79 | 2.84 |
| Ubiquitin D | 1.96 | 21.04 | 15.36 | ADAM-like, decysin 1 | * | 2.11 | 2.83 |
| Ia-associated invariant chain | 3.18 | 11.9 | 15.06 | Interferon gamma inducible protein, 47 kDa | 1.83 | 2.92 | 2.81 |
| Histocompatibility 2, class II antigen A, alpha | 3.75 | 13.98 | 10.5 | Retinol binding protein 1, cellular | * | 2.74 | 2.8 |
| Tubulin, beta 2 | * | * | 7.4 | Hydroxyacid oxidase (glycolate oxidase) 3 | * | * | 2.72 |
| Chemokine (C-X-C motif) ligand 13 | * | 4.61 | 5.99 | Expressed sequence AW112010 | 2.02 | 2.84 | 2.68 |
| Apoptosis inhibitor 6 | 2.38 | 4.77 | 5.99 | Tubulin, beta 3 | * | * | 2.68 |
| Glycoprotein 49 A | * | 3.04 | 5.69 | Tubulin, beta 5 | * | * | 2.67 |
| Cathepsin S | 2.35 | 4.24 | 5.38 | CREBBP/EP300 inhibitory protein 1 | * | 2.24 | 2.63 |
| Insulin-like growth factor binding protein 1 | * | * | 5.31 | Retinoic acid early transcript gamma | * | 1.69 | 2.63 |
| ADP-ribosyltransferase 2a | 3.37 | 5.47 | 5.07 | Carbon catabolite repression 4 homolog (*S. cerevisiae*) | * | 2.03 | 2.6 |
| Chemokine (C-X-C motif) ligand 9 | 2.16 | 17.3 | 5.05 | Paired-Ig-like receptor A1 | * | 3.24 | 2.6 |
| Procollagen, type IV, alpha 1 | * | 2.08 | 5.04 | Vascular cell adhesion molecule 1 | 4.06 | 4.64 | 2.59 |
| Immunoglobulin kappa chain variable 28 (V28) | * | * | 4.93 | Histocompatibility 2, class II, locus Mb1 | 2.95 | 5.94 | 2.59 |
| CD53 antigen | 1.84 | 3.82 | 4.92 | Histocompatibility 2, class II antigen E beta | 2.44 | 5.06 | 2.53 |
| Fc receptor, IgE, high affinity I, gamma polypeptide | * | 5.82 | 4.79 | Transporter 2, ATP-binding cassette, subfamily B (MDR/TAP) | 1.76 | 3.1 | 2.52 |
| Phospholipase A2 group VII (platelet-activating factor acetylhydrolase, plasma) | * | 4.02 | 4.71 | Orosomucoid 2 | * | 1.94 | 2.52 |
| | | | | Protamine 2 | 2.08 | * | 2.52 |
| | | | | Solute carrier family 4 (anion exchanger), member 4 | * | * | 2.49 |
| Chemokine (C-C) receptor 5 | * | 5.33 | 4.7 | Glutathione S-transferase, mu 2 | * | 2.3 | 2.48 |
| Complement component 1, q subcomponent, beta polypeptide | 1.91 | 4.6 | 4.69 | Cystatin B | * | 2.96 | 2.48 |
| Proteosome (prosome, macropain) subunit, beta type 8 (large multifunctional protease 7) | 3.7 | 5.93 | 4.59 | Cluster Incl U38967:Prothymosin beta | 1.56 | 2.88 | 2.48 |
| | | | | Reticulon 4 | 1.9 | 2.88 | 2.48 |
| | | | | Cytochrome b-245, alpha polypeptide | 1.53 | 3.04 | 2.47 |
| Complement component 1, q subcomponent, alpha polypeptide | 1.81 | 4.33 | 4.09 | Lipoprotein lipase | * | * | 2.44 |
| | | | | Intercellular adhesion molecule | * | 2.19 | 2.44 |
| Expressed sequence AU046135 | * | 2.88 | 3.82 | IQ motif containing GTPase activating protein 1 | * | 2.11 | 2.42 |
| Glycoprotein 49 B | * | * | 3.81 | | | | |
| Lysozyme | * | 5.82 | 3.79 | Amyloid beta (A4) precursor protein-binding, family B, member 1 interacting protein | * | 2.52 | 2.4 |
| Leukocyte specific transcript 1 | 1.68 | 4.54 | 3.78 | | | | |
| Complement component 1, q subcomponent, c polypeptide | 1.79 | 4.15 | 3.71 | Lymphocyte antigen 6 complex, locus E | 2.01 | 2.92 | 2.36 |
| | | | | Myristoylated alanine rich protein kinase C substrate | * | 1.91 | 2.34 |
| Cytochrome P450, 2b9, phenobarbitol inducible, type a | * | * | 3.62 | | | | |
| | | | | Histocompatibility 2, D region locus 1 | 1.73 | 2.64 | 2.31 |
| Serum amyloid A 3 | 2.21 | 15.37 | 3.6 | Fibrinogen-like protein 2 | 2.21 | 4.3 | 2.31 |
| H19 fetal liver mRNA | * | * | 3.56 | Lipoprotein lipase | * | * | 2.31 |
| Proteoglycan, secretory granule | * | 3.02 | 3.52 | Intracisternal A particles | * | 1.95 | 2.3 |
| Protein tyrosine phosphatase, nonreceptor type substrate 1 | * | 3.43 | 3.51 | TAP binding protein | 1.64 | 3.42 | 2.3 |
| | | | | MARCKS-like protein | * | 1.96 | 2.28 |
| Cytochrome P450, 2b13, phenobarbitol inducible, type c | * | * | 3.46 | Lipopolysaccharide binding protein | 1.71 | 2 | 2.27 |
| | | | | Circadian locomoter output cycles kaput | * | * | 2.27 |
| Serum amyloid A 2 | 5.14 | 2.22 | 3.29 | Eukaryotic translation initiation factor 1A | * | * | 2.26 |
| ESTs, Moderately similar to hypothetical protein FLJ11127 (Homo sapiens) (H. sapiens) | * | 3.54 | 3.28 | Interferon gamma-induced GTPase | 2.86 | 3.97 | 2.26 |
| | | | | Mitogen activated protein kinase kinase kinase 1 | * | * | 2.24 |
| Mus musculus, Similar to hypothetical protein FLJ20509, clone IMAGE:3489119, mRNA, partial cds | * | * | 3.27 | Ribosomal protein L7 | * | * | 2.23 |
| | | | | Secreted phosphoprotein 1 | * | * | 2.21 |
| | | | | Chloride intracellular channel 1 | * | 2.56 | 2.2 |
| ESTs, Weakly similar to RIKEN cDNA 0610011E17 (Mus musculus) (M. musulus) | * | * | 3.21 | Decorin | * | * | 2.17 |
| | | | | Annexin A1 | * | 1.98 | 2.16 |
| Histocompatibility 2, T region locus 17 | 2.11 | 2.85 | 3.19 | Expressed sequence AW547365 | * | * | 2.16 |
| CD52 antigen | 2 | 4.71 | 3.17 | Transporter 1, ATP-binding cassette, subfamily B (MDR/TAP) | 1.84 | 2.99 | 2.15 |
| Lectin, galactose binding, soluble 3 | * | 5.28 | 3.14 | | | | |
| TAP binding protein | 1.64 | 3.42 | 3.14 | Long chain fatty acyl elongase | −1.46 | * | 2.14 |
| Signal transducer and activator of transcription 1 | 2.57 | 5.75 | 3.11 | Acidic (leucine-rich) nuclear phosphoprotein 32 family, member A | * | * | 2.14 |
| Proteosome (prosome, macropain) subunit, beta type 9 (large multifunctional protease 2) | 3.77 | 6.28 | 3.1 | Lymphocyte antigen 86 | 1.58 | 2.39 | 2.13 |
| | | | | CD9 antigen | * | 1.93 | 2.12 |
| | | | | ADP-ribosylation-like factor 6 interacting protein 5 | * | * | 2.1 |
| Chemokine (C-X-C motif) ligand 1 | * | 4 | 3.1 | | | | |
| Cluster Incl M17790:Serum amyloid A pseudogene/cds = (0,251)/gb = M17790/gi = 200920/ug = Mm.56949/len = 252 | 4.22 | 13.87 | 3.06 | Polymerase (DNA directed), gamma | * | * | 2.1 |
| | | | | Hypothetical protein MGC47434 | * | * | 2.08 |
| | | | | Properdin factor, complement | 1.42 | 2.92 | 2.07 |
| Macrophage receptor with collagenous structure | 6.49 | * | 3 | B-cell translocation gene 1, anti-proliferative | * | * | 2.06 |
| | | | | Erythroid differentiation regulator | * | * | 2.06 |
| C-type (calcium-dependent, carbohydrate recognition domain) lectin, superfamily member 13 | 1.43 | * | 2.99 | Tubulin, alpha 6 | * | * | 2.06 |
| | | | | Annexin A5 | * | 2.39 | 2.03 |
| | | | | Guanylate nucleotide binding protein 3 | 3.03 | 6.67 | 2.03 |
| RIKEN cDNA 2310057H16 gene | * | * | 2.96 | Chemokine (C-X-C motif) ligand 1 | * | 4 | 2.02 |
| Lymphocyte antigen 6 complex, locus A | 6.45 | 5.38 | 2.95 | Flavin containing monooxygenase 3 | * | * | 2 |
| Histocompatibility 2, T region locus 10 | 2.14 | 2.99 | 2.95 | Dystroglycan 1 | * | * | 2 |

TABLE 2.—Genes with down-regulated transcription in the livers of *H. hepaticus*-infected male A/JCr mice with severe disease versus sham-infected controls (fold decrease).

| Gene | 3 months | 6 months | 12 months |
|---|---|---|---|
| Hydroxysteroid dehydrogenase-5, delta(5)-3-beta | −3.32 | −13.47 | −28 |
| Aminolevulinic acid synthase 1 | * | * | −5.45 |
| D site albumin promoter binding protein | * | * | −5.37 |
| Cytochrome P450, 7b1 | * | −2.09 | −4.68 |
| Thyroid hormone responsive SPOT14 homolog (Rattus) | * | * | −3.94 |
| Metallothionein 1 | +4.3 | +2.14 | −3.59 |
| Kidney expressed gene 1 | * | * | −3.57 |
| Cytochrome P450, 7b1 | * | * | −3.36 |
| RIKEN cDNA 2410041F14 gene | * | * | −2.99 |
| Epidermal growth factor receptor | * | * | −2.97 |
| Expressed sequence AI467657 | * | * | −2.88 |
| G0/G1 switch gene 2 | * | * | −2.83 |
| Homocysteine-inducible, endoplasmic reticulum stress-inducible, ubiquitin-like domain member 1 | * | * | −2.78 |
| Sialyltransferase 9 (CMP-NeuAc:lactosylceramide alpha-2,3-sialyltransferase) | +2.24 | * | −2.78 |
| Cluster Incl V00722:Mouse gene for beta-1-globin | * | * | −2.65 |
| Sulfotransferase-related protein SULT-X1 | * | * | −2.64 |
| 11–19 lysine-rich leukemia gene | * | −1.94 | −2.58 |
| Ubiquitin specific protease 2 | * | * | −2.56 |
| Serine (or cysteine) proteinase inhibitor, clade E, member 2 | * | * | −2.53 |
| Expressed sequence AI266885 | +1.51 | | −2.5 |
| Period homolog 2 (Drosophila) | * | * | −2.39 |
| Solute carrier family 10 (sodium/bile acid cotransporter family), member 1 | * | * | −2.36 |
| MAP kinase-interacting serine/threonine kinase 2 | * | * | −2.35 |
| Glucose-6-phosphatase, transport protein 1 | * | * | −2.24 |
| Expressed sequence C77405 | * | * | −2.24 |
| Amiloride-sensitive sodium channel | * | * | −2.23 |
| Hemoglobin, beta adult major chain | * | * | −2.21 |
| Angiopoietin-like 4 | * | * | −2.19 |
| Pre-B-cell colony-enhancing factor | +1.51 | +1.58 | −2.18 |
| P450 (cytochrome) oxidoreductase | * | * | −2.17 |
| Peroxisomal delta3, delta2-enoyl-Coenzyme A isomerase | * | −1.61 | −2.14 |
| DnaJ (Hsp40) homolog, subfamily A, member 1 | * | * | −2.11 |
| Epidermal growth factor receptor | * | * | −2.1 |
| BCL2/adenovirus E1B 19 kDa-interacting protein 1, NIP3 | * | * | −2.03 |
| Elastase 1, pancreatic | −1.43 | −1.85 | −2.01 |
| Colony stimulating factor 2 receptor, beta 1, low-affinity (granulocyte-macrophage) | * | * | −2.01 |
| Interleukin 1 receptor, type I | +1.82 | * | −2 |

persisted throughout the 12-month experimental period, while other clusters arose at 6 months or at 12-months. (Gene categories and protein domains are standardized vocabulary defined by the Gene Ontology consortium (http://www.geneontology.org)). A Venn diagram (Figure 1) presents this scenario in a simplified form for illustrative purposes. Tables 3 and 4 represent the 3-month, 6-month, and 12-month time points. Group 1 represents all the genes, gene categories, and protein domains exhibited at 3, 6, and 12 months. It contains many signatures of an acute-phase response that persisted over 12 months. Group 2 represents most, but not all, of the Group 1 clusters, plus new genes, gene categories, and protein domains at 6 months. Group 2 encompasses biological processes of both the acute immune response of Group 1, plus a more mature or chronic immune response. Tables 5 and 6 lists genes within the Gene Ontology category corresponding to the immune response and the pathogen response. Group 3 again intersects most of Group 1 and Group 2, but new entries indicate tubulin, microtubule, cytoskeletal, peroxisome, scavenger, and structural and proliferative activity. Table 7 lists specific genes in the Gene Ontology categories of cell proliferation, growth, and death. Genes expressed during fetal development or imprinted genes are also evident in Group 3.

TABLE 3.—Gene ontology clusters.

| Gene categories at 3, 6, and 12 months | |
|---|---|
| Endoplasmic reticulum (3, 6, 12) | Mitochondrion (3, 12) |
| Cytosol (3, 6, 12) | GTPase (3) |
| Defense response (3, 6, 12) | Microsome (3) |
| Acute-phase response (3, 6, 12) | Chemokine activity (6, 12) |
| Immune response (3, 6, 12) | Electron transport (6, 12) |
| Cell surface (3, 6, 12) | Integral to plasma membrane (6, 12) |
| Membrane (3, 6, 12) | Lipid transporter activity (6, 12) |
| Integral to membrane (3, 6, 12) | Inflammatory response (6) |
| Antigen presentation, endogenous antigen (3, 6, 12) | Extracellular (6) |
| Antigen presentation, exogenous antigen (3, 6, 12) | Catalytic activity (6) |
| Antigen processing, endogenous antigen via MHC class I (3, 6, 12) | GTPase activity (12) |
| Antigen processing, exogenous antigen via MHC class II (3, 6, 12) | GTP binding (12) |
| MHC Class I receptor activity (3, 6, 12) | Microtubule (12) |
| MHC class II receptor activity (3, 6, 12) | Carboxylic ester hydrolase activity (12) |
| Extracellular space (3, 6, 12) | Microtubule-based process (12) |
| Lysosome (3, 6, 12) | Microtubule-based movement (12) |
| Plasma membrane (3, 6, 12) | Serine esterase activity (12) |
| Monooxygenase activity (3, 6, 12) | Peroxisome organization and biogenesis (12) |
| Oxidoreductase activity (3, 6, 12) | Scavenger receptor activity (12) |
| Complement activation (3, 6) | Structural molecule activity (12) |
| External side of plasma membrane (3, 6) | Structural constituent of cytoskeleton (12) |
| Antigen presentation, exogenous antigen via MHC class II (3, 6) | Signal transduction (12) |
| Complement activation /classical pathway (3, 6) | Transporter activity (12) |
| Peptidase activity (3, 6) | Structural constituent of ribosome (12) |

### *Genes Up-Regulated and Down-Regulated*

Age matched *H. hepaticus* infected mice with progressive disease, exhibiting altered gene expression as defined by dChip software with default settings (Li and Wong, 2001b), yielded 188 differentially expressed genes at 3 months, 401 at 6 months, and 678 at 12 months. Immune response genes, including the acute phase response,

TABLE 4.—Protein domain clusters.

| Protein domains at 3, 6, and 12 months |
|---|
| ATP/GTP-binding site motif A (P-loop) (3, 6, 12) |
| Immunoglobulin/major histocompatibility complex (3, 6, 12) |
| Immunoglobulin-like (3, 6, 12) |
| Serum amyloid A protein (6) |
| Small chemokine, interleukin 8-like (6) |
| Immunoglobulin, C-type (6, 12) |
| Small chemokine, C-X-C subfamily (6, 12) |
| Tubulin family (12) |
| Tyrosine protein kinase, active site (12) |

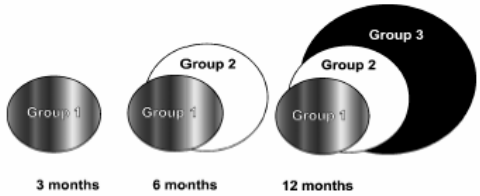


FIGURE 1.—Simplified Venn diagram representation of clusters of hepatic differential gene expression, gene categories, and protein domains arising during the course of the *H. hepaticus* experimental infection of male A/JCr mice. Group 1 figuratively represents the acute phase of lobular hepatitis observed histologically throughout the course of the experiment due to persistent infection. Group 2 intersects Group 1 and additionally represents the maturation of inflammatory response and the portal hepatitis first recognized at 6 months that became progressively more severe. Group 3 intersects Group 1 and Group 2 and additionally represents tubulin, microtuble, scavenger, peroxisome, and structural gene categories, plus genes suggestive of hepatic preneoplasia.

histocompatibility, macrophage, T and B cell development, and complement represented most of the up-regulated genes at 3 months (Table 1). These genes continued to be up-regulated throughout the 12-month experiment. The acute phase lipocalin family and serum amyloid family are represented in this group. At 6 months, there was a further increase in expression of these genes plus new differential expression levels of genes suggestive of further inflammatory response and repair including chemokine ligands (such as lymphocyte attracting chemokines Cxcl9 and Cxc13), chemokine receptors of the CC motif, ADAM family members, lysozyme, procollagen, cellular retinol binding protein (Lepreux et al., 2004), and detoxification enzymes.

At 12 months post *H. hepaticus* infection, new genes up-regulated represented more structurally related genes and more detoxification genes including tubulin, growth factors, carriers, and cytochrome P450 genes. Genes historically linked to neoplasia and up-regulated in the 12 month group included H19, intestinal trefoil factor 3, the ras family, and Jun-B. Up-regulated genes predominated over down-regulated genes at all time points for *H. hepaticus* infected A/J mice with hepatic lesions. Interestingly, the vast majority of down-regulated genes were at 12 months (Table 2). Down-regulated genes at 12 months were associated with steroid hormones, heme metabolism, and sodium/bile acid cotransport (Fraser et al., 2003; Jung et al., 2004). There was a consistent segregation of the most highly up-regulated and select down-regulated genes for *H. hepaticus*-infected mice with lesions. Genes up-regulated or down-regulated at 12 months, along with their corresponding values at 3 and 6 months are exhibited in Tables 1 and 2, respectively.

### *Gene Ontology Clusters*

Gene ontology ⟨www.geneontology.org⟩ describes gene products in 3 structured controlled vocabularies related to biological process, cellular components, and molecular functions. Microarray analysis generated multiple biological process ontology clusters for hepatic lesions of *H. hepaticus* infected A/JCr mice at all 3 time points (Table 3). There were several biological processes involved over the entire 12-month time period pertaining to an active infection including gene products associated with the defense response, immune response, acute phase response, antigen presentation and processing, MHC receptor activity, lysosomes, and others represented in Table 3. At 6 months post-*H. hepaticus* infection, the 3-month inflammatory biological processes were maintained and a chemokine activity cluster was added. Gene products associated with electron transport and lipid transport demonstrated increased activity (Table 3). At 12 months, new clusters of biological processes indicated gene products involved with structural change, increased signal transduction, and peroxisome organization (Table 3).

TABLE 5.—Gene ontology category: Immune response. Genes with up-regulated transcription in the livers of *H. hepaticus*-infected male A/JCr mice with severe disease versus sham-infected age-matched controls (fold increase).

| Symbol | Gene | 3 months | 6 months | 12 months |
|---|---|---|---|---|
| Ii | Ia-associated invariant chain | 3.18 | 11.9 | 15.06 |
| H2-Aa | Histocompatibility 2, class II antigen A, alpha | 3.75 | 13.98 | 10.5 |
| Cxcl13 | Chemokine (C-X-C motif) ligand 13 | * | 4.61 | 5.99 |
| Cxcl9 | Chemokine (C-X-C motif) ligand 9 | 2.16 | 17.3 | 5.05 |
| Igk-V8 | Immunoglobulin kappa chain variable 8 (V8) | * | * | 4.93 |
| Pla2g7 | Phospholipase A2, group VII (platelet-activating factor acetylhydrolase, plasma) | * | 4.02 | 4.71 |
| C1qb | Complement component 1, q subcomponent, beta polypeptide | 1.91 | 4.6 | 4.69 |
| Psmb8 | Proteosome (prosome, macropain) subunit, beta type 8 (large multifunctional protease 7) | 3.7 | 5.93 | 4.59 |
| C1qa | Complement component 1, q subcomponent, alpha polypeptide | 1.81 | 4.33 | 4.1 |
| C1qg | Complement component 1, q subcomponent, gamma polypeptide | 1.79 | 4.15 | 3.71 |
| Saa3 | Serum amyloid A 3 | 2.21 | 15.37 | 3.6 |
| Saa2 | Serum amyloid A 2 | 5.14 | 12.87 | 3.29 |
| Cxcl1 | Chemokine (C-X-C motif) ligand 1 | * | 4 | 3.1 |
| Psmb9 | Proteosome (prosome, macropain) subunit, beta type 9 (large multifunctional protease 2) | 3.77 | 6.28 | 3.1 |
| H2-T10 | Histocompatibility 2, T region locus 10 | 2.14 | 2.99 | 2.95 |
| Gbp2 | Guanylate nucleotide binding protein 2 | 2.55 | 7.62 | 2.91 |
| H2-DMb1 | Histocompatibility 2, class II, locus Mb1 | 2.95 | 5.94 | 2.59 |
| H2-Eb1 | Histocompatibility 2, class II antigen E beta | 2.44 | 5.06 | 2.53 |
| Tap2 | Transporter 2, ATP-binding cassette, subfamily B (MDR/TAP) | 1.76 | 3.1 | 2.53 |
| Orm2 | Orosomucoid 2 | * | 2.92 | 2.52 |
| H2-D1 | Histocompatibility 2, D region locus 1 | 1.73 | 2.64 | 2.3 |
| Tap1 | Transporter 1, ATP-binding cassette, subfamily B (MDR/TAP) | 1.84 | 2.99 | 2.16 |
| Ly86 | Lymphocyte antigen 86 | 1.58 | 2.39 | 2.13 |
| Pfc | Properdin factor, complement | 1.42 | 2.92 | 2.07 |
| Il1rn | Interleukin 1 receptor antagonist | * | * | 2.05 |
| Gbp3 | Guanylate nucleotide binding protein 3 | 3.03 | 6.67 | 2.03 |

TABLE 6.—Gene ontology category: Pathogen response. Genes with up and down regulated transcription in the livers of *H. hepaticus*-infected male A/JCr mice with severe disease versus sham-infected controls (fold increase/decrease).

| Symbol | Gene | 3 months | 6 months | 12 months |
|---|---|---|---|---|
| Cxcl13 | Chemokine (C-X-C motif) ligand 13 | * | 4.61 | 5.99 |
| Cxcl9 | Chemokine (C-X-C motif) ligand 9 | 2.16 | 17.3 | 5.05 |
| Igk-V8 | Immunoglobulin kappa chain variable 8 (V8) | * | * | 4.93 |
| Pla2g7 | Phospholipase A2, group VII (platelet-activating factor acetylhydrolase, plasma) | * | 4.02 | 4.71 |
| C1qb | Complement component 1, q subcomponent, beta polypeptide | 1.91 | 4.6 | 4.69 |
| C1qa | Complement component 1, q subcomponent, alpha polypeptide | 1.81 | 4.33 | 4.1 |
| C1qg | Complement component 1, q subcomponent, gamma polypeptide | 1.79 | 4.15 | 3.71 |
| Saa3 | Serum amyloid A 3 | 2.21 | 15.37 | 3.6 |
| Saa2 | Serum amyloid A 2 | 5.14 | 12.87 | 3.29 |
| Cxcl1 | Chemokine (C-X-C motif) ligand 1 | * | 4 | 3.1 |
| Orm2 | Orosomucoid 2 | * | 2.92 | 2.52 |
| Ly86 | Lymphocyte antigen 86 | 1.58 | 2.39 | 2.13 |
| Dnaja1 | DnaJ (Hsp40) homolog, subfamily A, member 1 | * | * | −2.11 |
| Herpud1 | Homocysteine-inducible, endoplasmic reticulum stress-inducible, ubiquitin-like domain member 1 | * | * | −2.78 |

### *Protein Domain Clusters*

Protein domain clusters produced via microarray analysis indicated regulatory proteins and systems involved during *H. hepaticus* pathogenesis (Table 4). These domains often mediate interactions of regulatory protein construction or have enzymatic activity (Pawson and Nash, 2003). As with the gene ontology clusters, some protein domain clusters were involved throughout the 12-month experimental period and were immunoglobulin related (Table 4). The immunoglobulin C-type protein domain involvement began at 6 months, as did chemokine and serum amyloid protein interactions (Table 4). At 12 months, structural activity promoted by tubulin domains was evident (Table 4).

### *Immune Response Gene Expression*

The individual genes members of the immune response biological process and their differential response at 3, 6, and 12 months are presented in Table 5. Four hundred and sixteen genes are members of this gene ontology biological process category. Table 5 genes include individual histocompatibility, chemokine, serum amyloid, and complement, and confirm the gene category clusters and protein domain clusters results.

### *Pathogen Response Gene Expression*

The Gene Ontology pathogen response biological process category consists of 241 genes and is a subcategory of the immune response. The individual genes and their differential response at 3, 6, and 12 months are presented in Table 6. This pattern of individual chemokine, immunoglobulin, acute phase, and complement genes change expression putatively due to *H. hepaticus* infection.

TABLE 7.—Gene ontology category: Cell proliferation, growth, and death.

| Symbol | Gene | 3 months | 6 months | 12 months |
|---|---|---|---|---|
| Cxcl1 | Chemokine (C-X-C motif) ligand 1 | * | 4 | 3.1 |
| Tgfa | Transforming growth factor alpha | * | * | 2.9 |
| Prm2 | Protamine 2 | 2.08 | −1.62 | 2.52 |
| Polg | Polymerase (DNA directed), gamma | * | * | 2.1 |
| Btg1 | B-cell translocation gene 1, anti-proliferative | * | * | 2.06 |
| Cdkn1a | Cyclin-dependent kinase inhibitor 1A (P21) | 2.95 | 2.96 | 1.95 |
| Nfkbia | Nuclear factor of kappa light chain gene enhancer in B-cells inhibitor, alpha | * | 1.39 | 1.92 |
| Ahr | Aryl-hydrocarbon receptor | * | * | 1.9 |
| Kras2 | Kirsten rat sarcoma oncogene 2, expressed | * | * | 1.69 |
| Macf1 | Microtubule-actin cross-linking factor 1 | * | * | 1.54 |
| Ccnd1 | Cyclin D1 | 1.69 | 3.21 | 1.53 |
| Ifnar2 | Interferon (alpha and beta) receptor 2 | * | * | 1.51 |
| Gas2 | Growth arrest specific 2 | * | * | 1.46 |
| Stat6 | Signal transducer and activator of transcription 6 | * | * | 1.44 |
| Junb | Jun-B oncogene | * | * | 1.3 |
| Cul4a | Cullin 4A | * | * | −1.42 |
| Gspt2 | G1 to phase transition 2 | * | * | −1.45 |
| Nfix | Nuclear factor I/X | * | * | −1.62 |
| Ches1 | Checkpoint suppressor 1 | * | * | −1.67 |
| Fgf1 | Fibroblast growth factor 1 | * | −1.71 | −1.71 |
| G0s2 | G0/G1 switch gene 2 | * | * | −2.83 |
| Egfr | Epidermal growth factor receptor | * | * | −2.97 |

* No differential expression.

Genes with up and down regulated transcription in the livers of of *H. hepaticus*-infected male A/JCr mice with severe disease versus sham-infected controls (fold increase/decrease).

### *Cell Proliferation, Growth, and Death*

Gene ontology categories suggestive of preneoplasia were investigated and included cell proliferation, cell growth, and cell death (Table 7). Some of the genes, as would be expected, suggest inflammatory cell turnover. Other genes do not necessarily fit into the inflammatory category including two oncogenes, the Kirsten rat sarcoma oncogene 2 (K-ras) and the Jun-B oncogene, that were slightly up-regulated 12 months postinfection.

### *Microarray Model Validation*

Microarray results were tightly correlated ($r > 0.99$ for controls and $r > 0.97$ for mice with lesions) between biological replicates (individual mouse liver per array) (Figure 2A). There was a moderate correlation between infected male mice that did not develop significant disease and uninfected controls (Figure 2C). In contrast, the correlation lessened substantially ($r < 0.83$) between infected mice that developed severe disease and uninfected controls (Figure 2D). These results confirm that histologic assessment of lesion severity is reflected by global gene expression profile alterations, represented by all the genes not on the linear scatterplot as seen in Figure 2D. These genes have differential expression as compared to the controls in Figure 2A.

### *Differential Gene Expression for Aging*

The experimental design enabled comparisons of transcription profiles due to aging. Aging control mice yielded

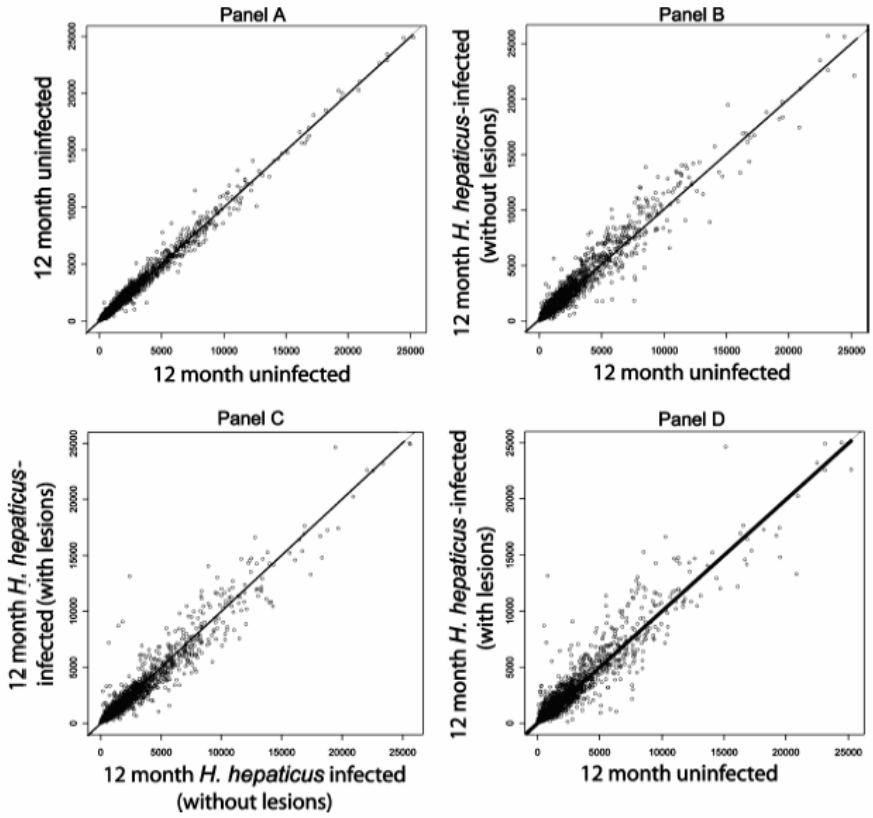


FIGURE 2.—Scatterplots highlighting variable degrees of correlation between microarray results from different groups of male A/JCr mice at 12 months. (a) High correlation between biological replicates ($r > 0.99$). (b) *H. hepaticus*-infected mice that did not develop disease are better correlated with sham-infected controls ($r > 0.97$). (c) than with infected diseased mice. (d) Marked discorrelation between infected mice with disease and sham-infected controls ($r > 0.79$).

402 differentially expressed genes at 6 months versus 3 months, 675 at 12 months versus 3 months, and 437 at 12 months versus 6 months. Although a large number of genes were associated with aging, the magnitude of hepatic expression differences was small ($-6$ to $+10$). Additional aging results are presented under linear discriminant analysis and principal component analysis.

### *Hierarchical Clustering*

Hierarchical clustering allowed age-matched A/JCr mice pairs with lesions to be differentiated from controls. The dChip option of combined hierarchical clustering of mouse microarray samples and genes produced very similar "heatmap" patterns between mouse microarray sample pairs within 6 groups, with each group displaying a different pattern (Figure 3). The increasing intensity of red (green) in the heatmap indicates an increasing (decreasing) expression level. The mice groups are labeled at the top of each column of the heatmap and consisted of the following pairs of arrays: (1) 3-month controls (3u1, 3u2) (u: uninfected), (2) 6-month controls (6u1, 6u2) (3) 12-month controls (12u1, 12u2), (4) 3 month *H. hepaticus*-infected A/J mice with lesions (3L1, 3L2) (L: lesions), (5) 6 month *H. hepaticus*-infected A/J mice with lesions (6L1, 6L2), and (6) 12 month *H. hepaticus*-infected A/J mice with lesions (12L1, 12L2) (Figure 3).

### *Linear Discriminant Analysis and Principal Component Analysis*

Linear discriminant analysis also differentiated between controls and *H. hepaticus*-infected A/J mice with hepatic

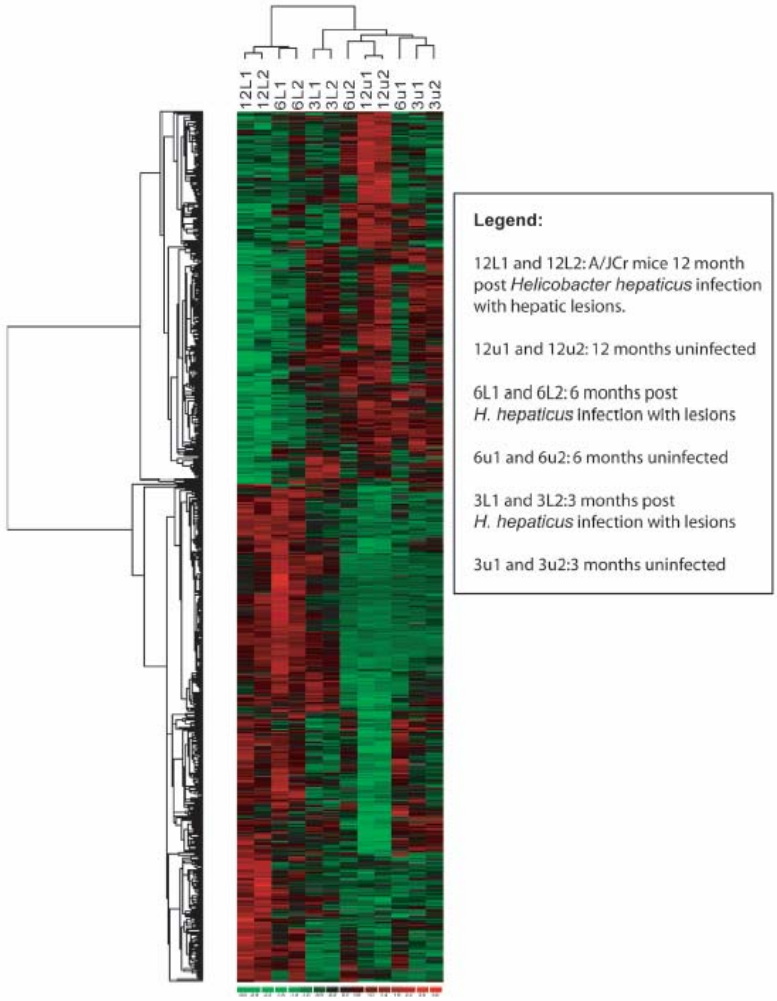


FIGURE 3.—Hierarchical clustering and two dimensional dendrogram. Columns represent individual A/JCr mice and rows represent genes. Every 2 columns represent the same group with a total of 6 groups. Columns exhibiting similar patterns are representative of groups of mice based on age and lesion status. The A/JCr mice illustrated are *H. hepaticus* infected with lesions and age-matched uninfected controls.

lesions (Figure 4). The control mice and the mice with hepatic lesions occupied opposite sides of the plot. Principal component analysis provided even more powerful classification of A/JCr mice groups. This algorithm produced regions of different ages for controls and for age groups of ***H. hepaticus***-infected A/J mice with lesions (Figure 5). However, these clear demarcations occurred only when the analysis omitted the transcription profile data for infected mice without lesions. Therefore, the LDA and PCA did not clearly differentiate the infection status of the mice when the livers were histologically normal at 3 and 6 months, but did indicate differences at 12 months postinfection (data not shown).

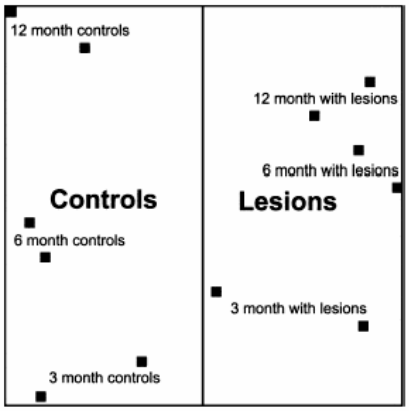


FIGURE 4.—Linear discriminant analysis demonstrating differentiation of the 6 groups by lesion status. Each box represents an A/JCr mouse. Note the mice on different sides of the plot. The A/JCr mice illustrated are *H. hepaticus* infected with lesions and age-matched controls.

### *Microarray Result Verification by Quantitative Real-Time RT-PCR*

The Assay on Demand results validated the Affymetrix microarray values except for 2 data points where fold changes were less than 2 for both methods (Figure 6).

## DISCUSSION

Microarray analysis of the livers of *H. hepaticus*-infected A/JCr mice demonstrated reproducible changes in global transcription profiles at 3, 6, and 12 months that were indicative of the progressive liver disease illustrated by histopathology. The progressive severity of hepatitis and dysplasia in infected mice was associated with an increasing number of differentially expressed genes and a specific transcription profile. The gene expression signature of age-matched controls and age-matched infected mice with lesions could be differentiated from each other utilizing hierarchical clustering and principal component analysis. Whether the hepatic transcription profile can be used to identify the age at infection, the time postinfection, and the temporal course of the molecular pathogenesis will require additional study.


FIGURE 5.—Principal component analysis demonstrating differentiation of the groups by age and lesion status. Each box represents an A/JCr mouse. Note the mice are clustered in separate regions. The A/JCr mice illustrated are *H. hepaticus* infected with lesions and age-matched controls.

The gene expression signature complements histopathology and PCR techniques and aids in diagnosis and prognosis for this experimental infection.

Whether another strain of *H. hepaticus*, a different liver pathogen, or other liver insult yields a unique gene expression signature over time in various strains of mice is under investigation. Recent studies indicate a specific gene signature for virally induced HCC (Iizuka et al., 2004). Many of the same differentially expressed genes in mice infected with *H. hepaticus* have also been documented in other models of murine hepatic injury and hepatic tumor promotion (Nyska et al., 1997; Graveel et al., 2001; Meyer et al., 2003). Some studies suggest the transcription profile of a small set of highly up-regulated or down-regulated genes are indicative of a particular disease while other studies indicate even very modest changes in a larger set of genes and pathways are suggestive of a specific disease (Etzioni et al., 2003; Mootha et al., 2003a).

### *Genes Associated with Neoplasia and Proliferation*

Two putative tumor markers, H19 fetal liver mRNA and intestinal trefoil factor 3 (Table 1), were increasingly up-regulated over time in mice with progressive hepatocellular dysplasia. Despite its name, the endproduct of the H19 gene is considered a nonmessenger polyadenylated RNA molecule (Brannan et al., 1990). H19 has putative regulatory roles in normal development, hepatocyte proliferation, and in oncogenesis (Kaplan et al., 2003; Yamamoto et al., 2004). H19 shares the nonprotein coding property with a rapidly growing number of novel transcripts, and recent experiments indicate that as much as an order of magnitude more chromosomal DNA is transcribed than accounted for by currently predicted and characterized exons (Kapranov et al., 2002). H19 is an imprinted gene with maternal allele expression. Loss of imprinting is a recognized human cancer risk, including genes H19, insulin-like growth factor 2 (Igf2), and cyclin dependent kinase inhibitor 1C (p57, KIP, CDK1NC) (Brannan and Bartolomei, 1999; Vernucci et al., 2000; Kaplan et al., 2003). H19 and Igf2 are reciprocally imprinted, with Igf2 being expressed from the paternal allele (Vernucci et al., 2000).

Igf2 is an anti-apoptotic factor associated with hepatocarcinogenesis, and is putatively activated and regulated by H19 (Vernucci et al., 2000). Although Igf2 up-regulation was not observed at 12 months by microarray analysis, there was nearly 2-fold down-regulation of the Igf2 receptor (Table 2), and an inverse relationship has been observed between epidermal growth factor and its cognate

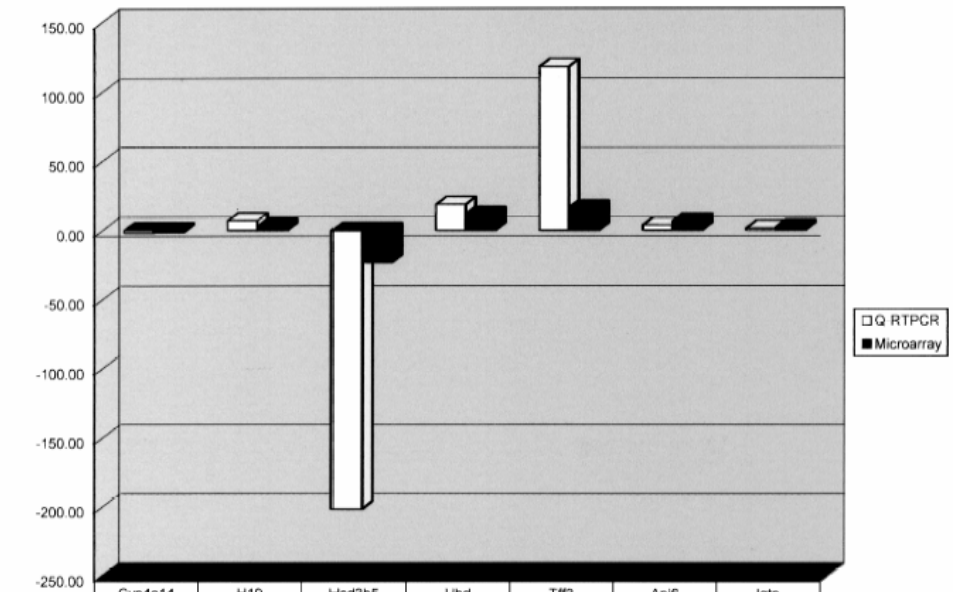


| | Cyp4a14 | H19 | Hsd3b5 | Ubd | Tff3 | Api6 | Igtp |
|---|---|---|---|---|---|---|---|
| Q-RTPCR | -1.78 | 6.99 | -201.55 | 18.70 | 118.19 | 3.71 | 1.26 |
| Microarray | -1.28 | 3.14 | -23.25 | 11.58 | 16.28 | 6.53 | 2.05 |

FIGURE 6.—Microarray (Affymetrix) result validation with RT-PCR (Assay on Demand). Rank invariant normalization to a baseline microarray was used for the microarray results (dChip). Normalization to GAPDH is used for the quantitative real-time RT-PCR.

receptor in mice infected with *H. hepaticus* (Ramljak et al., 1998). Insulin-like growth factor 1 (Igf1) is an acute phase protein that is decreased in plasma serum levels during systemic responses to inflammation (Gabay and Kushner, 1999). Insulin-like growth factor binding protein 1 (Igfbp1) (Table 1) was highly up-regulated in *H. hepaticus*-infected A/JCr mice at 12 months with liver lesions and foci of altered hepatocytes.

Igfbp1 binds both Igf1 and Igf2 with high affinity. Igfbp1 putatively functions as a critical survival factor in the liver by suppressing the level and activation of specific proapoptotic factors via its regulation of integrin-mediated signaling (Leu et al., 2003). Igf1 is important in fetal growth and development (along with Igf2, the imprinted gene described previously). Igf1 is expressed predominantly in the liver, and targeted gene knockout results in embryonic lethality in mice (Le Roith et al., 1999; Yakar et al., 1999; Scharf et al., 2001). Intestinal trefoil factor 3 is associated with enterohepatic inflammation, gastric cancer, colon cancer, pancreatic cancer, and breast cancer (Al-azzeh et al., 2002; Kimura et al., 2002; Leung et al., 2002; Katoh, 2003; Khan et al., 2003; Rodrigues et al., 2003). This factor promotes epithelial cell migration and mucosal restitution during inflammation, and is differentially expressed in primary biliary cirrhosis (Kimura et al., 2002).

Cyclin D1 is overexpressed in many human and murine tumors (Hinds et al., 1994; Hinds and Weinberg, 1994; Parker et al., 2003). Cyclin D1 (Ccnd1) affects G1 and was slightly up-regulated. Cyclin-dependent kinase inhibitor 1A (p21) (Cdkn1a) was also slightly up-regulated (Table 7). It maintains the G2 checkpoint and, after DNA damage, can arrest cells in G2. Cytolethal distending toxin (CDT) in several *Helicobacter* spp. including *H. hepaticus* causes cell cycle arrest in the G2/M phase resulting in cell distension in selected cell culture lines (Young et al., 2000; Taylor et al., 2003). An isogenic mutant of *H. hepaticus* lacking CDT activity when inoculated into C57BL/6 IL-$10^{-/-}$ produced less inflammatory bowel disease (IBD) when compared to its wild-type counterpart (Young et al., 2004). In another isogenic CDT mutant study, wild-type *Campylobacter jejuni* infected NF-$\kappa$B deficient mice exhibited a moderately severe gastritis and proximal duodenitis at 4 months postinfection while *C. jejuni* CDT mutant infected NF-$\kappa$B deficient mice were consistently cleared of *C. jejuni* at 4 months postinfection. These results suggest CDT plays a role in inflammation and potentially participates in avoiding the immune response (Fox et al., 2004).

In addition to CDT's possible role in inflammation, dChip analysis indicates cytoskeletal organization effects by *H. hepaticus*, possibly in part due to CDT activity in the liver.

Protein domain clusters associated with tubulin (Table 3) and gene category clusters associated with structural constituents of the cytoskeleton, structural molecule movement, and microtubules are evident at 12 months (Table 4). CDT reportedly damages DNA via its CdtB subunit, a homologue of mammalian type I Dnase. CDT has putative nuclear localization signals and may induce apoptosis through activation of caspase 2 and caspase 7 (Lara-Tejero and Galan, 2000; McSweeney and Dreyfus, 2004; Ohara et al., 2004). Caspase 3 and caspase 2 were slightly upregulated in this study, but caspase 7 was not.

Two oncogenes, K-ras and Jun-B, were slightly upregulated at 12 months post *H. hepaticus* infection. The ras family, K-ras, N-ras, and H-ras are guanine nucleotide binding proteins involved in cell proliferation, differentiation, and survival (Chan et al., 2004). K-ras mediates cytokine signaling in formation of E-cadherin based adherens junctions in hepatocyte development (Matsui et al., 2002). Jun-B suppresses cell proliferation through its inhibition of activation protein transcription factor (AP-1), however overexpression of Jun-B putatively perpetuates undifferentiated cancers (Song et al., 2004). LPS from gram-negative bacteria induces AP-1, but there was no differential expression of any of the subunits of the AP-1 complex in this study. Mutations and increased expression in these genes have been reported in myeloproliferative disease, colon cancer, breast cancer, prostate cancer, and metastases to the liver (Matsui et al., 2002; Edwards et al., 2003; Frasor et al., 2003; Palmer et al., 2003; Chan et al., 2004; Selvamurugan et al., 2004; Song et al., 2004). Although K-ras mutations have been reported in chemically induced hepatocellular carcinoma in the A/J mouse (Bai et al., 2003), K-ras, H-ras, and N-ras mutations have not been reported in A/J mice infected with *H. hepaticus* (Diwan et al., 1997; Sipowicz et al., 1997b). These data, indicating that *H. hepaticus* is nongenotoxic, are further documentation that *H. hepaticus* is acting as a tumor promoter.

### *Genes Associated with Inflammation*

Chronic inflammation is a risk factor for cancer, and acute-phase proteins indicative of ongoing inflammation persisted at high levels over time in *H. hepaticus*-infected male mice with progressive disease (Gabay and Kushner, 1999; Rogers and Fox, 2004). One acute-phase protein, lipocalin 2 (Table 1), was prominently up-regulated in the liver as a result of *H. hepaticus* infection. Lipocalin 2 is highly expressed in hepatocellular carcinoma via genotoxic or peroxisomal mechanisms (Meyer et al., 2003) and the lipocalin family is expressed in other forms of cancer including pancreatic, colorectal, and ovarian (Bartsch and Tschesche, 1995; Nielsen et al., 1996; Furutani et al., 1998; Bratt, 2000). Lipocalin 2 (Lpn2, uterocalin, 24p3, NGAL, SIP24) was discovered as a secreted, inducible protein from BALB/c 3T3 cells (Nilsen-Hamilton et al., 1982) and later identified as a product of mouse 24p3 mRNA and as an acute-phase protein (Liu and Nilsen-Hamilton, 1995). Lipocalin 2 in the Gene Ontology system is considered a transporter. Reported roles of lipocalin 2 include mucosal immunity, epithelial development in the kidney, signaling, transport of non-transferrin-bound iron, chaperoning, apoptosis, retinol transport, prostaglandin synthesis, and male scent expression (Cavaggioni and Mucignat-Caretta, 2000; Xu and Venge, 2000; Devireddy et al., 2001; Tong et al., 2003; Yang et al., 2003). Other lipocalins, up-regulated in this study include orosomucoid and retinol-binding protein. Other acute-phase proteins were up-regulated in *H. hepaticus*-infected male A/JCr mice with severe disease. For example, serum amyloid A (Tables 4 and 5) is a hallmark indicator of active inflammation, and putatively activates neutrophils in addition to direct antimicrobial properties (Hatanaka et al., 2003; Ribeiro et al., 2003). Also up-regulated was properdin factor (Table 5), a member of the alternative complement pathway of the innate immune system which binds to microbial surfaces. Ceruloplasmin, a plasma metalloprotein, binds copper and is involved in transferrin peroxidation. Haptoglobin protects against microbial growth by binding hemoglobin and preventing microbial access to iron (Eaton et al., 1982). Hemopexin binds heme and transports it to the liver for iron recovery.

### *Genes Associated with Cytochrome P450*

As seen in other rodent and human studies of hepatic injury, *H. hepaticus* infection in male A/JCr resulted in altered expression of several members of the cytochrome P450 (CYP) family. At 3 months, CYP2c37, 4a10, and 4a14 were down-regulated (Table 2) while CYP2b10 was up-regulated (Table 1). At 6 months, CYP2c37, 4a10, 4a14, 51, and 7b1 were down-regulated (Table 2). At 12 months, the previously listed group remained down-regulated (Table 2) while CYP2b9, 2b10, and 2b13 were up-regulated (Table 1). Phenobarbital also up-regulates Cyp2b10 (Rivera-Rivera et al., 2003; Yoshinari et al., 2003). Phenobarbital promotes hepatic tumors initiated by compounds such as *N*-nitrosodiethylamine (NDMA) (Thirunavukkarasu and Sakthisekaran, 2003). This data is consistent with the hypothesis that *H. hepaticus* is a tumor promoter in the mouse liver initiated by NDMA (Diwan et al., 1997; Sipowicz et al., 1997b). Members of the cytochrome P450 family are integral to detoxification, and play key roles in steroid, lipid, and bile acid metabolism. Reactive oxygen species are postulated to contribute to DNA damage and tumorigenesis, and electrophilic cytochrome P450 molecules are a major source of these highly reactive radicals (Bondy and Naderi, 1994). Oxidative DNA damage including increased 8-hydroxydeoxyguanosine adducts have been reported in *H. hepaticus*-infected A/JCr mice, along with alterations in glutathione S-transferase and CYP2a5 (Chomarat et al., 1997; Sipowicz et al., 1997a). It has been noted, however, that CYP2a5 induction may not be dependent on oxidative damage alone given reactive oxygen species are also produced in liver injury caused by LPS, which results in CYP2a5 down-regulation (Bautista and Spitzer, 1990).

### *Genes Associated with Steroids*

The male predominance of HCC in humans suggests sex steroid involvement but epidemiological studies of serum levels have been controversial (Kuper et al., 2001; Tanaka et al., 2000). Therapeutic trials of steroid receptor inhibitors on patients with diagnosed HCC yielded mixed results (Nowak et al., 2004). One gene prominently and consistently down-regulated (Table 2) in *H. hepaticus*-infected male A/JCr mice with severe hepatitis and preneoplastic liver lesions was hydroxysteroid dehydrogenase-5, delta⟨5⟩-3-beta (Hsd3b5).

This 3-ketosteroid reductase gene, expressed only in the male mouse liver after puberty, reduces dihydrotestosterone to the relatively inactive 3$\beta$,17$\beta$-androstanediol, in preparation for conjugation and elimination (Payne et al., 1997). Hsd3b5 is also down-regulated in the liver of mice exposed to peroxisome proliferators and genotoxins (Wong and Gill, 2002; Wong et al., 2002).

*Genes Associated with Aging*

Splicing factor 3b subunit 1 (Sf3b1), a subunit of the spliceosome complex; peroxisome proliferation-activated receptor alpha (Ppara), a transcription factor involved in regulation of fatty acid oxidation, glycerol metabolism, and amino acid metabolism in the liver (Kersten et al., 2001; Patsouris et al., 2004); pre-B cell colony enhancing factor 1 (Pbef1), a growth factor for early stage B cells and recently identified as an inflammatory cytokine affecting neutrophil apoptosis (Jia et al., 2004); and D site albumin promoter binding protein (Dbp), a liver enriched transcription factor, were up-regulated greater than 5-fold at 12 months of age versus 3 months of age. Syndecan (Sdc4), a heparan sulfate proteoglycan promotes focal adhesion and stress fibers and delays healing and impairs angiogenesis when deleted in mice (Echtermeyer et al., 2001; Keum et al., 2004); and tubulin beta 2 (Tubb2) were down-regulated by 5-fold. Although there were few genes substantially up-regulated or down-regulated with aging, the principal component analysis graph spatially clustered regions of age groups at 3, 6, and 12 months in the A/JCr mouse. Aging may be associated with slight but coordinated changes in gene expression over time, implying that coregulated groups of genes or pathways may be modified more predictably as a group pattern change rather than individual gene changes. Future analysis should examine this approach (Mootha et al., 2003b). For example, aging is associated with an increased level of inflammation, and the present analysis confirms inflammation-associated genes being differentially expressed, but few individual genes change substantially over the course of 12 months. It is interesting to note that some genes such as insulin-like growth factor binding protein 1 (Igfbp1), apoptosis inhibitor 6 (now named CD5 antigen-like (Cd5l)), lysozyme (Lyzs), complement component 1 subcomponents (C1qa, C1qb, C1qg), tubulin beta 2 (Tubb2), Ia associated invariant chain (Ii), lipoprotein lipase (Lp1), and vascular cell adhesion molecule (Vcam1) are up-regulated due to ***H. hepaticus*** related lesions but are down-regulated with aging. In the aggregate, however, aging down-regulates more genes than it up-regulates in this study and others (Cao et al., 2001).

*Similar Studies Analyzing Gene Expression in* H. hepaticus *Infected A/JCr Mice*

***H. hepaticus*** initially colonizes the lower bowel before migrating to the liver. Although infection generally results in minimal-to-moderate inflammation in the lower bowel in immunocompetent mice, this murine pathogen induces severe typhlocolitis and lower bowel cancer in mutant mice with targeted immune dysfunctions (Erdman et al., 2003; Tomczak et al., 2003; Rogers and Fox, 2004). In an ***H. hepaticus*** infection study in A/JCr mice, a cDNA array consisting of 1176 genes demonstrated 31 up-regulated and 2 down-regulated genes in the cecum at 3 months postinfection (Myles et al., 2003). Some up-regulated genes in common in both studies at the 3 month time point included Ia associated invariant chain (Ii), interferon gamma inducible protein (Ifi47), and chemokine (CXC motif) ligand 9 (Cxcl9), and several different serum amyloid A components. Opioid receptor sigma 1 (Oprs1) was slightly up-regulated at 12 months in the present study. Continued study of host responses to ***H. hepaticus*** in the lower bowel may help identify factors responsible for protection or susceptibility to typhlocolitis as well as ***H. hepaticus*** translocation to the liver.

Hepatic proliferation is a key component of the development of HCC in the livers of mice infected with ***H. hepaticus*** (Fox et al., 1996a; Hailey et al., 1998). In agreement with a previous study of ***H. hepaticus*** infection in 6–18-month-old mice, we documented increased transcription of cyclin D1 and decreased epidermal growth factor receptor 2 in mice with progressive hepatic disease (Ramljak et al., 1998). However, our microarray results did not confirm previously reported differences in other genes including c-myc, cyclin-dependent kinase 4, hepatocyte growth factor, and transforming growth factor-$\alpha$ (Ramljak et al., 1998). Further studies are required to determine the contribution of different cell proliferation pathways related to tumorigenesis and their transcriptional, translational, and posttranslational regulatory mechanisms.

*Summary*

In summary, we characterized time-dependent gene expression signatures in the ***H. hepaticus*** infected A/J mouse liver with progressively severe liver disease. Transcription profiles in the livers of ***H. hepaticus***-infected male A/JCr mice exhibiting liver lesions yield a consistent ranking of differentially expressed genes. Importantly, the bimodal distribution of disease severity in infected male mice, as demonstrated by histopathology, corresponds with global hepatic gene expression differences. The reasons for the variable ***H. hepaticus*** colonization density and disease susceptibility in males, however, remain unexplained. There was an increased number of genes exhibiting differential expression for aging mice, in both ***H. hepaticus***-infected A/JCr mice and controls. Two putative tumor markers, intestinal trefoil factor 3 and H19 fetal liver mRNA were up-regulated in progressively dysplastic livers. Further investigations will determine if the gene expression signature of a target organ is diagnostic of a specific pathogen and whether there is prognostic value in data derived from this type of analysis. Global gene expression profiling by microarray analysis will continue to play an important role in elucidating molecular events in preneoplasia and cancer induced by microbial agents.

## ACKNOWLEDGMENTS

The authors acknowledge support from the following grants NIH R01CA67529, R01A159052, P01CA26731, and T32RR07036 to J.G.F.

## REFERENCES

Al-azzeh, E., Dittrich, O., Vervoorts, J., Blin, N., Gott, P., and Luscher, B. (2002). Gastroprotective peptide trefoil factor family 2 gene is activated by upstream stimulating factor but not by c-Myc in gastrointestinal cancer cells. *Gut* **51**, 685–90.

Avenaud, P., Marais, A., Monteiro, L., Le Bail, B., Biculac Sage, P., Balabaud, C., and Megraud, F. (2000). Detection of *Helicobacter* species in the liver of patients with and without primary liver carcinoma. *Cancer* **89**, 1431–9.

Bai, F., Nakanishi, Y., Takayama, K., Pei, X. H., Inoue, K., Harada, T., Izumi, M., and Hara, N. (2003). Codon 64 of K-ras gene mutation pattern in hepatocellular carcinomas induced by bleomycin and 1-nitropyrene in A/J mice. *Teratog Carcinog Mutagen* **Suppl 1**, 161–70.

Bartsch, S., and Tschesche, H. (1995). Cloning and expression of human neutrophil lipocalin cDNA derived from bone marrow and ovarian cancer cells. *FEBS Lett* **357**, 255–9.

Bautista, A. P., and Spitzer, J. J. (1990). Superoxide anion generation by in situ perfused rat liver: effect of in vivo endotoxin. *Am J Physiol* **259**, G907–12.

Bondy, S. C., and Naderi, S. (1994). Contribution of hepatic cytochrome P450 systems to the generation of reactive oxygen species. *Biochem Pharmacol* **48**, 155–9.

Brannan, C. I., and Bartolomei, M. S. (1999). Mechanisms of genomic imprinting. *Curr Opin Genet Dev* **9**, 164–70.

Brannan, C. I., Dees, E. C., Ingram, R. S., and Tilghman, S. M. (1990). The product of the H19 gene may function as an RNA. *Mol Cell Biol* **10**, 28–36.

Bratt, T. (2000). Lipocalins and cancer. *Biochim Biophys Acta* **1482**, 318–26.

Cao, S. X., Dhahbi, J. M., Mote, P. L., and Spindler, S. R. (2001). Genomic profiling of short- and long-term caloric restriction effects in the liver of aging mice. *Proc Natl Acad Sci USA* **98**, 10630–5.

Cavaggioni, A., and Mucignat-Caretta, C. (2000). Major urinary proteins, alpha(2U)-globulins and aphrodisin. *Biochim Biophys Acta* **1482**, 218–28.

Chan, I. T., Kutok, J. L., Williams, I. R., Cohen, S., Kelly, L., Shigematsu, H., Johnson, L., Akashi, K., Tuveson, D. A., Jacks, T., and Gilliland, D. G. (2004). Conditional expression of oncogenic K-ras from its endogenous promoter induces a myeloproliferative disease. *J Clin Invest* **113**, 528–38.

Chomarat, P., Sipowicz, M. A., Diwan, B. A., Fornwald, L. W., Awasthi, Y. C., Anver, M. R., Rice, J. M., Anderson, L. M., and Wild, C. P. (1997). Distinct time courses of increase in cytochromes P450 1A2, 2A5 and glutathione S-transferases during the progressive hepatitis associated with *Helicobacter hepaticus*. *Carcinogenesis* **18**, 2179–90.

Devireddy, L. R., Teodoro, J. G., Richard, F. A., and Green, M. R. (2001). Induction of apoptosis by a secreted lipocalin that is transcriptionally regulated by IL-3 deprivation. *Science* **293**, 829–34.

Diwan, B. A., Ward, J. M., Ramljak, D., and Anderson, L. M. (1997). Promotion by *Helicobacter hepaticus*-induced hepatitis of hepatic tumors initiated by *N*-nitrosodimethylamine in male A/JCr mice. *Toxicol Pathol* **25**, 597–605.

Eaton, J. W., Brandt, P., Mahoney, J. R., and Lee, J. T., Jr. (1982). Haptoglobin: a natural bacteriostat. *Science* **215**, 691–3.

Echtermeyer, F., Streit, M., Wilcox-Adelman, S., Saoncella, S., Denhez, F., Detmar, M., and Goetinck, P. (2001). Delayed wound repair and impaired angiogenesis in mice lacking syndecan-4. *J Clin Invest* **107**, R9–R14.

Edwards, J., Krishna, N. S., Witton, C. J., and Bartlett, J. M. (2003). Gene amplifications associated with the development of hormone-resistant prostate cancer. *Clin Cancer Res* **9**, 5271–81.

Erdman, S. E., Poutahidis, T., Tomczak, M., Rogers, A. B., Cormier, K., Plank, B., Horwitz, B. H., and Fox, J. G. (2003). CD4(+) CD25(+) Regulatory T lymphocytes inhibit microbially induced colon cancer in Rag2-deficient mice. *Am J Pathol* **162**, 691–702.

Etzioni, R., Urban, N., Ramsey, S., McIntosh, M., Schwartz, S., Reid, B., Radich, J., Anderson, G., and Hartwell, L. (2003). The case for early detection. *Nat Rev Cancer* **3**, 243–52.

Fox, J. G., Dewhirst, F. E., Shen, Z., Feng, Y., Taylor, N. S., Paster, B. J., Ericson, R. L., Lau, C. N., Correa, P., Araya, J. C., and Roa, I. (1998). Hepatic *Helicobacter* species identified in bile and gallbladder tissue from Chileans with chronic cholecystitis. *Gastroenterology* **114**, 755–63.

Fox, J. G., Dewhirst, F. E., Tully, J. G., Paster, B. J., Yan, L., Taylor, N. S., Collins, M. J., Jr., Gorelick, P. L., and Ward, J. M. (1994). *Helicobacter hepaticus* sp. nov., a microaerophilic bacterium isolated from livers and intestinal mucosal scrapings from mice. *J Clin Microbiol* **32**, 1238–45.

Fox, J. G., Drolet, R., Higgins, R., Messier, S., Yan, L., Coleman, B. E., Paster, B. J., and Dewhirst, F. E. (1996a). *Helicobacter canis* isolated from a dog liver with multifocal necrotizing hepatitis. *J Clin Microbiol* **34**, 2479–82.

Fox, J. G., Li, X., Yan, L., Cahill, R. J., Hurley, R., Lewis, R., and Murphy, J. C. (1996b). Chronic proliferative hepatitis in A/JCr mice associated with persistent *Helicobacter hepaticus* infection: a model of *helicobacter*-induced carcinogenesis. *Infect Immun* **64**, 1548–58.

Fox, J. G., Rogers, A. B., Whary, M. T., Ge, Z., Taylor, N. S., Xu, S., Horwitz, B. H., and Erdman, S. E. (2004). Gastroenteritis in NF-κB-deficient mice is produced with wild-type *Camplyobacter jejuni* but not with *C. jejuni* lacking cytolethal distending toxin despite persistent colonization with both strains. *Infect Immun* **72**, 1116–25.

Fox, J. G., Wang, T. C., Rogers, A. B., Poutahidis, T., Ge, Z., Taylor, N., Dangler, C. A., Israel, D. A., Krishna, U., Gaus, K., and Peek, R. M., Jr. (2003). Host and microbial constituents influence *Helicobacter pylori*-induced cancer in a murine model of hypergastrinemia. *Gastroenterology* **124**, 1879–90.

Fraser, D. J., Zumsteg, A., and Meyer, U. A. (2003). Nuclear receptors constitutive androstane receptor and pregnane X receptor activate a drug-responsive enhancer of the murine 5-aminolevulinic acid synthase gene. *J Biol Chem* **278**, 39392–401.

Frasor, J., Danes, J. M., Komm, B., Chang, K. C., Lyttle, C. R., and Katzenellenbogen, B. S. (2003). Profiling of estrogen up- and down-regulated gene expression in human breast cancer cells: insights into gene networks and pathways underlying estrogenic control of proliferation and cell phenotype. *Endocrinology* **144**, 4562–74.

Furutani, M., Arii, S., Mizumoto, M., Kato, M., and Imamura, M. (1998). Identification of a neutrophil gelatinase-associated lipocalin mRNA in human pancreatic cancers using a modified signal sequence trap method. *Cancer Lett* **122**, 209–14.

Gabay, C., and Kushner, I. (1999). Acute-phase proteins and other systemic responses to inflammation. *N Engl J Med* **340**, 448–54.

Graveel, C. R., Jatkoe, T., Madore, S. J., Holt, A. L., and Farnham, P. J. (2001). Expression profiling and identification of novel genes in hepatocellular carcinomas. *Oncogene* **20**, 2704–12.

Hailey, J. R., Haseman, J. K., Bucher, J. R., Radovsky, A. E., Malarkey, D. E., Miller, R. T., Nyska, A., and Maronpot, R. R. (1998). Impact of *Helicobacter hepaticus* infection in B6C3F1 mice from twelve National Toxicology Program two-year carcinogenesis studies. *Toxicol Pathol* **26**, 602–11.

Hatanaka, E., Pereira Ribeiro, F., and Campa, A. (2003). The acute phase protein serum amyloid A primes neutrophils. *FEMS Immunol Med Microbiol* **38**, 81–4.

Hinds, P. W., Dowdy, S. F., Eaton, E. N., Arnold, A., and Weinberg, R. A. (1994). Function of a human cyclin gene as an oncogene. *Proc Natl Acad Sci USA* **91**, 709–13.

Hinds, P. W., and Weinberg, R. A. (1994). Tumor suppressor genes. *Curr Opin Genet Dev* **4**, 135–41.

Ihrig, M., Schrenzel, M. D., and Fox, J. G. (1999). Differential susceptibility to hepatic inflammation and proliferation in AXB recombinant inbred mice chronically infected with *Helicobacter hepaticus*. *Am J Pathol* **155**, 571–82.

Iizuka, N., Oka, M., Yamada-Okabe, H., Hamada, K., Nakayama, H., Mori, N., Tamesa, T., Okada, T., Takemoto, N., Matoba, K., Takashima, M., Sakamoto, K., Tangoku, A., Miyamoto, T., Uchimura, S., and Hamamoto, Y. (2004). Molecular signature in three types of hepatocellular carcinoma with different viral origin by oligonucleotide microarray. *Int J Oncol* **24**, 565–74.

Jia, S. H., Li, Y., Parodo, J., Kapus, A., Fan, L., Rotstein, O. D., and Marshall, J. C. (2004). Pre-B cell colony-enhancing factor inhibits neutrophil apoptosis in experimental inflammation and clinical sepsis. *J Clin Invest* **113**, 1318–27.

Jung, D., Hagenbuch, B., Fried, M., Meier, P. J., and Kullak-Ublick, G. A. (2004). Role of liver-enriched transcription factors and nuclear receptors in regulating the human, mouse, and rat NTCP gene. *Am J Physiol Gastrointest Liver Physiol* **286**, G752–61.

Kaplan, R., Luettich, K., Heguy, A., Hackett, N. R., Harvey, B. G., and Crystal, R. G. (2003). Monoallelic up-regulation of the imprinted H19 gene in airway epithelium of phenotypically normal cigarette smokers. *Cancer Res* **63**, 1475–82.

Kapranov, P., Cawley, S. E., Drenkow, J., Bekiranov, S., Strausberg, R. L., Fodor, S. P., and Gingeras, T. R. (2002). Large-scale transcriptional activity in chromosomes 21 and 22. *Science* **296**, 916–9.

Katoh, M. (2003). Trefoil factors and human gastric cancer (Review). *Int J Mol Med* **12**, 3–9.

Kersten, S., Mandard, S., Escher, P., Gonzalez, F. J., Tafuri, S., Desvergne, B., and Wahli, W. (2001). The peroxisome proliferator-activated receptor alpha regulates amino acid metabolism. *FASEB J* **15**, 1971–8.

Keum, E., Kim, Y., Kim, J., Kwon, S., Lim, Y., Han, I., and Oh, E. S. (2004). Syndecan-4 regulates localization, activity and stability of protein kinase C-alpha. *Biochem J* **378**, 1007–14.

Khan, Z. E., Wang, T. C., Cui, G., Chi, A. L., and Dimaline, R. (2003). Transcriptional regulation of the human trefoil factor, TFF1, by gastrin. *Gastroenterology* **125**, 510–21.

Kimura, Y., Leung, P. S., Kenny, T. P., Van De Water, J., Nishioka, M., Giraud, A. S., Neuberger, J., Benson, G., Kaul, R., Ansari, A. A., Coppel, R. L., and Gershwin, M. E. (2002). Differential expression of intestinal trefoil factor in biliary epithelial cells of primary biliary cirrhosis. *Hepatology* **36**, 1227–35.

Kuper, H., Mantzoros, C., Lagiou, P., Tzonou, A., Tamimi, R., Mucci, L., Benetou, V., Spanos, E., Stuver, S. O., and Trichopoulos, D. (2001). Estrogens, testosterone and sex hormone binding globulin in relation to liver cancer in men. *Oncology* **60**, 355–60.

Lara-Tejero, M., and Galan, J. E. (2000). A bacterial toxin that controls cell cycle progression as a deoxyribonuclease I-like protein. *Science* **290**, 354–7.

Le Roith, D., Karas, M., Yakar, S., Qu, B. H., Wu, Y., and Blakesley, V. A. (1999). The role of the insulin-like growth factors in cancer. *Isr Med Assoc J* **1**, 25–30.

Lepreux, S., Bioulac-Sage, P., Gabbiani, G., Sapin, V., Housset, C., Rosenbaum, J., Balabaud, C., and Desmouliere, A. (2004). Cellular retinol-binding protein-1 expression in normal and fibrotic/cirrhotic human liver: different patterns of expression in hepatic stellate cells and (myo)fibroblast subpopulations. *J Hepatol* **40**, 774–80.

Leu, J. I., Crissey, M. A., and Taub, R. (2003). Massive hepatic apoptosis associated with TGF-beta1 activation after Fas ligand treatment of IGF binding protein-1-deficient mice. *J Clin Invest* **111**, 129–39.

Leung, W. K., Yu, J., Chan, F. K., To, K. F., Chan, M. W., Ebert, M. P., Ng, E. K., Chung, S. C., Malfertheiner, P., and Sung, J. J. (2002). Expression of trefoil peptides (TFF1, TFF2, and TFF3) in gastric carcinomas, intestinal metaplasia, and non-neoplastic gastric tissues. *J Pathol* **197**, 582–8.

Li, C., and Hung Wong, W. (2001a). Model-based analysis of oligonucleotide arrays: model validation, design issues and standard error application. *Genome Biol* **2**, RESEARCH0032.

Li, C., and Wong, W. H. (2001b). Model-based analysis of oligonucleotide arrays: expression index computation and outlier detection. *Proc Natl Acad Sci USA* **98**, 31–6.

Liu, Q., and Nilsen-Hamilton, M. (1995). Identification of a new acute phase protein. *J Biol Chem* **270**, 22565–70.

Matsui, T., Kinoshita, T., Morikawa, Y., Tohya, K., Katsuki, M., Ito, Y., Kamiya, A., and Miyajima, A. (2002). K-Ras mediates cytokine-induced formation of E-cadherin-based adherens junctions during liver development. *EMBO J* **21**, 1021–30.

McSweeney, L. A., and Dreyfus, L. A. (2004). Nuclear localization of the *Escherichia coli* cytolethal distending toxin CdtB subunit. *Cell Microbiol* **6**, 447–58.

Meyer, K., Lee, J. S., Dyck, P. A., Cao, W. Q., Rao, M. S., Thorgeirsson, S. S., and Reddy, J. K. (2003). Molecular profiling of hepatocellular carcinomas developing spontaneously in acyl-CoA oxidase deficient mice: comparison with liver tumors induced in wild-type mice by a peroxisome proliferator and a genotoxic carcinogen. *Carcinogenesis* **24**, 975–84.

Mootha, V. K., Bunkenborg, J., Olsen, J. V., Hjerrild, M., Wisniewski, J. R., Stahl, E., Bolouri, M. S., Ray, H. N., Sihag, S., Kamal, M., Patterson, N., Lander, E. S., and Mann, M. (2003a). Integrated analysis of protein composition, tissue diversity, and gene regulation in mouse mitochondria. *Cell* **115**, 629–40.

Mootha, V. K., Lindgren, C. M., Eriksson, K. F., Subramanian, A., Sihag, S., Lehar, J., Puigserver, P., Carlsson, E., Ridderstrale, M., Laurila, E., Houstis, N., Daly, M. J., Patterson, N., Mesirov, J. P., Golub, T. R., Tamayo, P., Spiegelman, B., Lander, E. S., Hirschhorn, J. N., Altshuler, D., and Groop, L. C. (2003b). PGC-1α-responsive genes involved in oxidative phosphorylation are coordinately downregulated in human diabetes. *Nat Genet* **34**, 267–73.

Myles, M. H., Livingston, R. S., Livingston, B. A., Criley, J. M., and Franklin, C. L. (2003). Analysis of gene expression in ceca of *Helicobacter hepaticus*-infected A/JCr mice before and after development of typhlitis. *Infect Immun* **71**, 3885–93.

Nielsen, B. S., Borregaard, N., Bundgaard, J. R., Timshel, S., Sehested, M., and Kjeldsen, L. (1996). Induction of NGAL synthesis in epithelial cells of human colorectal neoplasia and inflammatory bowel diseases. *Gut* **38**, 414–20.

Nilsen-Hamilton, M., Hamilton, R. T., and Adams, G. A. (1982). Rapid selective stimulation by growth factors of the incorporation by BALB/C 3T3 cells of [35S]methionine into a glycoprotein and five superinducible proteins. *Biochem Biophys Res Commun* **108**, 158–66.

Nilsson, H. O., Mulchandani, R., Tranberg, K. G., and Wadstrom, T. (2001). *Helicobacter* species identified in liver from patients with cholangiocarcinoma and hepatocellular carcinoma. *Gastroenterology* **120**, 323–4.

Nowak, A., Findlay, M., Culjak, G., and Stockler, M. (2004). Tamoxifen for hepatocellular carcinoma. *Cochrane Database Syst Rev*, CD001024.

Nyska, A., Maronpot, R. R., Eldridge, S. R., Haseman, J. K., and Hailey, J. R. (1997). Alteration in cell kinetics in control B6C3F1 mice infected with *Helicobacter hepaticus*. *Toxicol Pathol* **25**, 591–6.

Ohara, M., Hayashi, T., Kusunoki, Y., Miyauchi, M., Takata, T., and Sugai, M. (2004). Caspase-2 and caspase-7 are involved in cytolethal distending toxin-induced apoptosis in Jurkat and MOLT-4 T-cell lines. *Infect Immun* **72**, 871–9.

Palmer, H. G., Sanchez-Carbayo, M., Ordonez-Moran, P., Larriba, M. J., Cordon-Cardo, C., and Munoz, A. (2003). Genetic signatures of differentiation induced by 1alpha,25-dihydroxyvitamin D3 in human colon cancer cells. *Cancer Res* **63**, 7799–806.

Parker, M. A., Deane, N. G., Thompson, E. A., Whitehead, R. H., Mithani, S. K., Washington, M. K., Datta, P. K., Dixon, D. A., and Beauchamp, R. D. (2003). Over-expression of cyclin D1 regulates Cdk4 protein synthesis. *Cell Prolif* **36**, 347–60.

Patsouris, D., Mandard, S., Voshol, P. J., Escher, P., Tan, N. S., Havekes, L. M., Koenig, W., Marz, W., Tafuri, S., Wahli, W., Muller, M., and Kersten, S. (2004). PPARalpha governs glycerol metabolism. *J Clin Invest* **114**, 94–103.

Pawson, T., and Nash, P. (2003). Assembly of cell regulatory systems through protein interaction domains. *Science* **300**, 445–52.

Payne, A. H., Abbaszade, I. G., Clarke, T. R., Bain, P. A., and Park, C. H. (1997). The multiple murine 3 beta-hydroxysteroid dehydrogenase isoforms: structure, function, and tissue- and developmentally specific expression. *Steroids* **62**, 169–75.

Ponzetto, A., Pellicano, R., Leone, N., Cutufia, M. A., Turrini, F., Grigioni, W. F., D'Errico, A., Mortimer, P., Rizzetto, M., and Silengo, L. (2000). *Helicobacter* infection and cirrhosis in hepatitis C virus carriage: is it an innocent bystander or a troublemaker? *Med Hypotheses* **54**, 275–7.

Ramljak, D., Jones, A. B., Diwan, B. A., Perantoni, A. O., Hochadel, J. F., and Anderson, L. M. (1998). Epidermal growth factor and transforming growth factor-alpha-associated overexpression of cyclin D1, Cdk4, and c-Myc during hepatocarcinogenesis in *Helicobacter hepaticus*-infected A/JCr mice. *Cancer Res* **58**, 3590–7.

Ribeiro, F. P., Furlaneto, C. J., Hatanaka, E., Ribeiro, W. B., Souza, G. M., Cassatella, M. A., and Campa, A. (2003). mRNA expression and release of interleukin-8 induced by serum amyloid A in neutrophils and monocytes. *Mediators Inflamm* **12**, 173–8.

Rivera-Rivera, I., Kim, J., and Kemper, B. (2003). Transcriptional analysis in vivo of the hepatic genes, Cyp2b9 and Cyp2b10, by intravenous administration of plasmid DNA in mice. *Biochim Biophys Acta* **1619**, 254–62.

Rodrigues, S., Attoub, S., Nguyen, Q. D., Bruyneel, E., Rodrigue, C. M., Westley, B. R., May, F. E., Thim, L., Mareel, M., Emami, S., and Gespach, C. (2003). Selective abrogation of the proinvasive activity of the trefoil peptides pS2

and spasmolytic polypeptide by disruption of the EGF receptor signaling pathways in kidney and colonic cancer cells. *Oncogene* **22**, 4488–97.

Rogers, A. B., and Fox, J. G. (2004). Inflammation and Cancer I. Rodent models of infectious gastrointestinal and liver cancer. *Am J Physiol Gastrointest Liver Physiol* **286**, G361–6.

Scharf, J. G., Dombrowski, F., and Ramadori, G. (2001). The IGF axis and hepatocarcinogenesis. *Mol Pathol* **54**, 138–44.

Selvamurugan, N., Kwok, S., and Partridge, N. C. (2004). Smad3 interacts with JunB and Cbfa1/Runx2 for transforming growth factor-beta1-stimulated collagenase-3 expression in human breast cancer cells. *J Biol Chem* **279**, 27764–73.

Sipowicz, M. A., Chomarat, P., Diwan, B. A., Anver, M. A., Awasthi, Y. C., Ward, J. M., Rice, J. M., Kasprzak, K. S., Wild, C. P., and Anderson, L. M. (1997a). Increased oxidative DNA damage and hepatocyte overexpression of specific cytochrome P450 isoforms in hepatitis of mice infected with *Helicobacter hepaticus*. *Am J Pathol* **151**, 933–41.

Sipowicz, M. A., Weghorst, C. M., Shiao, Y. H., Buzard, G. S., Calvert, R. J., Anver, M. R., Anderson, L. M., and Rice, J. M. (1997b). Lack of p53 and ras mutations in *Helicobacter hepaticus*-induced liver tumors in A/JCr mice. *Carcinogenesis* **18**, 233–6.

Song, X., Tao, Y. G., Deng, X. Y., Jin, X., Tan, Y. N., Tang, M., Wu, Q., Lee, L. M., and Cao, Y. (2004). Heterodimer formation between c-Jun and Jun B proteins mediated by Epstein-Barr virus encoded latent membrane protein 1. *Cell Signal* **16**, 1153–62.

Tanaka, K., Sakai, H., Hashizume, M., and Hirohata, T. (2000). Serum testosterone:estradiol ratio and the development of hepatocellular carcinoma among male cirrhotic patients. *Cancer Res* **60**, 5106–10.

Taylor, N. S., Ge, Z., Shen, Z., Dewhirst, F. E., and Fox, J. G. (2003). Cytolethal distending toxin: a potential virulence factor for *Helicobacter cinaedi*. *J Infect Dis* **188**, 1892–7.

Thirunavukkarasu, C., and Sakthisekaran, D. (2003). Effect of dietary selenite on N-nitrosodiethylamine-induced and phenobarbital promoted multistage hepatocarcinogenesis in rat: reflection in some minerals. *Biomed Pharmacother* **57**, 416–21.

Tomczak, M. F., Erdman, S. E., Poutahidis, T., Rogers, A. B., Holcombe, H., Plank, B., Fox, J. G., and Horwitz, B. H. (2003). NF-kappaB is required within the innate immune system to inhibit microflora-induced colitis and expression of IL-12 p40. *J Immunol* **171**, 1484–92.

Tong, Z., Wu, X., and Kehrer, J. P. (2003). Increased expression of the lipocalin 24p3 as an apoptotic mechanism for MK886. *Biochem J* **372**, 203–10.

Vernucci, M., Cerrato, F., Besnard, N., Casola, S., Pedone, P. V., Bruni, C. B., and Riccio, A. (2000). The H19 endodermal enhancer is required for Igf2 activation and tumor formation in experimental liver carcinogenesis. *Oncogene* **19**, 6376–85.

Ward, J. M., Fox, J. G., Anver, M. R., Haines, D. C., George, C. V., Collins, M. J., Jr., Gorelick, P. L., Nagashima, K., Gonda, M. A., Gilden, R. V., and et al. (1994). Chronic active hepatitis and associated liver tumors in mice caused by a persistent bacterial infection with a novel *Helicobacter* species. *J Natl Cancer Inst* **86**, 1222–7.

Wong, J. S., and Gill, S. S. (2002). Gene expression changes induced in mouse liver by di(2-ethylhexyl) phthalate. *Toxicol Appl Pharmacol* **185**, 180–96.

Wong, J. S., Ye, X., Muhlenkamp, C. R., and Gill, S. S. (2002). Effect of a peroxisome proliferator on 3 beta-hydroxysteroid dehydrogenase. *Biochem Biophys Res Commun* **293**, 549–53.

Xu, S., and Venge, P. (2000). Lipocalins as biochemical markers of disease. *Biochim Biophys Acta* **1482**, 298–307.

Yakar, S., Liu, J. L., Stannard, B., Butler, A., Accili, D., Sauer, B., and LeRoith, D. (1999). Normal growth and development in the absence of hepatic insulin-like growth factor I. *Proc Natl Acad Sci USA* **96**, 7324–9.

Yamamoto, Y., Nishikawa, Y., Tokairin, T., Omori, Y., and Enomoto, K. (2004). Increased expression of H19 non-coding mRNA follows hepatocyte proliferation in the rat and mouse. *J Hepatol* **40**, 808–14.

Yang, J., Mori, K., Li, J. Y., and Barasch, J. (2003). Iron, lipocalin, and kidney epithelia. *Am J Physiol Renal Physiol* **285**, F9–18.

Yoshinari, K., Kobayashi, K., Moore, R., Kawamoto, T., and Negishi, M. (2003). Identification of the nuclear receptor CAR:HSP90 complex in mouse liver and recruitment of protein phosphatase 2A in response to phenobarbital. *FEBS Lett* **548**, 17–20.

Young, V. B., Knox, K. A., Pratt, J. S., Cortez, J. S., Mansfield, L. S., Rogers, A. B., Fox, J. G., and Schauer, D. B. (2004). In vitro and in vivo characterization of *Helicobacter hepaticus* cytolethal distending toxin mutants. *Infect Immun* **72**, 2521–7.

Young, V. B., Knox, K. A., and Schauer, D. B. (2000). Cytolethal distending toxin sequence and activity in the enterohepatic pathogen *Helicobacter hepaticus*. *Infect Immun* **68**, 184–91.